SARAJI EAST MINING LEASE PROJECT

Groundwater Modelling Technical Report

Prepared for:

AECOM Australia Pty Ltd
540 Wickham Street Fortitude Valley, Brisbane 4006

SLR Ref: 620.31025.00000-R01
Version No: -v4.1
May 2023

PREPARED BY

SLR Consulting Australia Pty Ltd
ABN 29 001 584 612
Level 16, 175 Eagle Street
Brisbane QLD 4000 Australia
(PO Box 26 Spring Hill QLD 4004)
T: +61 7 3858 4800
E: brisbane@slrconsulting.com www.slrconsulting.com

BASIS OF REPORT

DOCUMENT CONTROL

Reference	Date	Prepared	Checked	Authorised
620.31025.00000-R01-v4.1	31 May 2023	Vahid Shapoori / Ryan Davies	Brian Rask / Derwin Lyons	Derwin Lyons

CONTENTS

DOCUMENT REFERENCES

TABLES

FIGURES

APPENDICES

1 Introduction

SLR Consulting Australia Pty Ltd (SLR) has been engaged by AECOM Australia Pty Ltd (AECOM) to conduct groundwater modelling in support of response to submissions received on the recent Saraji East Mining Lease Project (SEMLP) Environmental Impact Statement (EIS) approval submission, which was developed by AECOM. The SEMLP is proposed by BM Alliance Coal Operations Pty Ltd (BMA) and comprises an underground longwall coal mine development located immediately east of BMA's Saraji Mine in Queensland's Bowen Basin.

As a part of the updated SEMLP Groundwater Assessment being prepared in response to submissions, AECOM requested SLR to update the existing regulatory accepted BMA regional groundwater model to include known local hydrogeologic features and mining operations (historic, approved and proposed) in the vicinity of the SEMLP, in order to provide estimates of potential impacts to groundwater and relevant receptors. This new modelling supersedes the earlier groundwater modelling works completed for the SEMLP by AECOM (2019), AECOM (2016) and AGE (2012).

1.1 Background

The updated regional groundwater model, referred to as the SEMLP numerical groundwater model in this report, builds on the regional scale Olive Downs Project model (i.e. the foundational model) (HydroSimulations, 2018). The foundational model was subsequently updated for the Moorvale South Project in 2019 (SLR, 2019), Winchester South Project in 2020 (SLR, 2020), Caval Ridge Mine (CVM) and Horse Pit Extension (HPE) Project in 2021 (SLR, 2021a), Lake Vermont North (LVN) Extension Project (SLR, 2021b), Millennium Mine Mavis Extension (SLR, 2021c), and for the Daunia Mine (DNM) Water Licence Review (SLR, 2021d). This regional scale model has been reviewed and accepted twice by State agencies and once by the Commonwealth for other project approval applications (Such as Olive Downs Coking Coal Project). Additionally, BMA has used the model to support various State mining compliance reporting requirements. Data sharing agreements have been established by these project proponents that allow the sharing of groundwater information and modelling. Under these agreements, the groundwater models developed as part of each project's groundwater assessment were adopted as a base for the SEMLP model, where relevant.

A range of updates to the BMA regional groundwater model were required for the model to be considered fit for purpose for the SEMLP. The updates to the model design are as follow:

- Updated fracture zone depth and hydraulic property changes above the proposed SEMLP longwalls (LW) based on the SEMLP subsidence modelling report (Minserve 2022).
- Updated model layer geometry based on the Peak Downs (PDM), Saraji (SRM), SEMLP and Saraji South latest BMA geological models.
- Implemented historic and approved future mining operations at SRM and PDM and the proposed underground operations at SEMLP.
- Refined surface elevations and hydrologic features.

Further detail on these updates is provided in this report.

1.2 Modelling Objectives

The overall objectives of this groundwater modelling are to:

- Estimate the groundwater inflow to the SEMLP mine workings as a function of mine position and timing.
- Simulate and predict the extent of groundwater level drawdown due to the SEMLP.
- Identify areas of potential environmental risk, where groundwater impact management measures may be necessary.

1.3 This Report

This report has been prepared documenting technical details of the SEMLP numerical groundwater model, to support the SEMLP and other future applications of the model.

Further details on the model updates completed for the SEMLP are discussed in **Section 0** of this modelling report, which presents how the conceptualisation has been developed as a numerical groundwater model, and **Section 2.6** presents how well the model replicates observed data (calibration). Details on how the model represents the SEMLP and other future mining activities approved or under assessment within the model domain is outlined within **Section 3** of this report.

It is important to note that this report does not present an updated groundwater impact assessment for the SEMLP. The updated groundwater impact assessment is being developed by AECOM separately, based in part on the modelling results reported herein. Similarly, conceptualisation of the groundwater regime relevant to the SEMLP is included in the updated groundwater impact assessment.

2 Model Construction and Development

2.1 Model Code

MODFLOW-USG Transport was used as the model code (Panday *et al.* 2013). MODFLOW-USG is the recent version of industry standard MODFLOW code and was determined to be the most suitable modelling code for accomplishing the model objectives. MODFLOW-USG optimises the model grid and increases numerical stability by using unstructured, variably sized cells. These cells take any polygonal shape, with variable size constraints allowing for refinement in areas of interest (i.e., geological or mining features).

Where previous MODFLOW versions restricted interlayer flow to vertical connectivity, MODFLOW-USG offers lateral connectivity between model layers. Lateral connectivity enables more accurate representations of hydrostratigraphic units, particularly those that pinch out, outcrop, or cross geological faults.

MODFLOW-USG is also able to simulate unsaturated conditions, allowing progressive mine dewatering and post mining rewetting to be represented by the model. For the SEMLP model, vadose zone properties have been excluded, and the unsaturated zone was simulated using the upstream-weighting method.

Fortran code and a MODFLOW-USG edition of the Groundwater Data Utilities (Watermark Numerical Computing) were used to construct the MODFLOW-USG input files.

2.2 Model Extent and Mesh Design

The groundwater model extent is shown in **Figure 2-1.** The model is a regional scale model with the domain extent designed to meet environmental approvals application requirements for cumulative impact assessment, (i.e., the domain is large enough to appropriately consider all potential overlapping groundwater impacts from resource operations in the Bowen Basin).

The model domain extent has been kept consistent from the previous (Caval Ridge Mine Horse Pit Extension) CVM HPE version of the model (SLR, 2021a). The model domain is intended to place boundary conditions sufficiently distant from the SEMLP and surrounding mines to allow the extent of potential impacts from mining activities on the groundwater system to be assessed. At its widest extents, the model is approximately 62 km west-east by 95 km north-south. The model domain from the CVM HPE version of the model is deemed appropriate for the SEMLP model based on the following considerations:

- The western boundary is represented by the outcrop boundary of the Back Creek Group, which is considered the regional low permeability basement for the purpose of this modelling.
- The northern boundary contains the primary geological unit being targeted by the SEMLP and is 30 km away from the proposed longwall panels.
- The southern boundary is set along the Stephens Creek 30 km south of the SEMLP and is expected to be far outside the range of predicted SEMLP related drawdown.
- The eastern boundary is set along the Delvin Creek 40 km east of the SEMLP and is expected to be far outside the range of predicted Project related drawdown.

To allow stable numerical modelling of the large spatial area of the model domain, an unstructured grid with varying Voronoi cell sizes was designed using Algomesh (HydroAlgorithmics, 2014). Varying Voronoi cell sizes allowed refinement around areas of interest, while a coarser resolution elsewhere reduces the total cell count to a manageable size. The model domain was vertically discretised into 19 layers, each layer comprising a cell count up to 121,225. The total number of cells in the model is 1,362,485. This is after pinching out areas in layers 3 to 19 where a layer is not present based on the mapped geology.

The following features have been included in the grid design:

- The Isaac River is represented in the model with a 50 metre (m) Voronoi cell size constraint.
- Longwall mining for the SEMLP is represented with a 100 m cell size constraint.
- Open cut mine areas for the opencut mines including PDM, SRM, CVM, Poitrel, Daunia, Millennium, Lake Vermont, Winchester South, and Olive Downs have a 100 m Voronoi cell size constraint.
- Longwall mining at Grosvenor and Eagle Downs has an oriented regular grid of 100 m width squares to represent longwalls.
- Faults are represented using a 200 m Voronoi cell constraint.

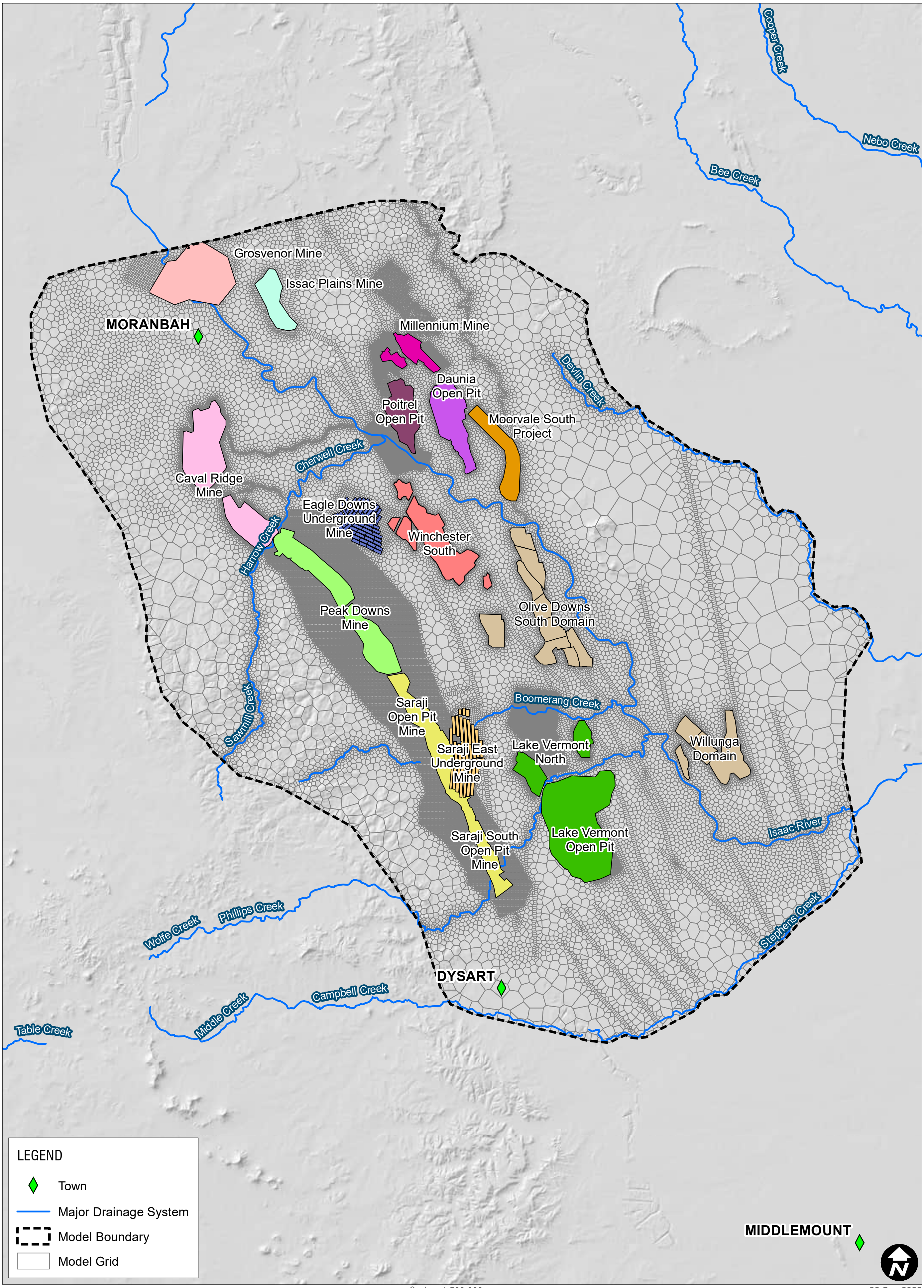

H:\Projects-SLR\620-BNE\620-BNE\620.31025.00000 Saraji East GW Modelling\03 SLR Data\01 CADGIS\GIS\62031025 F2-1 Model Domain.mxd

Scale: 1:500,000
GDA 1994 MGA Zone 55

22-Dec-2022
620.31025

Sheet Size : A4

SLR
www.slrconsultingaustralia.com

0 5 10 15 km

Model Domain

FIGURE 2-1

2.3 Model Layers

Topography within the model domain has been defined using numerous sources of varying accuracy. Data extents of the sources used to construct model topography are shown in **Figure 2-2**. High resolution (1 m) Digital Elevation Model (DEM) data, provided by BMA, was used to define local surface elevation within the SEMLP area. Outside the extents of the DEM dataset for the SEMLP, LiDAR data from the Moorvale South Project, Winchester South Project, and the Olive Downs Project and CVM were used to define surface elevation, where available. Public domain 25 m DEM data sourced from Geoscience Australia (with 3 m subtracted for consistency between datasets) was used to define topography in the remainder of the model domain.

The model domain is discretised into 19 layers, as listed in **Table 2-1**. **Table 2-1** also presents the average thicknesses across the model domain for each layer. Model layer extents (lateral and vertical) have been defined using data from the following sources:

- BMA, SRM site geological model
- BMA, Saraji South site geological model
- BMA, DNM site geological model
- BMA, CVM site geological model and bore hole logs
- BMC, PTM site geological model
- Jellinbah Mining Pty Ltd, Lake Vermont, Lake Vermont North and Lake Vermont Meadowbrook site geological models and bore hole logs
- Whitehaven WS Pty Ltd - Winchester South Project site geological model and bore hole logs
- MetRes Pty Ltd, Millennium site geological model
- Peabody Energy Limited, Moorvale South Project site geological model and bore hole logs
- Pembroke Resources Limited, Olive Downs Project site geological model and bore hole logs
- CSIRO Regolith depth survey
- Queensland Globe bore hole logs
- Queensland surface geology and basement geological maps.

Table 2-1 Model Layers and Thicknesses

Model Layer	Formation	Unit	Average Thickness (m)
1	Alluvium, colluvium, Tertiary basalt	Surface cover – alluvium, colluvium and Tertiary basalt	8.3
2	Tertiary sediments, Tertiary basalt	Tertiary and minor Triassic Clematis Group, weathered Permian, Tertiary basalt	19.2
3	Rewan Group	Triassic	117.7
4	Rangal Coal Measures	Leichhardt overburden	36.6
5		Leichhardt seam	4.6
6		Interburden	35.6
7		Vermont seam	3.8
8		Vermont underburden	34.1
9	Fort Cooper Coal Measures	Fort Cooper overburden	206.6
10		Fort Cooper seams (combined)	55.9
11		Fort Cooper underburden	56.1
12	Moranbah Coal Measures	Q Seam	3.3
13		Interburden	38.0
14		P Seam	2.9
15		Interburden	56.4
16		H Seam	5.5
17		Interburden	67.1
18		D Seam (target coal seam for SEMLP)	8.4
19		Base of Model - aquitard	100.0

Model Layer 1 is fully extensive across the model with an average thickness of 8.3 m. The base of Layer 1 is largely consistent with the previous CVM HPE version of the model, with local updates using the bore logs available for the SEMLP area. With respect to Boomerang Creek (the creek north of the SEMLP), the alluvium associated with the creek was set a uniform thickness of 3.75 m consistent with AECOM conceptualisation based on drill hole logs along the creek.

Model Layer 2 is also fully present across the model area with a minimum thickness of 1 m. The SRM, SEMLP, South Saraji, Peak Downs, Winchester South and CVM site geology models were used to define the base of model Layer 2. Outside these site geology models the base of Layer 2 was interpreted from CSIRO regolith survey depths and Queensland Globe bore log lithology data consistent with the previous CVM HPE version of the model.

The underlying Triassic and Permian layers are present only to their outcrop extents, with some inference made for the presence of older units beneath the surface outcrop due to folding and faulting. The layering above the Moranbah Coal Measures is generally consistent with the CVM HPE model.

With regards to Moranbah Coal Measures, eight layers were included to account for all the coal seam targets within the Moranbah Coal Measures at the CVM, PDM, SRM, and SEMLP sites. The PDM and SRM/SEMLP site geology models were used for updating the construction of layers 12 to 19 representing the Moranbah Coal Measures. It is not possible to represent every individual coal seam or ply in the model layers representing the Moranbah Coal Measures, therefore a 'combined thickness' totalling the approximate thickness of coal for the main seams has been simulated, consistent with the previous CVM HPE version of the model. The major coal seams represented in the model are the Q, P, H and D seams. In doing so, the thicknesses of each individual coal seam (typically < 1m thickness) were combined separately for the major coal seams and the combined thicknesses were used in the model. The base of the lowest coal seam at each group was used to assign the bottom of the model layer. Outside of the geology model extents, where bore logs with information on Moranbah Coal Measures were available this information was included in the layer elevations. Elsewhere, average thicknesses were extrapolated out into the extended model area and Queensland Surface Geology maps were used to pinch-out the layers when the geology unit discontinues and does not exist laterally.

Table 2-1 reports the average thicknesses of each layer over the entire model area. In order to provide an estimate of coal seam thicknesses within the mine area, the average thicknesses of major coal seams were calculated only within SRM/SEMLP area and reported as below:

- Q Seam thickness: 1.5 m
- P Seam Thickness: 2.5 m
- H Seam Thickness: 4.5 m
- D Seam Thickness: 8.5 m

The basement layer has the thickness of 100m and considered to replicate the Back Creek Group. The Back Creek Group in general has low permeability and will act as regional aquitard, suppressing downward vertical flow.

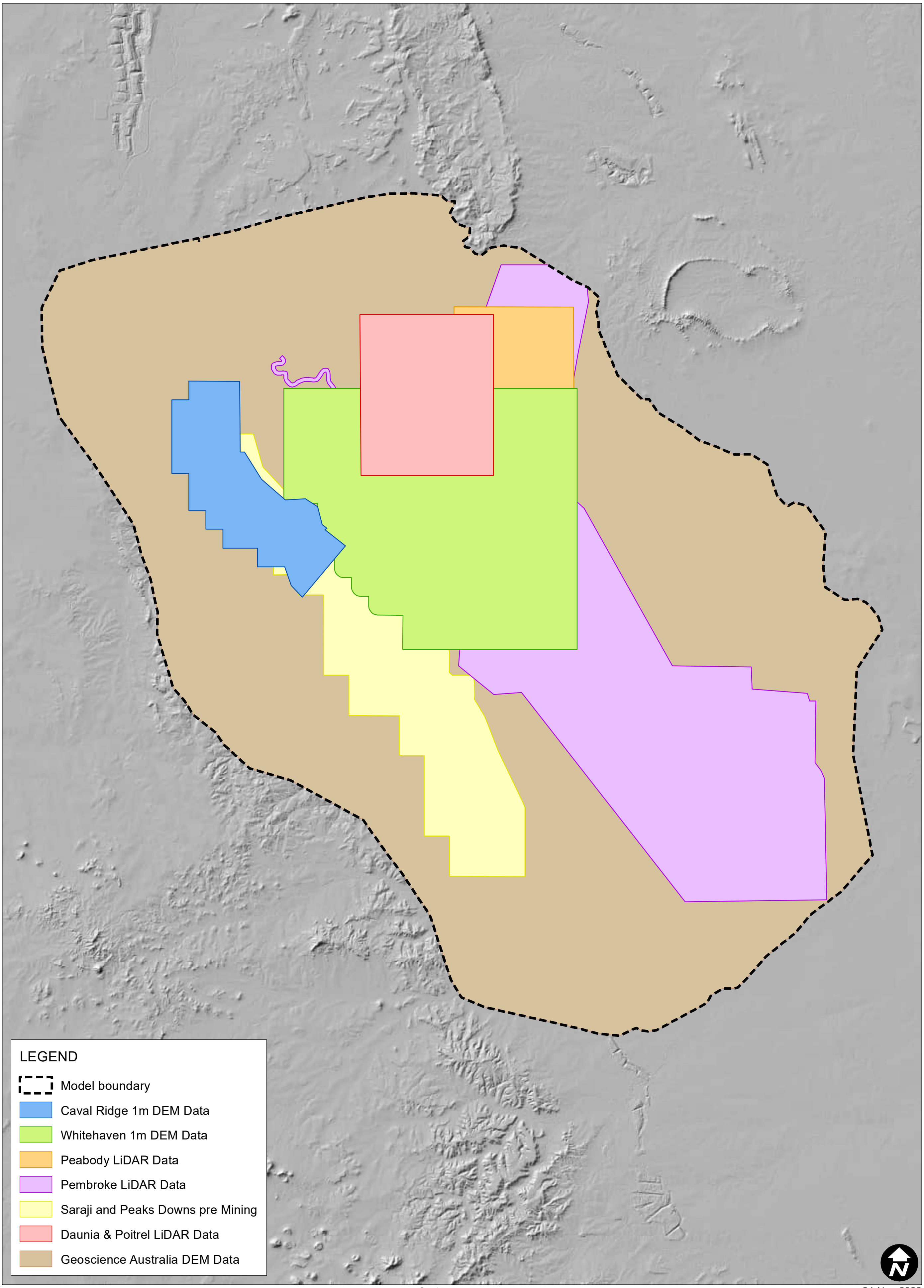

H:\Projects-SLR\620-BNE\620-BNE\620.31025.00000 Saraji East GW Modelling\03 SLR Data\01 CADGIS\GIS\62031025 F2-2 Topography data extents.mxd

Scale 1:500,000
GDA 1994 MGA Zone 55

24-Nov-2022
620.30125

Sheet Size : A4

SLR
www.slrconsultingaustralia.com

0 5 10 15 Kilometers

Topography Data Extents

FIGURE 2-2

2.3.1 Geological Faults

As discussed in the AECOM (2019) groundwater conceptualisation report, there are faults present in and around the SEMLP. The modelling of faults within the groundwater model domain is from the CVM HPE model using the fault mapping and site-specific geology models where available.

Local faults displacements derived from the PDM and SRM/SEMLP geological models have also been captured in the model layer elevations at these sites. There are three key regional northwest-southeast trending fault zones included in the model:

- Extending 50 km, 500 m to the east of SEMLP
- Extending 70 km, 12 km to the east of SEMLP
- Numerous shorter faults extending 25 km total, 15 km to the east of SEMLP
- Mesh refinement (200m) has been used along fault lines to allow for isolated changes of hydraulic properties along fault zones during calibration. **Figure 2-3** shows the locations of geological fault zones represented in the model.

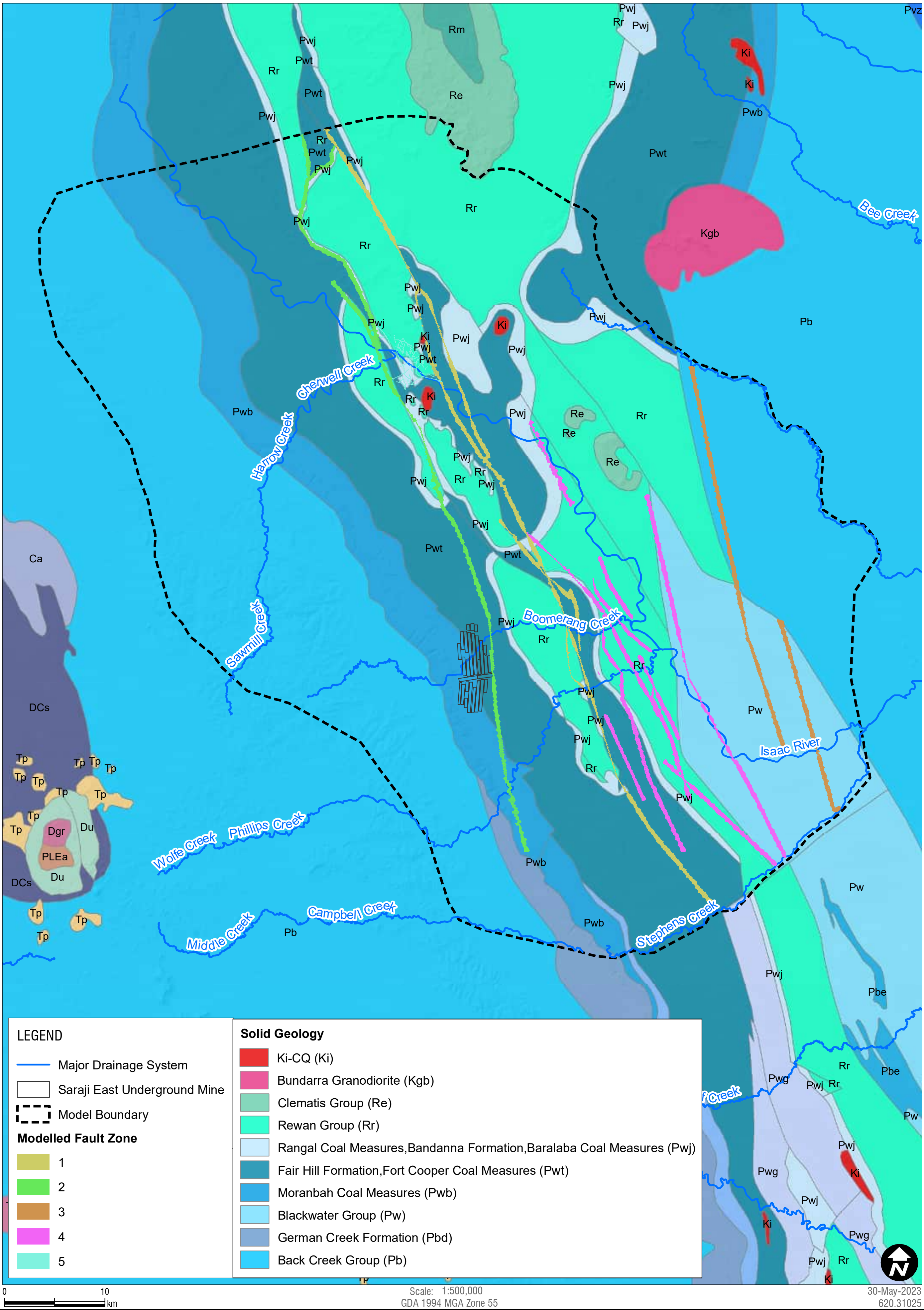

Modelled Fault Zones

FIGURE 2-3

2.4 Model Stresses and Boundary Conditions

2.4.1 Regional Groundwater Flow

General Head Boundary (GHB) have been specified along the eastern, southern, and part of the northern model boundaries. The GHB boundary condition is used to represent the regional flow into and out of the model area and has been assigned using GHB cells in all layers using pre-mining head elevations. Groundwater will enter the model where the head set in the GHB is higher than the modelled head in the adjacent cell and will leave the model when the water level is lower in the GHB. GHB conductance is calculated using the hydraulic conductivity and the dimensions of each GHB cells and is therefore variable in this model due to variable cell-size.

No flow boundary was applied to the western boundary of the model that represents the outcrop of the Back Creek Group.

A drain boundary condition was used in the northern model boundary to simulate the mining at the Grosvenor Mine.

2.4.2 Watercourses

Major rivers (including Isaac River) as well as minor creeks were built into the model using MODFLOW-USG RIV package. River cells in the model are shown in **Figure 2-4** . Streams within and around the SEMLP that were included in the RIV package are presented in **Table 2-2**.

Table 2-2 River and Surface Water Features in the Model

Boundary	River Stage (m)	River Bed Kz (m/day)
Isaac River	Warm Up Simulation - Long term Average (2008-2020) Calibration simulation - Historical Quarterly Averages Prediction simulation- Fixed Stage Height- Long term Average (2008-2020)	1.0×10^{-2}
One Mile Creek	0	1.0×10^{-1}
Boomerang Creek	0	1.0×10^{-1}
Other Minor Creeks	0	1.0×10^{-2} to 1.0×10^{-1}

Surveyed river stage data was available at several locations along the Isaac River. The closest gauging station to the site, located at Deverill, records average monthly water levels as shown in **Table 2-3**. This data was extrapolated to provide continuous stage elevations.

Table 2-3 Average Stage Heights (m) Used to Develop Transient Sequence

Station	Jan	Feb	Mar	Apr	May	Jun	Jul	Aug	Sep	Oct	Nov	Dec	Annual Average
Isaac River at Deverill	0.46	0.89	0.68	0.39	0.23	0.15	0.16	0.10	0.08	0.02	0.09	0.41	0.31

River and creek widths, thickness and conductance values were adopted from the CVM HPE model. The rivers are set with the riverbed 1 to 10 m below the surrounding topography to represent the steep-banked incised channels. The river widths were assumed to be fixed for each river in the model. The river widths were estimated using aerial photography and aligned with assumptions within the CVM HPE model.

The river conductance was calculated using river width, river length, riverbed thickness, and the vertical hydraulic conductivity of riverbed material (Kz). Therefore, the river conductance is variable due to the non-constant spatial discretisation in each of the model river cells. The vertical hydraulic conductivity of riverbeds for different rivers in the model were adopted from the CVM HPE model.

The river stage height in the minor tributaries or drainage lines was set to 0 m (i.e., river stage elevation was equal to river bottom elevation). Therefore, the minor tributaries or drainage lines act as drains to the groundwater system and do not result in any recharge from the watercourse to the groundwater system.

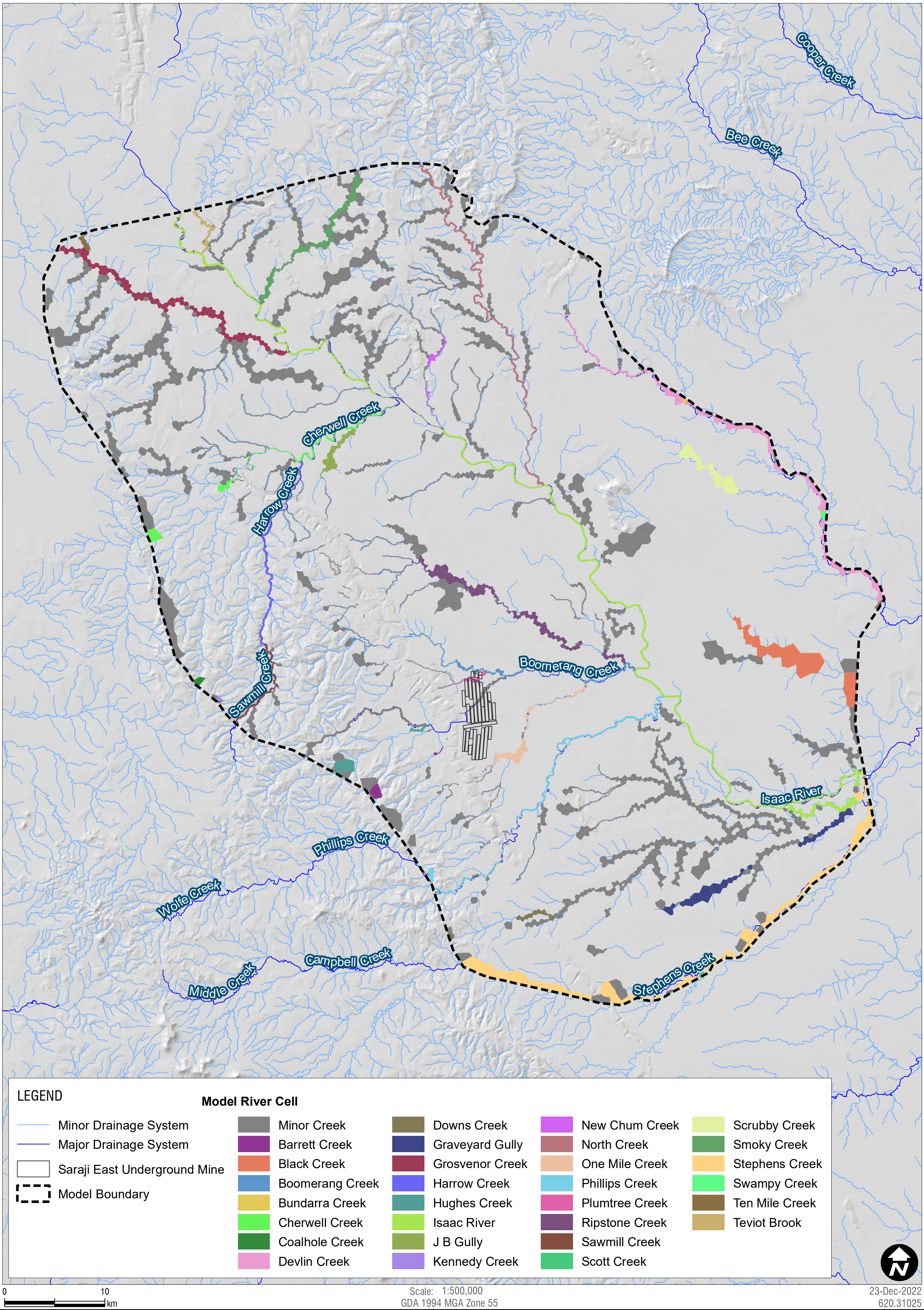

H:\Projects-SLR\620-BNE\620-BNE\620.31025.00000 Saraji East GW Modelling\03 SLR Data\01 CADGIS\GIS\62031025 F2-4 Stream and River Cells.mxd

SLR

Stream and River Cells

FIGURE 2-4

2.4.3 Rainfall Recharge

The dominant mechanism for recharge to the groundwater system is through diffuse infiltration of rainfall through the soil profile and subsequent deep drainage to underlying groundwater systems. Diffuse rainfall recharge to the model was represented using the MODFLOW-USG Recharge package (RCH).

The recharge rates were established through the calibration process, with bounds based on the conceptual understanding of the system and comparing them with other groundwater models prepared for the region. The starting values adopted in the calibration process were from the CVM HPE model. Rainfall recharge was imposed as a percentage of actual rainfall from the SILO Grid Point observations. Long-term average rainfall was used for the steady-state model. For the transient calibration model, quarterly averages of the historical rainfall data were used (2008 to 2020). For the prediction model, annual averages of 1990-2020 rainfall data was used.

The model included 7 recharge zones as listed below:

- Isaac River Flood Plain Alluvium
- Isaac River Channel Alluvium
- Alluvium – rest of the model
- Regolith
- Basalt
- Duaringa Formation
- Weathered Permian

An enhanced recharge of 100 % is applied to residual mine pit voids in the prediction model, where void lakes are not represented. No recharge is applied to constant head cells representing void lakes during recovery predictions. Recharge to mine spoil is set to 1 % of average annual rainfall (Mackie, C.D., 2009).

The calibrated recharge rates are discussed in **Section 2.9**. Overall, the recharge rates range from 0.1 to 2.3 mm/year.

2.4.4 Evapotranspiration

The MODFLOW Evapotranspiration (EVT) package was used to simulate evapotranspiration from the groundwater system.

Evapotranspiration Extinction depths were set to 2 m below ground across the model domain. The Evapotranspiration extinction depth parameter defines the maximum depth from which water can be extracted by vegetation through transpiration. Any water that is available below this depth is assumed to be unavailable to plants. Maximum potential rates were set using actual evapotranspiration values (from the Bureau of Meteorology), with the average value (600 mm/year) used as the transient calibration evapotranspiration rate. An EVT rate of 0 was assigned to the model cells representing the rivers.

2.4.5 Groundwater Use

Private groundwater pumping bores have not been included in the model due to lack of information regarding abstraction rates across the model domain. Due to generally low groundwater abstraction across the model area, it is likely that the bores have very localised drawdowns and will not significantly impact model results.

2.4.6 Mining

The MODFLOW Drain (DRN) package is used to simulate mine dewatering in the model for the SEMLP and surrounding mines. Boundary conditions for drain cells allow one-way flow of water out of the model. When the computed head drops below the stage elevation of the drain, the drain cells become inactive. This is an effective way of theoretically representing removal of water seeping into a mine over time, with the actual removal of water being via pumping and evaporation.

Longwall extraction at the SEMLP is represented as drain cells in model layer 18 (D Seam; lowermost coal seam in Moranbah Coal Measures) and the fractured zone extended above the H seam as will be discussed in **Section 2.4.6.2** below. The cover depth of overburden over SEMLP varies between 110 m and 470 m. The panel width and extraction height are 320m and 3.6m respectively.

The drain cells representing the surrounding mines are consistent with the CVM HPE version of the model. To simulate open cut mines in the model, drain cells are applied to all active layers from the surface to the base of the lowermost mined seam. Longwall extraction at Grosvenor Mine and Eagle Downs Mine are represented as drain cells in model layer 18 (D Seam; lowermost coal seam in Moranbah Coal Measures) and the fracture zone extended up to layer 10 consistent with the CVM HPE model.

2.4.6.1 Variation in Hydraulic Properties - Open Cut Mining

For open cut mining, Hawkins (1998) and Mackie (2009) indicate that spoil and waste rock are more permeable than the undisturbed strata. Completed open cut mining areas will be backfilled with waste overburden as the extraction proceeds. The model cell properties were updated to spoil properties guided by operational mine plans. The hydraulic properties were varied with time using the Time-variant materials (TVM) package of MODFLOW-USG Transport. Horizontal hydraulic conductivity of 0.3 m/day and vertical hydraulic conductivity of 0.1 m/day is applied to the spoil. The storage parameters used for the spoil were a specific yield of 0.1 and a storage coefficient of 1.0×10^{-5}.

2.4.6.2 Variation in Hydraulic Properties - Longwall Mining

As longwall mining progresses through the coal seam, the void left behind collapses (goaf) and fills with collapsed rock from the formations directly above the coal seam. There is a sag in the bedded formations above the goaf zone and the deformation causes generally vertical fractures to occur. These fractures can provide new flow paths for groundwater and alter the permeability of the strata overlying longwall mining areas. Therefore, they are included in the groundwater model using the TVM package.

Figure 2-5 provides the detail of fracturing applied in the groundwater model in the layers above the longwall panels. This is mainly derived from the subsidence report recently completed by Minserve (2022). Below are the major findings from the subsidence report (Minserve, 2022):

- When overburden thickness is less than 300m above the target D coal seam, the subsidence modelling results show continual volumetric strain and rock mass damage in the overburden strata extending from longwall edge to the surface. Shear cracks at the surface are predicted to form to a depth of 30m to 70m below the ground level.
- When the overburden thickness is more than 300m, the results indicate that the fractured zone extends to above 30m to 50m above the Harrow Creek seam (H Seam, layer 16 in the groundwater model). The overlying units will be undamaged rock mass. Longwall mining also induces shallow tension cracks, which are predicted to extend to a maximum depth of 15m below ground level.

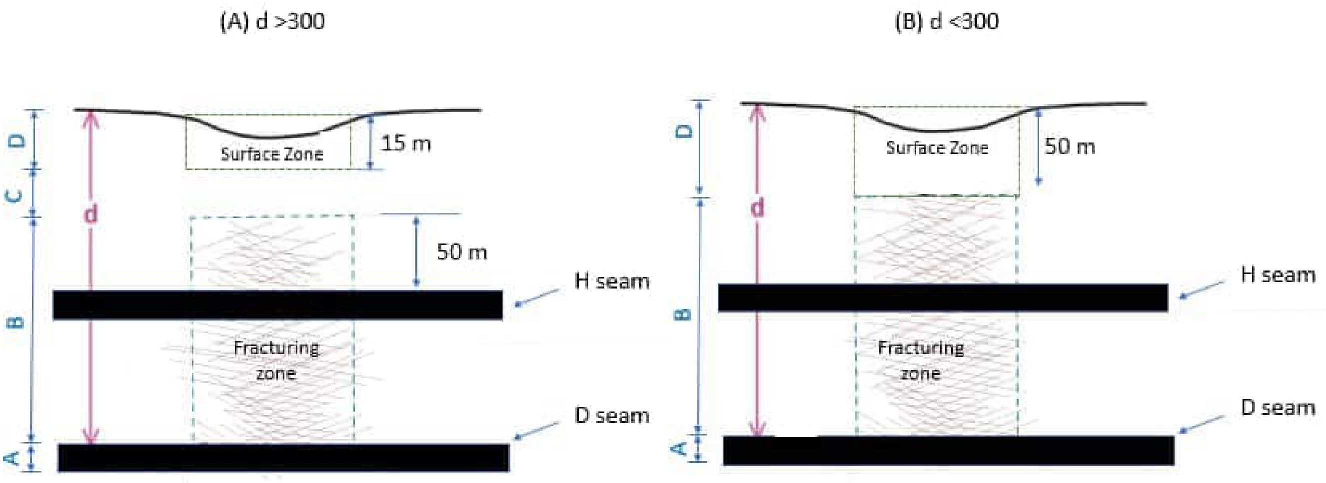

A = Mined zone, B = Fracture Zone, C = Constrained Zone, D = Surface cracking

Figure 2-5 Details of Fracture Zone

Based on the above subsidence findings, two different fracture zones were developed in the model; one for where the longwalls have an overburden thickness > 300m, and another where the longwalls have an overburden thickness < 300m. With respect to deeper longwalls (overburden thickness > 300 m), it was assumed that the fracture zone generally extends to 50m above the Harrow Creek seam (H Seam) and the surface cracking occurs up the depth of 15m. Over shallower longwalls (i.e., overburden thickness < 300m), the surface cracking extend to a depth of 50m. It was assumed here that the fracturing occurs above the longwall up to the surface cracking zone.

Table 2-4 shows the hydraulic parameter changes applied within the goaf induced fracture and surface shear crack zones. The values are the average numbers being used in the groundwater modelling to simulate the fracturing above the coal seam. In this study, it was assumed that any change to hydraulic and storage properties will be kept until the end of model predictive run, (i.e., there is no 'self-sealing of subsidence fracturing over time). This approach is considered to be conservative given that the overlying Tertiary sediments, particularly those at the surface zone, usually swell and self-seal over time, and therefore any surface cracks fill with sediments reducing their hydrological effect over time.

Table 2-4 Hydraulic Parameter Changes Within the Fracture Zone

Conceptual zone	Zone (refer Figure 2-5)	Change in the hydraulic properties
Surface Cracking	D	HK_host no change VK_host*10
Constrained Zone	C	No change
Fractured Zone	B	HK_host*3 VK_host*100
Mined Zone (Extracted seam)	A	HK 100 m/day VK 100 m/day Sy 0.16

2.4.6.3 Simulation of Incidental Mine Gas Extraction

Removal of gas from the Permian coal measures will be undertaken via pre-drainage wells as part of the SEMLP so that the underground mine workings are unhindered by seam gas emissions during extraction of the coal. Gas extraction ahead of mining also removes groundwater as associated water during the gas extraction process. AECOM (2019) adopted a conceptual gas extraction modelling developed by GeoGas (2016) for the SEMLP. For the groundwater model, the same approach was used to simulate the gas extraction. Based on GeoGas (2016), the underground layout was divided into five regions and the gas and associated water extraction were simulated from a number of pre-drainage wells. The mine gas extraction was assumed to be starting one year prior to underground mining and continued for a period of 8 years. Further details about the location of the wells and extraction volumes adopted in the model are provided in AECOM (2019).

Gas extraction from CSG operators is not simulated in the model.

2.5 Timing

A combined steady sate, transient warm-up and transient calibration model was developed, as follows:

- A steady state model with one stress period to simulate the water levels pre-mining
- A transient warm-up model with one 20-year stress period from January 1988 to December 2007)
- A transient calibration model with 56 quarterly stress periods from December 2007 to December 2021.

The first stress period of the model was steady-state and did not include any mining. The transient warm-up model was built to incorporate pre-2008 mining activities and their impacts on groundwater levels around the SEMLP. The warm-up model provided appropriate starting conditions for the calibration model (i.e., starting heads and hydraulic properties). Together, the steady state, warm-up and transient calibrations comprise 58 stress periods.

A summary of the calibration validation model stress periods and simulated active mine timings is shown in **Appendix D**. The first stress period of the warm-up model was steady-state and did not include any mining. This was to simulate the pre-mining conditions within the model domain.

A transient predictive model was then developed from the end of the transient calibration model from January 2022 to January 2044. The recovery model will then start from January 2044 to January 4044 for 2000 years.

To assist the model in overcoming the numerical difficulties, MODFLOW-USG Adaptive Time-Stepping (ATS) option was used. The ATS option of MODFLOW automatically decreases time-step size when the simulation becomes numerically difficult and increases it when the difficulty passes. The minimum time step size used in the simulations was 1 day.

2.6 Calibration

2.6.1 Calibration Method

The previous version of the model (CVM HPE) was calibrated using PEST++ and, upon review of model calibration statistics after the updates for SEMLP, was considered still reasonably calibrated. Therefore, the calibration methodology adopted for the SEMLP model involved running the model numerous times using different parameter sets and investigating which model produce the best calibration statistics. In doing so, the previously calibrated parameter set from the CVM HPE model was used as a starting point to establish 550 realisations of the SEMLP model, and the model was run using those 550 realisations. A full description of the parameter distribution across the 550 realisations is provided in **Section 6**.

After running the 550 calibration realisations, the calibration statistics were then calculated for each realisation and the realisation that produced the lowest Scaled Root Mean Square error (SRMS) was considered to be the best calibrated model for the purposes of the SEMLP. The calibration results described in this report section are from this particular realisation with the lowest SRMS error. The remaining 549 realisations were then used to quantify the model uncertainty with respect to simulated heads and predictive variables as discussed in **Section 6**.

2.6.2 Groundwater Levels

The groundwater levels recorded between January 2008 to December 2021 were used for the calculation of SRMS. In all, 3449 target heads were established for 281 bores from the following sites:

- SRM/SEMLP: included 34 groundwater level observation sites and VWPs
- Lake Vermont: included 30 groundwater level observations sites and VWPs
- Winchester South: 16 bores including 2 VWPs
- Olive Downs Project: included 38 groundwater level observations sites and VWPs
- Peak Downs Mine: included 6 bores
- Caval Ridge Mine: comprised 33 bores including VWPs
- Other sites: 124 other bores, including available data from Moorvale South Mine, Millennium Mine, Lake Vermont Meadowbrook Mine, Eagle Downs Mine, Poitrel Mine, Daunia Mine, Moranbah South Mine and some Queensland Globe bore monitoring observations.

Groundwater targets were selected where:

- Valid information on bore construction or geology information was available for the site
- Targets were manually reviewed to ensure the measurements were realistic.

During calibration, each groundwater bore was assigned a weight of 1, and the weight for each observed water level was calculated by dividing 1 by the number of groundwater levels recorded at each bore. Details on each of the observation points and their residuals are presented in **Appendix A** of this report. The locations of these bores are shown in **Figure 2-9**.

The hydraulic properties (i.e., horizontal, vertical conductivity, specific yield, and specific storage) and recharge rates were adjusted during the calibration to provide best match between the groundwater level measurements and model simulated heads.

2.6.3 Calibration Statistics

The overall transient calibration statistics are presented in **Table 2-5** for the best calibrated model**.** One of the industry standard methods to evaluate the calibration of the model is to examine the statistical parameters associated with the calibration. This is done by assessing the error between the modelled and observed (measured) water levels in terms of the root mean square (RMS). A RMS is expressed as:

$$\mathrm{RMS} = \left[1/n \sum (h_o - h_m)_i^{\,2} \right]^{0.5}$$

where: n = number of measurements

ho = observed water level

hm = simulated water level

RMS is considered to be the best measure of error if errors are normally distributed. The RMS error calculated for the calibrated model is 8.9 m.

The acceptable value for the calibration criterion depends on the magnitude of the change in heads over the model domain. If the ratio of the RMS error to the total head change in the system is small, the errors are considered small in relation to the overall model response(s). The total measured head change across the model domain is 156 m; therefore, the ratio of RMS to the total head change (i.e., scaled root mean square, SRMS) is 5.9 %. While there is no recommended universal SRMS error, the Australian Groundwater Modelling Guidelines suggests that setting SRMS targets such as 5 or 10 % may be appropriate in some circumstances (Barnett et al, 2012).

Table 2-5 Calibration Statistics – Best Calibrated Model

Statistic	Value
Sum of Squares (m^2)	275362.7
Mean of Squares (m)	79.8
Square Root of Mean of Squares (RMS) (m)	8.9
Scaled Root Mean Square (SRMS) (%)	**5.9**
Sum of Residuals (m)	23025.2
Mean Residual (m)	6.7
Scaled Mean Residual (%)	4.4
Coefficient of Determination (tend to unity)	1.2
Targets within ±2m (% of total)	740 (21%)
Targets within ±5m (% of total)	1728 (50%)
Targets within ±20m (% of total)	3327(96%)

Figure 2-6 presents the observed and simulated groundwater levels graphically as a scattergram for the historic transient calibration (2008 to 2022).

Figure 2-7 shows the observed and simulated groundwater levels graphically only for the SRM/SEMLP bores. The RMS for the SRM/SEMLP bores is 8.4 m, which is lower than the RMS for the entire model (8.9 m) indicating slightly better local calibration performance.

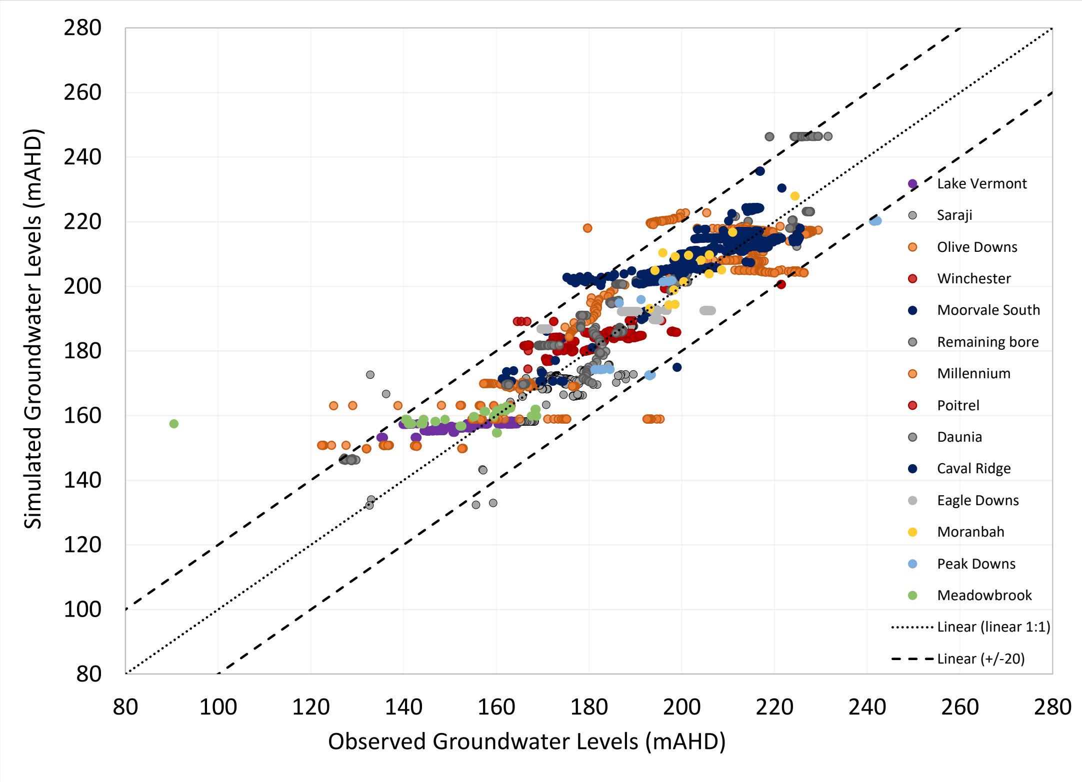

Figure 2-6 Calibration Scattergram – Modelled vs Observed Groundwater Levels (All Bores)

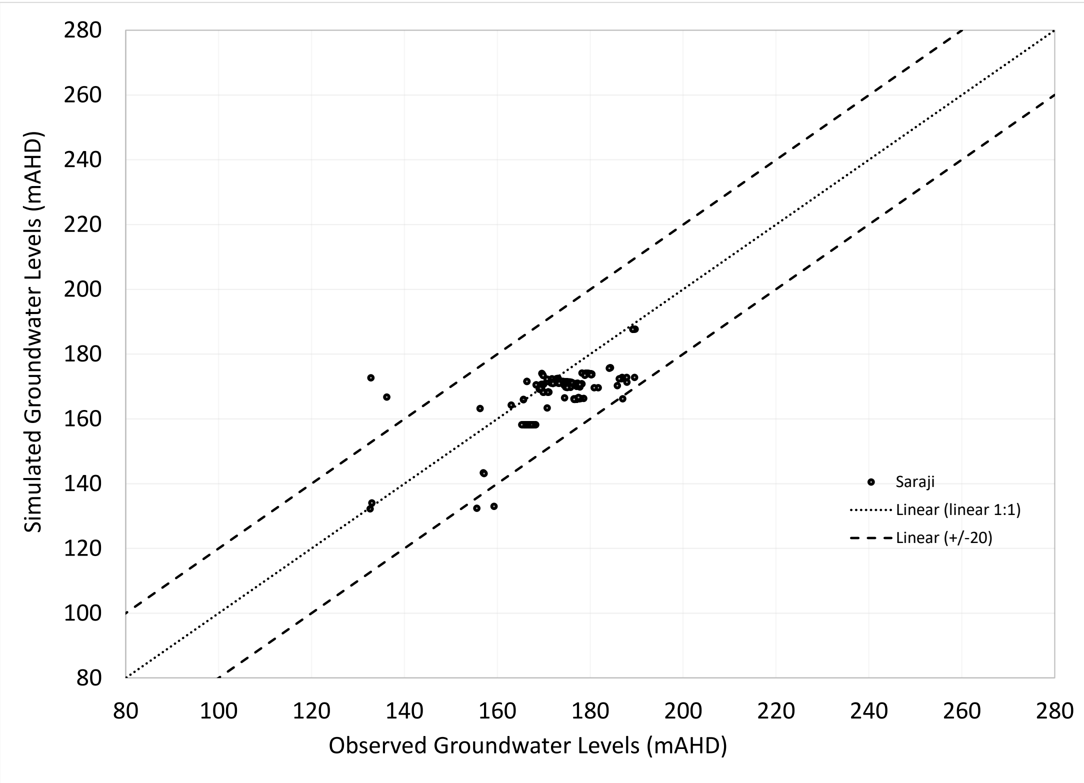

Figure 2-7 Calibration Scattergram – Modelled vs Observed Groundwater Levels (SEMLP Bores)

Figure 2-8 shows the distribution of calibration residuals for the entire model. As shown in the figure the calibration residuals in majority of the calibration data points are within ± 20 m. **Figure 2-8** indicates that in general the model tends to slightly over predict groundwater levels, but **Figure 2-7** suggests a tendency to local underprediction.

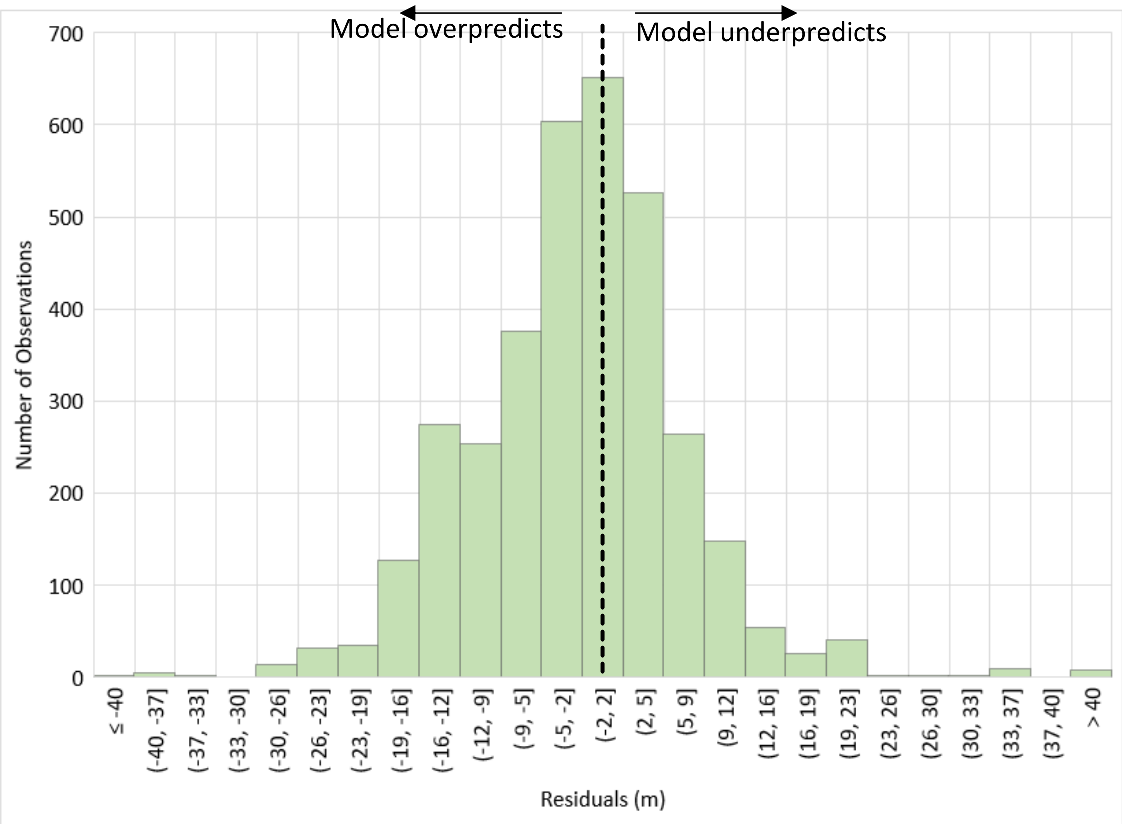

Figure 2-8 Calibration Residual Histogram Scattergram

Table 2-6 shows the average calibration residual and absolute average residual per model layer. The residual is the difference between the measured and the modelled water level at each bore. A negative residual represents an over estimation of water levels, while a positive residual represents an underestimate. **Table 2-6** shows an overall overestimation of water levels in the model layers across the model domain. The table shows layer 3 has the highest absolute average residual and layer 15 has the highest average residual. The table also show overall the simulated groundwater levels are closer to the observed groundwater levels in the model layers representing the Moranbah Coal Measures (layers 12 to 18), excluding layer 15 which has a small number of observation bores (5).

Table 2-7 shows the average calibration residual and absolute average residual per each site within the model domain. As indicated in the table, there is an average overestimation of 6.7 m in the bores. The table shows the PDM bores have the highest average absolute residuals.

Table 2-6 Average Residual by Model Layer

Model Layer	Formation	Unit	Average Residual (m)	Average Absolute Residual (m)	Number of Observation Targets	Number of bores
1	Alluvium, colluvium, Tertiary basalt	Surface cover	-5.1	5.8	212	18
2	Tertiary sediments, Tertiary basalt	Tertiary and minor Triassic Clematis, weathered Permian, Tertiary basalt	2.3	6.3	910	93
3	Rewan Group	Triassic	-6.0	17.6	153	15
4	Rangal Coal Measures	Leichhardt overburden	-4.6	6.8	251	10
5		Leichhardt seam	-2.3	7.0	358	28
6		Interburden	-7.2	9.2	123	6
7		Vermont seam	-7.4	9.3	259	23
8		Vermont underburden	-7.2	7.8	175	5
9	Fort Cooper Coal Measures	Fort Cooper overburden	1.3	3.8	338	23
10		Fort Cooper seams (combined)	2.9	9.3	90	10
11		Fort Cooper underburden	6.8	7.3	29	4
12	Moranbah Cooper Coal Measures	Q Seam	0.0	2.6	117	3
13		Interburden	-2.1	4.5	39	2
14		P Seam	-2.5	6.0	99	6
15		Interburden	-10.4	10.4	66	5
16		H Seam	-3.7	6.0	85	14
17		Interburden	-5.6	9.5	7	3
18		D Seam	-4.7	6.5	138	14
19*		Interburden	-	-	-	-

*There are no observation bores in Layer 19

Table 2-7 Average Residual by Project

Site	Average Residual (m)	Average Absolute Residual (m)	Number of Observation Targets	Number of Bores
Lake Vermont	-0.8	9.3	353	31
Saraji \ SEMLP	6.1	7.0	237	35
Caval Ridge	-3.2	5.6	599	33
Olive Downs South	-4.0	9.2	212	38
Winchester South	-2.9	5.1	488	16
Other Monitoring Bores	-3.9	8.6	232	27
Moorvale South	-5.7	6.6	21	13
Millennium	0.7	9.4	297	12
Poitrel	-2.8	5.3	324	11
Daunia	-6.6	7.1	333	9
Eagle Downs	-0.9	6.7	220	6
Moranbah	-3.3	5.1	15	15
Peak Downs	11.4	14.1	41	6
Lake Vermont Meadowbrook	-3.2	5.7	77	30

The spatial distribution of average residuals for each bore from the transient calibration is shown in **Figure 2-9**.

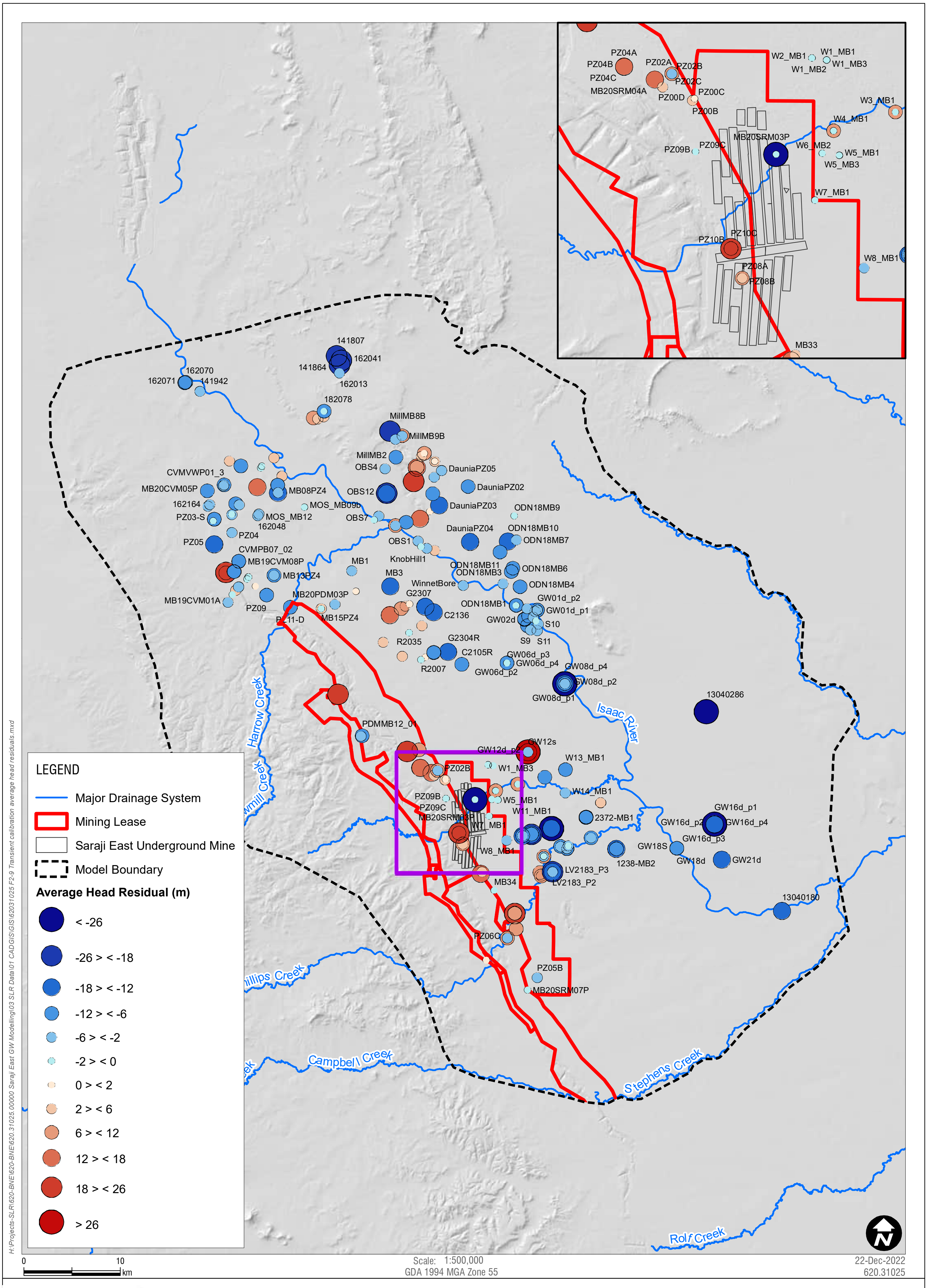

Transient Calibration Validation
Average Head Residuals (m)

FIGURE 2-9

2.6.4 Calibration Fit

This section provides discussion on the modelled to observed groundwater level trends (calibration hydrographs) for key bores across the SRM and SEMLP site. Calibration hydrographs for the full calibration dataset is presented as **Appendix B**.

2.6.4.1 Alluvium and Tertiary

It should be noted here that there are no bores screened in Alluvium within the SEMLP area. In order to show how the model simulates water level within alluvium, two Isaac alluvium bores were selected and shown in **Figure 2-10**. The two bores are GW08S and Knob Hill 2 close to Olive Downs and Winchester South mines respectively. As the graph indicate there is a good match between the observation and simulation and the model is able to simulate to some extent the water level fluctuations due to climatic variation.

Figure 2-10 also presents the fit between simulated and observed heads in the four bores (W2_MB1, W3_MB2, PZ00C and PZ00B) within the Tertiary sediments. The hydrograph for bores W2_MB1 and W3_MB2 located 4km northeast of the SEMLP (Figure 2-9) shows a very close match between simulated and measured groundwater levels.

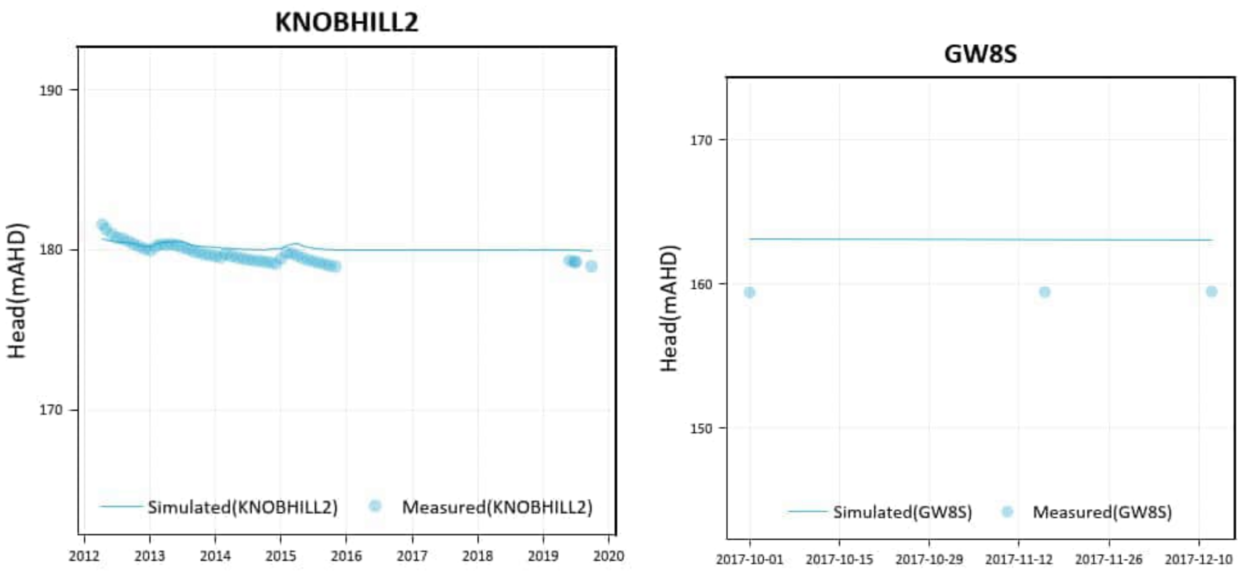

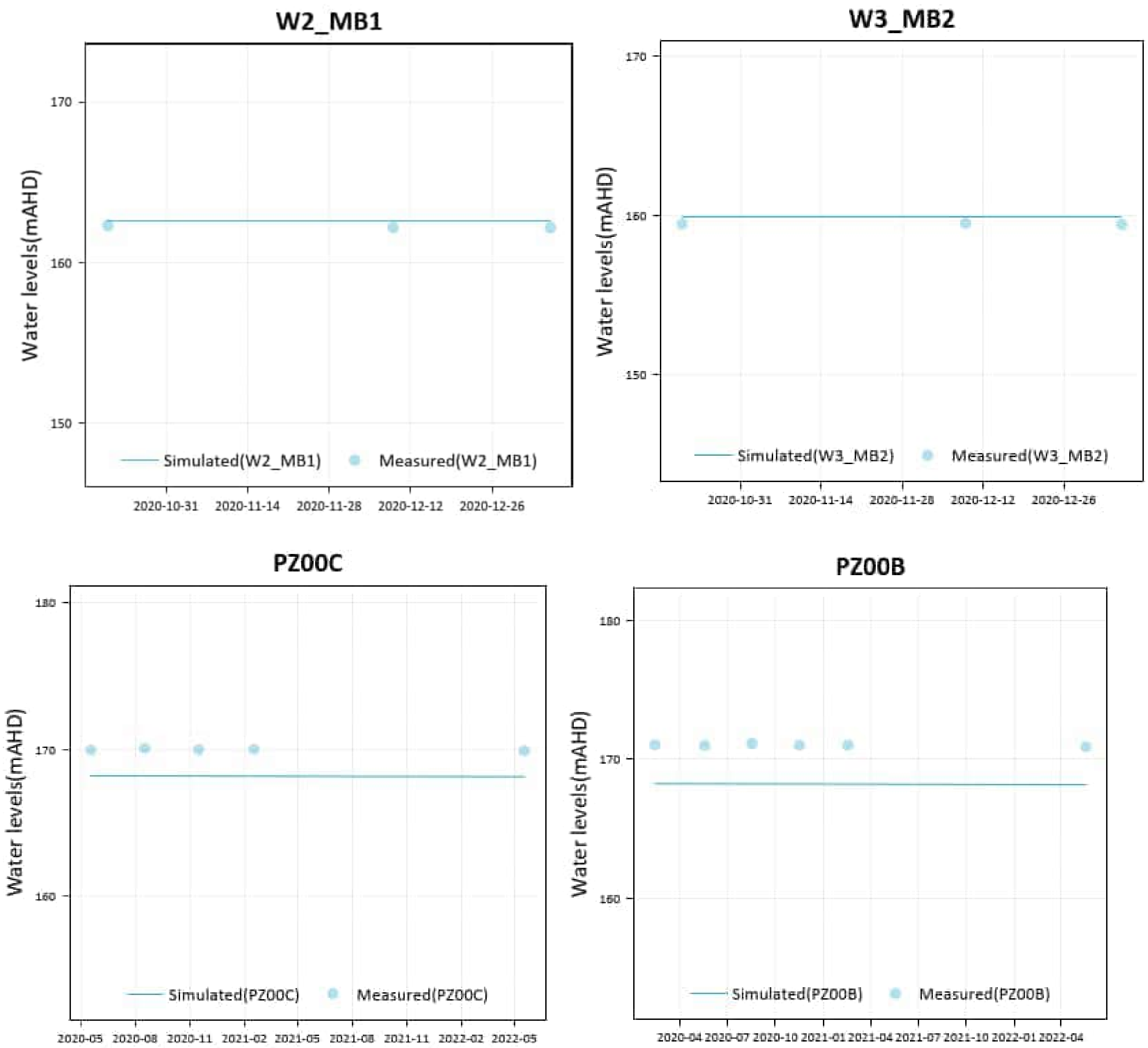

Figure 2-10 Calibration Fit - Alluvium Bores

The hydrograph for PZ00C and PZ00B located 1.5 Km northwest of the SEMLP shows the model slightly under predicts the groundwater levels at these bores by around 4.0 m. As shown in the hydrographs in **Appendix B**, regionally there is a good match between the simulated and measured groundwater levels in alluvial bores such as Olive Downs S series, Winchester South ODN series, Knob Hill 1 and Knob Hill 2.

2.6.4.2 Permian Coal Measures

The bores screened in the Permian Coal Measures within SEMLP have not been subject to monitoring for a significant period of time. Consequently, there is a restricted availability of water level information for Permian Coal Measures within the SEMLP area.

Figure 2-11 shows the water levels in the Permian Coal Measures, specifically in the D, Q, P, and H seams. Given the lack of water level data in SEMLP and in order to demonstrate the impact of mining on water levels within the Permian Coal Measures, two bores (i.e., PZ01 and PZ07D) bores were chosen from the Caval Ridge mine (CVM) mine and shown in **Figure 2-11**. The simulation results indicate that PZ01 successfully reproduces the water level decline attributable to CVM mining activities. PZ01 is located 25 km Northwest of SEMLP. Furthermore, PZ07D demonstrates that the model can replicate the minor water level decrease following 2016. PZ07D is located 20 km Northwest of SEMLP. The other bore is MB34 which is located 3 km South of SEMLP. The modelling results indicate the model can simulate the gradual decline observed in water level between 2016 and 2022.

2.6.4.3 Other Bores

Figure 2-12 shows the hydrographs for other site monitoring bores including the basalt and regolith bores. The hydrographs shows that the model results in a reasonable (± 10 m) fit between modelled and observed groundwater levels (PZ06-S, Pz12-S, R2008 and OBS10).

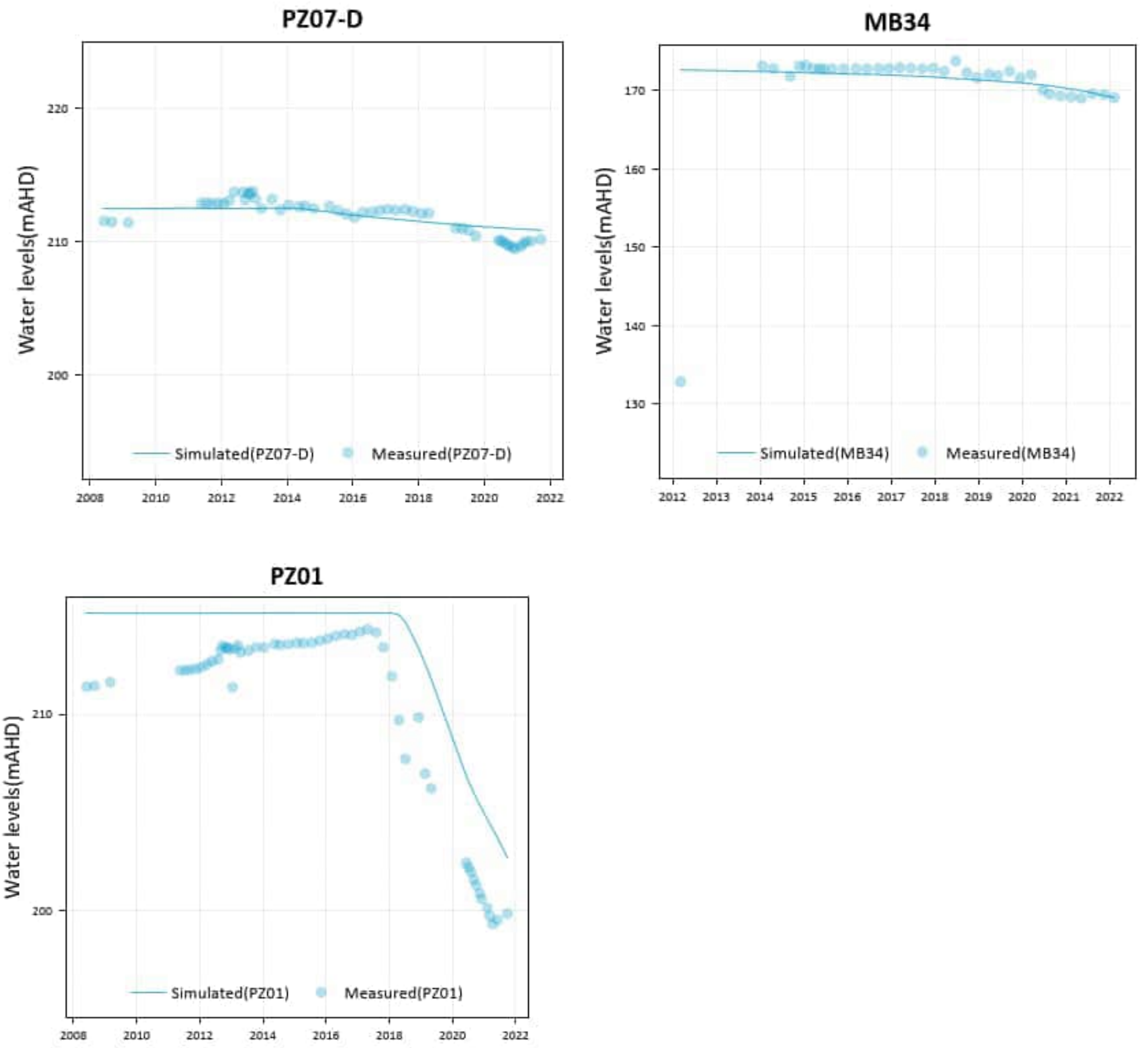

Figure 2-11 Calibration Fit - Permian Bores (D,Q, P and H seams)

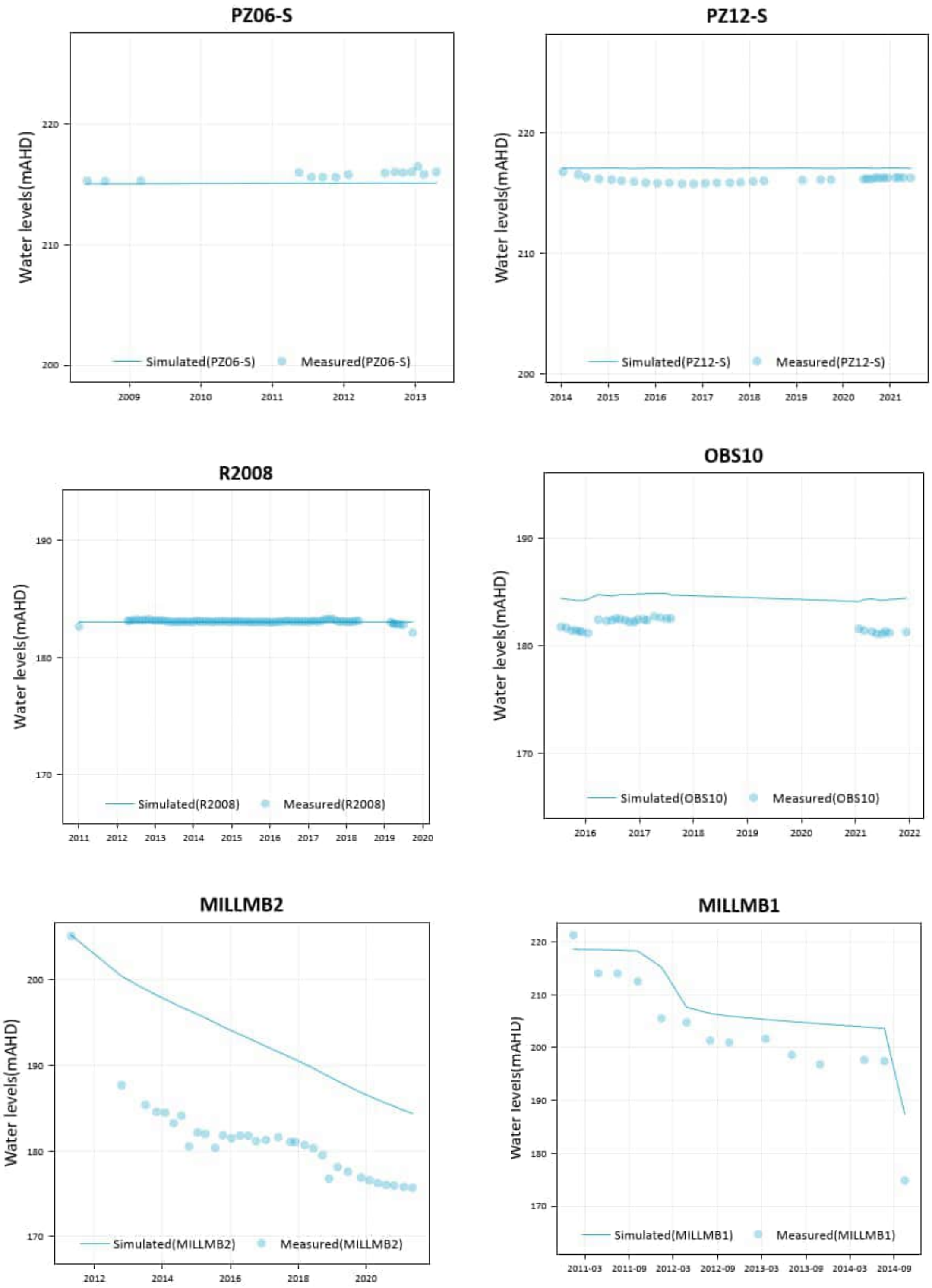

Figure 2-12 Calibration Fit - Other Bores

2.6.5 Model Water Balance

2.6.5.1 Steady State Calibration

The water balance for the steady state model calibration is shown in **Table 2-8**. The water balance for the steady-state model indicates that recharge was the largest net inflow contributor to the steady state model (4.2 ML/d). Regional groundwater inflow and outflow are 2.2 and 0.2 ML/d respectively, indicating that groundwater enters the model domain through this boundary.

A net outflow of 2.3 ML/d from the steady state model occurs due to baseflow seepage to the Isaac River (i.e. surface water and groundwater interaction in the Isaac River). Other factors that contribute to outflow from the groundwater system are evapotranspiration (3.1 ML/d outflow) and baseflow seepage to minor drainage systems (0.8 ML/d outflow). The mass balance error for the steady state calibration is 0.00 %, within the error threshold recommended by the Australian Groundwater Modelling Guidelines (Barnett et al., 2012), and indicating the model is stable and achieves an accurate numerical solution.

Table 2-8 Steady-State Model Water Balance

Component	Inflow (ML/d)	Percent of Total Inflow (%)	Outflow (ML/d)	Percent of Total Inflow (%)
Recharge (RCH)	4.20	29.91	0.00	0.00
ET (from GW) (EVT)	0.00	0.00	3.09	22.03
SW-GW Interaction Isaac River (RIV)	7.63	-54.37	9.97	71.06
SW-GW Interaction other rivers (RIV)*	0.00	0.00	0.76	5.40
Regional GW Flow (GHB)	2.21	15.72	0.21	1.51
Mines (DRN)	0.00	0.00	0.00	0.00
Storage	0.00	0.00	0.00	0.00
Total	14.03	100.00	14.03	100.00

* The other tributaries or drainage lines in the model are set as drains to the groundwater system and do not result in any recharge.

2.6.5.2 Transient Calibration

The model water balance for the transient simulation averaged over the duration of the calibration period is presented in **Table 2-9**. The mass balance error, that is the difference between calculated model inflows and outflows at the completion of the transient calibration, was 0.00 %, which indicates the model is stable and achieves an accurate numerical solution. **Table 2-9** shows 3.1 ML/d is lost to evapotranspiration in areas where the water table is within 2 m of the land surface. In total 11.4 ML/d is discharged via surface drainages, with the vast majority of that attributed to the Isaac River. A net flow loss of approximately 2.5 ML/d occurs to the Isaac River (reach within the model domain) indicates a net gaining condition in the river in the calibration period.

Table 2-9 Transient Model Water Balance

Component	Inflow (ML/d)	Percent of Total Inflow (%)	Outflow (ML/d)	Percent of Total Inflow (%)
Recharge (RCH)	4.68	18.17	0.00	0.00
ET (from GW) (EVT)	0.00	0.00	3.11	12.07
SW-GW Interaction Isaac River (RIV)	8.18	31.74	10.71	41.56
SW-GW Interaction other rivers (RIV)*	0.00	0.00	0.74	2.88
Regional GW Flow (GHB)	2.26	8.76	0.22	0.86
Mines (DRN)	0.00	0.00	6.32	24.55
Storage	10.65	41.33	4.66	18.08
Total	25.76	100.00	25.76	100.00

* The other tributaries or drainage lines in the model are set as drains to the groundwater system and do not result in any recharge.

Other rivers contribute to a loss of approximately 0.7 ML/d from the groundwater system over the transient calibration with no inflow component. The fluxes from the GHB component (inflow and outflow) are 2.3 and 0.2 ML/d respectively. The GHB net inflow is less than 5 % of the total inflow, and the GHB net outflow is less than 1 % of the total outflow. This indicates that a small volume of water enters the model domain through this boundary and therefore, this boundary condition does not have a significant influence on the model predictions.

6.3 ML/d is removed from the model by the Drain boundary condition that represents historical mining (1988-2022) in the model. The average simulated historical ingress for major active mines active during the calibration period are:

- SRM – 1.3 ML/d
- PDM – 1.6 ML/d
- CVM – 0.6 ML/d
- Daunia – 0.3 ML/d
- Poitrel – 0.3 ML/d
- Millennium – 0.6 ML/d
- Lake Vermont – 0.6 ML/d

2.7 Calibrated Hydraulic Parameters

Table 2-10 provides a summary of the model layer parameter values for horizontal and vertical hydraulic conductivity in the best calibrated model. The hydraulic parameter zones in all the model layers are presented in **Appendix C**.

Table 2-10 Hydraulic Conductivity – Best Calibrated Model

Model Layer	Formation	Unit	Horizontal Hydraulic Conductivity (m/day)	Anisotropy Kv/Kx
1	Isaac River Alluvium **	Surface cover	54	0.28
1	Regolith	Surface cover	4.6	0.04
1	Weathered Permian	Surface cover	0.35	0.4
1	Duaringa Formation	Surface cover	1.8	0.4
1 & 2	Tertiary Basalt	Tertiary basalt	2.7	0.1
2	Regolith	Surface cover	0.35	0.2
3	Rewan Group	Triassic	4.8×10^{-3}	0.5
4	Rangal Coal Measures	Leichhardt overburden	5.0×10^{-5} to 8.5×10^{-3}	0.1
5		Leichhardt seam	1.0×10^{-4} to 1.0×10^{-1}	0.15
6		Interburden	5.0×10^{-5} to 8.9×10^{-4}	0.002
7		Vermont seam	1.0×10^{-4} to 1.9×10^{-2}	0.5
8		Vermont underburden	5.0×10^{-5} to 7.6×10^{-3}	0.03
9	Fort Cooper Coal Measures	Fort Cooper overburden	5.0×10^{-5} to 6.3×10^{-3}	0.001
10		Fort Cooper seam	1.0×10^{-4} to 3.5×10^{-3}	0.5
11		Fort Cooper underburden	5.0×10^{-5} to 3.5×10^{-3}	0.2
12	Moranbah Coal Measures	Q Seam	1.0×10^{-4} to 5.9×10^{-2}	0.003
13		Interburden	5.0×10^{-5} to 1.0×10^{-2}	0.06
14		P Seam	1.0×10^{-4} to 1.0×10^{-1}	1
15		Interburden	5.0×10^{-5} to 1.0×10^{-2}	0.5
16		H Seam	1.0×10^{-4} to 7.4×10^{-2}	0.01
17		Interburden	25.0×10^{-5} to 1.0×10^{-3}	0.2
18		D Seam	1.0×10^{-4} to 4.9×10^{-2}	0.2
19		Interburden	5.0×10^{-5} to 6.6×10^{-5}	0.001

**Further explanation is provided in Section 6.1 for the horizontal hydraulic conductivity of Alluvium.

The hydraulic conductivity of the Permian interburden material in the Rangal Coal Measures, Fort Cooper Coal Measures and Moranbah Coal Measures reduces with depth to reflect field observations. As the decrease of Kx within the interburden rock units is driven by an increase in overburden pressure, the relationship between Kx and depth is different from that of coal seams. The hydraulic conductivity for the interburden material is capped at a minimum of 5.0×10^{-5} m/day and the hydraulic conductivity of the coal seams is capped at a minimum of 1.0×10^{-4} m/day.

The hydraulic conductivity of the interburden/overburden and coal seam layers decreases with depth according to Equations 1, 2 (exponential) and Equation 3 (power). Equations 1 and 2 were adopted from the Winchester South Project groundwater model. Equations 3 was suggested by AGE (2016) for the interburden units within the Moranbah Coal Measures based upon recent studies in the area. With regards to the faults, an exponential equation (Equation 4) was used to replicate changes in hydraulic conductivities of fault at depth.

Coal:	$HC = HC_0 \times e(-0.015 \times depth)$	(Eq. 1)
Interburden (RCM and FCCM):	$HC = HC_0 \times e(-0.018 \times depth)$	(Eq. 2)
Interburden (MCM):	$HC = HC_0 \times -2.1^{depth}$	(Eq. 3)
Fault:	$HC = HC_0 \times e(-0.018 \times depth)$	(Eq. 4)

Where:

- HC is horizontal hydraulic conductivity at specific depth
- HC_0 is horizontal hydraulic conductivity at depth of 0 m (intercept of the curve)
- Depth is depth of the floor of the layer (thickness of the cover material)
- Slope is a term representing slope of the formula (steepness of the curve).

HC_0 was estimated in the calibration. It varies for the coal seams and for the interburden and overburden units in the model. The slope function and coefficient of the coal and interburden depth dependence equations were not calibrated. The Kx vs depth relationships for the interburden/overburden are presented in **Figure 2-13**, while the calibrated relationships for coal units are presented in **Figure 2-14**. The figures present the Olive Downs site data (2018), Winchester South site data, Lake Vermont North site data and Coffey (2014) Bowen Basin data. The AGE (2016) and the hydraulic conductivity measurements in the Moranbah Coal Measures are also shown in the figures.

Figure 2-14 presents the lower and upper range for coal horizontal conductivity against depth relationship in Moranbah Coal Measures estimated during the calibration. **Figure 2-14** also shows the coal horizontal conductivity against depth relationship for the Leichhardt and the Vermont Seam of the Rangal Coal Measures.

Figure 2-15 illustrates the range in horizontal hydraulic conductivity obtained from site testing and publicly available data. The data are focused on the key site units, being the alluvium, regolith, Rewan Group and the coal and interburden sequences of the Rangal and Moranbah Coal Measures. The data are compared to the horizontal hydraulic conductivity values used in the model. A depth dependence equation for the coal measures was used in the numerical groundwater model and therefore the calibrated hydraulic conductivity values vary across the model domain. As shown in **Figure 2-15**, the modelled horizontal hydraulic conductivity values are all within the range of field data.

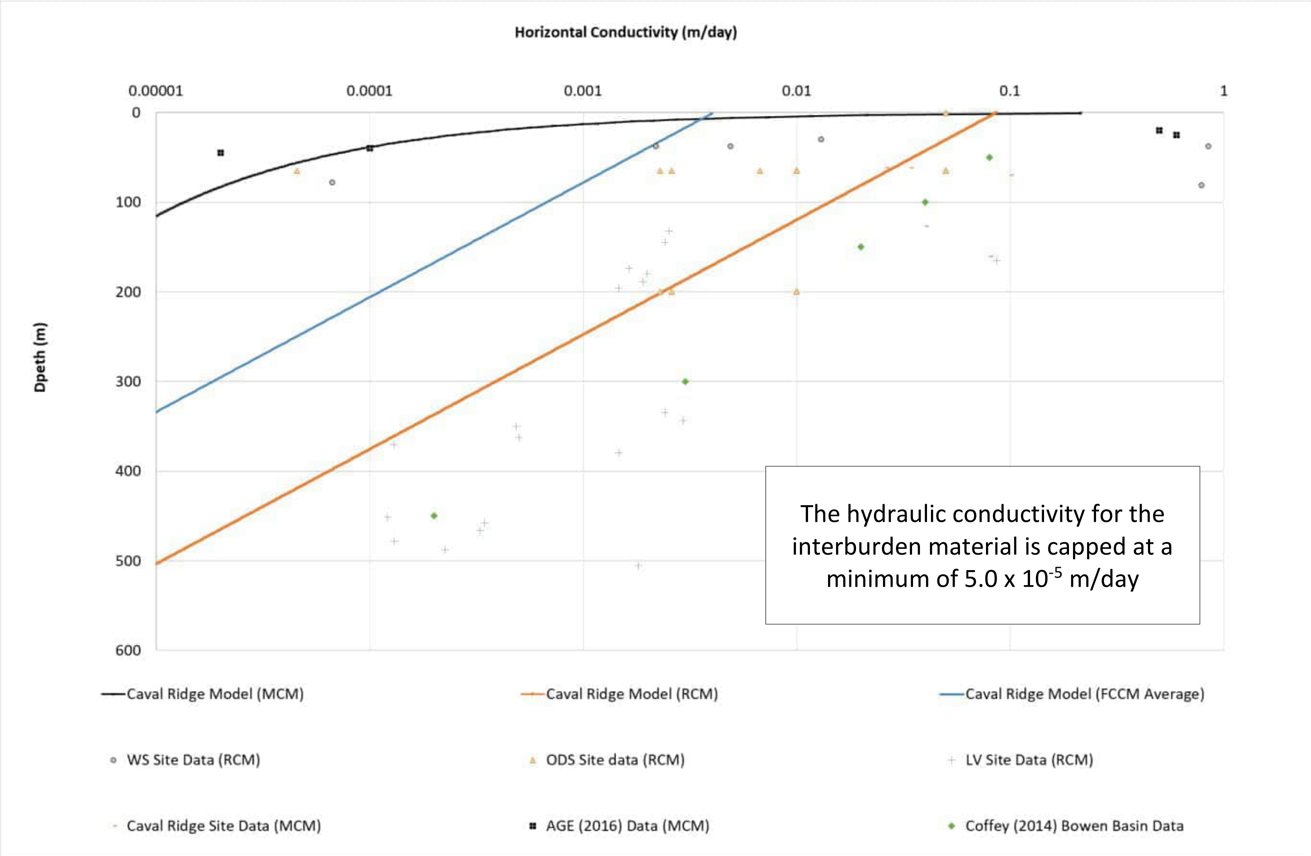

Figure 2-13 Hydraulic Conductivity vs Depth – Interburden/Overburden

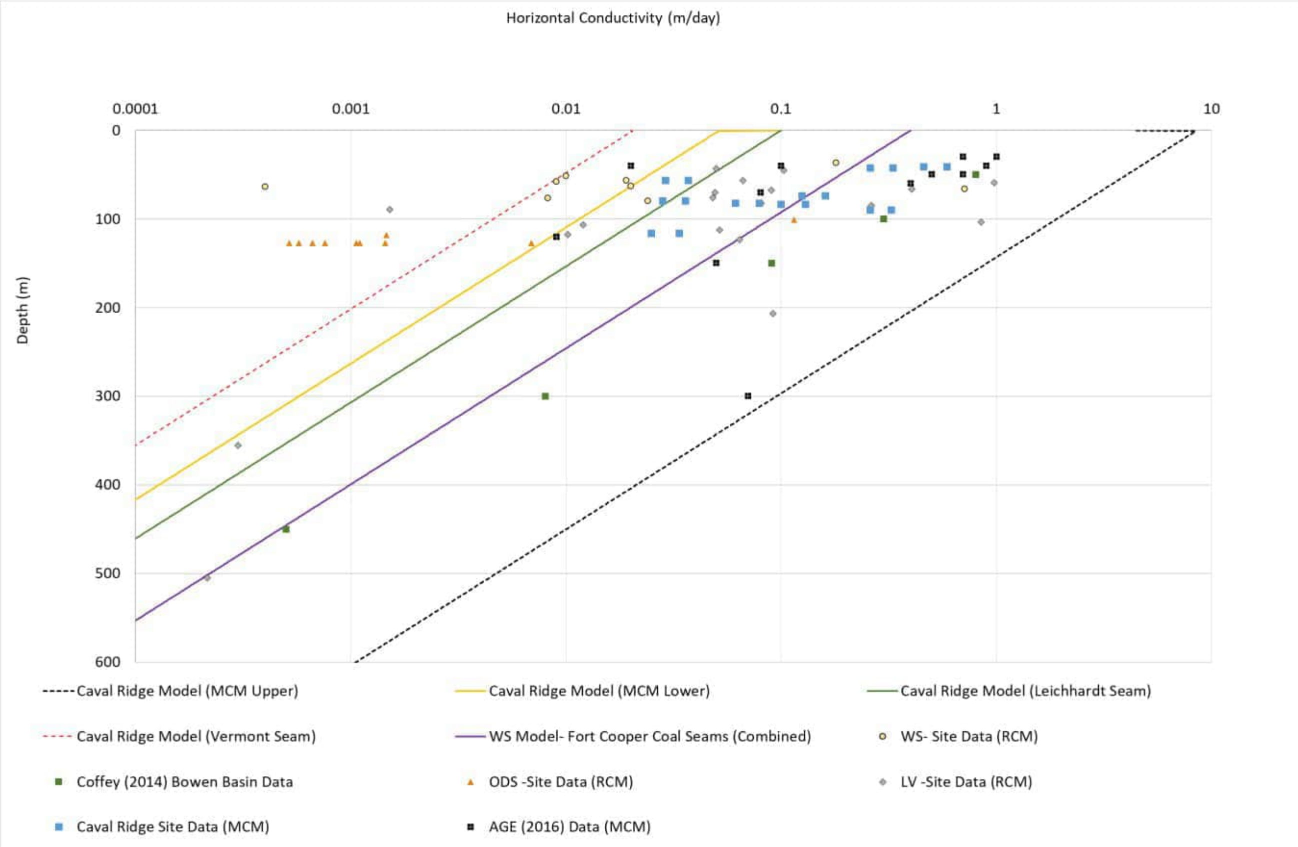

Figure 2-14 Hydraulic Conductivity vs Depth – Coal

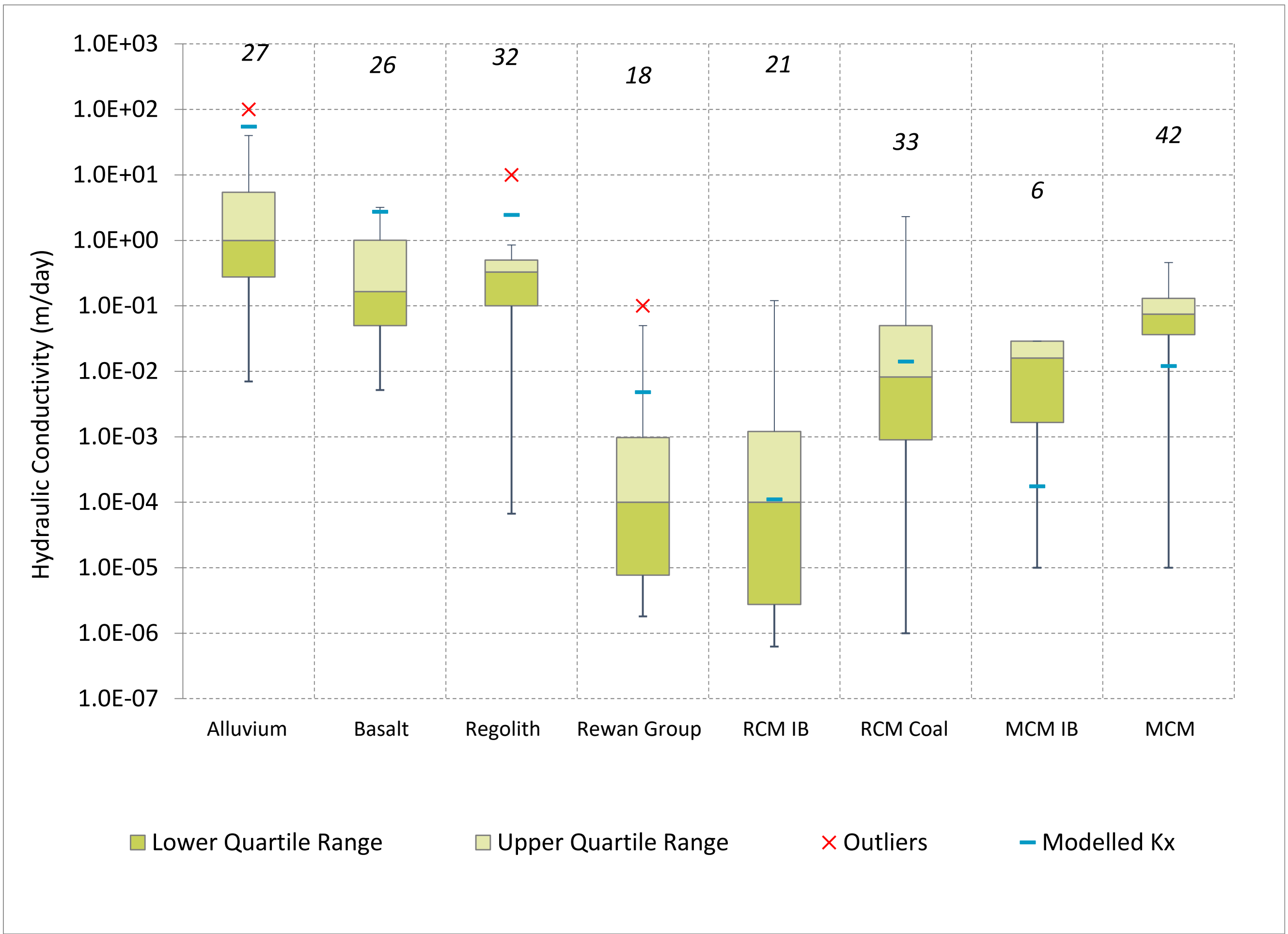

Figure 2-15 Hydraulic Parameters Estimates vs Best Calibrated Hydraulic Parameters

In order to show how the hydraulic conductivities changes at depth within the faults, the hydraulic parameters within faults were calculated for each layer and shown in **Table 2-11**.

Table 2-11 Hydraulic Conductivity of Faults – Best Calibrated Model

Model Layer	Formation	Unit	Average Horizontal Hydraulic Conductivity (m/day)	Anisotropy Kv/Kx
3	Rewan Group		9.8×10^{-3}	0.35
4	Rangal Coal Measures	Leichhardt overburden	9.1×10^{-3}	0.34
5		Leichhardt seam	9.0×10^{-3}	0.32
6		Interburden	8.5×10^{-3}	0.30
7		Vermont seam	8.0×10^{-3}	0.29
8		Vermont underburden	7.7×10^{-3}	0.27
9	Fort Cooper Coal Measures	Fort Cooper overburden	7.3×10^{-3}	0.35
10		Fort Cooper seam	6.3×10^{-3}	0.18
11		Fort Cooper underburden	4.9×10^{-3}	0.12
12	Moranbah Coal Measures	Q Seam	4.3×10^{-3}	0.17
13		Interburden	4.1×10^{-3}	0.19
14		P Seam	3.8×10^{-3}	0.19
15		Interburden	3.7×10^{-3}	0.23
16		H Seam	3.3×10^{-3}	0.21
17		Interburden	3.0×10^{-3}	0.22
18		D Seam	2.6×10^{-3}	0.21
19		Interburden	1.9×10^{-3}	0.18

2.8 Calibrated Storage Properties

Table 2-12 summarises the calibrated values of specific storage and specific yield for the hydrostratigraphic units.

Table 2-12 Calibrated Storage Parameters – Best Calibrated Model

Model Layer	Formation	Unit	Specific Yield Sy (%)	Specific Storage Ss (m^{-1})
1	Alluvium	Surface cover	4.2	1.0×10^{-5}
1	Regolith	Surface cover	3.6	5.5×10^{-6}
1	Weathered Permian	Surface cover	1.0	1.0×10^{-6}
1	Duaringa Formation	Surface cover	2.1	1.0×10^{-6}
1 & 2	Tertiary Basalt	Tertiary basalt	3.4	1.2×10^{-6}

Model Layer	Formation	Unit	Specific Yield Sy (%)	Specific Storage Ss (m^{-1})
2	Regolith	Surface cover	2.8	1.0×10^{-6}
3	Rewan Group	Triassic	4.2	7.0×10^{-7}
4	Rangal Coal Measures	Leichhardt overburden	2.8	4.7×10^{-6}
5		Leichhardt Seam	0.8	9.0×10^{-7}
6		Interburden	0.1	7.0×10^{-7}
7		Vermont Seam	0.2	3.1×10^{-6}
8		Vermont underburden	0.2	1.6×10^{-6}
9	Fort Cooper Coal Measures	Fort Cooper overburden	0.1	7.0×10^{-7}
10		Fort Cooper seam	0.5	3.2×10^{-6}
11		Fort Cooper underburden	0.6	1.9×10^{-6}
12	Moranbah Coal Measures	Q Seam	0.1	4.8×10^{-6}
13		Interburden	0.4	1.7×10^{-6}
14		P Seam	0.1	9.0×10^{-6}
15		Interburden	0.13	1.4×10^{-6}
16		H Seam	0.1	9.0×10^{-6}
17		Interburden	0.32	3.4×10^{-6}
18		D Seam	0.1	9.7×10^{-6}
19		Interburden	0.39	3.5×10^{-6}
	Fault		0.2 to 3.9	7.0×10^{-7} to 6.3×10^{-6}
	Spoil		5	1.0×10^{-5}

2.9 Calibrated Recharge

Table 2-13 presents the calibrated recharge rates for each geological unit in the model. These calibrated recharge rates have been adopted into the predictive model. The recharge zones in the model layers are presented in **Appendix C**. The mean annual rainfall was assumed to 565 mm/year.

Table 2-13 Calibrated Rainfall Recharge – Best Calibrated Model

Model Geology Zone	(mm/year)	% Mean annual rainfall
Isaac River Flood Plain Alluvium	1.3	0.24
Isaac River Channel Alluvium	0.3	0.05
Other Alluvium	0.7	0.13
Duaringa Formation	0.2	0.03
Tertiary basalts	2.3	0.4
Weathered Permian	0.5	0.1

Model Geology Zone	(mm/year)	% Mean annual rainfall
Regolith	0.1	0.01

Figure 2-16 compares the calibrated recharge rates in the model against the recharge rates previously estimated using a chloride mass balance (CMB) method for the various units (SLR, 2021a).

As per the conceptual model, higher recharge occurs through the alluvium and lower recharge in regolith and Permian outcrops. Increased recharge through the alluvium of the Isaac River channel has been used to simulate the potential for the Isaac River to provide rapid recharge to the alluvial groundwater system during rainfall events.

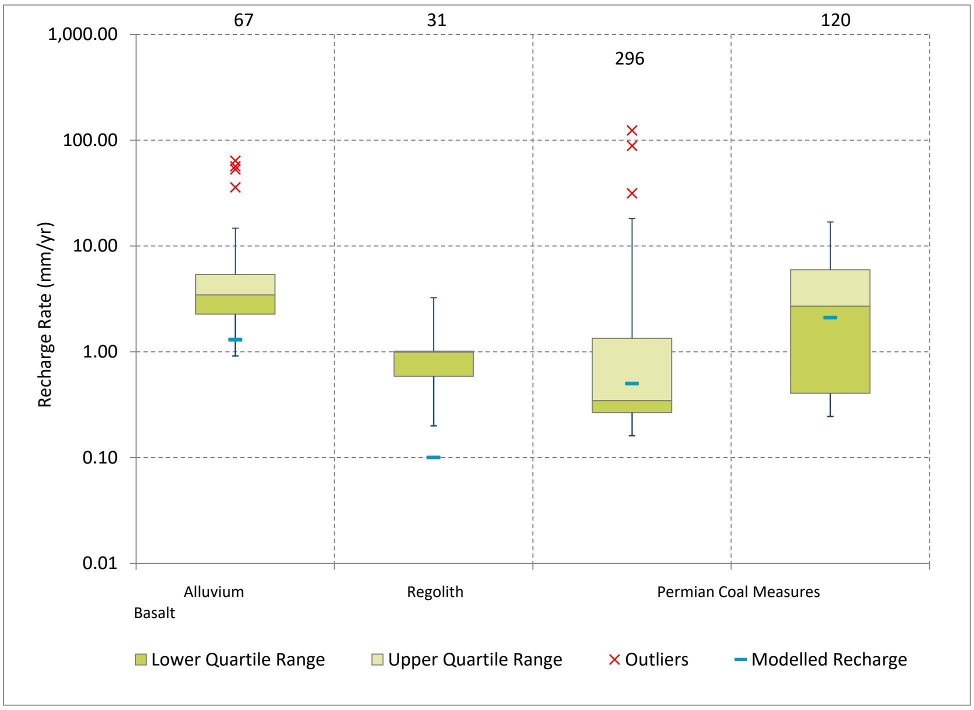

Figure 2-16 CMB Recharge Estimates vs Modelled Recharge

3 Predictive Modelling

3.1 Timing and Mining

Transient predictive modelling was used to simulate the proposed mining at the SEMLP as well as mining at other approved and foreseeable mines within the model domain. The predictive part of the model comprises annual stress periods, starting from January 2021 until January 2044. The predictive model stress period setup is detailed in **Appendix D**, alongside simulated mine timings.

Transient predictive models have been developed for three model scenarios:

- Project – all approved and foreseeable mining in region including SRM open cut plus SEMLP.
- Approved – all approved and foreseeable mining in region includes SRM open cut only.
- Null Run – no mining within region.

Mining cells progressed annually and drain cells simulating the mined coal were projected down to the base of the lowermost target coal seam (i.e. the D seam). A three-year operational window was assumed for mine cells at the SRM open cut, after which time the drains were removed and the MODFLOW Time Varying Materials (TVM) package was used to assign spoil properties to the cells. The drains at the SEMLP remain active during active mining and one year following the completion of the panel.

All mines included in the model were simulated using the MODFLOW Drain (DRN) package. A nominally high drain conductance of 100 square metres per day (m^2/day) was applied to drain cells to simulate rapid removal of water from the system. Where there is an overlap between the SRM opencut and SEMLP future mine plans, the opencut mine has been removed and replaced by the SEMLP longwall mining. **Figure 3-1** shows the SEMLP and the revised version of the SRM opencut used in the Project model scenario.

Predictive modelling results presented in this report section are based on the single model (i.e. best calibrated model realisation discussed in **Section 2.6)** and uncertainty with respect to the model predictions is investigated in detail in **Section 6**.

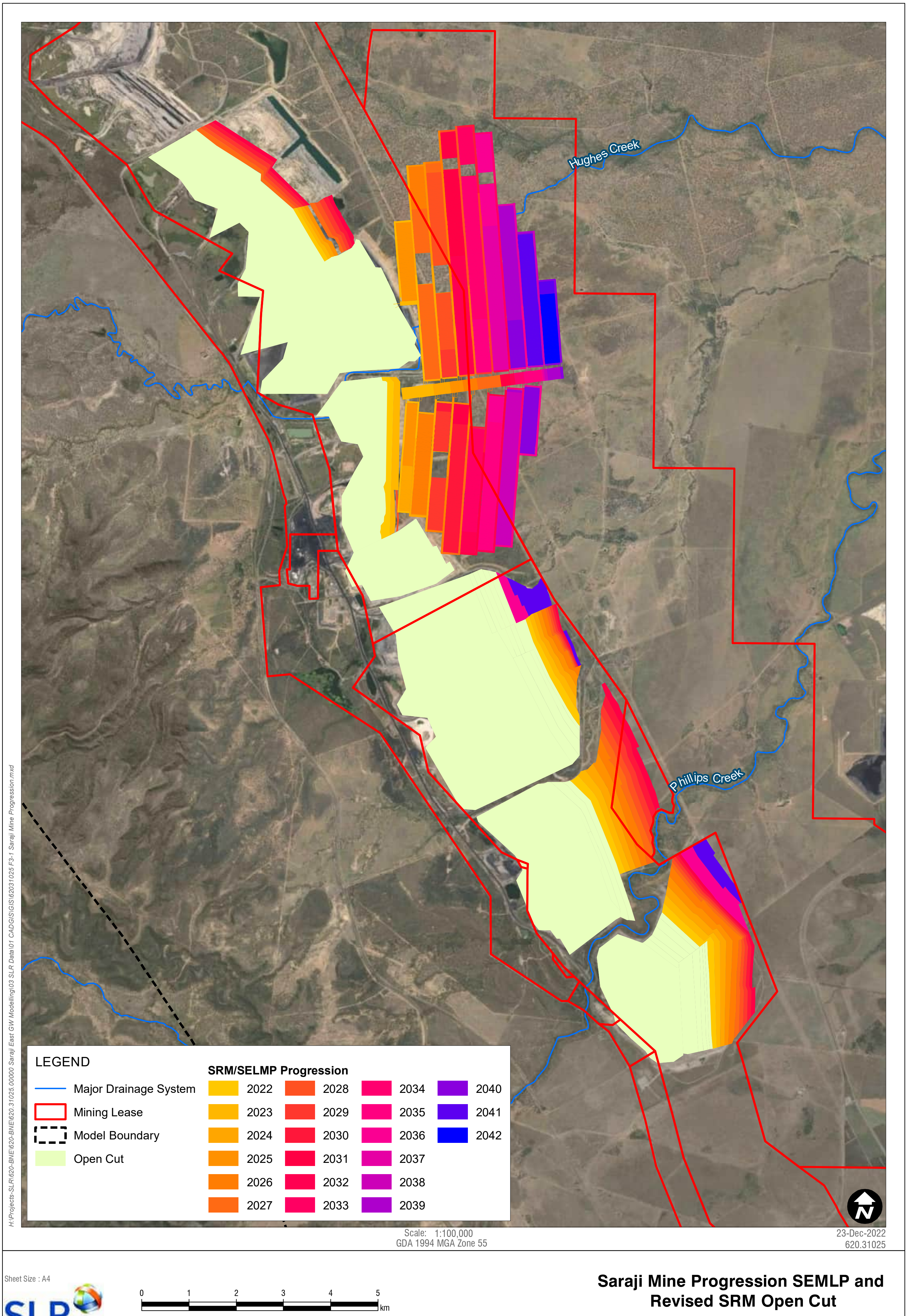

Sheet Size : A4

SLR

www.slrconsultingaustralia.com

Saraji Mine Progression SEMLP and Revised SRM Open Cut

FIGURE 3-1

3.2 Water Balance

Table 3-1 to **Table 3-3** provide average flow rates for water transfer into and out of the predictive model for the three model scenarios. The mass balance error for three scenarios was 0.0 % indicating that the model was stable and achieved an accurate numerical solution. All scenarios maintained mass balance errors below 1 % for all time steps throughout the simulations. The low error achieved indicates that the predictive model is stable, and the solution achieved is accurate (Barnett *et al*., 2012).

The tables show that simulated recharge increased from 4.2 ML/d in the Null scenario to around 7.5 ML/d in the Project and Approved scenarios. The increase in recharge is due to the presence of open cut mining and enhanced recharge through the spoil to the groundwater system in the Project and Approved scenarios.

Table 3-1 to **Table 3-3** show in all the three model scenarios, groundwater enters the model through regional groundwater flow (GHB). The GHB net flow is less than 2 % of the total flow in water balance for all the scenarios indicating the model boundary conditions do not have an influence on the model predictions.

Evapotranspiration for the predictive models is approximately 2.8 ML/d for the Project and Approved scenarios and 3.1 ML/d for the Null Run. The loss to evapotranspiration happens where the water table is within 2 m of the land surface across the model domain, which is primarily along the saturated extent of Isaac River alluvium near the Isaac River. It should be mentioned that the open cut void lakes are not generated during the predictive period of active mining and the groundwater model does not simulate a loss to evaporation. Therefore, the evapotranspiration component reported here only replicates evapotranspiration from shallow water tables particularly within alluvium.

Table 3-3 shows a negative river net baseflow (-2.1 ML/d) in the Null Run indicating flow from the groundwater system to Isaac River within the model domain. However, **Table 3-1** shows that in the Approved scenario the net river exchange flux (RIV) is positive (5.9 ML/d), which indicates that overall, the Isaac River is losing water to the groundwater system. The difference in river net fluxes is likely due to the modelled influence from all mining activities from 2021, resulting in lower groundwater levels and an increase in modelled leakage (along reaches where it occurs) from the Isaac River to the groundwater system. **Table 3-2** indicates that Project scenario creates the same river loss as Approved scenario, indicating that the proposed SEMLP mining activities do not impact the flow out of the Isaac River. Further detail about the impact of proposed SEMLP on the Isaac River is provided in **Section 3.6**.

Groundwater outflow from the model mostly occurs via drain cells, used to simulate open cut and underground mining activity in the model. **Table 3-1** and **Table 3-2** show that the SEMLP in the Project scenario resulted in an increase in the average drain outflow (33.5 ML/d from 33.1 ML/d predicted for the Approved scenario) (i.e. 0.4 ML/d or 161 ML/yr).

Table 3-1 Average Simulated Water Balance over the Prediction Period – Project

Component	Inflow (ML/d)	Percent of Total Inflow (%)	Outflow (ML/d)	Percent of Total Inflow (%)
Recharge (direct rainfall)	7.43	12.52	0.00	0.00
Evapotranspiration (ET)	0.00	0.00	2.82	4.75
SW/GW Interaction Isaac River (RIV)	12.45	20.98	6.58	11.09
SW/GW Interaction Other Rivers (RIV)*	0.00	0.00	0.61	1.02
Regional GW flow (GHB)	3.05	5.14	0.21	0.35
Drains (Mine inflows)	0.00	0.00	33.54	56.51
Storage	36.42	61.36	15.57	26.23
Gas drainage wells (WEL)	0.00	0.00	0.02	0.03
Total	59.35	100.00	59.35	99.99

* The other tributaries or drainage lines in the model are set as drains to the groundwater system and do not result in any recharge.

Table 3-2 Average Simulated Water Balance over the Prediction Period – Approved

Component	Inflow (ML/d)	Percent of Total Inflow (%)	Outflow (ML/d)	Percent of Total Inflow (%)
Recharge (direct rainfall)	7.53	12.83	0.00	0.00
Evapotranspiration (ET)	0.00	0.00	2.82	4.80
SW/GW Interaction Isaac River (RIV)	12.45	21.22	6.58	11.22
SW/GW Interaction Other Rivers (RIV)*	0.00	0.00	0.61	1.03
Regional GW flow (GHB)	3.05	5.20	0.21	0.36
Drains (Mine inflows)	0.00	0.00	33.10	56.40
Storage	35.64	60.74	15.37	26.19
Gas drainage wells (WEL)	0.00	0.00	0.00	0.00
Total	58.68	100.00	58.68	100.00

* The other tributaries or drainage lines in the model are set as drains to the groundwater system and do not result in any recharge.

Table 3-3 Average Simulated Water Balance over the Prediction Period – Null Run

Component	Inflow (ML/d)	Percent of Total Inflow (%)	Outflow (ML/d)	Percent of Total Inflow (%)
Recharge (direct rainfall)	4.20	29.7	0.00	0.0
Evapotranspiration (ET)	0.00	0.0	3.08	21.8
SW/GW Interaction Isaac River (RIV)	7.70	54.4	9.83	69.5
SW/GW Interaction Other Rivers (RIV)*	0.00	0.0	0.76	5.3
Regional GW flow (GHB)	2.22	15.7	0.21	1.5
Drains (Mine inflows)	0.00	0.0	0.00	0.0
Storage	0.04	0.3	0.27	1.9
Gas drainage wells (WEL)	0.00	0.0	0.00	0.0
Total	14.15	100.0	14.15	100.0

* The other tributaries or drainage lines in the model are set as drains to the groundwater system and do not result in any recharge.

3.3 Predicted Groundwater Level Change

Predicted groundwater levels at the end of mining operations for the Approved and Project scenarios are provided in **Figure 3-2** to **Figure 3-7**. The gaps in the water level grids represent unsaturated areas (i.e., where the simulated water level elevation is below the base of cell).

These predicted groundwater levels indicate that there is no change to alluvial groundwater levels when comparing the Project to the Approved mining scenario (**Figure 3-2** and **Figure 3-5**).

Figure 3-3 and **Figure 3-6** show predicted groundwater levels in the regolith at the end of mining for the Project and Approved mining scenarios. Dewatering of the Regolith caused by the SEMLP can be seen by slightly larger unsaturated zone within the SEMLP area for the Project scenario (**Figure 3-6**), relative to the Approved mining scenario (**Figure 3-3**).

Figure 3-4 and **Figure 3-7** show the predicted water levels in the target D coal seam (Layer 18) at the end of mining for Project and Approved mining scenarios. Respectively, a regional south-easterly hydraulic gradient can be observed, reflecting the downstream flow gradient of the Isaac River. Zones of depressurisation at the SEMLP and surrounding mines are shown to cause localised interruptions to the regional flow gradient. A discussion on groundwater drawdown within the Permian Coal Measures is included in **Section 3.4**.

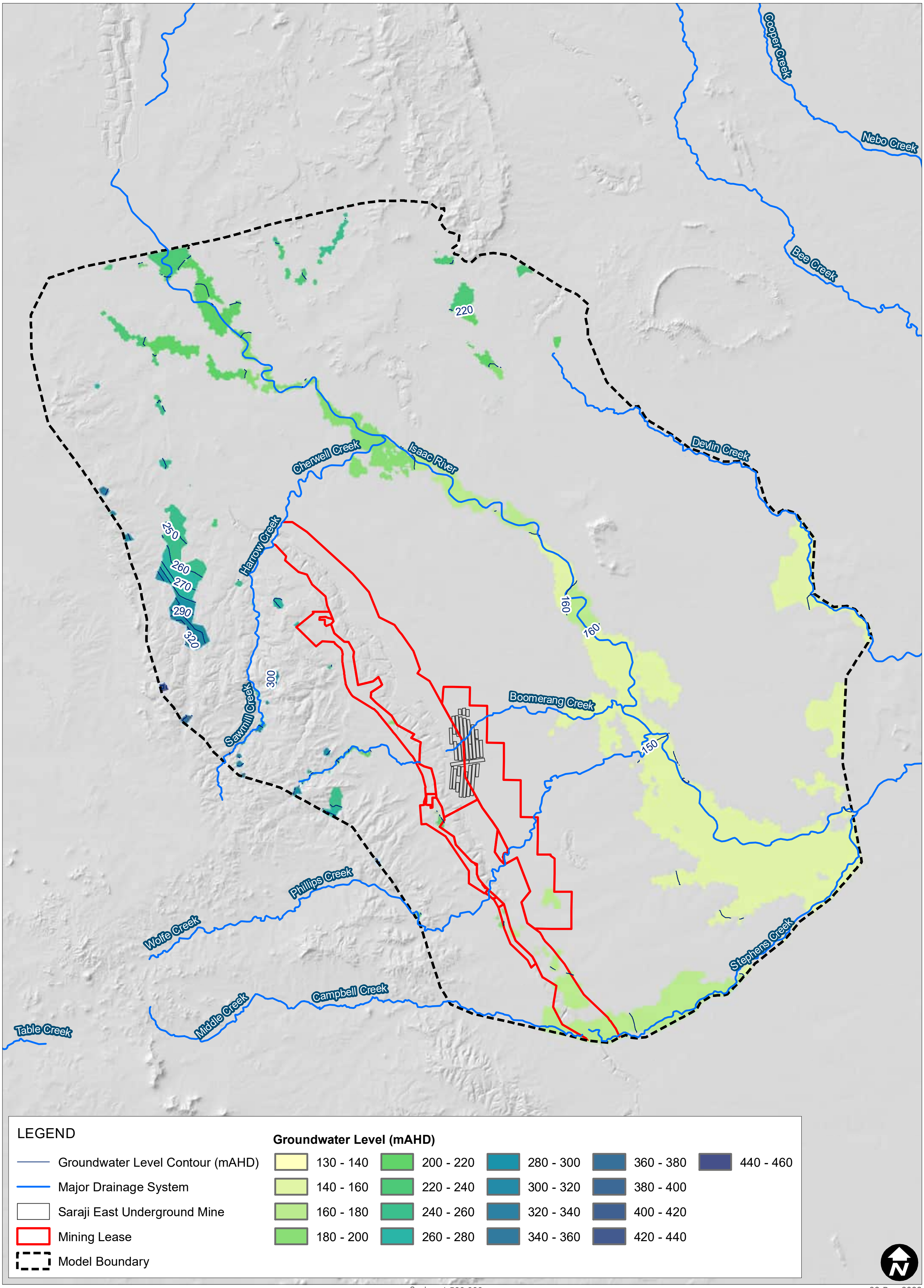

H:\Projects-SLR\620-BNE\620-BNE\620.31025.00000 Saraji East GW Modelling\03 SLR Data\01 CADGIS\GIS\62031025 F3-2 Predicted WL in Alluvium.mxd

Scale: 1:500,000
GDA 1994 MGA Zone 55

22-Dec-2022
620.30125

Sheet Size : A4

0 5 10 15 20 km

www.slrconsultingaustralia.com

Predicted Water Level within Quaternary Alluvium (Layer 1) at End of Mining – Approved Scenario

FIGURE 3-2

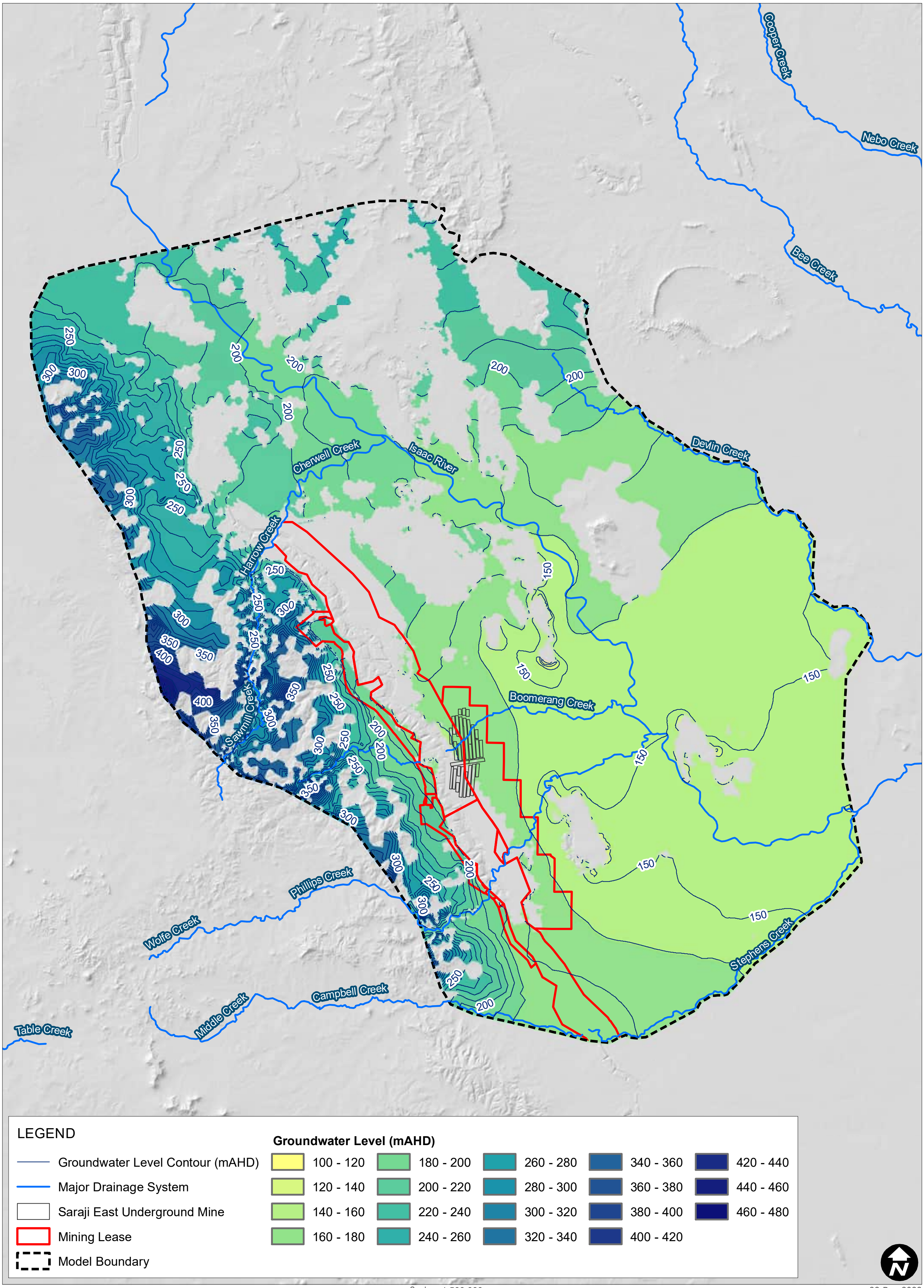

H:\Projects-SLR\620-BNE\620-BNE\620.31025.00000 Saraji East GW Modelling\03 SLR Data\01 CADGIS\GIS\62031025 F3-3 Predicted WL in Regolith.mxd

Scale: 1:500,000
GDA 1994 MGA Zone 55

22-Dec-2022
620.31025

Sheet Size : A4

SLR
www.slrconsultingaustralia.com

0 5 10 15 20 km

Predicted Water Level within Regolith (Layer 2) at End of Mining – Approved Scenario

FIGURE 3-3

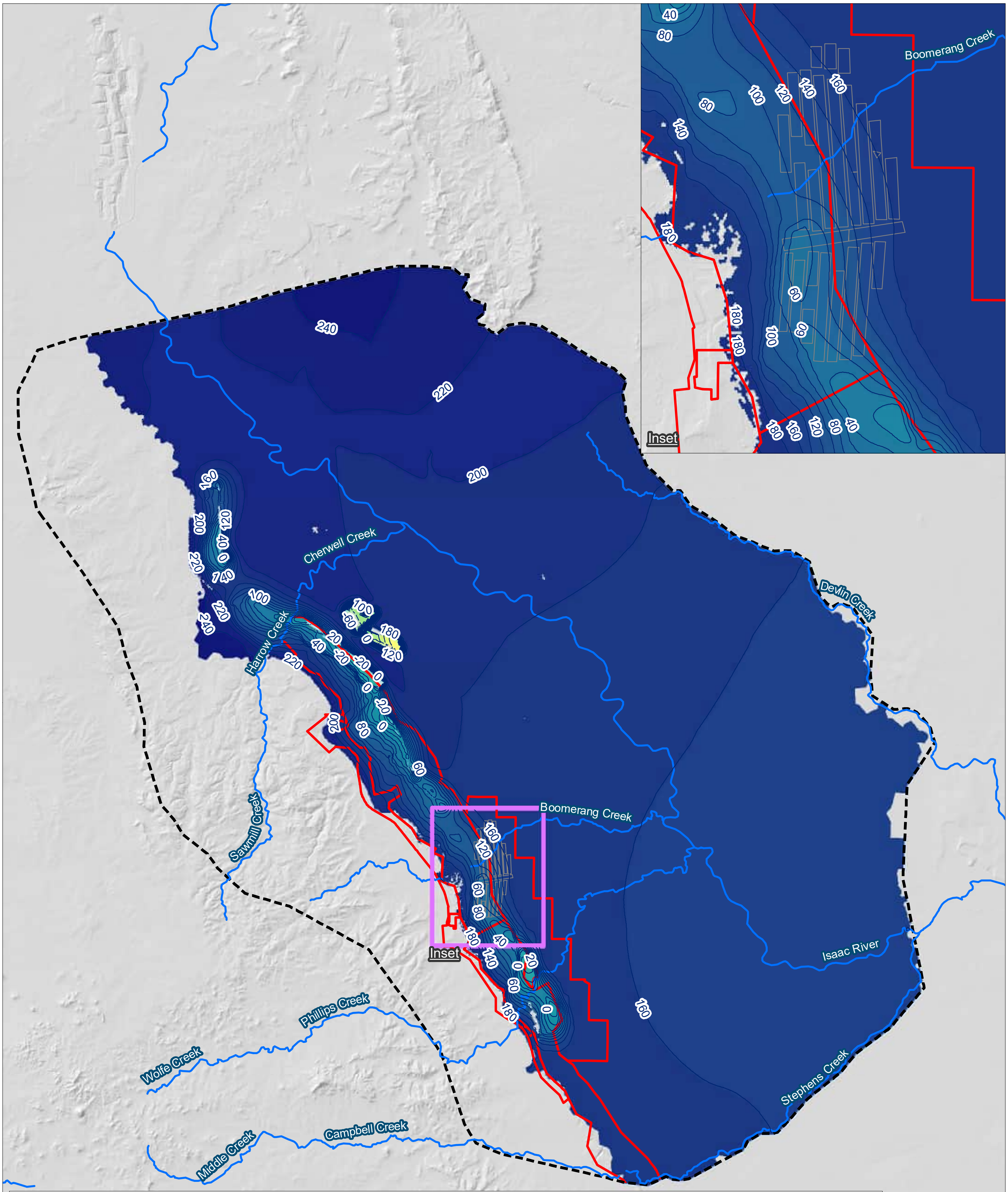

LEGEND

- Groundwater Level Contour (mAHD)
- Major Drainage System
- Saraji East Underground Mine
- Mining Lease
- Model Boundary

Groundwater Level (mAHD)

-300 - -280	-180 - -160	-60 - -40	60 - 80	180 - 200
-280 - -260	-160 - -140	-40 - -20	80 - 100	200 - 220
-260 - -240	-140 - -120	-20 - 0	100 - 120	220 - 240
-240 - -220	-120 - -100	0 - 20	120 - 140	240 - 260
-220 - -200	-100 - -80	20 - 40	140 - 160	260 - 280
-200 - -180	-80 - -60	40 - 60	160 - 180	

H:\Projects-SLR\620-BNE\620-BNE\620.31025.00000 Saraji East GW Modelling\03 SLR Data\01 CADGIS\GIS\62031025 F3-4 Predicted WL in Permain Coal.mxd

Scale: 1:500,000
GDA 1994 MGA Zone 55

22-Dec-2022
620.31025

Sheet Size : A4

0 5 10 15 20 km

www.slrconsultingaustralia.com

Predicted Water Level within Permain Coal Measures (Layer 18) at End of Mining – Approved Scenario

FIGURE 3-4

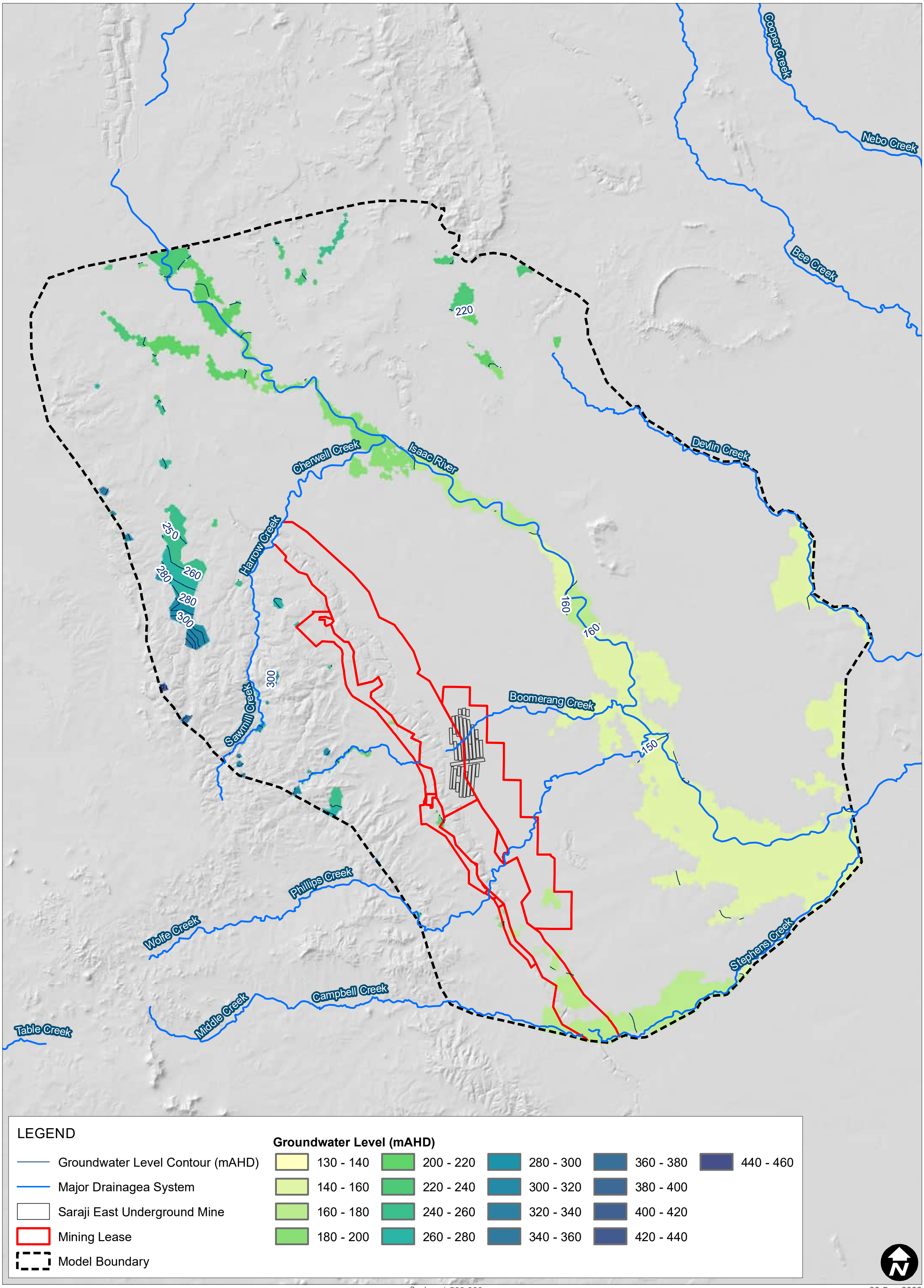

H:\Projects-SLR\620-BNE\620-BNE\620.31025.00000 Saraji East GW Modelling\03 SLR Data\01 CADGIS\GIS\62031025 F3-5 Predicted WL in Alluvium Project.mxd

Scale: 1:500,000
GDA 1994 MGA Zone 55

22-Dec-2022
620.31025

Sheet Size : A4

SLR
www.slrconsultingaustralia.com

0 5 10 15 20 km

Predicted Water Level within Quaternary Alluvium (Layer 1) at End of Mining – Project Scenario

FIGURE 3-5

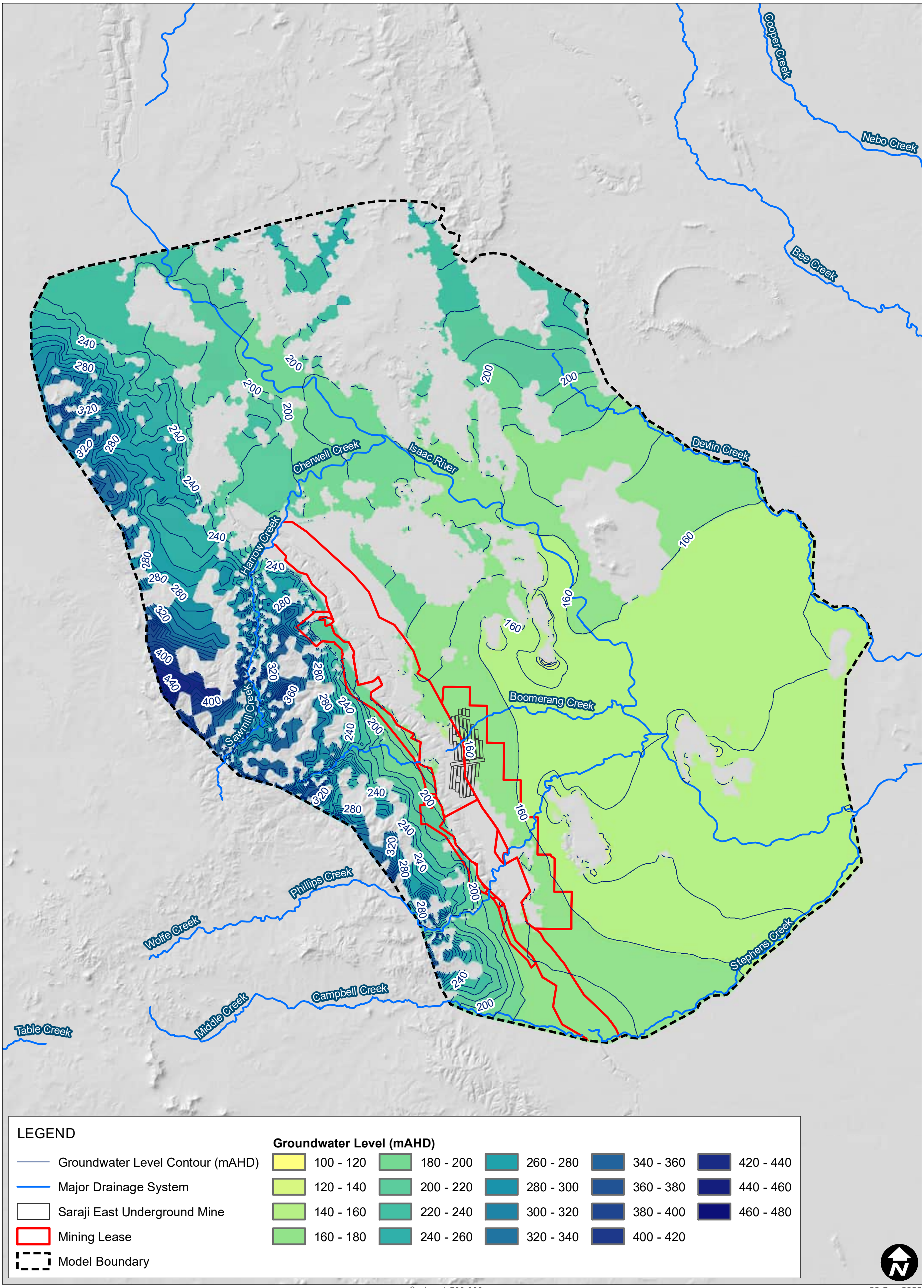

SLR
www.slrconsultingaustralia.com

Predicted Water Level within Regolith (Layer 2) at End of Mining – Project Scenario

FIGURE 3-6

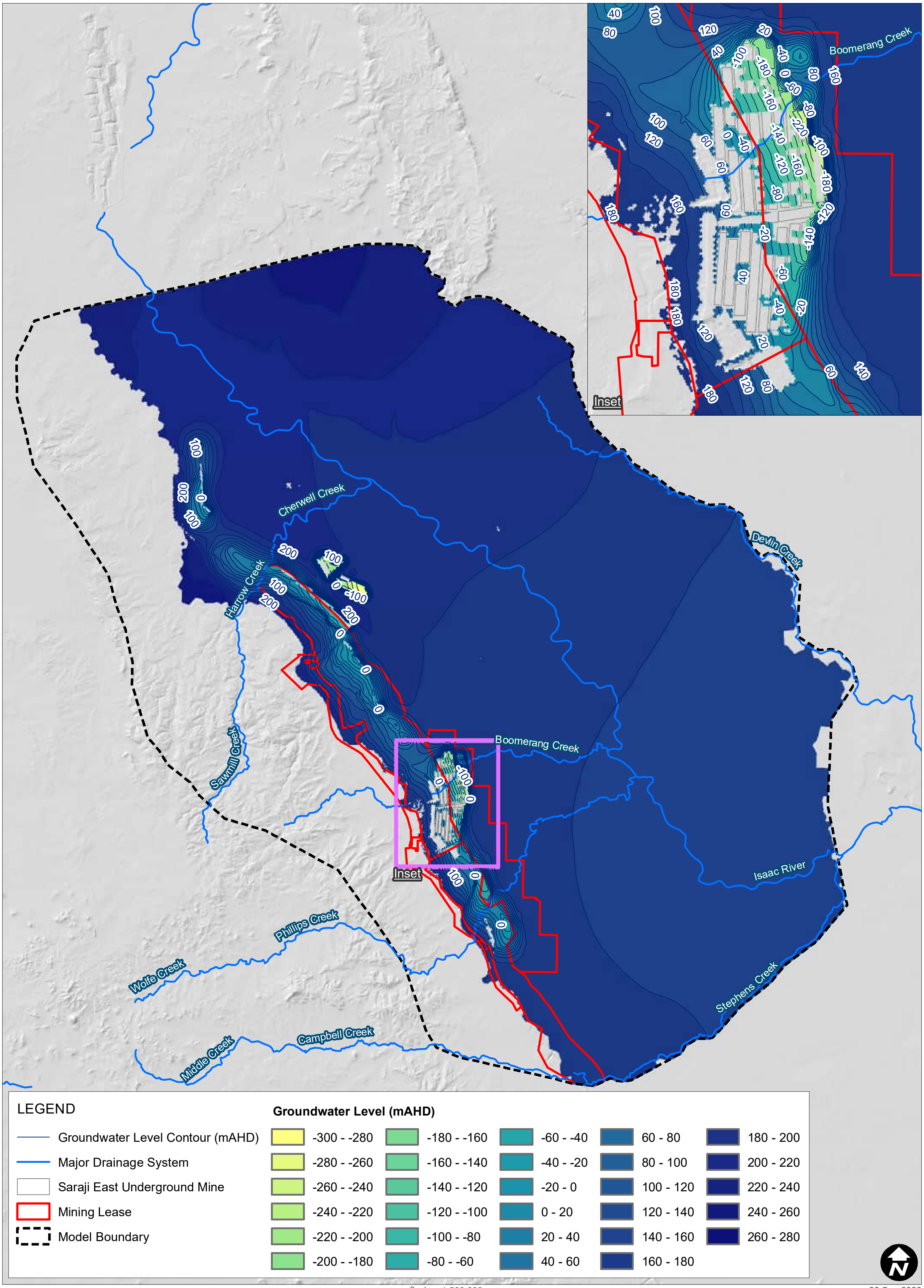

Scale: 1:500,000
GDA 1994 MGA Zone 55

22-Dec-2022
620.31025

H:\Projects-SLR\620-BNE\620-BNE\620.31025.00000 Saraji East GW Modelling\03 SLR Data\01 CADGIS\GIS\62031025 F3-7 Predicted WL in Permain Coal Project.mxd

Sheet Size : A4

SLR
www.slrconsultingaustralia.com

0 5 10 15 20 km

Predicted Water Level within Permain Coal Measures (Layer 18) at End of Mining – Project Scenario

FIGURE 3-7

3.4 Maximum Predicted Drawdowns

3.4.1 Incremental Drawdown

The process of mining directly removes water from the groundwater system and reduces water levels in surrounding groundwater units. The extent of the zone affected is dependent on the properties of the aquifers/aquitards and is referred to as the zone of drawdown. Groundwater drawdown is greatest at the working coalface and decreases with distance from the mine workings. Predictive modelling results presented in this report section are based on the single model (i.e. best calibrated model realisation discussed in **Section 2.6** and uncertainty with respect to the model predictions is investigated in detail in **Section 6**.

In this report, maximum incremental drawdown refers to the drawdown impact associated with the SEMLP only and is obtained by comparing the difference in predicted aquifer groundwater levels for the Approved scenario and the Project scenario at matching times. The maximum incremental drawdown represents the maximum drawdown values recorded at each model cell at any time over the model predictive simulation duration. Predicted drawdown figures (**Figure 3-8** to **Figure 3-13**) show where maximum incremental drawdown impacts are predicted to exceed 1 m.

Figure 3-8 shows that no incremental drawdown impacts are predicted for the Quaternary alluvium as a result of mining at the SEMLP.

The maximum predicted incremental drawdown impacts associated with the SEMLP within the regolith is shown in **Figure 3-9.** The incremental drawdown extent within the regolith (Layer 2) is largely confined to the SEMLP MLA or downdip of only the northern panel area and is influenced by the distribution of predicted saturated zones in the regolith. At the northern panels, 1 m drawdown influence is predicted to extend 4.2 km northeast of the SEMLP mine extent.

The coal seams of the Moranbah Coal Measures are the primary groundwater bearing strata at the SEMLP and will experience drawdowns as a result of mining at the SEMLP. Groundwater level drawdown within the mined coal seams is influenced by unit structure and is confined to unit extents. **Figure 3-10** to **Figure 3-13** show the maximum predicted incremental drawdown for Q, P, H and D seam in the Moranbah Coal Measures. The figures show the extent of maximum predicted depressurisation of the Permian aged coal seams is limited to the west of the SEMLP due to the depositional geology (i.e. coal seams subcrop).

The extents of maximum predicted incremental drawdown impacts in the Moranbah Coal Measures coal seams are generally elongated along strike in the northeast-southwest direction and extents maximum of 5 km and 8 km northwest and southeast of the SEMLP mine extent, respectively. Drawdowns propagate further within the shallower coal seams (i.e., Q and P seam) when compared to the D seam (i.e., coal seam target). Given the use of depth dependant equation for assigning the hydraulic properties in the model, the shallower units have higher hydraulic conductivities in comparison to deeper ones which facilitates the drawdowns.

The influence of fault near the SEMLP is also evident and it appears that it limits the drawdown propagation to the east.

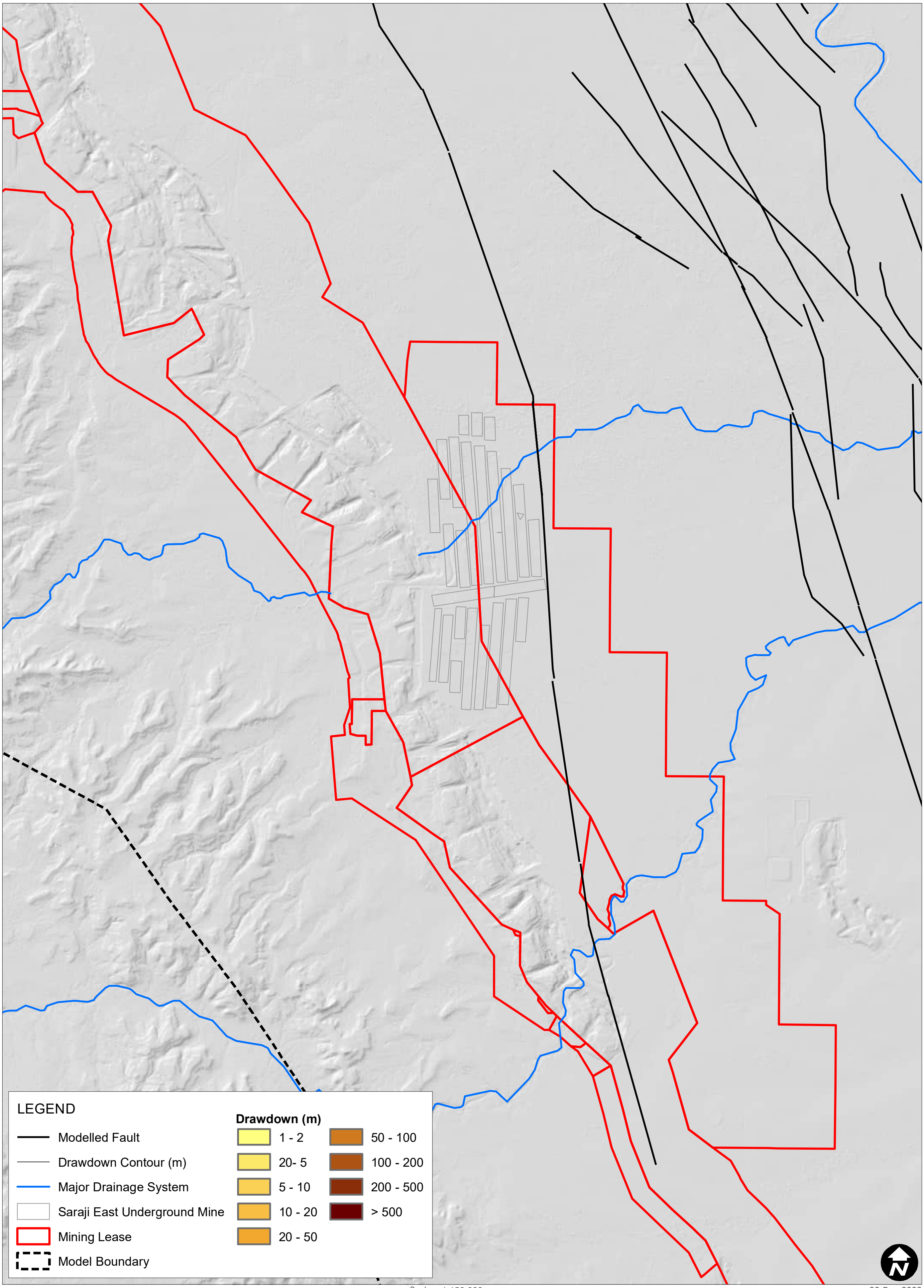

Scale: 1:150,000
GDA 1994 MGA Zone 55

22-Dec-2022
620.31025

Sheet Size : A4

SLR
www.slrconsultingaustralia.com

0 1 2 3 4 5 km

Maximum Incremental Drawdown in Quaternary Alluvium (Layer 1)

FIGURE 3-8

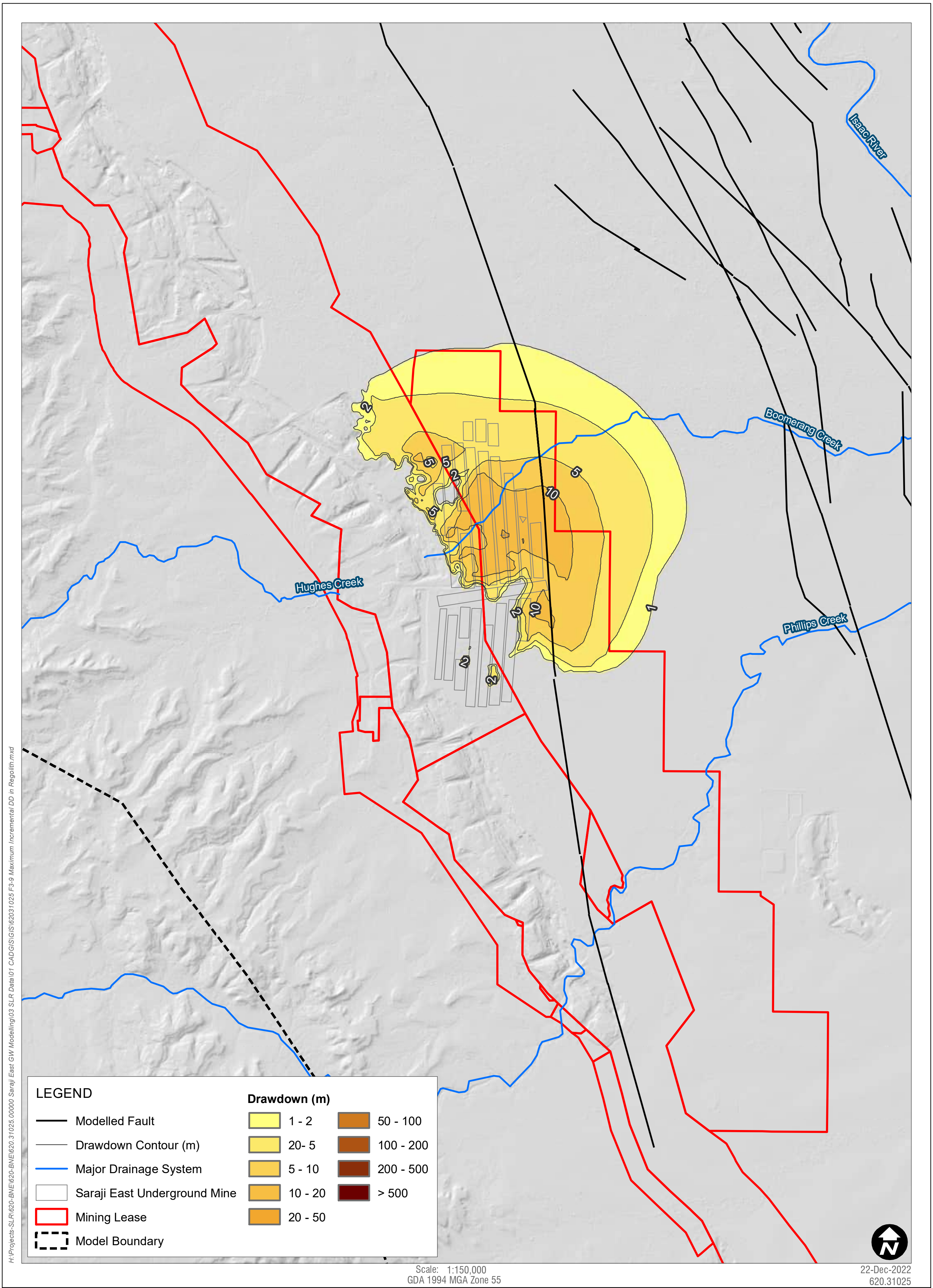

Scale: 1:150,000
GDA 1994 MGA Zone 55

22-Dec-2022
620.31025

Sheet Size : A4

0 1 2 3 4 5 km

www.slrconsultingaustralia.com

Maximum Incremental Drawdown in Regolith (Layer 2)

FIGURE 3-9

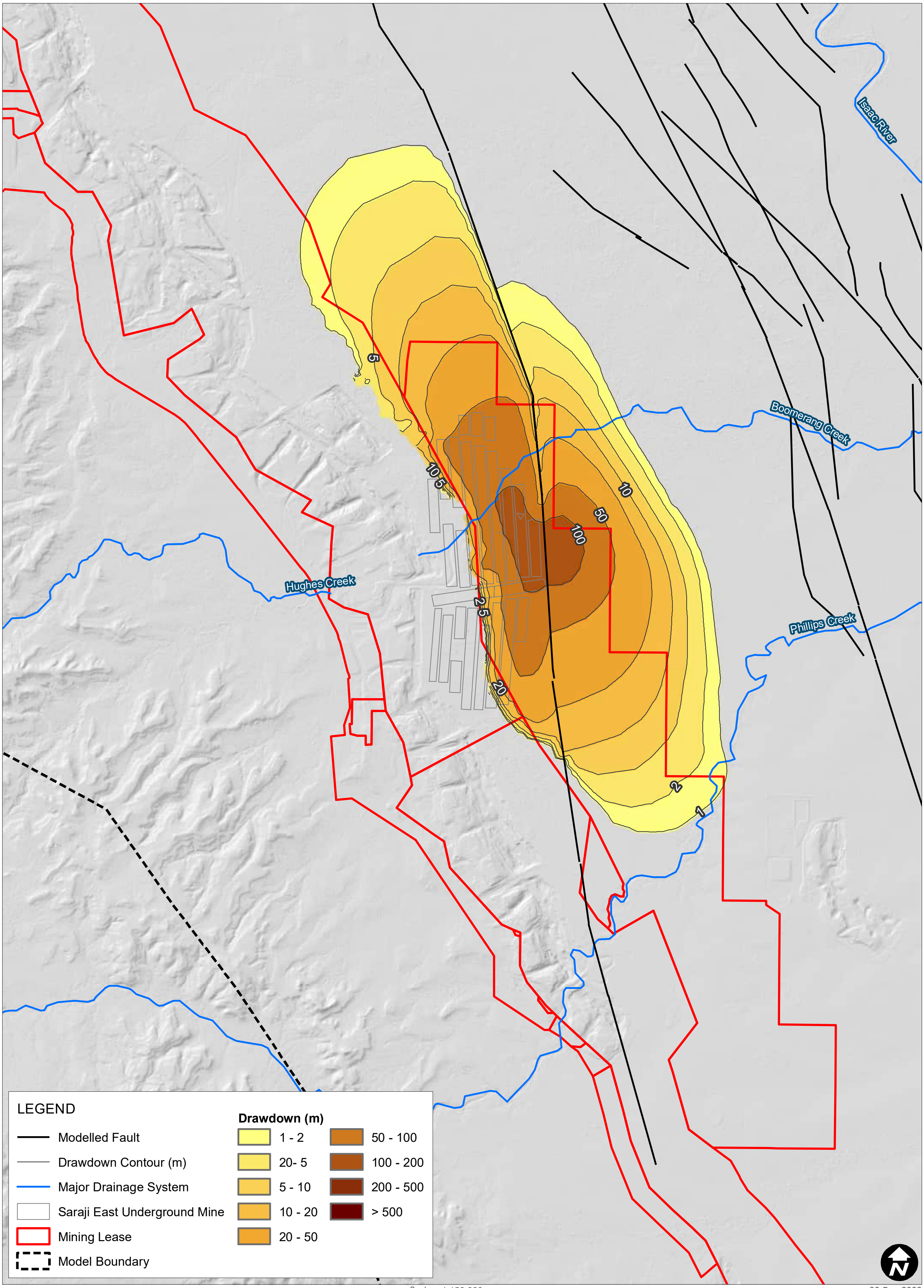

H:\Projects-SLR\620-BNE\620-BNE\620.31025.00000 Saraji East GW Modelling\03 SLR Data\01 CADGIS\GIS\62031025 F3-10 Maximum Incremental DD in Q Seam.mxd

Scale: 1:150,000
GDA 1994 MGA Zone 55

22-Dec-2022
620.31025

Sheet Size : A4

SLR
www.slrconsultingaustralia.com

0 1 2 3 4 5
km

Maximum Incremental Drawdown in Q Seam (Layer 12)

FIGURE 3-10

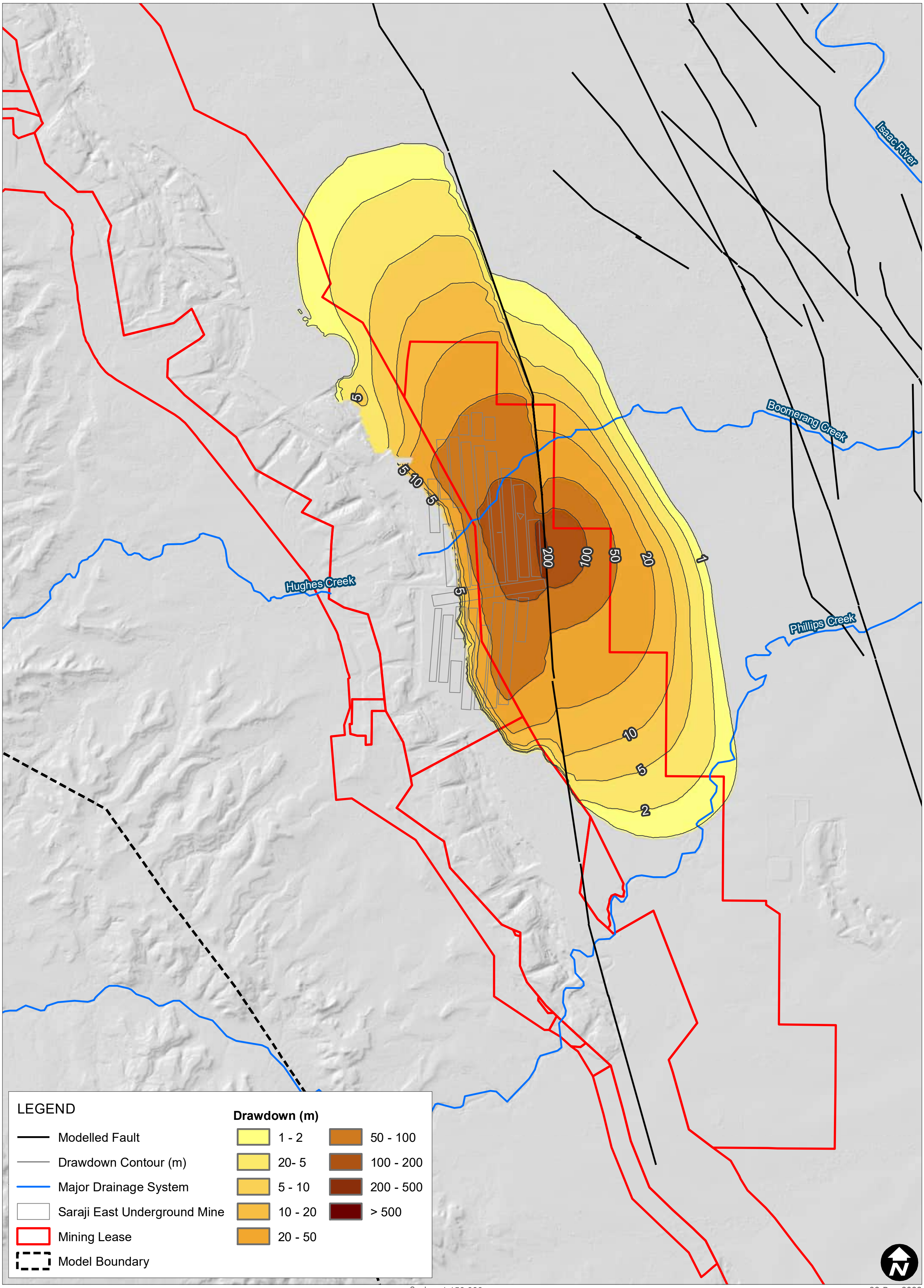

Scale: 1:150,000
GDA 1994 MGA Zone 55

22-Dec-2022
620.30125

Sheet Size : A4

0 1 2 3 4 5 km

SLR
www.slrconsultingaustralia.com

Maximum Incremental Drawdown in P Seam (Layer 14)

FIGURE 3-11

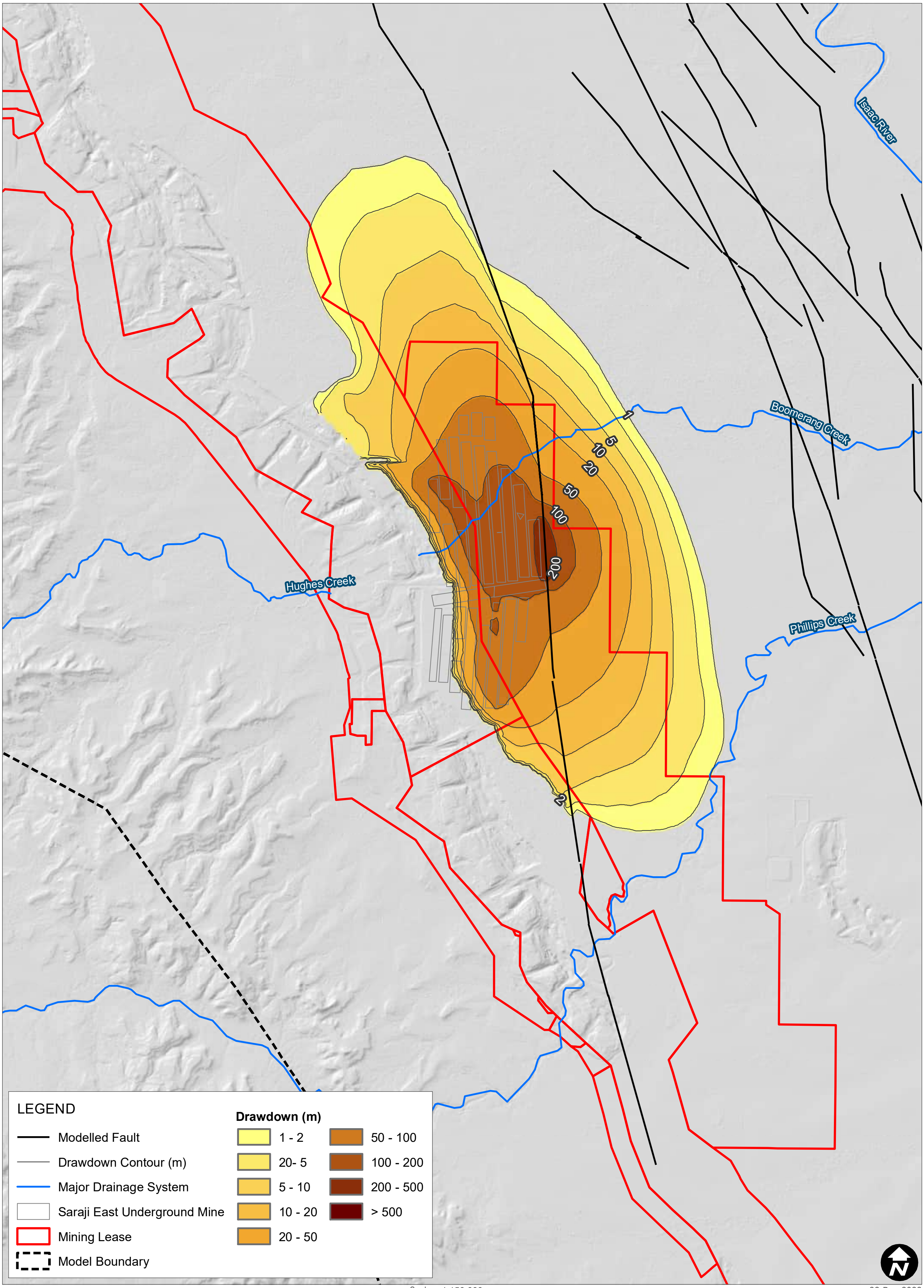

Scale: 1:150,000
GDA 1994 MGA Zone 55

22-Dec-2022
620.31025

Sheet Size : A4

0 1 2 3 4 5 km

SLR
www.slrconsultingaustralia.com

Maximum Incremental Drawdown in H Seam (Layer 16)

FIGURE 3-12

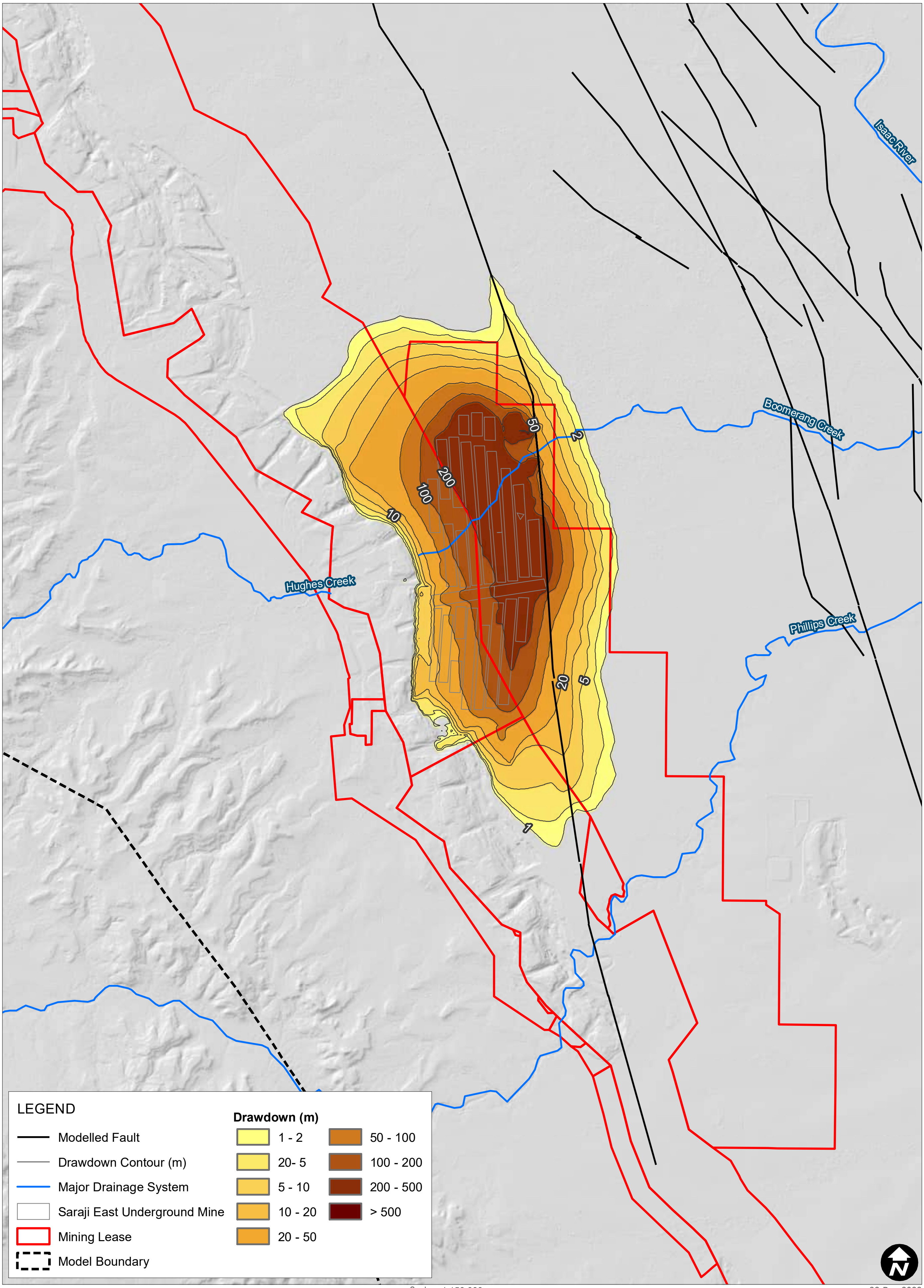

Scale: 1:150,000
GDA 1994 MGA Zone 55

22-Dec-2022
620.30125

Sheet Size : A4

SLR
www.slrconsultingaustralia.com

0 1 2 3 4 5 km

Maximum Incremental Drawdown in D Seam (Layer 18)

FIGURE 3-13

3.4.2 Cumulative Drawdown

The simulated cumulative drawdown presented in this section show the impacts on different hydrostratigraphic units due to the existing approved mining within the model domain. The simulated cumulative drawdown shows whether the zone of impact from the neighbouring operations is predicted to interact with the zone of impact predicted for the SEMLP in different aquifers (alluvium none, regolith, MCM coal seams – only).

Maximum cumulative drawdown impacts in proximity to the SEMLP are shown in **Figure 3-14** to **Figure 3-21**. Maximum cumulative drawdown predictions covering the entire model domain are provided in **Appendix E**. These drawdowns represent the total impact to modelled groundwater levels resulting from all mining within the model domain, by comparing the maximum difference in aquifer groundwater levels for the Project model scenario with those in the theoretical "no mining" Null Run scenario, for all times during the predictive model period. The vast majority of these predicted cumulative drawdown impacts are not related to the SEMLP but result from existing mining activities represented in the model.

There are no cumulative drawdown impacts predicted for the Quaternary alluvium within or around the SEMLP (**Figure 3-14)**.

Cumulative impacts within the regolith can be seen connecting the Project-related drawdown to the drawdown impacts at the PDM and SRM open cuts (**Figure 3-15**).

For the Leichhardt and Vermont coal seams of the Rangal Coal Measures, there was no drawdown interaction between the SEMLP area and the neighbouring mines since these seams are not present in the SEMLP area (**Figure 3-16** and **Figure 3-17**).

Figure 3-18 to **Figure 3-21** show the maximum predicted cumulative drawdown in Q, P, H and D seams in the Moranbah Coal Measures. As shown in the figures the cumulative drawdown is predicted to interact with zone of impact from the PDM and SRM open cuts.

Figure 3-21 shows that drawdowns occur along the north-south trending fault located on the east of SRM.

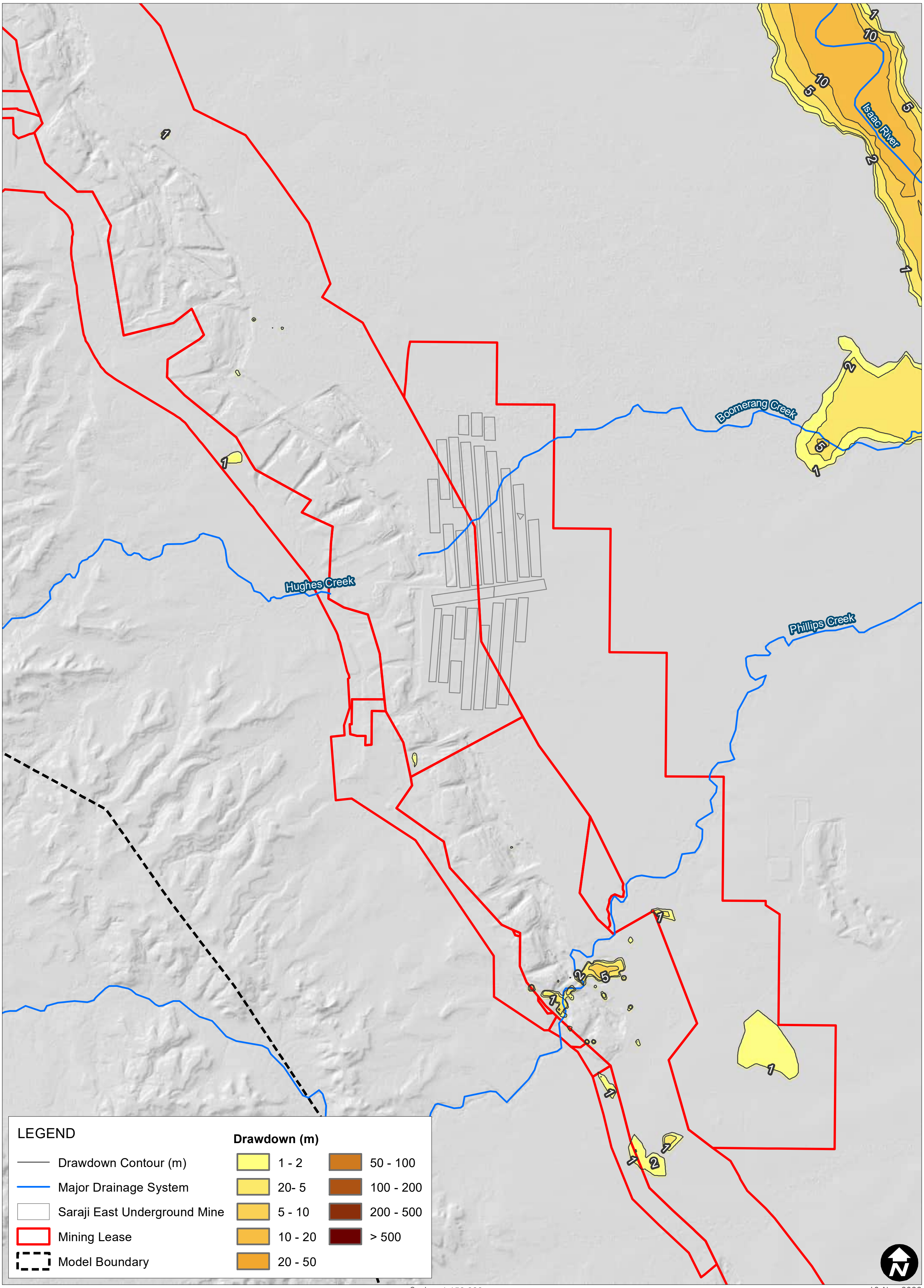

H:\Projects-SLR\620-BNE\620-BNE\620.31025.00000 Saraji East GW Modelling\03 SLR Data\01 CADGIS\GIS\62031025 F3-14 Maximum Cumulative DD in Alluvium.mxd

Scale: 1:150,000
GDA 1994 MGA Zone 55

18-Nov-2022
620.31025

Sheet Size : A4

SLR
www.slrconsultingaustralia.com

0 1 2 3 4 5 km

Maximum Cumulative Drawdown in Quaternary Alluvium (Layer 1)

FIGURE 3-14

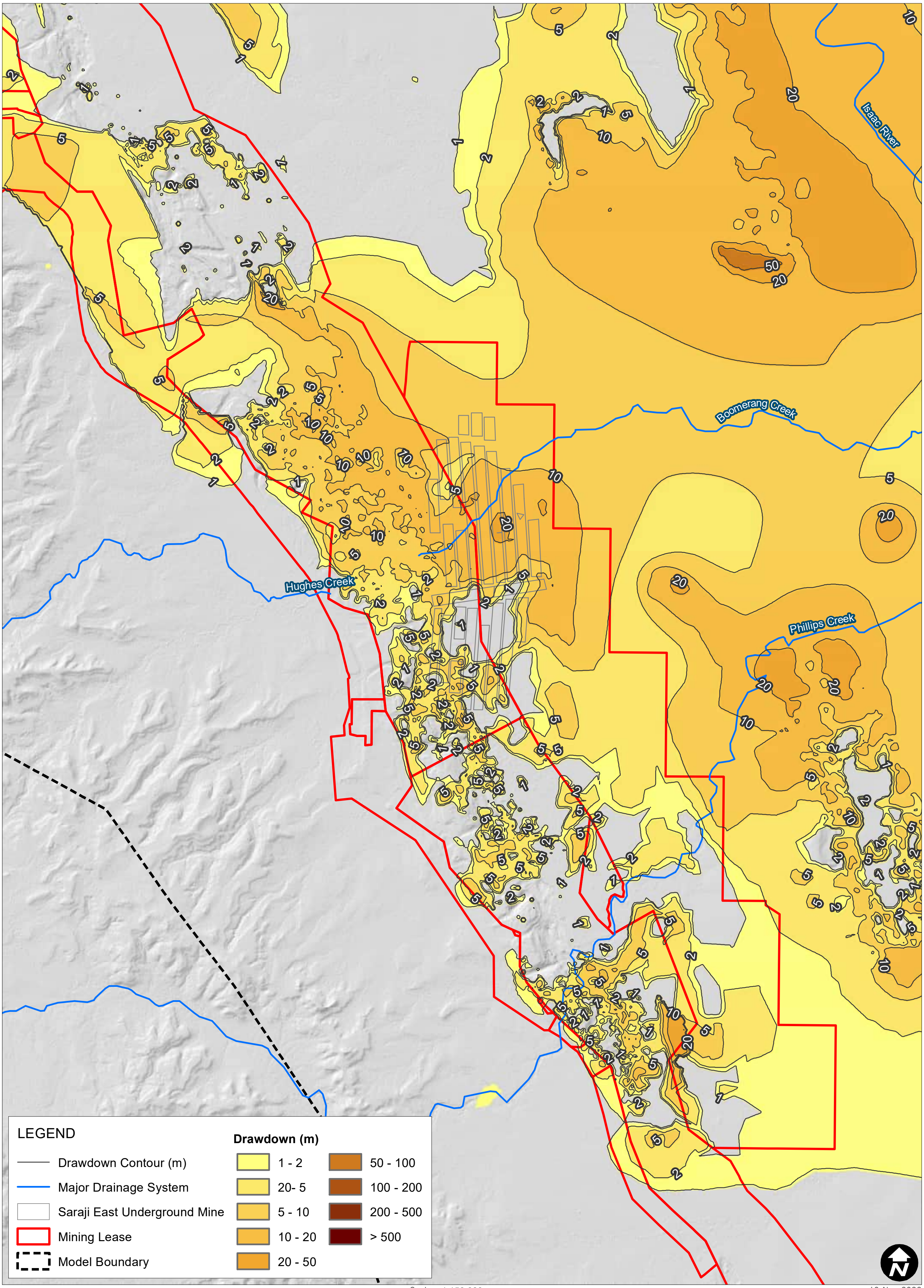

H:\Projects-SLR\620-BNE\620-BNE\620.31025.00000 Saraji East GW Modelling\03 SLR Data\01 CADGIS\GIS\62031025 F3-15 Maximum Cumulative DD in Regolith.mxd

Scale: 1:150,000
GDA 1994 MGA Zone 55

18-Nov-2022
620.31025

Sheet Size : A4

SLR
www.slrconsultingaustralia.com

0 1 2 3 4 5 km

Maximum Cumulative Drawdown in Regolith (Layer 2)

FIGURE 3-15

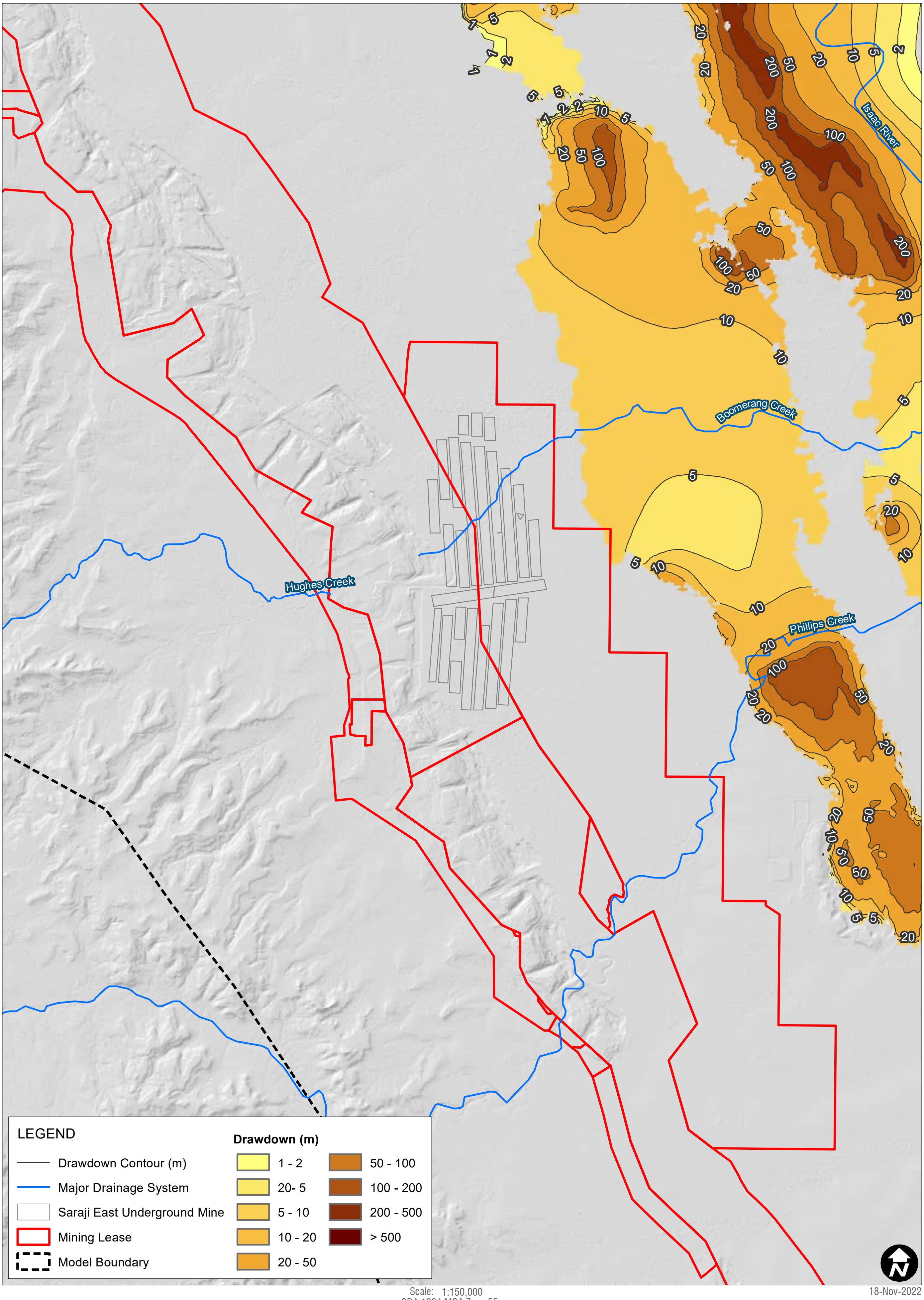

H:\Projects-SLR\620-BNE\620-BNE\620.31025.00000 Saraji East GW Modelling\03 SLR Data\01 CADGIS\GIS\62031025 F3-16 Maximum Cumulative DD in Leichardt.mxd

Scale: 1:150,000
GDA 1994 MGA Zone 55

18-Nov-2022
620.31025

Sheet Size : A4

SLR
www.slrconsultingaustralia.com

0 1 2 3 4 5 km

Maximum Cumulative Drawdown in Leichhardt Seam (Layer 5)

FIGURE 3-16

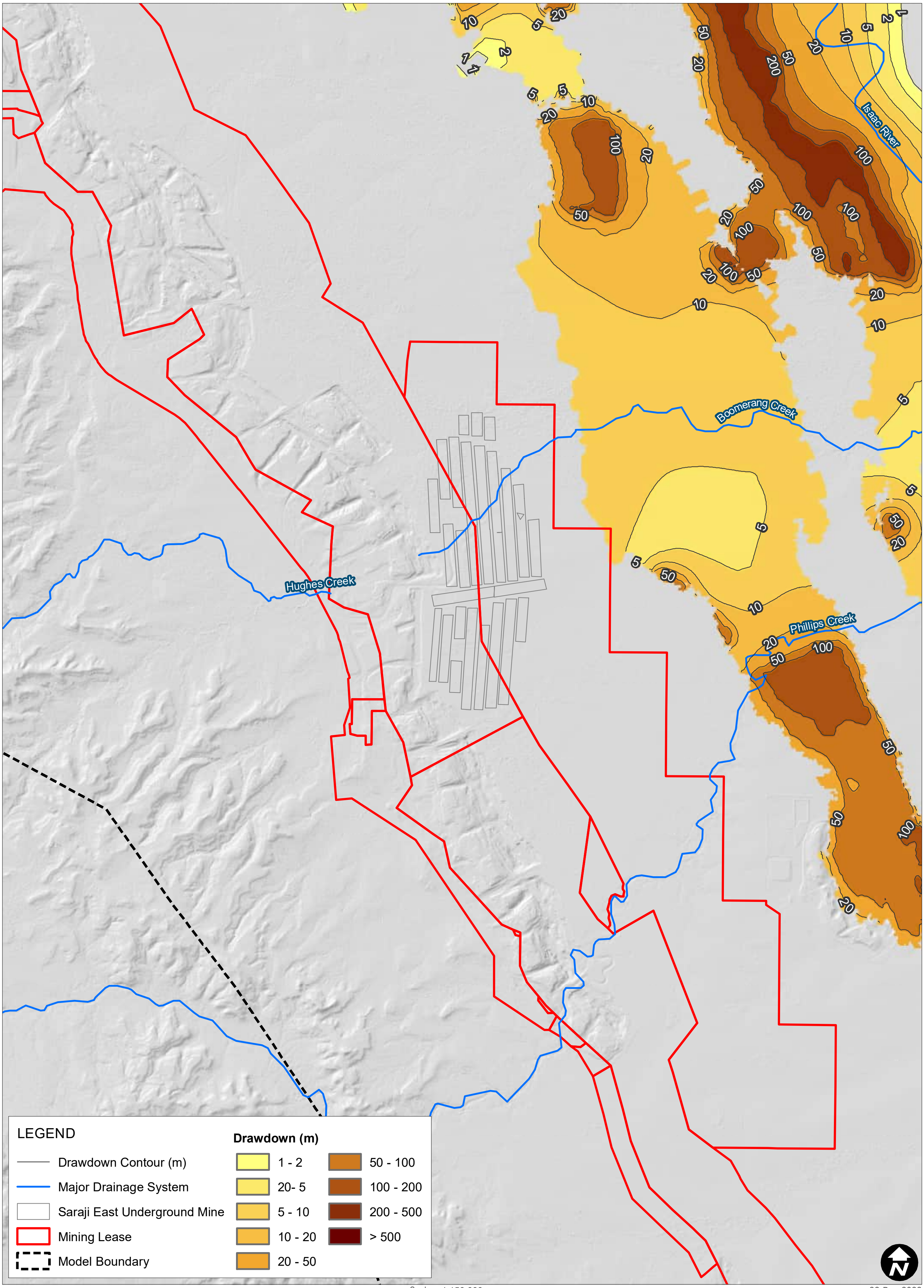

H:\Projects-SLR\620-BNE\620-BNE\620.31025.00000 Saraji East GW Modelling\03 SLR Data\01 CADGIS\GIS\62031025 F3-17 Maximum Cumulative DD in Vermont.mxd

Scale: 1:150,000
GDA 1994 MGA Zone 55

22-Dec-2022
620.31025

Sheet Size : A4

SLR
www.slrconsultingaustralia.com

0 1 2 3 4 5 km

Maximum Cumulative Drawdown in Vermont Seam (Layer 7)

FIGURE 3-17

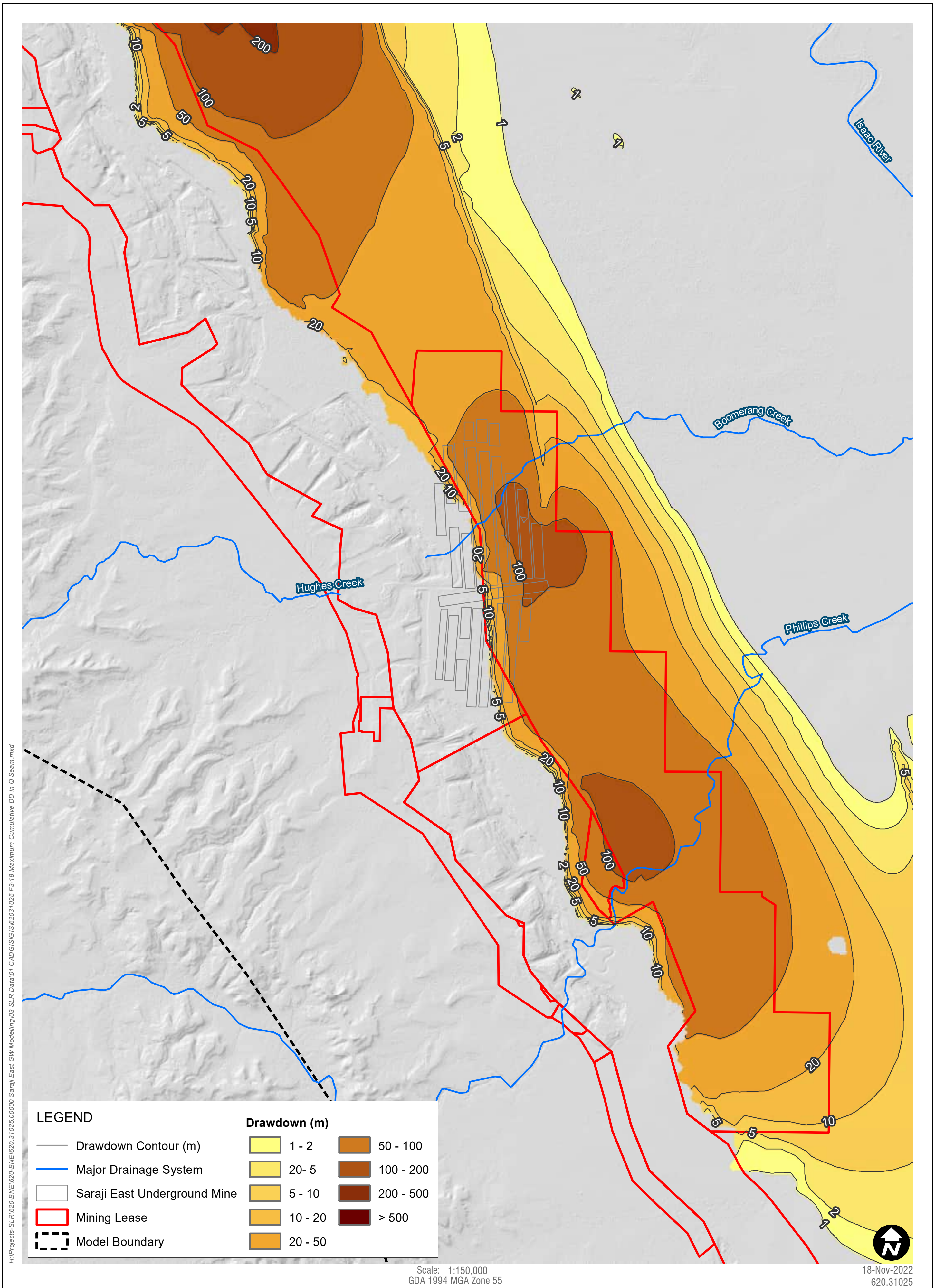

Maximum Cumulative Drawdown in Q Seam (Layer 12)

FIGURE 3-18

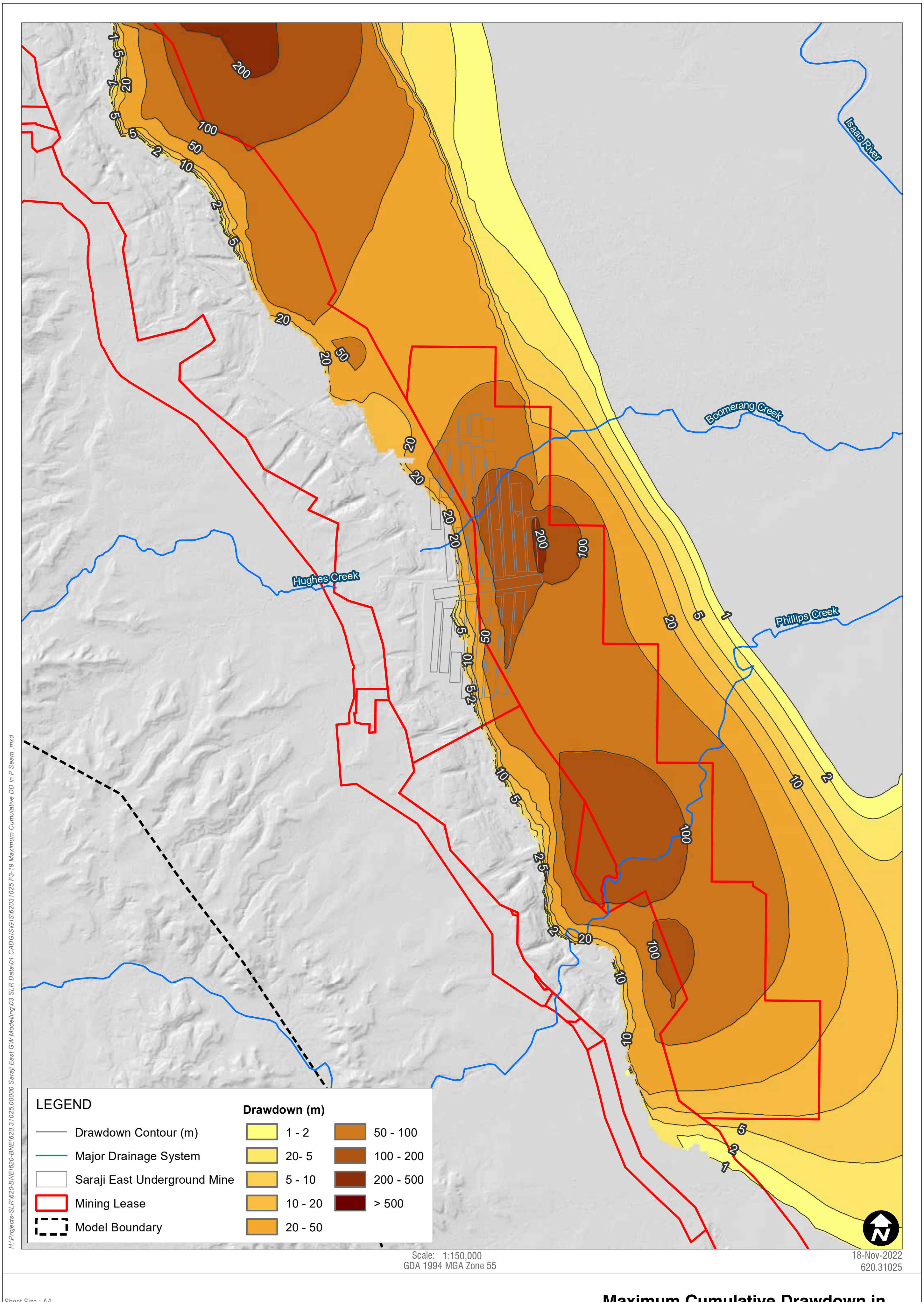

Maximum Cumulative Drawdown in P Seam (Layer 14)

FIGURE 3-19

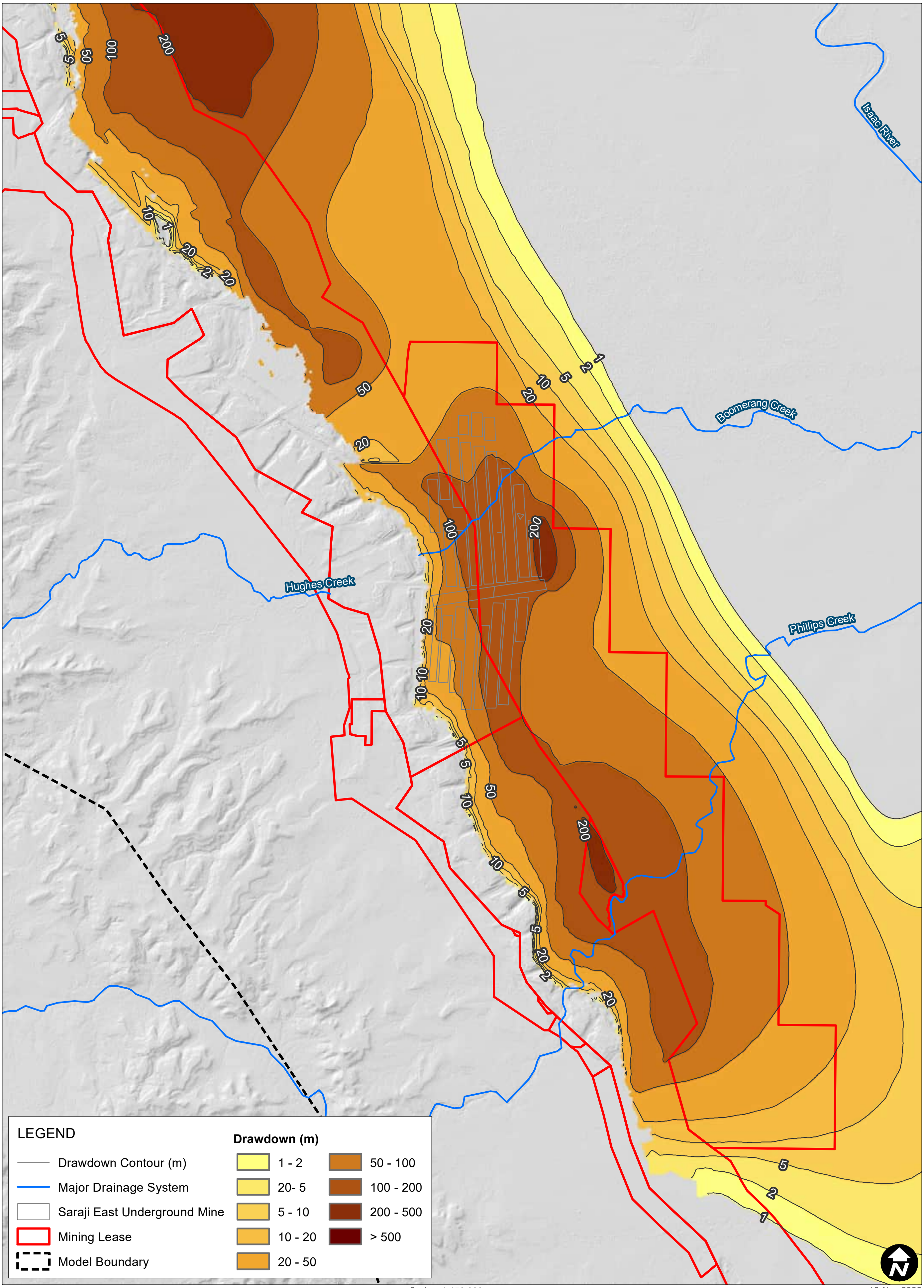

Scale: 1:150,000
GDA 1994 MGA Zone 55

18-Nov-2022
620.31025

H:\Projects-SLR\620-BNE\620-BNE\620.31025.00000 Saraji East GW Modelling\03 SLR Data\01 CADGIS\GIS\62031025 F3-20 Maximum Cumulative DD in H Seam.mxd

Sheet Size : A4

SLR
www.slrconsultingaustralia.com

0 1 2 3 4 5 km

Maximum Cumulative Drawdown in H Seam (Layer 16)

FIGURE 3-20

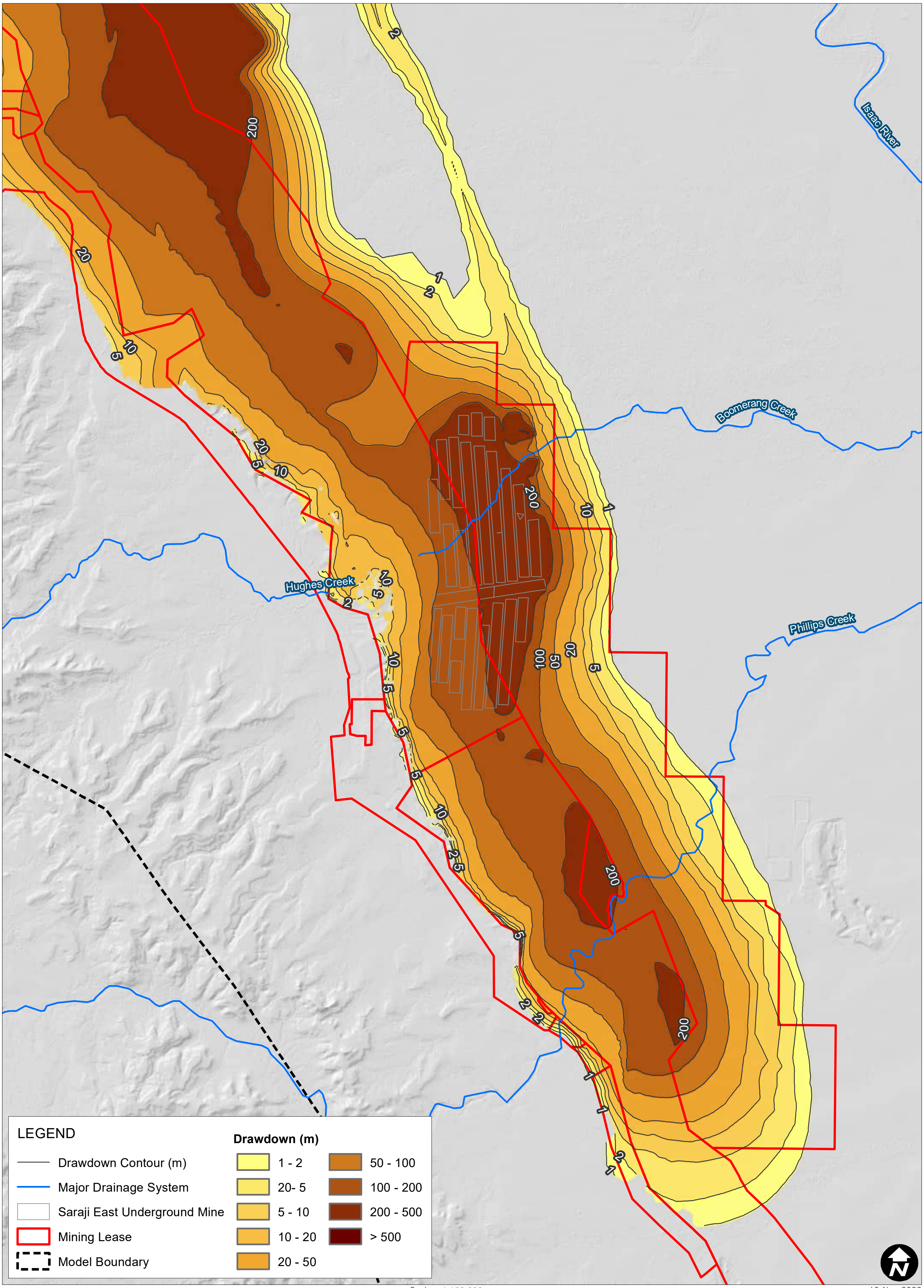

SLR
www.slrconsultingaustralia.com

Maximum Cumulative Drawdown in D Seam (Layer 18)

FIGURE 3-21

3.5 Predicted Groundwater Ingress

Project mine pit inflow volumes have been estimated as time weighted averages of the outflow reported by ZoneBudget software for drain cells representing mining at the SEMLP. The predicted inflows for both the SEMLP and the SRM open cut pits are presented in **Figure 3-22**.

As shown in **Figure 3-22**, inflows at the SEMLP are predicted to reach a maximum peak in year 16 with 500 ML/yr (1.4 ML/d). The average inflow rate at the SEMLP is 183 ML/yr (0.5 ML/d).. The current model includes all the recent model structure updates from site geological information and the changes to the hydraulic properties based on the new calibration undertaken on the more recent observation data.

The predicted groundwater inflows to the SRM open cut pits, due to size and strike length, are much larger than the SEMLP inflows between years 1 and 9, approximately 1,200 to 1,400 ML/yr (3.3 to 3.8 ML/d. It should be mentioned that year 9 is the final year of the approved SRM opencut mining. The inflows then decrease gradually and remain around 100 ML/yr (0.3 ML/d) between years 10 and 20. It should be noted that the drain cells representing the SRM open cut were kept active for the areas close to the SEMLP in order to ensure that the SRM pits will act as sink.

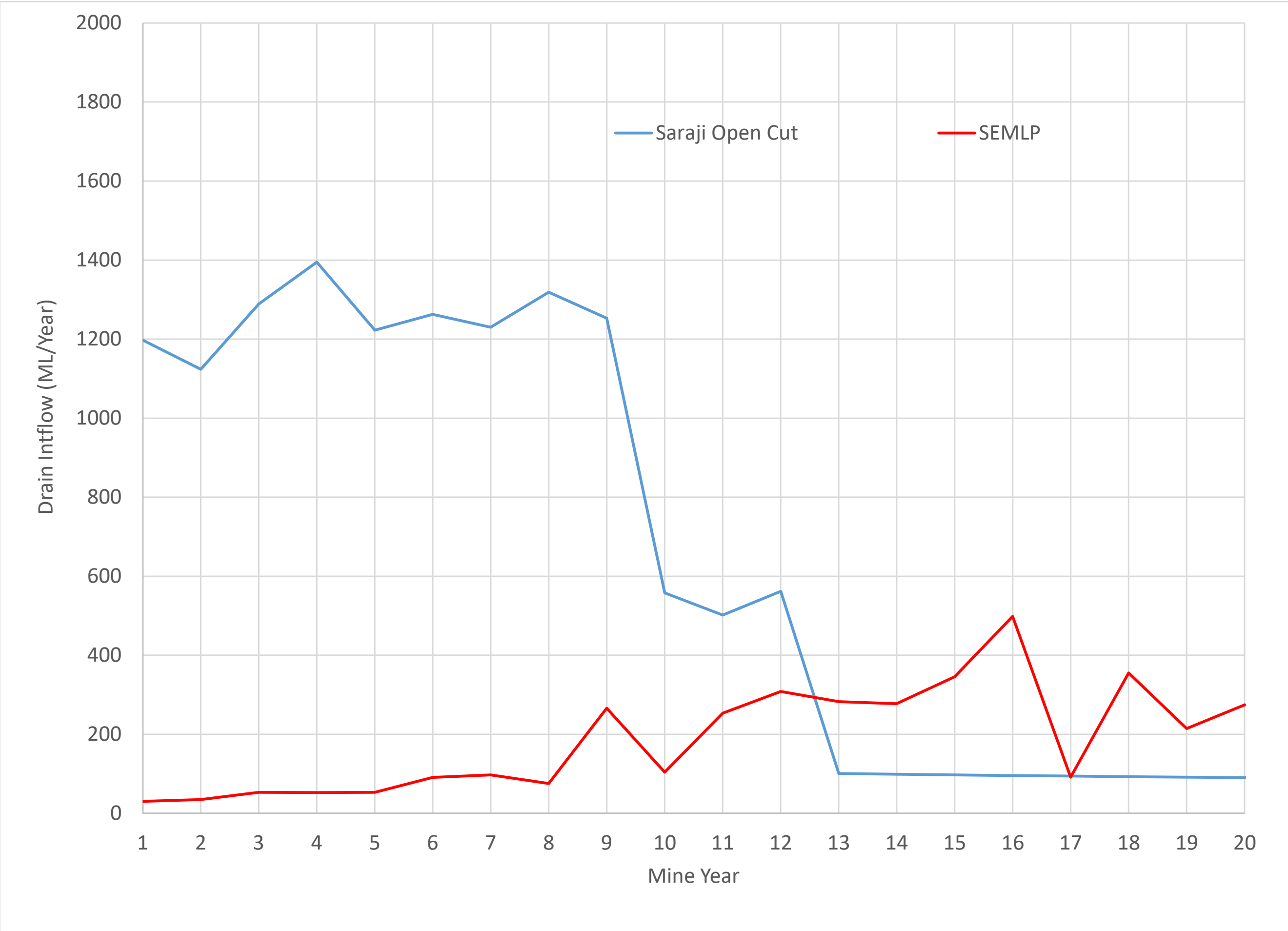

Figure 3-22 Predicted Groundwater Inflows

3.6 Incidental Water Impacts

3.6.1 Influence on Alluvium

The change in alluvial water resources was assessed by comparing water budgets for alluvial zones using the Project and Approved scenarios of the predictive model. Interference of the alluvial groundwater can occur due to the potential for increased leakage, due to goaf.

Over the extent of Boomerang Creek alluvium, the predicted loss of water from alluvium as a result of the SEMLP is predicted to be zero. With regards to the Isaac River alluvium, the model predicts that the alluvium take due to the SEMLP is also zero.

It should be noted that any change in flux below than 0.01 ML/d is beyond the model ability to be able to predict it. Therefore, any flux changes derived from the model that are below than 0.01 ML/d are considered to be in the range of model error.

3.6.2 Groundwater – Surface Water Interaction

The change in surface water drainage leakage to groundwater due to the SEMLP was assessed by comparing the River cell flow budgets for the Isaac River in the Project scenario against the Approved scenario. This comparison showed that over the life of the Project, the change in the Isaac River net flow attributable to the SEMLP is zero.

Boomerang, Hughes, and Plumtree creeks located within the SEMLP area are all set up with a stage height of 0.0 which means they are simulated as gaining systems (i.e., negative net flow). The results indicate that there is no change to the estimated net flow for the above creeks as the result of SEMLP.

4 Recovery Model

The post-mining recovery modelling included simulation of groundwater level recovery in the SEMLP underground workings as well as the SRM open cuts. A 2,000-year transient model was created to ascertain post-mining recovery.

All drain cells representing the SEMLP were removed at the start of the recovery period to allow groundwater levels in the underground workings and the overlying water-bearing strata to recover.

In the SRM open pits, all the mine areas changed to spoil and only the sections of open cut near the SEMLP and mined at the final year were not backfilled and remained as a void. The void cells were assigned high horizontal and vertical hydraulic conductivities (1,000 m/day) and storage parameters based on the compressibility of water (specific yield of 1.0, storage coefficient of 5.0 x 10^{-6} m^{-1}), to simulate free water movement within the cells. No extra recharge or evapotranspiration are applied to the voids, and it was assumed that it will be filled through groundwater recovery. With regards to the spoil, the horizontal hydraulic conductivity of 0.3 m/day and vertical hydraulic conductivity of 0.1 m/day is applied to the spoil. The storage parameters used for the spoil were a specific yield of 0.1 and a specific storage of 1.0 x 10^{-5} m^{-1}.

In the SEMLP area, the parameters adopted in the model cells to reflect mined-out areas and goaf effects were consistent with the properties at the end the prediction model that includes enhanced vertical and horizontal hydraulic conductivity in the fractured layers overlying longwall panels and specific yield set at 0.16 (16%) in the mined seam to replicate increased storage.

Figure 4-1 shows the predicted filling of the SEMLP workings over time. **Figure 4-1** shows the model predicts the groundwater system will reach equilibrium approximately 1,800 years post-mining. As shown in **Figure 4-1**, in both northern and southern longwall panels, the groundwater level recovers to approximately 176.5 mAHD, which is approximately 7.0 m above the pre-mining (all open cut and underground mining) groundwater levels. The pre-mining groundwater level was derived from steady state run. The ground levels are 197.6 and 187.1 m for the two points chosen at the northern and southern longwall panels. This indicates that the recovered water level is between 10-20 m below ground level.

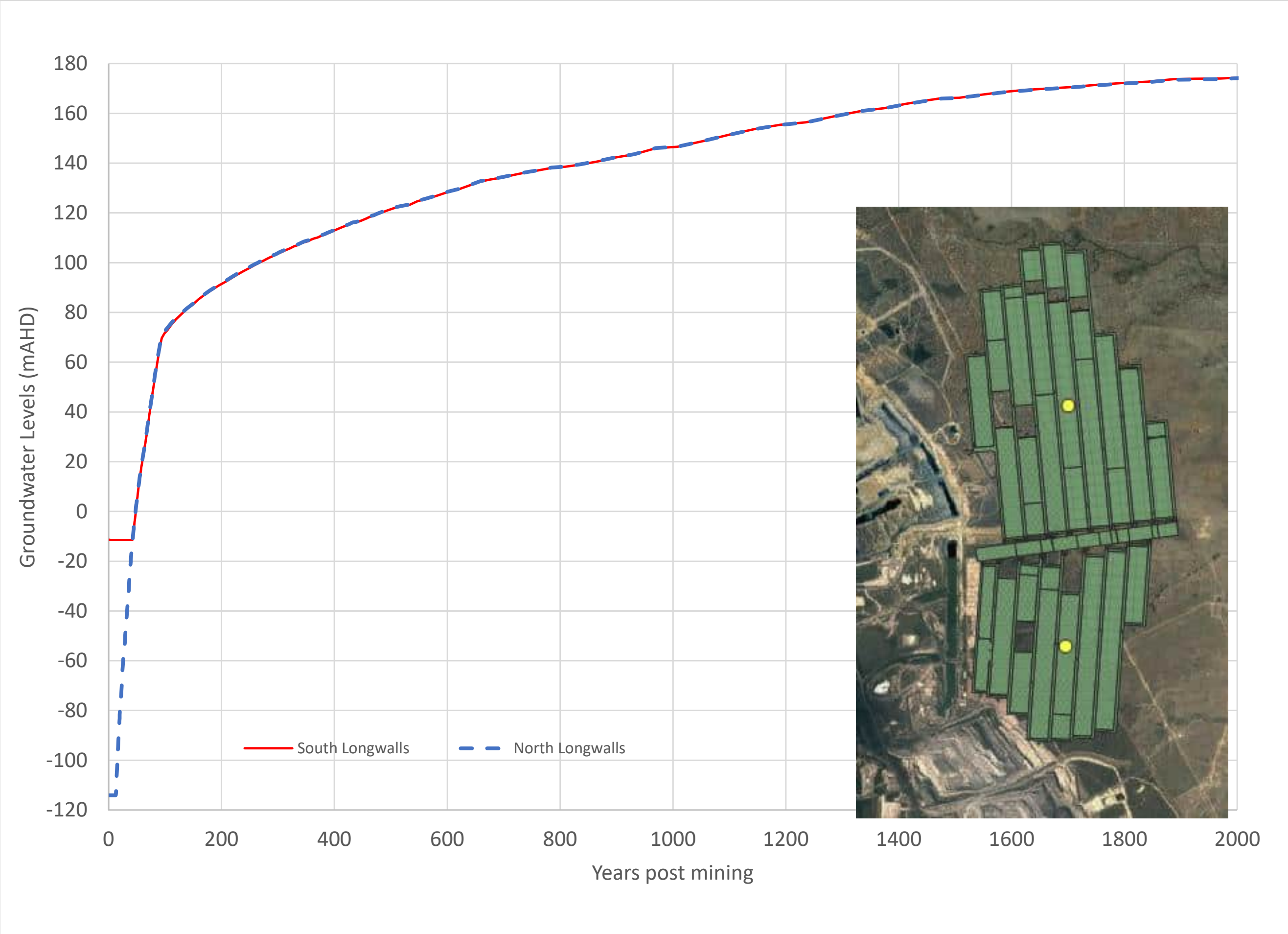

Figure 4-1 Predicted Groundwater Recovery within the SEMLP Workings

5 Sensitivity Analysis

5.1 Sensitivity Analysis

5.1.1 Calibration Identifiability

Identifiability describes a parameter's capability to be constrained by the model calibration. Identifiability values range from zero to one. As identifiability approaches one, the parameter is increasingly able to be constrained. Likewise, as values approach zero the parameter is increasingly unable to be constrained by the calibration and uncertainty of model results is not reduced through calibration.

The PEST utility GENLINPRED was used to provide an estimate of parameter identifiability for each of the model parameters. Estimated identifiability values for the calibrated parameters horizontal hydraulic conductivity, anisotropy, specific yield, and recharge are summarised in **Figure 5-1** through **Figure 5-5**.

Figure 5-1 indicates that in general the calibration process was successful in constraining the horizonal hydraulic conductivity. Notably, the horizontal hydraulic conductivity of Rewan Group, Leichhardt Seam, Vermont Seam, MCM D Seam and Q Seam units are well constrained by calibration (high identifiability values above 0.80).

The horizontal hydraulic conductivity of most of the faults generally has not been able to be constrained well during calibration, relative to their surrounding unit. The exception to this is the Isaac fault zone (i.e., Kx_Fault_1), which has been constrained during the calibration.

Identifiability of hydraulic conductivity anisotropy for model zones is presented in **Figure 5-2**. Anisotropy in the weathered Permian, Moranbah Coal Measures interburden, Fort Cooper Coal Measures interburden and Moranbah Coal Measures interburden have high identifiability values indicating these can be constrained and contribute to reducing model uncertainty. All other zones feature low values (equal to and below 0.40) and are less constrained by calibration.

Figure 5-3 shows that specific yield of Regolith, Rewan Group, and Isaac fault zone is highly identifiable, whilst other zones in the model domain have low identifiability.

Figure 5-4 shows that the specific storage of D seam appears to be the most identifiable parameters among the zones.

Figure 5-5 shows that the recharge zones for all the zones except the Isaac River Channel, are constrained by the calibration. Note that the stream channel alluvium represents a narrow zone along the Isaac River, with a small area relative to the other recharge zones. It is, therefore, considered less impactful to model predictions.

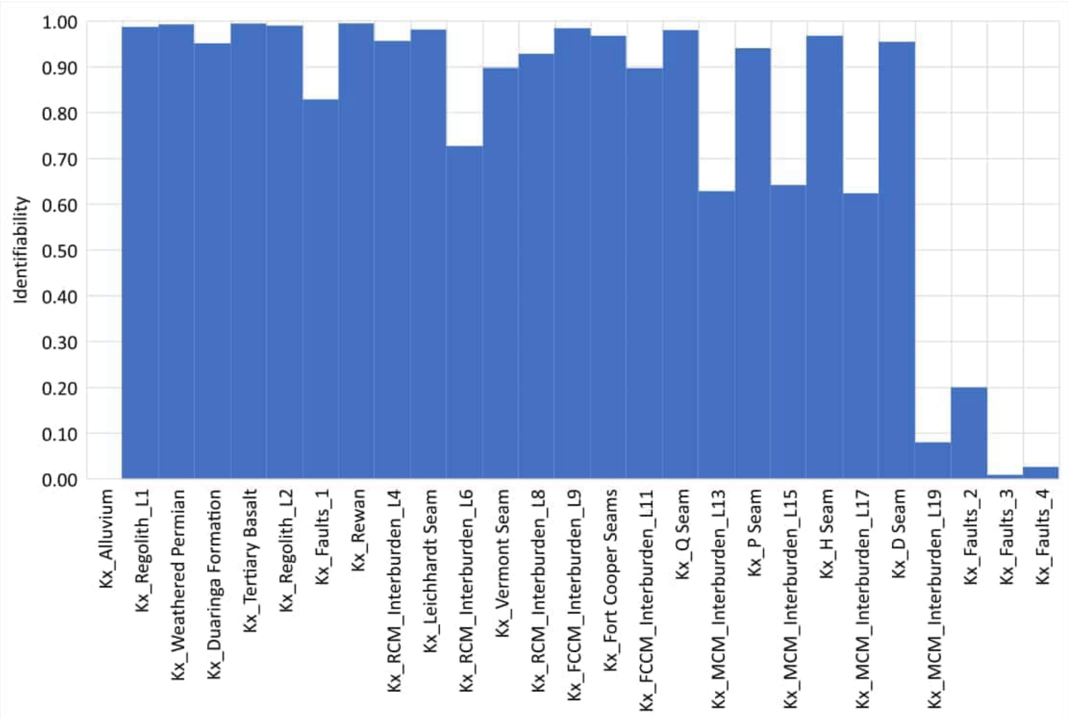

Figure 5-1 Identifiability – Horizontal Hydraulic Conductivity (Kx)

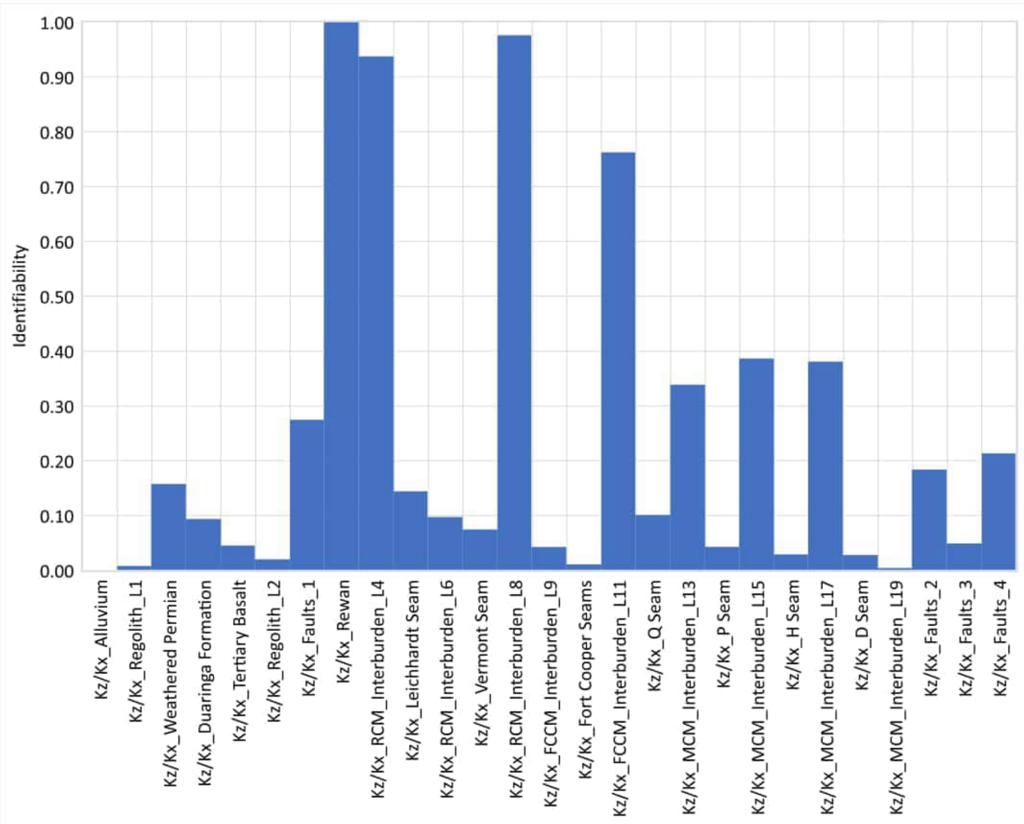

Figure 5-2 Identifiability – Anisotropy (Kv/Kx)

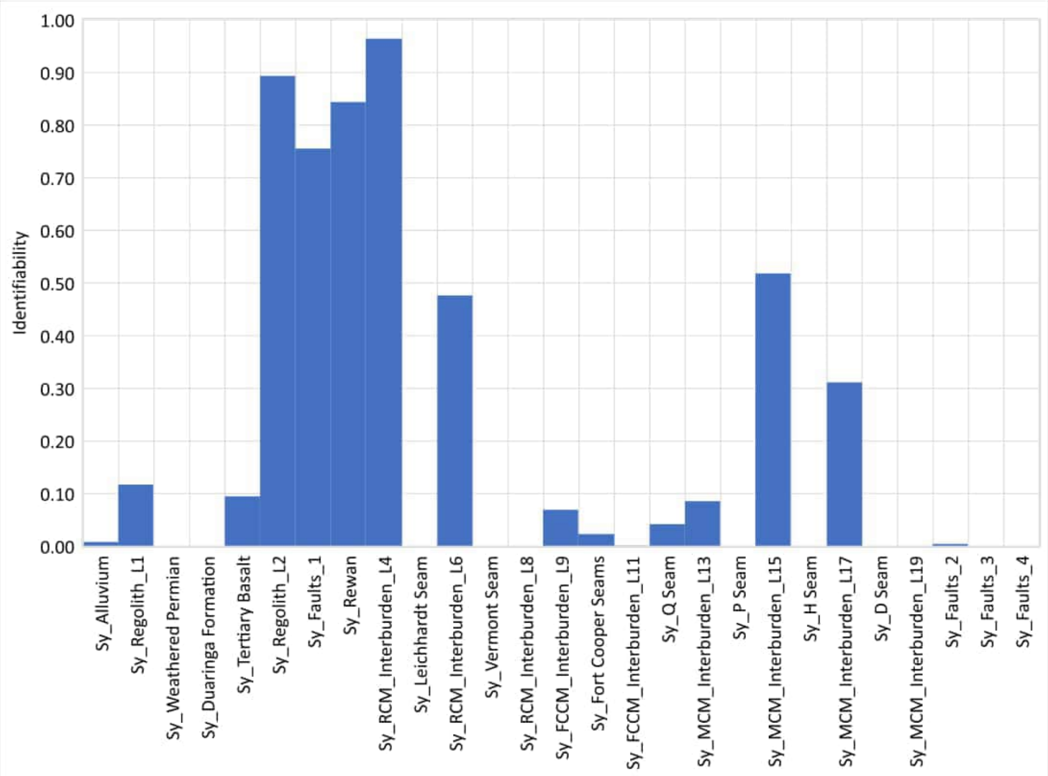

Figure 5-3 Identifiability – Specific Yield (Sy)

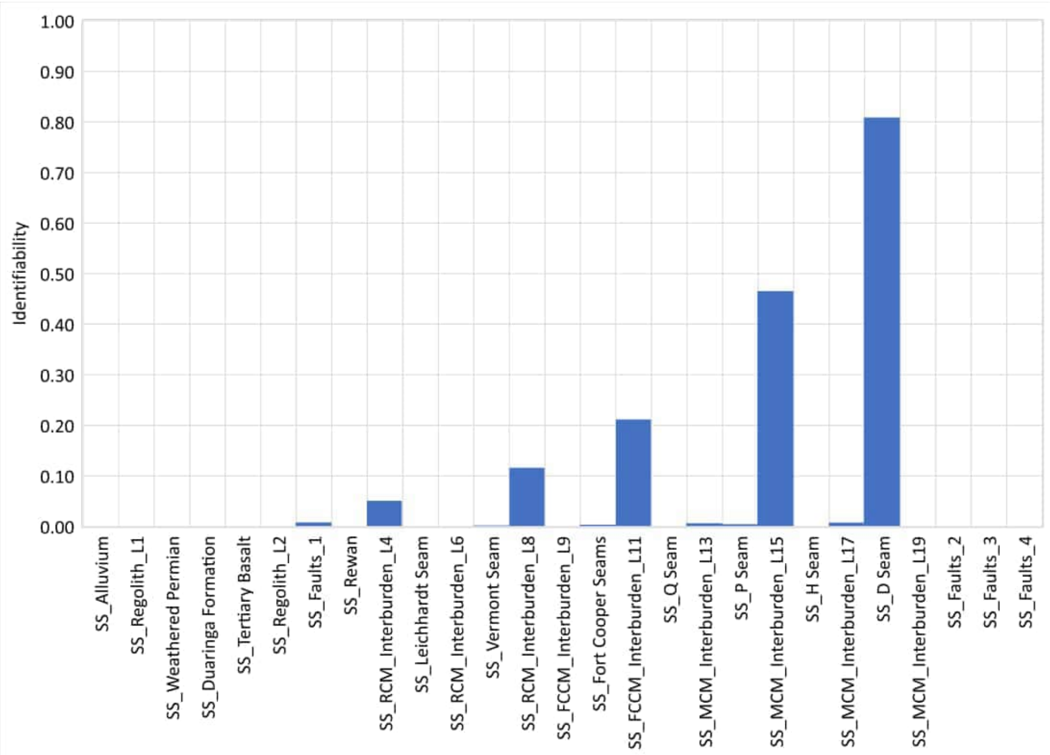

Figure 5-4 Identifiability – Specific Storage (SS)

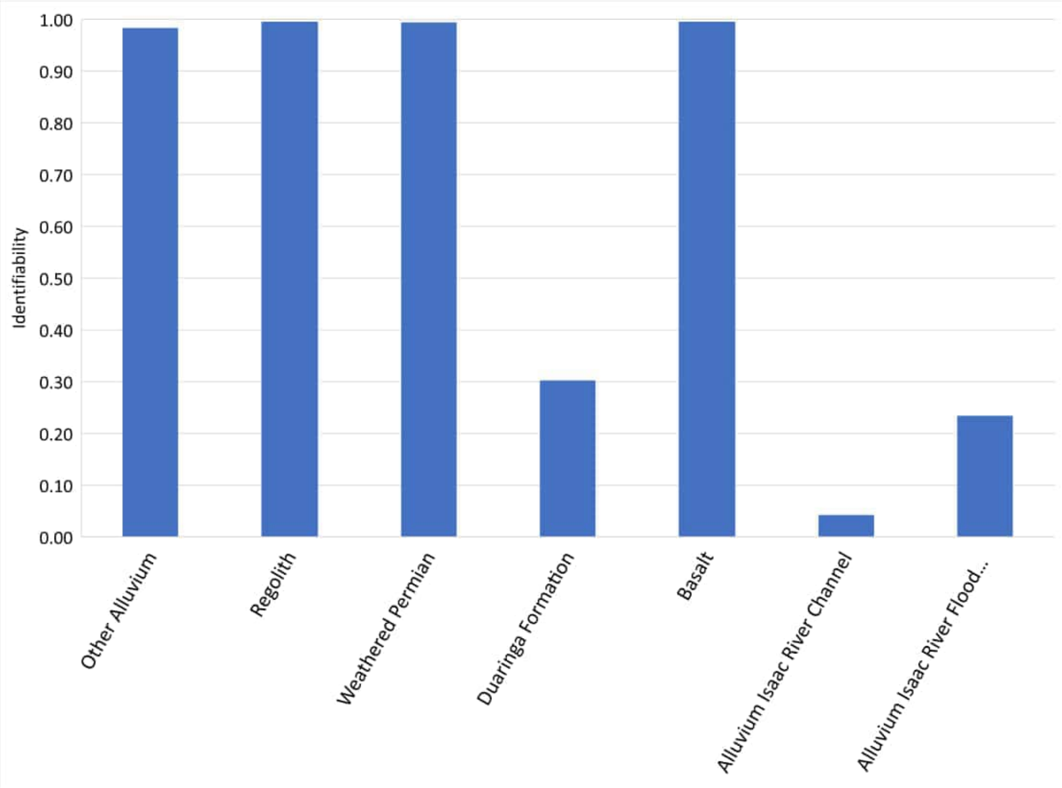

Figure 5-5 Identifiability – Recharge (RCH)

5.1.2 Prediction Identifiability

Prediction identifiability describes parameters capability on influencing the model predictions. To calculate the prediction identifiability the groundwater model is run once per each parameter. The predictions included in the analysis were the project only inflows and maximum incremental drawdowns. The analysis then utilised the GENLINPRED utility to provide an estimate of parameter identifiability for each of the model parameters.

As identifiability approaches one, the parameter is increasingly able to change model predictions. On the contrary, as values approach zero the parameter is increasingly unable to change model predictions.

The Murray Darling Basin Modelling Guidelines (MDBC, 2000) recommends classifying sensitivity by the resultant changes (or contribution) to the model calibration and predictions. According to this process models can be classified as one of the four main types:

- Type I: Insignificant changes to calibration (low identifiability) and prediction (low uncertainty contribution)
- Type II: Significant changes to calibration (high identifiability) – insignificant changes to predictions (low uncertainty contribution)
- Type III: Significant changes to calibration (high identifiability) –significant changes to predictions (high uncertainty contribution)
- Type IV: Insignificant changes to calibration (low identifiability) –significant changes to predictions (high uncertainty contribution).

Types I-III are of less concern, as these Types have an insignificant impact on model predictions or constrained by calibration. Type IV is classed as ‘a cause for concern’ as non-uniqueness in a model input might allow a range of valid calibrations but the choice of value impacts significantly on a prediction (MDBC, 2000).

To classify the sensitivity contribution to the model calibration and predictions for each model parameter, the calibration and prediction Identifiability were compared against each other for each parameter.

Figure 5-6 presents the relationship between the identifiability of the SEMLP inflows and the identifiability of the calibration. Sensitivity classifications for the sensitivity types have been assigned using judgement based on the range of the identifiability. The results show that the key parameters that require further work to reduce their influence on predictive uncertainty in relation to groundwater inflows include the specific yield of the Moranbah Coal Measures interburden (model layer 13) and anisotropy of the fault to the east of the SEMLP.

Figure 5-7 presents the relationship between identifiability of the maximum predicted drawdown and the identifiability of the calibration. Sensitivity classifications for the sensitivity types have been assigned using judgement based on the range of the posterior predictions. The results show that the key parameter that require further work to reduce its influence on predictive uncertainty in relation to the maximum drawdown extent are specific storage of the Moranbah Coal Measures interburden_L17 (i.e., interburden above the SEMLP coal seam mining target), specific yield for 2 overlying interburden layers (Layers 9 and 13) and the anisotropy of the fault to the east of the SEMLP.

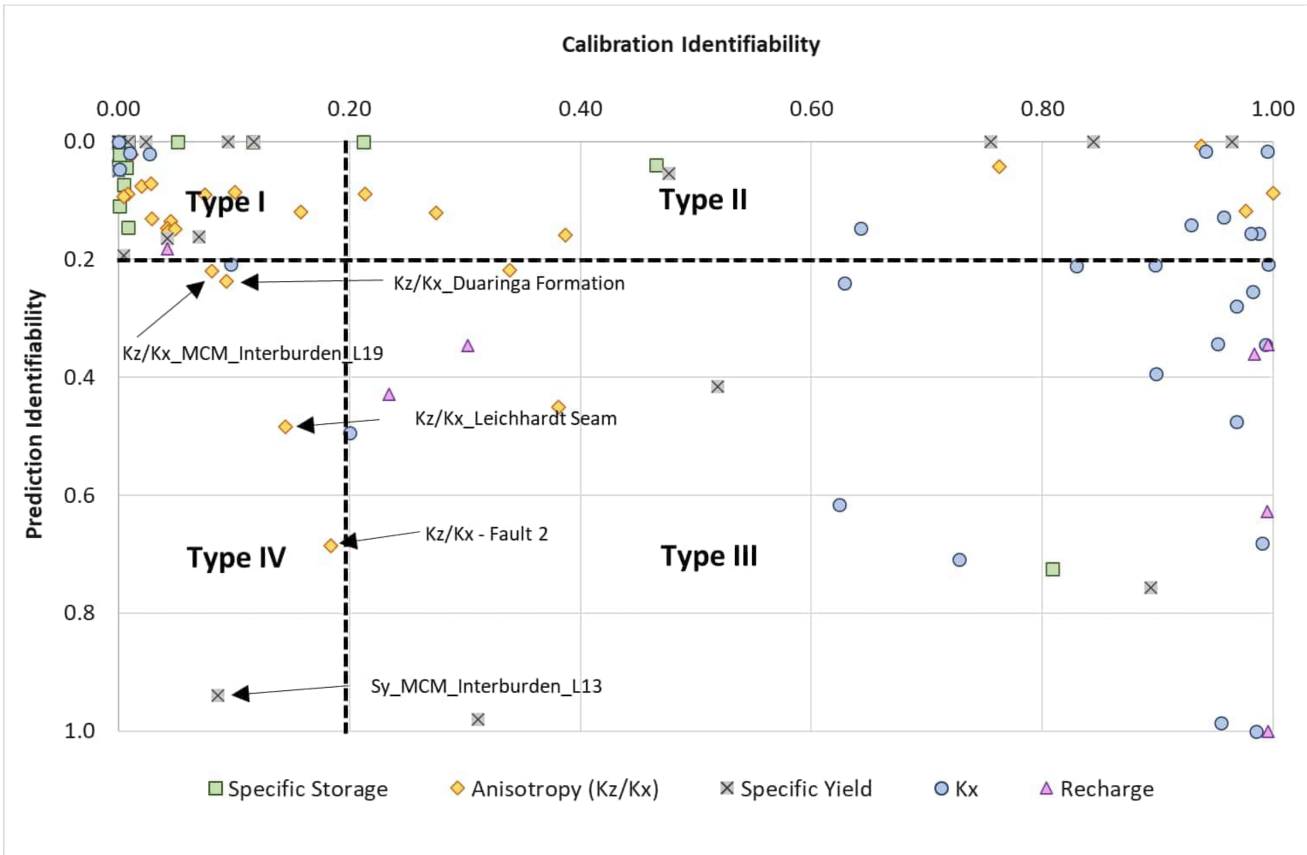

Figure 5-6 Uncertainty Contribution (predicted mine inflow) versus Identifiability

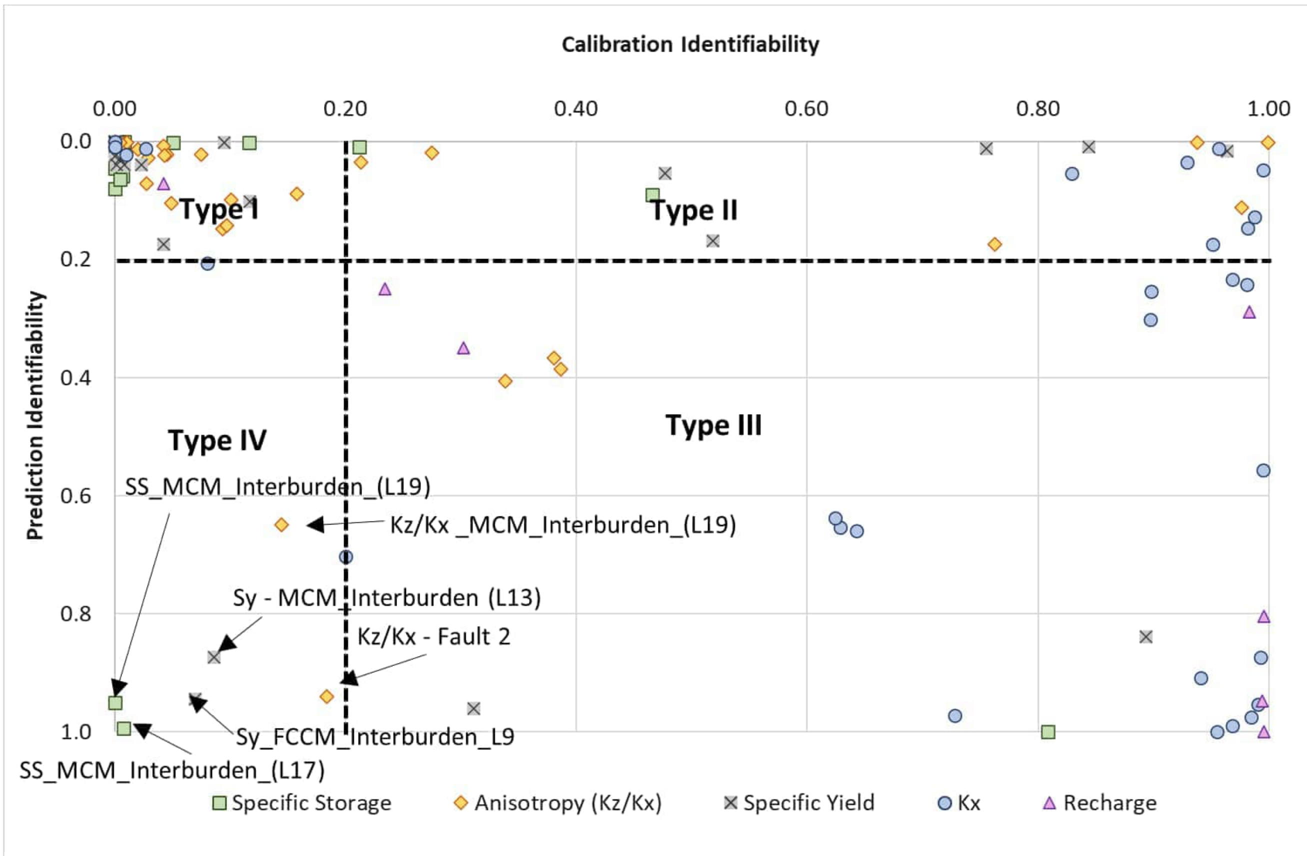

Figure 5-7 Uncertainty Contribution (maximum incremental drawdown) versus Identifiability

6 Uncertainty Analysis

A Type 3 Monte Carlo uncertainty analysis (IESC, 2018) was undertaken to estimate the uncertainty in the future impacts predicted by the model. This method operates by generating numerous alternative sets of input parameters to the deterministic groundwater flow model (realisations), executing the model independently for each realisation, and then aggregating the results for statistical analysis.

The first step in Monte Carlo analysis is to define the parameter distribution and range. For SEMLP, the parameters are assumed to be log-normally distributed around the optimum value derived from the calibration and the standard deviation attributed to the log (base 10) of parameter is 0.5. The distribution for each parameter were checked and constrained such that upper or lower ranges do not go beyond ranges in literature for physical constraints. 550 model realisations were generated, each having differing values of key parameters. The realisations were run, and calibration quality was assessed.

Of the 550 model runs, 95 model runs were accepted as sufficiently calibrated, with SRMS values ranging between 5.9% and 7.9%. These were used in all model scenarios (Project Mining, Approved Mining) and statistically analysed for uncertainty analysis.

6.1 Parameter Distribution

Table 6-1 to **Table 6-5** show the parameter ranges explored during the uncertainty analysis simulation.

Parameters were assumed to possess a log-Normal distribution. Instead of simple random sampling, the Latin Hypercube Sampling (LHS) method was used to create random realisations from parameter distribution. LHS aims to spread the sample points evenly across all possible values. In doing so, it divides parameter space into N intervals of equal probability and chooses one sample from each interval. The generated random numbers derived from LHS approach is distributed sufficiently across the parameter space even at the small sample size. The main advantage of LHS over simple random sampling is that a lower number of realisations are needed to obtain a reasonable convergence of the uncertainty results. The parameter distributions for prior (i.e. from the 550 model realisations) and posterior (i.e. from 95 accepted realisations) are provided as **Appendix F**.

Upon review of parameter distributions, it was noted that the horizontal hydraulic conductivity of Alluvium for the basecase (i.e. the one used in **Section 2.6**) is at the upper range of parameter distribution. **Figure 6-1** presents the parameter distribution of horizontal hydraulic conductivity of Alluvium from the uncertainty analyses and the value used in the basecase scenario. As **Figure 6-1** shows, the majority of realisations are centred around the 10 m/day with a few of realisations up to 50 m/day. This indicates that although 54 m/day used in the basecase is considered to be extreme, the uncertainty analysis results are based on a more probable value (i.e. 10 m/day). In addition, the sensitivity analysis in **Section 5** indicates the horizontal hydraulic conductivity of alluvium is considered to be type 1 meaning that it will not have significant influence on the modelling predictions.

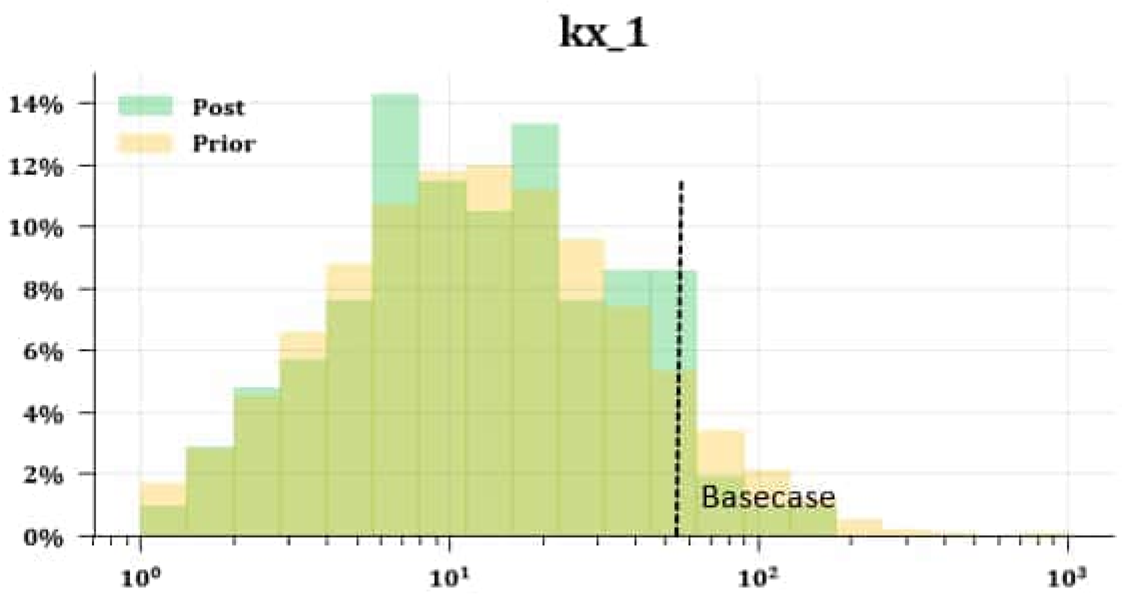

Prior : Prior distribution from 550 realisations. Post : Posterior distribution from 95 accepted realisations

Figure 6-1 Horizontal Hydraulic Conductivity of Alluvium Parameter Distribution

Table 6-1 Uncertainty Parameter Range for Horizontal Hydraulic Conductivity

Zone	Layer - Unit	Horizontal Hydraulic Conductivity (m/day)	
		Mean (Log10)	Constraint
1	Layer 1 - Alluvium	1.08	No constraint
2	Layer 1 - Regolith	0.00	< Kx_Alluvium
3	Layer 1 - Weathered Permian	-0.19	< Kx_Alluvium
4	Layer 1 - Duaringa Formation	-0.30	< Kx_Alluvium
5	Layer 1/2 - Tertiary Basalt	0.51	< Kx_Alluvium
6	Layer 2 - Regolith	0.00	< Kx_Alluvium
7	Layer 3-19- Faults_zone1	-0.91	No constraint
8	Layer 3-Rewan	-2.63	< Kx_Alluvium
9	Layer 4 - RCM O/B	-2.16	< Kx_Alluvium
10	Layer 5 - Leichhardt Seam	-1.02	< Kx_Alluvium
11	Layer 6 - RCM I/B	-2.93	< Kx_Alluvium
12	Layer 7 - Vermont Seam	-1.96	< Kx_Alluvium
13	Layer 8 - RCM U/B	-3.00	< Kx_Alluvium
14	Layer 9 - FCCM O/B	-3.00	< Kx_Alluvium
15	Layer 10 - FCCM Seam	-2.94	< Kx_Alluvium
16	Layer 11 - FCCM U/B	-0.39	< Kx_Alluvium
17	Layer 12 - Q Seam	-1.00	< Kx_Alluvium

Zone	Layer - Unit	Horizontal Hydraulic Conductivity (m/day)	
		Mean (Log10)	Constraint
18	Layer 13 - MCM U/B	0.69	< Kx_Alluvium
19	Layer 14 - P Seam	0.69	< Kx_Alluvium
20	Layer 15 -MCM I/B	-0.52	< Kx_Alluvium
21	Layer 16 - H Seam	-0.98	< Kx_Alluvium
22	Layer 17 - MCM I/B	-0.65	< Kx_Alluvium,
23	Layer 18 - D Seam	-1.00	< Kx_Alluvium
24	Layer 19 - MCM U/B	-0.56	< Kx_Alluvium
25	Layer 3-19 - Faults zone 2	-0.46	No constraint
26	Layer 7 - Faults zone 3	-0.32	No constraint
27	Layer 8 - Faults zone 4	-0.40	No constraint
28	Layer 3-7 Faults zone 5	-3.00	No constraint

Standard deviation = 0.5 order of magnitude for all units.
O/B = Overburden.
I/B = Interburden.
U/B = Underburden.
RCM = Rangal Coal Measures.
FCCM = Fort Cooper Coal Measures.
MCM = Moranbah Coal Measures.

Table 6-2 Uncertainty Parameter Range for Vertical to Horizontal Conductivity (Kv/Kx)

Zone	Layer - Unit	Anisotropy (Kv/Kx)	
		Mean (Log10)	Constraint
1	Layer 1 - Alluvium	-0.70	< 1.0
2	Layer 1 - Regolith	-1.00	< 1.0
3	Layer 1 - Weathered Permian	-1.18	< 1.0
4	Layer 1 - Duaringa Formation	-1.25	< 1.0
5	Layer 1/2 - Tertiary Basalt	-1.00	< 1.0
6	Layer 2 - Regolith	-1.52	< 1.0
7	Layer 3-19 - Faults zone1	-1.02	< 1.0
8	Layer 3 - Rewan	-1.11	< 1.0
9	Layer 4 - RCM O/B	-1.01	< 1.0
10	Layer 5 - Leichhardt Seam	-2.66	< 1.0
11	Layer 6 - RCM I/B	-0.97	< 1.0
12	Layer 7 - Vermont Seam	-1.43	< 1.0
13	Layer 8 - RCM U/B	-2.65	< 1.0
14	Layer 9 - FCCM O/B	-1.00	< 1.0
15	Layer 10 - FCCM Seam	-0.79	< 1.0
16	Layer 11 - FCCM U/B	-2.33	< 1.0
17	Layer 12 - Q Seam	-0.70	< 1.0
18	Layer 13 - MCM U/B	-0.70	< 1.0
19	Layer 14 - P Seam	-1.29	< 1.0
20	Layer 15 -MCM I/B	-1.33	< 1.0
21	Layer 16 - H Seam	-2.14	< 1.0
22	Layer 17 - MCM I/B	-1.21	< 1.0
23	Layer 18 - D Seam	-1.42	< 1.0
24	Layer 19 - MCM U/B	-2.23	< 1.0
25	Layer 3-19 - Faults zone 2	-1.02	< 1.0
26	Layer 7 - Faults zone 3	-2.99	< 1.0
27	Layer 8 - Faults zone 4	-2.21	< 1.0
28	Layer 3-7 - Faults zone 5	-2.00	< 1.0

Standard deviation = 0.5 order of magnitude for all units.

Table 6-3 Uncertainty Parameter Range for Specific Yield

Zone	Layer - Unit	Specific Yield (Sy)	
		Mean (Log10)	Constraint
1	Layer 1 - Alluvium	-1.60	< 0.20
2	Layer 1 - Regolith	-1.67	< Sy_Alluvium; < 0.05
3	Layer 1 - Weathered Permian	-2.73	< Sy_Alluvium; < 0.05
4	Layer 1 - Duaringa Formation	-1.71	< Sy_Alluvium; < 0.05
5	Layer 1/2 - Tertiary Basalt	-1.74	< Sy_Alluvium; < 0.05
6	Layer 2 - Regolith	-1.30	< Sy_Alluvium; < 0.05
7	Layer 3-19- Faults_zone 1	-2.09	< Sy_Alluvium; < 0.05
8	Layer 3-Rewan	-2.02	< Sy_Alluvium; < 0.05
9	Layer 4 - RCM O/B	-2.00	< Sy_Alluvium; < 0.02
10	Layer 5 - Leichhardt Seam	-3.00	< Sy_Alluvium; < 0.02
11	Layer 6 - RCM I/B	-2.00	< Sy_Alluvium; < 0.02
12	Layer 7 - Vermont Seam	-2.68	< Sy_Alluvium; < 0.02
13	Layer 8 - RCM U/B	-2.40	< Sy_Alluvium; < 0.02
14	Layer 9 - FCCM O/B	-2.98	< Sy_Alluvium; < 0.02
15	Layer 10 - FCCM Seam	-2.46	< Sy_Alluvium; < 0.02
16	Layer 11 - FCCM U/B	-2.34	< Sy_Alluvium; < 0.02
17	Layer 12 - Q Seam	-3.00	< Sy_Alluvium; < 0.02
18	Layer 13 - MCM U/B	-2.76	< Sy_Alluvium; < 0.02
19	Layer 14 - P Seam	-2.80	< Sy_Alluvium; < 0.02
20	Layer 15 -MCM I/B	-2.57	< Sy_Alluvium; < 0.02
21	Layer 16 - H Seam	-2.74	< Sy_Alluvium; < 0.02
22	Layer 17 - MCM I/B	-2.99	< Sy_Alluvium; < 0.02
23	Layer 18 - D Seam	-3.00	< Sy_Alluvium; < 0.02
24	Layer 19 - MCM U/B	-2.42	< Sy_Alluvium; < 0.02
25	Layer 3-19 - Faults zone 2	-2.60	< Sy_Alluvium; < 0.05
26	Layer 7 - Faults zone 3	-2.22	< Sy_Alluvium; < 0.05
27	Layer 8 - Faults zone 4	-2.67	< Sy_Alluvium; < 0.05
28	Layer 3-7 Faults zone 5	-2.00	< Sy_Alluvium; < 0.05

Standard deviation = 0.5 order of magnitude for all units.

Table 6-4 Uncertainty Parameter Range for Specific Storage (1/m)

Zone	Layer - Unit	Specific Storage (SS) 1/m	
		Mean (Log10)	Constraint
1	Layer 1 - Alluvium	-5.83	< 1 x 10^{-5}
2	Layer 1 - Regolith	-5.55	< SS_Alluvium;< 1 x 10^{-5}
3	Layer 1 - Weathered Permian	-6.99	< SS_Alluvium;< 1 x 10^{-5}
4	Layer 1 - Duaringa Formation	-6.49	< SS_Alluvium;< 1 x 10^{-5}
5	Layer 1/2 - Tertiary Basalt	-6.17	< SS_Alluvium;< 1 x 10^{-5}
6	Layer 2 - Regolith	-6.75	< SS_Alluvium;< 1 x 10^{-5}
7	Layer 3-19- Faults zone1	-5.52	< SS_Alluvium;< 1 x 10^{-5}
8	Layer 3-Rewan	-6.25	< SS_Alluvium;< 1 x 10^{-5}
9	Layer 4 - RCM O/B	-5.48	< SS_Alluvium;< 1 x 10^{-5}
10	Layer 5 - Leichhardt Seam	-6.30	< SS_Alluvium;< 1 x 10^{-5}
11	Layer 6 - RCM I/B	-6.30	< SS_Alluvium;< 1 x 10^{-5}
12	Layer 7 - Vermont Seam	-6.30	< SS_Alluvium;< 1 x 10^{-5}
13	Layer 8 - RCM U/B	-5.89	< SS_Alluvium;< 1 x 10^{-5}
14	Layer 9 - FCCM O/B	-6.28	< SS_Alluvium;< 1 x 10^{-5}
15	Layer 10 - FCCM Seam	-5.64	< SS_Alluvium;< 1 x 10^{-5}
16	Layer 11 - FCCM U/B	-5.66	< SS_Alluvium;< 1 x 10^{-5}
17	Layer 12 - Q Seam	-5.60	< SS_Alluvium;< 1 x 10^{-5}
18	Layer 13 - MCM U/B	-5.43	< SS_Alluvium;< 1 x 10^{-5}
19	Layer 14 - P Seam	-5.64	< SS_Alluvium;< 1 x 10^{-5}
20	Layer 15 -MCM I/B	-5.30	< SS_Alluvium;< 1 x 10^{-5}
21	Layer 16 - H Seam	-6.16	< SS_Alluvium;< 1 x 10^{-5}
22	Layer 17 - MCM I/B	-5.87	< SS_Alluvium;< 1 x 10^{-5}
23	Layer 18 - D Seam	-5.32	< SS_Alluvium;< 1 x 10^{-5}
24	Layer 19 - MCM U/B	-6.15	< SS_Alluvium;< 1 x 10^{-5}
25	Layer 3-19 - Faults zone 2	-6.24	< SS_Alluvium;< 1 x 10^{-5}
26	Layer 7 - Faults zone 3	-5.42	< SS_Alluvium;< 1 x 10^{-5}
27	Layer 8 - Faults zone 4	-6.13	< SS_Alluvium;< 1 x 10^{-5}
28	Layer 3-7 Faults zone 5	-5.00	< SS_Alluvium;< 1 x 10^{-5}

Standard deviation = 0.5 order of magnitude for all units.

Table 6-5 Uncertainty Ranges for Recharge Rates

Zone	Unit	Mean % of rainfall	Constraints
1	Other Alluvium	0.23	No Constraint
2	Regolith	0.01	< Other Alluvium
3	Weathered Permian	0.06	< Other Alluvium
4	Duaringa Formation	0.01	< Other Alluvium
5	Tertiary Basalt	0.32	No Constraint
6	Alluvium Isaac River Channel	0.53	No Constraint
7	Alluvium Isaac River	0.23	No Constraint

Standard deviation = 0.5 order of magnitude for all units.

6.2 Uncertainty Results

6.2.1 Number of Realisations

65 realisations were selected as calibrated realisations and used for uncertainty analysis. The predictive model was run using the 65 parameters sets. The results from the predictive model were used to conduct statistical analyses to assess if additional realisations were likely to provide results that would significantly change the reported predictive results. The 95 % confidence interval was calculated for the mine inflows and the maximum drawdown.

Figure 6-2 and **Figure 6-3** show the 95 % confidence intervals of the median and maximum drawdown and predicted inflows, as well as the variance of the median and maximum drawdown and predicted inflows as more realisations are added to the uncertainty analysis. For example, the 95% confidence interval for the maximum drawdown is calculated by first estimating the maximum drawdown for each realisation and then calculating the 95 % confidence interval of the maximum drawdowns as each realisation is added to the dataset. As shown in **Figure 6-2** and **Figure 6-3**, additional realisations will not significantly increase or decrease the confidence intervals of predictions of mine inflows and maximum drawdowns. Therefore, the results from the 65 realisations are considered sufficient for the estimation of uncertainty with respect to inflows and other prediction variables.

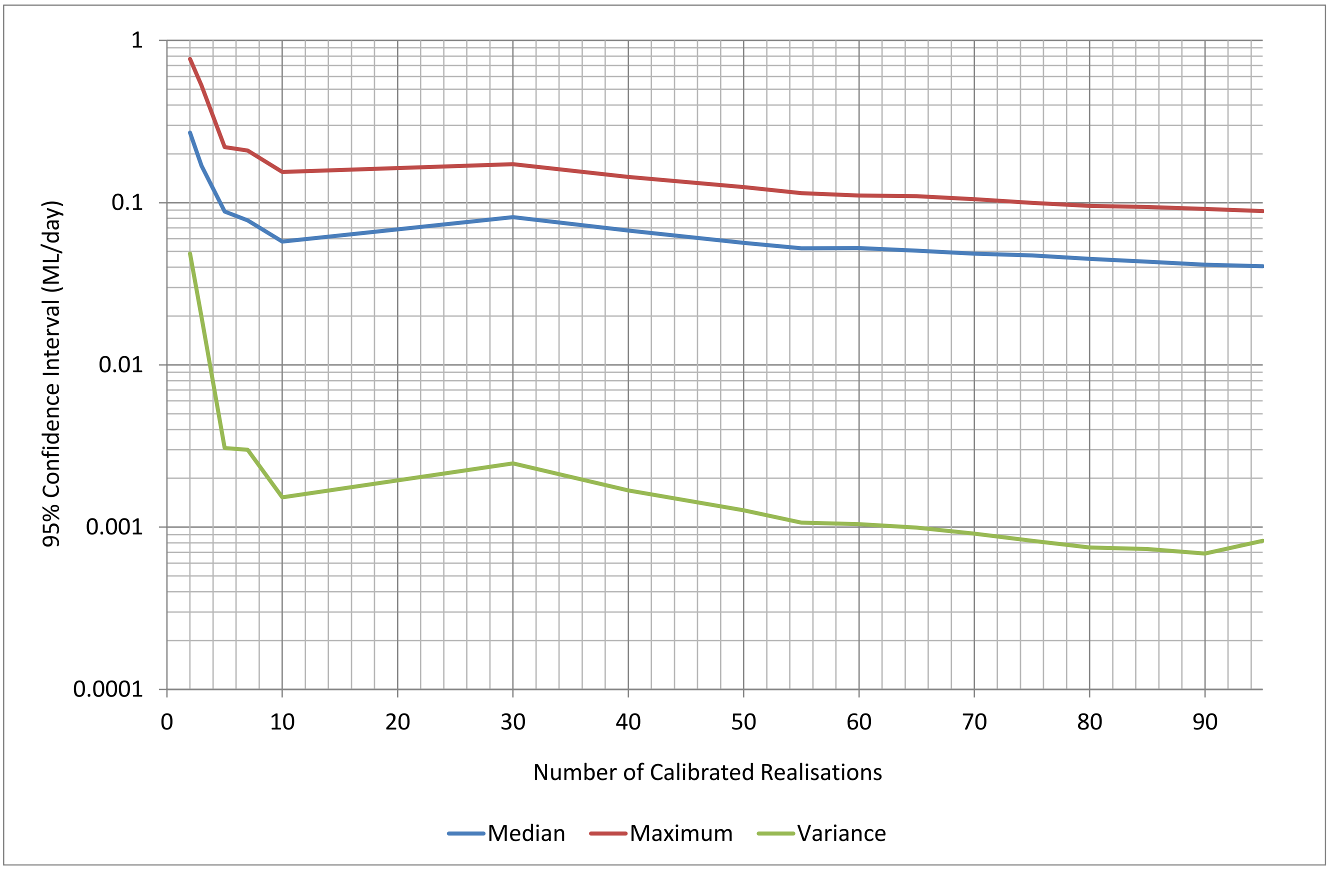

Figure 6-2 95 % Confidence Interval for Pit Inflows

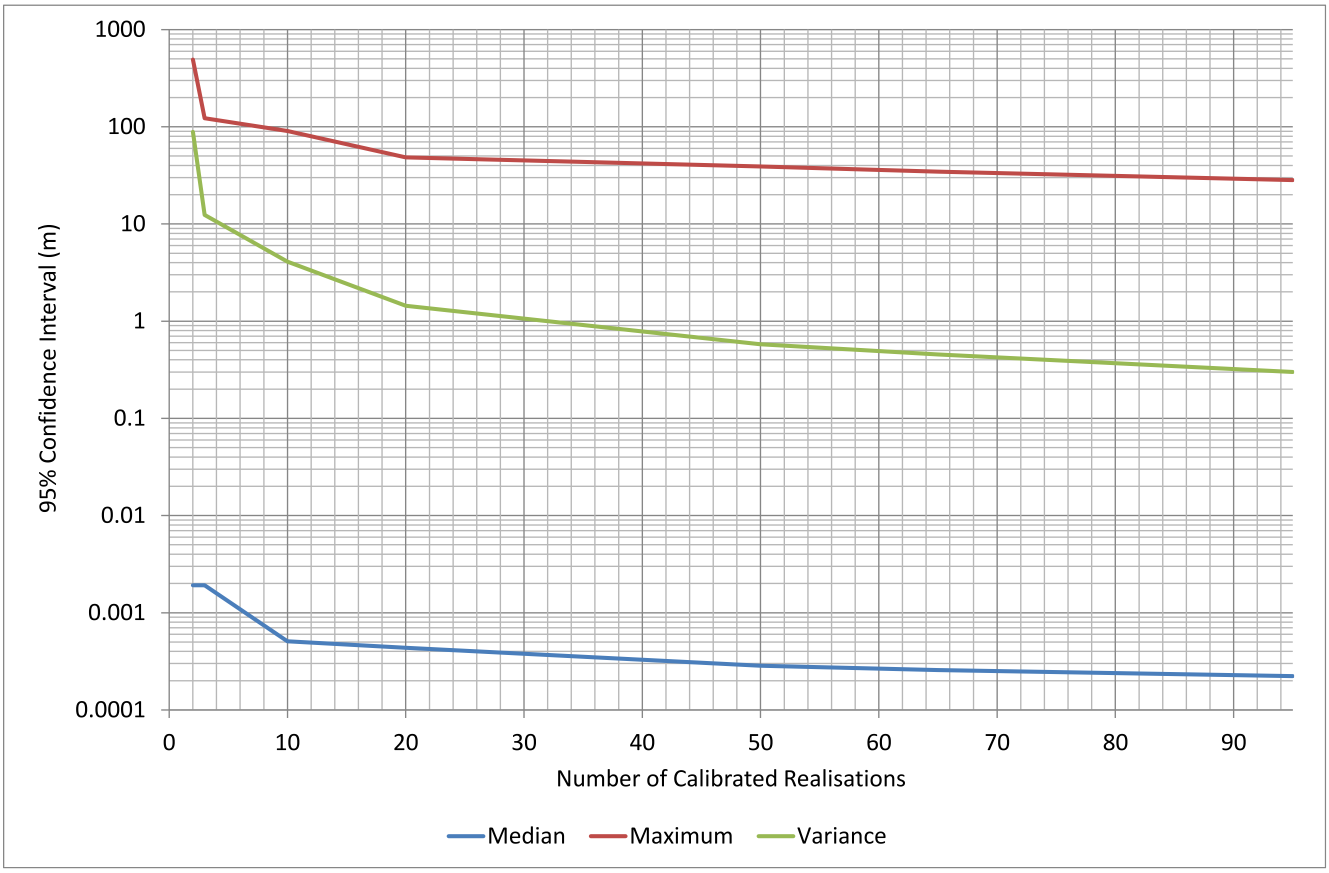

Figure 6-3 95 % Confidence Interval for Maximum Drawdowns

6.2.2 Uncertainty of Mine Ingress

Figure 6-4shows the predicted inflows for the SEMLP and different percentiles including 10th, 33rd, 50th, 67th and 90th prediction bounds. Based on the IESC (2018) guidelines these percentiles represent:

- 10th percentile indicates it is very likely the outcome is larger than this value,
- 10th – 33rd indicates it is likely that the outcome is larger than this value,
- 33rd - 67th indicate it is as likely as not that the outcome is larger or smaller than this value,
- 67th - 90th indicates it is unlikely that the outcome is larger than this value, and
- 90th percentile indicates it is very unlikely the outcome is larger than this value.

The bounds in the figure demonstrate the uncertainty within the predicted inflow rate. The bounds show that the calibrated model generally match the 50th percentile.

As shown in **Figure 6-4**, the maximum mine inflow in the uncertainty analysis was 1,188 ML/yr (3.25 ML/d) (i.e. very unlikely that the outcome is larger than this value). The average inflows for the 10th to 90th percentiles are 111.4 ML/yr (0.31 Ml/d) and 271.5 ML/yr (0.74 ML/day) respectively.

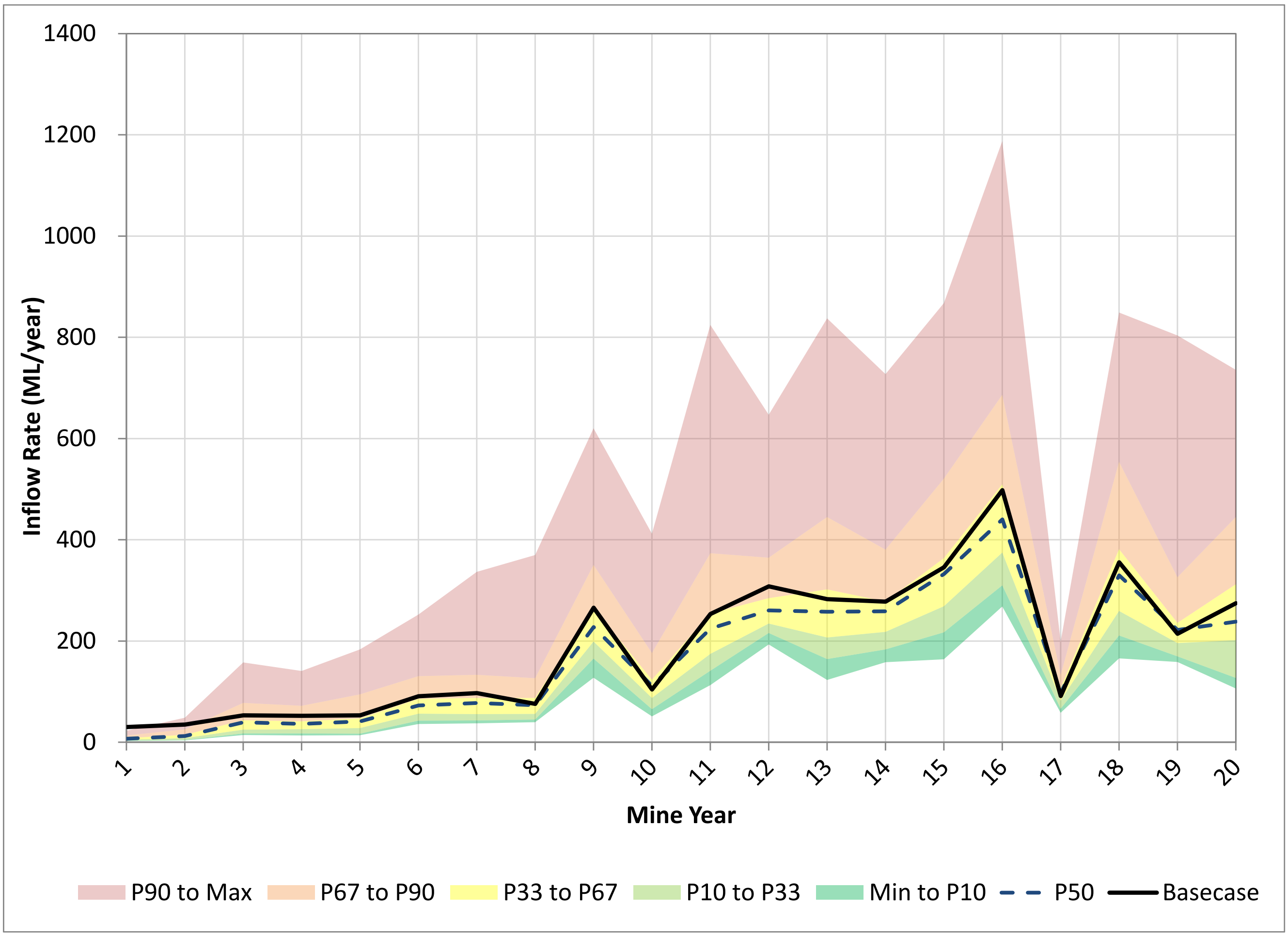

Figure 6-4 Mine Inflow Uncertainty

6.2.3 Groundwater Drawdowns

To illustrate the level of uncertainty in the extent of predicted drawdown, the 1 m drawdown due SEMLP project is compared to 5th, 50th and 95th percentiles maximum drawdown from the uncertainty analysis.

Figure 6-5 shows the 5th, 50th and 95th percentile maximum drawdowns in Alluvium. The uncertainty results indicate that the SEMLP project does not impact alluvium even at the 95th percentile (i.e., the most unlikely percentile).

Figure 6-6 shows the uncertainty in the extent of predicted 1 m maximum incremental drawdown in regolith. As shown in this figure, the 5th, 50th and 95th percentile maximum drawdowns in the regolith are localised around the Northern panels at SEMLP. With respect to the 95th percentile, the drawdown extends approximately 5 km northeast of SEMLP.

Figure 6-7 and **Figure 6-8** show the uncertainty in the extent of predicted 1 m maximum incremental drawdown in the Q Seam and D Seam. The figures show that the 95th percentile drawdown in H Seam and D Seam extends between 10 and 12 km to the northwest and southeast of the SEMLP.

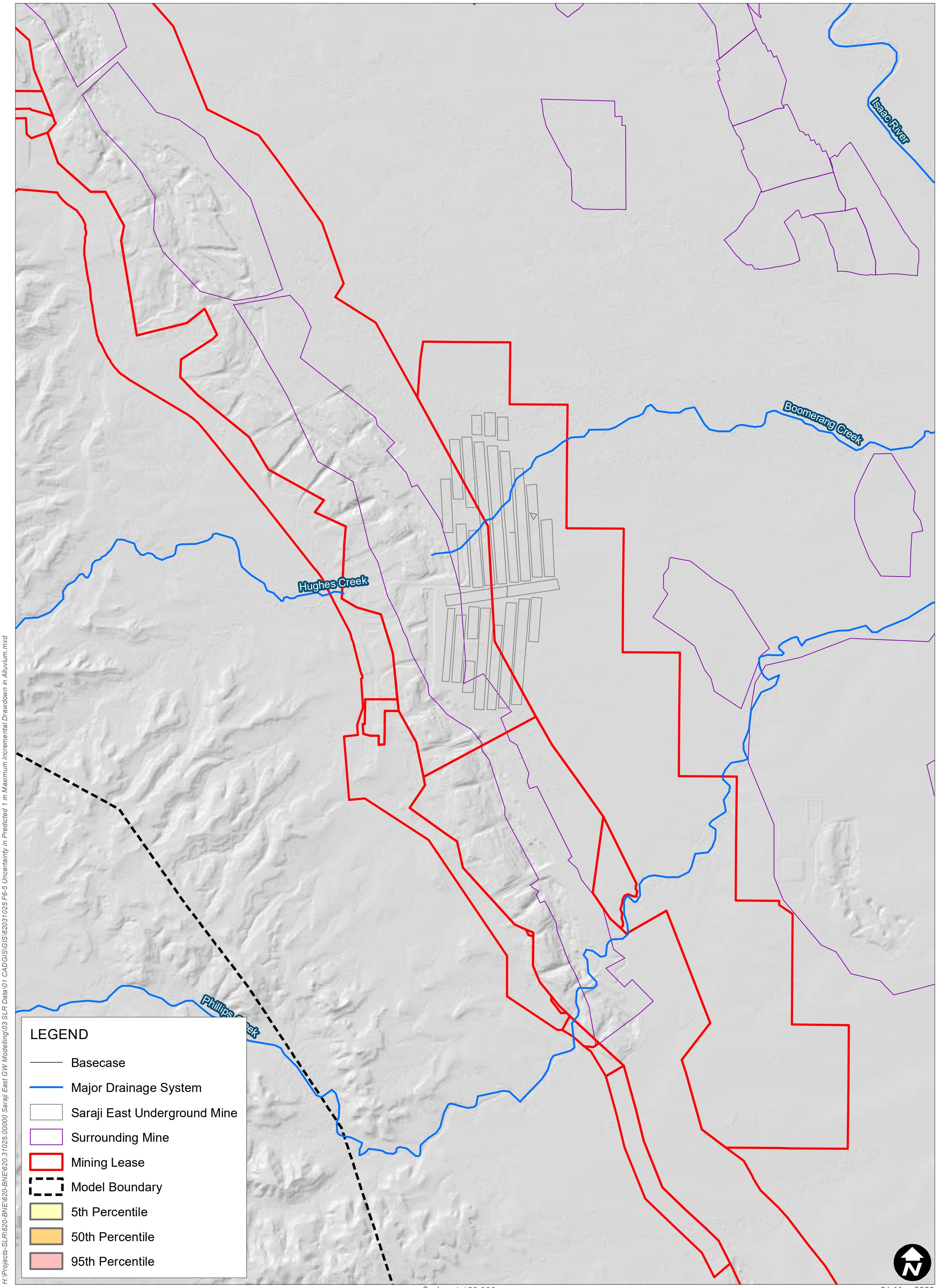

Scale: 1:150,000
GDA 1994 MGA Zone 55

31-May-2023
620.31025

Sheet Size : A4

SLR
www.slrconsultingaustralia.com

0 1 2 3 4 5 km

Uncertainty in Predicted 1 m Maximum Incremental Drawdown in Alluvium (Layer 1)

FIGURE 6-5

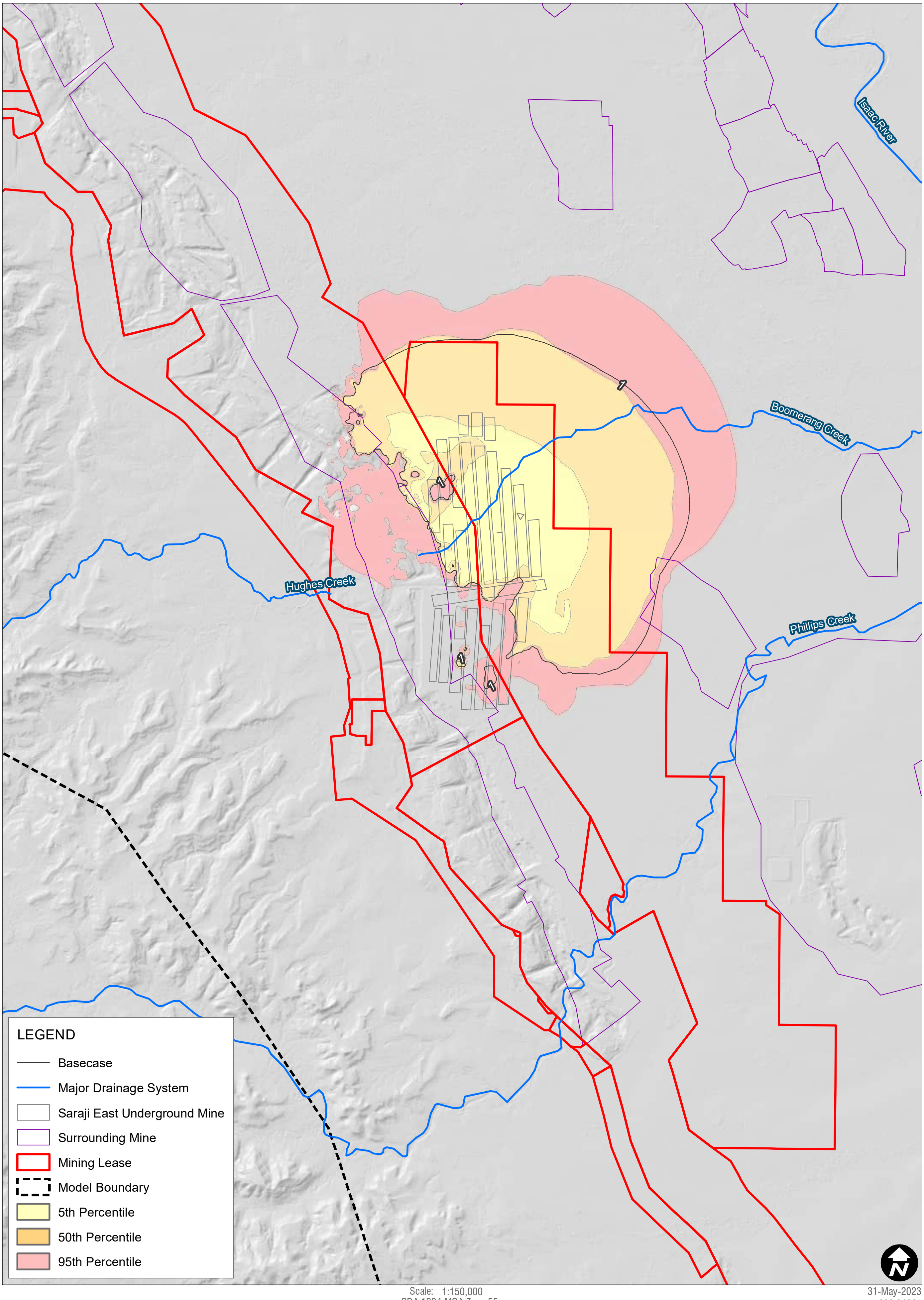

H:\Projects-SLR\620-BNE\620-BNE\620.31025.00000 Saraji East GW Modelling\03 SLR Data\01 CADGIS\GIS\62031025 F6-6 Uncertainty in Predicted 1 m Maximum Incremental Drawdown in Regolith.mxd

Sheet Size : A4

SLR

www.slrconsultingaustralia.com

Uncertainty in Predicted 1 m Maximum Incremental Drawdown in Regolith (Layer 2)

FIGURE 6-6

H:\Projects-SLR\620-BNE\620-BNE\620.31025.00000 Saraji East GW Modelling\03 SLR Data\01 CADGIS\GIS\62031025 F6-7 Uncertainty in Predicted 1 m Maximum Incremental Drawdown in Q Seam.mxd

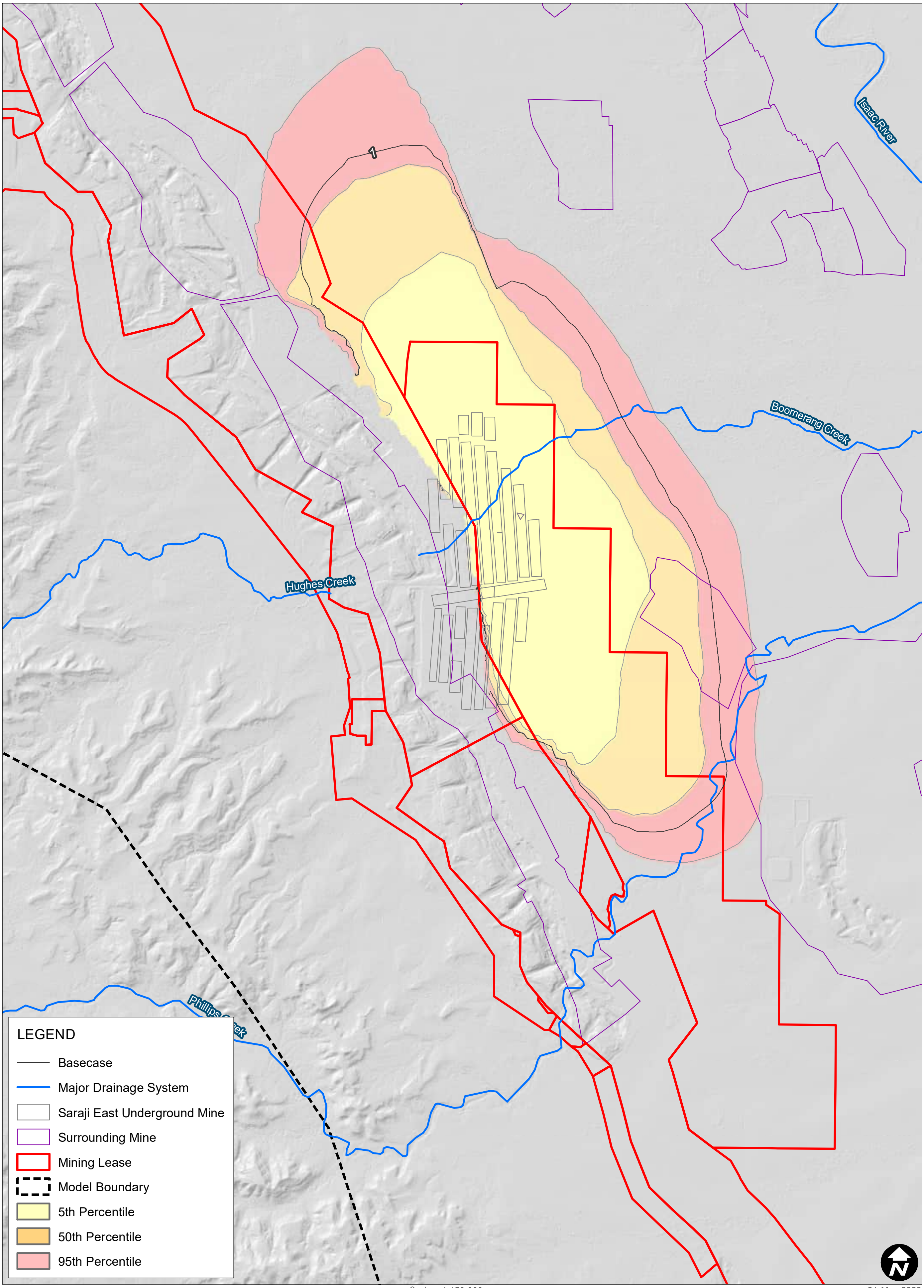

Scale: 1:150,000
GDA 1994 MGA Zone 55

31-May-2023
620.31025

Sheet Size : A4

SLR
www.slrconsultingaustralia.com

0 1 2 3 4 5 km

Uncertainty in Predicted 1 m Maximum Incremental Drawdown in Q Seam (Layer 12)

FIGURE 6-7

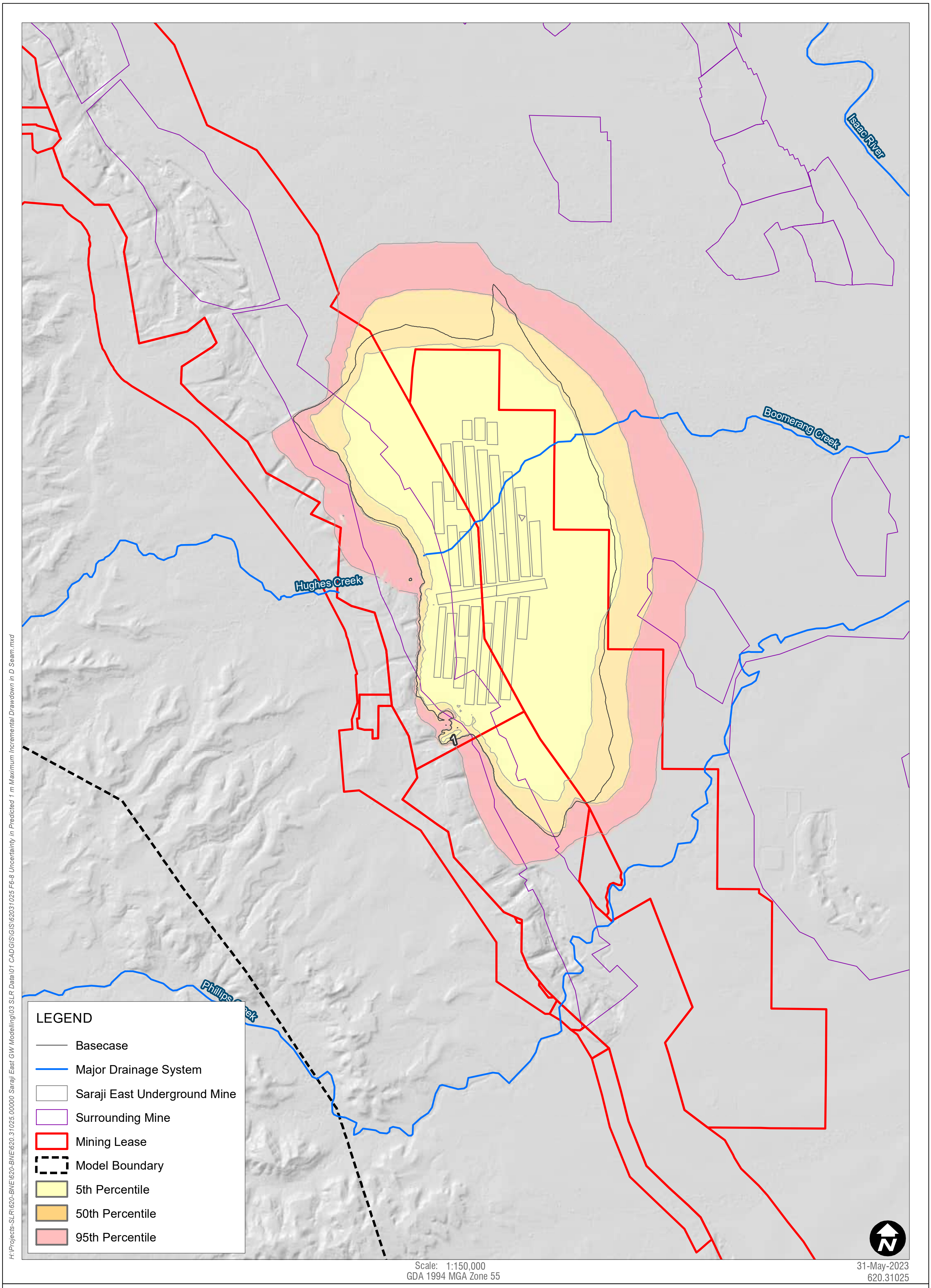

Uncertainty in Predicted 1 m Maximum Incremental Drawdown in D Seam (Layer 18)

FIGURE 6-8

6.2.4 Uncertainty of Influence on Alluvium and Surface Water Flow

The uncertainty analysis results showed that even for the 90th percentile prediction, which is a very unlikely outcome, the take from the Isaac River and Boomerang creek alluvium due to SEMLP were insignificant and considered to be in the range of model errors. The uncertainty analysis also indicates that there is no change to the net flow of Isaac River and local creeks as the result of SEMLP.

7 Model Confidence Level Classification

The groundwater modelling was conducted in accordance with the Australian Groundwater Modelling Guidelines (Barnett et al. 2012), the Murray Darling Basin Commission (MDBC) Groundwater Flow Modelling Guideline (MDBC, 2001) and the released IESC Explanatory Note for Uncertainty Analysis (IESC, 2018). These are mostly generic guides and do not include specific guidelines on special applications, such as underground coal mine modelling.

The 2012 Australian Groundwater Modelling Guidelines has replaced the model complexity classification of the previous MDBC guideline by a "model confidence level" (Class 1, Class 2, or Class 3 in order of increasing confidence) typically depending on:

- Available data (and the accuracy of that data) for the conceptualisation, design, and construction.
- Calibration procedures that are undertaken during model development.
- Consistency between the calibration and predictive analysis.
- Level of stresses applied in predictive models.

It is generally expected that a model confidence level of Class 2 is required for mining environmental impact assessment; the 2012 Australian Groundwater Modelling Guidelines state that a Class 2 model may be used for assessing impacts associated with mine dewatering (Barnett et al. 2012).

Table 7-1 summarises the subjective qualitative criteria allowing model classification, per Table 2.1 of the 2012 Australian Groundwater Modelling Guidelines. The classification of the SEMLP model as presented in **Table 7-1** has been assessed subjectively by a Principal level groundwater modeller and reviewed by a Technical Director level hydrogeologist/modeller, whereby:

1. The classification table was subjectively reviewed, and the specialists mutually decided, in their professional opinion, which box most appropriately describes the various characteristics of the model.
2. Thereafter, the assessors assigned an overall classification class for the model based on the characteristics selected, i.e. which class has the most selected characteristics.

The assessment shown in **Table 7-1** indicates that, overall, the SEMLP groundwater model can be classified as primarily Class 3 using the 2012 Australian Groundwater Modelling Guidelines classification system (effectively “high confidence”), with some aspects meeting the lower Class 2 (“medium confidence”) criteria. This is considered an appropriate level for the SEMLP groundwater assessment context.

Table 7-1 Groundwater Model Classification Table[1,2]

Class	Model Characteristics					
	Data		Calibration		Prediction	
1		Few or poorly distributed data points		Not possible		Predictive timeframe >> calibration timeframe
		Unavailable or sparse data in areas of greatest interest		Unacceptable levels of error		Temporal discretisation is different to calibration
	✓	No metered groundwater extraction data		Inadequate distribution of data		Transient prediction but steady state calibration
		Remote climate data		Targets incompatible with model purpose		Unacceptable validation
		Little or no useful data on land-use, soils, or river flows and stage elevations				
2		Some data but may not be adequate throughout domain	✓	Reasonable calibration statistics with errors in parts of the model	✓	Predictive timeframe > calibration timeframe
		Some metered groundwater extraction data		Long-term trends not replicated in all parts of domain		Long stress periods compared to calibration
	✓	Streamflow and stage measurements are available at some points		Transient calibration not extending to present day		New stresses not in calibration
		Reliable irrigation application data available in part	✓	Weak seasonal replication		Poor validation
				No use of calibration targets compatible with model purpose		
			✓	Validation not undertaken		
3	✓	Spatial and temporal distribution of data adequate	✓	Scaled RMS error or other calibration statistics are acceptable		Predictive timeframe ~ calibration timeframe
		Clearly defined aquifer geometry	✓	Long-term trends adequately replicated where important	✓	Temporal discretisation in predictive model consistent with transient calibration
		Reliable metered groundwater extraction data		Seasonal fluctuations adequately replicated	✓	Similar stresses to those in calibration
	✓	Rainfall and evaporation data is available	✓	Transient calibration is current		Steady state prediction consistent with steady state calibration
	✓	Aquifer testing data to define key parameters	✓	Model is calibrated to heads and fluxes		Model validation suggests calibration is appropriate
	✓	Good quality and adequate spatial coverage of DEM	✓	Key modelling outcomes dataset used in calibration		Steady-state predictions when the model is calibrated in steady-state
		Streamflow and stage measurements are available at many points				
		Reliable land-use and soil-mapping data available				
		Reliable irrigation application data available				

1. Refer Table 2.1 of the 2012 Australian Groundwater Modelling Guidelines (Barnett et al. 2012)
2. Green highlighted cells = model has been subjectively assessed to meet the classification criteria for that Class

8 Groundwater Model and Data Limitation

The IESC *Uncertainty analysis – Guidance for groundwater modelling within a risk management framework* (2018) identifies four key sources of scientific uncertainty affecting groundwater model simulations:

- Structural/conceptual.
- Parameterisation.
- Measurement error.
- Scenario uncertainties.

These four sources of scientific uncertainty have been qualitatively assessed with regards key aspects of the SEMLP groundwater model, as presented in **Table 8-1**.

Overall, the model captures depressurisation due to active mining. The model is numerically stable with no mass balance error. The model shows a reasonable fit between observed and modelled groundwater levels (**Section 2.6.4**). A depth dependence function was used for hydraulic conductivity, with the calibrated values showing a good fit to observed data as presented in **Section 2.7**. Overall, the model is considered fit for purpose to achieve the objectives outlined in **Section 1** based on the data provided and the project timeframe.

In case of future use of the model, updates could be conducted to further refine the model if it was deemed that an increase in model confidence level was required, but the applicability of this would be dependent on the purpose of the future modelling and availability of data to inform future changes. As it stands, the current model is deemed fit for purpose for the Project impact assessment.

Table 8-1 Groundwater Model and Data Limitations

Type	Part	Status	Comment
Structural/ Conceptual	Grid and Model Extent	Fit for purpose	The model has an unstructured Voronoi grid that includes detailed cell refinement around site, neighbouring mines and along drainage features.
	Layers	Fit for purpose	Top of layer 1 incorporates site LiDAR data from SEMLP and SRM.
		Fit for purpose	Representation of alluvium based on CSIRO (2015) regolith mapping and refined based on site drill data.
	Conceptualisation – Geological Structure	Fit for purpose	The local structure of the geology is based on detailed data at site, and regional model geometry (outside of site) interpolated based on neighbouring mines geology models (Winchester South, Lake Vermont, Moorvale South and Olive Downs South) and geological mapping. Geophysical surveys across the Project Area have identified minor faulting in the SEMLP area. Faulting is typically confined to the coal seams of the Moranbah Coal Measures. No geological structures (i.e. faults) have been included within the Project area in the model other than through layer displacements from the site geological model. The most significant geological structure in the area is the Fault which is located 500m from the site and will not be intersected by mining.
	Conceptualisation – Surface Water Groundwater Interactions	Fit for purpose	The Permian coal measures outcrop along the western edge of the site. Therefore, how this is captured within the model influences the model predictions. The structure of the coal seams was checked to ensure it matches observed and mapped geology. The predictions of drawdown adjacent to mining was checked and the model shows a good fit between modelled and observed trends.
	Conceptualisation – Saturated Extent of Alluvium and Regolith	Fit for purpose	For the extent and thickness of alluvium in the vicinity of the Project Area (i.e., alluvium along Boomerang Creek) auger hole logs and Google satellite imagines were used. Any additional data or study on alluvium extent and thickness at SEMLP should be reviewed and captured (where relevant) in future updates of the model. Such improvements are not deemed required for the Project impact assessment however.
Parameterisation	Hydraulic Conductivity – Depth Dependence	Fit for purpose, future improvements possible	Field testing of hydraulic conductivity (horizontal and to a lesser extent vertical) has been conducted in the area. Hydraulic conductivity test results from the other sites within the model domain were also considered. The data shows a general decline in hydraulic conductivity with depth that is replicated in the model. Further conductivity tests and measurements of storage properties can improve model calibration and refine model predictions but are not deemed required for the Project impact assessment.

Type	Part	Status	Comment
	Spoil Properties	Fit for purpose, future improvements possible	Limited site-specific data is available for the spoil. Spoil properties were adopted using the previous studies.
	Rivers	Fit for purpose, future improvements possible	Isaac River stage height is changed temporally in the historical calibration model based on observed levels from government stream gauges, and long term annual average level assumed in the predictive model. Watercourses within and in the vicinity of the Project Area such as Boomerang Creek are ephemeral and only flow briefly after rainfall. Therefore, river stage height of zero was assigned to these watercourses in the model. Measurements of flow rates and stage height in the rivers can help with improving the model calibration and refining the model predictions but are not deemed required for the Project impact assessment.
	Recharge	Fit for purpose	Recharge zonation is based on mapped surface geology and calibrated recharge rates.
Measurement Error	Observation Data Quality	Fit for purpose	Bore logs and construction details available for most site bores, and long-term site water level data available for various units.
	Landholder Bore Data Quality	Fit for purpose	Impacts on registered landholder bores are influenced by the assumptions of the bore design, target geology and use.
	Temporal spread	Fit for purpose	Timeseries water level data from the site as well as the neighbouring mines (Winchester South, Moorvale South, Olive Downs South and Lake Vermont, Peak Downs, Moranbah South) for the alluvium and Permian coal measures.
Scenario Uncertainties Future stresses/ conditions	Calibration	Fit for purpose	Transient warm-up (1988-2008) and transient (2008 to 2022) calibration model set up and a depth dependence function used and calibration to water levels conducted using automated (PEST) and manual methods.
	Predictive	Fit for purpose	Model captures approved and proposed underground at SEMLP. The model also includes future mining at Saraji, Peak Downs mainly based on publicly available data. The actual future mine progression for these sites may vary.
	Sensitivity and uncertainty	Fit for purpose	Uncertainty analysis has been conducted by stochastic modelling using an adapted Monte Carlo method with modern software packages. The Latin Hypercube Sampling (LHS) method was used to create random realisations from parameter and PEST++ was used to orchestrate the model runs. The uncertainty analysis quantified the variability in predictions with changes in maximum predicted drawdowns, mine inflows, impact on alluvium flow and impacts on surface water flow.

9 Conclusions

A numerical groundwater model for the SEMLP was developed using BMA's CVM HPE numerical groundwater model (SLR, 2021a) as the foundation. The numerical groundwater model developed for the SEMLP has successfully achieved the modelling objectives, as outlined in **Section 1**.

The SEMLP numerical groundwater model covered a large domain due to extensive historic and approved mining within the region. Existing and approved mines are represented in the model.

A new model calibration was undertaken to match best the latest observation datasets. In doing so, new observation data was included in the calibration data set where it was available. The calibrated model showed a reasonable match between simulated and observed water levels across the model domain and therefore the model parameterisation was considered appropriate for the SEMLP model.

The key conclusions from the modelling are summarised as follows:

- Predicted total groundwater inflows (basecase) to the SEMLP amount to 183 ML/year on average (between 2022 and 2042) and ranging up to a peak in the order of 500 ML/year in the year 2038.
- There is no groundwater drawdown predicted in the alluvium due to the SEMLP.
- Groundwater drawdown in the regolith occurs above the northern SEMLP panels where the model predicts the regolith is saturated.
- Groundwater drawdown in Permian coal seams is limited to the west due to coal seam subcrops/existing open pit mining, and extends a maximum of 5 km east and 8 km north and south of the SEMLP.
- No change in surface water flows in the local creeks including Boomerang Creek is predicted due to the SEMLP. Similarly, no change is predicted to surface water flows in the Isaac River due to the SEMLP.

10 References

AECOM, 2016. Saraji Open-Cut Extension Project – Groundwater Technical. Report.

AECOM, 2019. Saraji East Mining Lease Project, Environmental Impact Statement Appendix F-1, Ground water Technical Report, Project No. 60507031.

AGE, 2012. Saraji East Project Groundwater Impact Assessment, For Sinclair Knight Merz, Project No. G1549.

AGE, 2016. G200s Project Grosvenor Groundwater Impact Assessment Report, For Hansen Bailey Pty Ltd, Project Number G1807A.

Barnett, B., Townley, L.R., Post, V., Evans, R.E., Hunt, R.J., Peters, L., Richardson, S., Werner, A.D., Knapton, A. and Boronkay, A. ,2012. Australian Groundwater Modelling Guidelines. Waterlines Report Series No. 82.

Groundwater Imaging Pty Ltd (Allen, D), 2018. Moorvale South AgTEM survey for Groundwater Investigation, near Coppabella, Bowen Basin, QLD. Report for Peabody Energy.

Hawkins, J.W., 1998. Hydrogeologic characteristics of surface-mine spoil. In Coal Mine Drainage Prediction and Pollution Prevention in Pennsylvania, ed. Brady, Smithy and Schueck. Harrisburg, Pennsylvania. Available at: http://www.techtransfer.osmre.gov/nttmainsite/Library/pub/cmdpppp/chapter3.pdf.

HydroAlgorithmics,2014. AlgoMesh User Manual.

HydroSimulations, 2018. Olive Downs South and Willunga. Appendix B. Modelling Appendix. Report for Pembroke Resources Pty Ltd.

IESC, 2018, Uncertainty analysis – Guidance for groundwater modelling within a risk management framework.

Mackie, C.D., 2009. Hydrogeological characterisation of Coal Measures and overview of impacts of coal mining on groundwater systems in the upper Hunter Valley of NSW. PhD thesis at University of Technology, Sydney.

MDBC (Middlemis, H., Merrick, N., and Ross, J.), 2000. Murray-Darling Basin Commission – Groundwater Flow Modelling Guideline. Report for MDBC.

Minserve, 2022. Subsidence over Longwall Panels Saraji East Underground Mine.

Panday, S., Langevin, C.D., Niswonger, R.G., Ibaraki, M., and Hughes, J.D., 2013., MODFLOW–USG version 1: An unstructured grid version of MODFLOW for simulating groundwater flow and tightly coupled processes using a control volume finite-difference formulation: USGS Techniques and Methods 6-A45.

SLR, 2019. Moorvale South Groundwater Assessment. Appendix B1 Groundwater Modelling Technical Appendix. Report for Peabody Energy.

SLR, 2020. Winchester South Project EIS. Groundwater Impact Assessment Baseline Report. Report for Whitehaven Coal.

SLR, 2021. BHP - Horse Pit Approvals November 2020 Bore Survey. Report for BMA.

SLR, 2021a. Caval Ridge Mine Horse Pit Extension Project. Groundwater Assessment Report. Report for BMA.

SLR, 2021b. Caval Ridge Mine Horse Pit Extension Project. Surface Water Assessment Report. Report for BMA.

SLR, 2021c. Millennium Mine Groundwater Mavis Underground Operations. Groundwater Impact Assessment. Groundwater Modelling Technical Report. Report for MetRes Pty Ltd.

SLR, 2021d. Daunia Mine FY21 Water Licence Performance Review Report . Groundwater Modelling Technical Report. Report for BHP Billiton Mitsubishi Alliance.

Appendix A:

CalibratiSon Residuals

ID	Easting	Northing	Layer	Average Residual	Min	Max
141807	621693	7573807	2	-25.8	-28.6	-23.4
141864	621978	7572901	2	-19.6	-29.6	-11.3
141942	607531	7570131	1	-5.5	-5.5	-5.5
162013	621998	7572002	2	-5.6	-15.4	-1.8
162041	622162	7573331	3	-20.9	-27.5	-14.9
162043	613496	7560208	2	12.4	12.4	12.4
162044	615613	7560397	2	-8.2	-8.2	-8.2
162048	613513	7557249	2	-3.5	-3.5	-3.5
162068	605993	7571041	2	-10.1	-10.1	-10.1
162070	606033	7571055	2	-10.7	-10.7	-10.7
162071	605990	7571006	2	-10.3	-10.3	-10.3
162141	613846	7562175	2	-0.6	-0.6	-0.6
162143	616018	7561336	2	3.0	3.0	3.0
162164	608384	7558233	2	-5.7	-5.8	-5.7
162165	608920	7556710	2	-1.8	-7.1	2.3
162169	611129	7551675	2	0.6	0.3	1.2
162171	612441	7550671	2	-0.7	-0.8	-0.6
162173	611249	7549500	2	4.2	1.6	5.7
162549	619260	7567365	2	6.3	5.3	6.7
162550	620351	7567479	2	4.4	3.7	4.6
162682	641151.5	7546517	2	-7.0	-7.5	-6.8
162684	642471.2	7547492	2	-3.7	-4.0	-3.4
182078	620368	7568049	2	-6.7	-15.4	-1.8
182079	620368	7568046	2	-1.2	-1.6	-0.8
182080	619740	7567253	2	3.4	3.3	3.5
13040180	667824	7516333	1	-17.8	-19.6	-16.5
13040286	659983	7536966	2	-27.1	-27.6	-26.8
1238-MB1	650670.9	7522741	2	-10.5	-10.7	-10.3
1238-MB2	650670.4	7522744	7	-17.8	-18.1	-17.5
2218-MB2	645525.7	7522756	3	-4.2	-5.0	-3.3
2218-MB3	645523	7522754	5	-4.5	-5.0	-4.0

ID	Easting	Northing	Layer	Average Residual	Min	Max
2226-MB2	643134.1	7521947	4	3.6	3.0	4.1
2226-MB3	643133.3	7521950	5	0.5	0.3	0.7
2372-MB1	647519.8	7526012	2	-10.2	-10.4	-10.0
2372-MB2	647519.3	7526010	4	-9.9	-10.1	-9.7
2372-MB3	647517.7	7526008	7	-9.2	-9.3	-9.0
2375-MB2	648041.7	7523874	9	-12.0	-12.1	-11.9
2393-MB1	645696.1	7523043	2	-1.9	-2.4	-1.4
2393-MB2	645693.5	7523043	5	-4.0	-4.4	-3.5
2393-MB3	645690.9	7523043	7	-4.2	-4.8	-3.4
2394-MB1	644897.8	7522962	2	-6.3	-6.4	-6.1
2394-MB2	644895.2	7522962	3	-4.2	-4.4	-4.0
C2105R	634650	7541857	5	-7.6	-7.6	-7.6
C2136	631742	7547243	5	-15.4	-15.7	-15.2
CVMMB16_02	611247.7	7558493	16	-6.7	-6.8	-6.5
CVMPB07_01	611564.7	7552523	2	6.6	6.6	6.6
CVMPB07_02	611564.7	7552540	14	-6.3	-6.3	-6.3
CVMVWP01_3	610027.7	7560450	16	-8.5	-9.1	-7.8
CVMVWP01_4	610027.7	7560450	18	-4.8	-6.0	-3.7
DauniaPZ01	632534	7561905	8	-3.6	-4.9	-2.7
DauniaPZ02	635300	7560237	6	-6.9	-14.9	10.5
DauniaPZ03	632332	7558326	8	-12.1	-12.9	-9.0
DauniaPZ04	635531	7554554	8	-12.0	-12.7	-8.2
DauniaPZ05	632576	7561914	8	-2.6	-4.6	-1.0
DauniaPZ06	631776	7561217	7	-3.9	-11.7	-0.1
DauniaPZ07	631627	7559539	10	-9.8	-10.7	-8.7
G2304R	633245	7543171	7	-13.2	-13.2	-13.2
G2307	630881	7547844	7	-14.8	-14.9	-14.6
GW01d_p1	642475.4	7547489	7	-7.9	-9.1	-6.6
GW01d_p2	642475.4	7547489	5	-11.8	-12.6	-10.5
GW01d_p3	642475.4	7547489	3	-6.4	-6.6	-5.9
GW01d_p4	642475.4	7547489	3	-4.2	-4.4	-3.5
GW01s	642471.2	7547492	2	-3.0	-3.3	-2.8
GW02d	641148.2	7546512	7	-7.1	-7.2	-7.1
GW02s	641151.5	7546517	2	-7.2	-7.2	-7.1
GW06d_p1	639333.8	7542009	9	7.7	7.3	8.0
GW06d_p2	639333.8	7542009	10	-1.4	-1.9	-1.0
GW06d_p3	639333.8	7542009	9	-1.7	-2.0	-1.5

ID	Easting	Northing	Layer	Average Residual	Min	Max
GW06d_p4	639333.8	7542009	9	-6.2	-7.0	-4.1
GW08d_p1	645312	7539846	5	-12.2	-15.0	-10.6
GW08d_p2	645312	7539846	3	-6.6	-6.8	-6.4
GW08d_p3	645312	7539846	3	0.0	0.0	0.1
GW08d_p4	645312	7539846	3	-32.2	-38.2	-24.4
GW12d_p1	641492.4	7532790	5	1.6	0.4	6.0
GW12d_p2	641492.4	7532790	5	-3.3	-4.2	-2.0
GW12d_p3	641492.4	7532790	3	15.1	12.2	16.3
GW12d_p4	641492.4	7532790	3	34.5	33.6	36.4
GW12s	641497.8	7532791	2	-2.2	-2.2	-2.2
GW16d_p1	660834	7525288	7	-27.1	-28.5	-23.2
GW16d_p2	660834	7525288	5	-15.1	-15.2	-15.0
GW16d_p3	660834	7525288	3	-14.8	-15.0	-14.5
GW16d_p4	660834	7525288	3	-14.1	-14.2	-13.9
GW18d	656890.7	7522809	7	-8.3	-8.3	-8.3
GW18S	656884.6	7522810	1	-7.7	-7.9	-7.6
GW21d	661579.5	7521648	10	-17.8	-17.8	-17.7
GW21s	661580.2	7521653	2	2.9	2.7	3.0
GW8S	645323.5	7539847	1	-3.6	-3.7	-3.6
KnobHill1	631005	7553874	1	-3.5	-3.7	-3.3
KnobHill2	630431	7554061	1	-0.4	-1.0	0.9
LH13	627200	7546952	9	13.0	12.3	13.9
LV2183_P2	644067.9	7520358	5	-3.9	-5.6	-1.8
LV2183_P3	644067.9	7520358	6	-22.8	-23.8	-21.7
LV2183_P4	644067.9	7520358	7	-15.5	-17.4	-13.0
LV2218_P1	645525.9	7522753	5	-5.7	-7.1	-5.2
LV2218_P2	645525.9	7522753	6	-8.8	-9.3	-8.6
LV2218_P3	645525.9	7522753	7	-8.0	-9.4	-7.3
LV2226_P1	643129.4	7521950	4	5.0	4.6	5.3
LV2226_P2	643129.4	7521950	5	-0.4	-1.6	0.5
LV2226_P3	643129.4	7521950	6	-1.8	-2.5	-1.2
LV2226_P4	643129.4	7521950	7	-3.7	-3.8	-3.5
LV2370W	648036.5	7523878	2	-4.0	-4.2	-3.9
LV2371W	643131.4	7521947	2	6.1	5.5	7.1
LV2372R_P1	647515.2	7526007	6	-8.4	-9.7	-6.7
LV2372R_P4	647515.2	7526007	7	-10.3	-10.9	-8.1
MB08PZ4	615638	7559628	16	-14.5	-14.5	-14.5

ID	Easting	Northing	Layer	Average Residual	Min	Max
MB1	623254	7551541	9	-3.2	-5.2	-1.6
MB13PZ4	615195	7551070	16	-10.6	-10.6	-10.6
MB15PZ4	620083	7547608	16	-1.0	-1.0	-1.0
MB19CVM01A	610443	7548264	2	-2.0	-2.3	-1.6
MB19CVM03T	610214	7551338	2	9.9	7.6	11.1
MB19CVM04P	610215	7551344	18	24.1	24.1	24.1
MB19CVM05T	611082	7551428	2	-9.8	-11.9	-7.0
MB19CVM06P	611075	7551429	16	-8.5	-10.3	-5.5
MB19CVM07T	611578	7552537	2	5.1	4.9	5.6
MB19CVM08P	611579	7552526	16	-6.3	-7.4	-3.5
MB19CVM09A	612560	7550879	2	1.9	1.6	2.4
MB19CVM10P	613294	7549948	16	0.7	-1.1	3.6
MB19SRM01A	640145.8	7516041	1	20.9	20.9	20.9
MB19SRM02T	640139.8	7516048	2	10.9	10.9	10.9
MB19SRM03P	640131.8	7516057	9	10.9	10.9	10.9
MB19SRM04P	637173.7	7511222	2	1.8	1.6	2.1
MB2	623684	7549391	9	2.0	1.4	2.4
MB20CVM01A	610028	7560466	2	0.2	-0.3	1.1
MB20CVM04T	608307	7559829	2	2.7	2.3	3.4
MB20CVM05P	608312	7559824	18	-8.2	-10.9	-6.1
MB20CVM06T	610921	7549067	2	-1.5	-3.6	-0.8
MB20PDM03P	621512.8	7548051	15	-4.7	-5.4	-3.9
MB20PDM05P	630220.5	7533012	14	8.2	7.0	10.3
MB20PDM06T	628975.9	7532808	2	20.5	20.4	20.8
MB20PDM07T	621822.7	7538727	2	21.4	21.1	21.9
MB20SRM02T	636027.9	7527850	9	-1.1	-1.1	-1.1
MB20SRM03P	636020.9	7527857	18	-30.5	-30.5	-30.5
MB20SRM04A	631510.9	7530650	1	15.7	15.7	15.7
MB20SRM06A	636595.8	7520189	2	16.7	16.7	16.7
MB20SRM07P	641475.7	7508141	18	-1.5	-1.5	-1.5
MB3	627240	7549946	3	-16.6	-17.2	-15.6
MB34	638039.8	7518450	14	-0.6	-39.8	2.2
MB35	642759.8	7520291	2	8.7	7.2	10.2
MB36	640263.8	7514464	2	6.0	4.2	6.7
MB39	640131.8	7516057	10	11.4	10.4	12.3
MB4	626507	7544152	9	4.0	3.8	4.2
MB40	640139.8	7516048	2	10.9	10.6	11.2

ID	Easting	Northing	Layer	Average Residual	Min	Max
MB5	628491	7542693	9	5.0	4.1	5.4
MillMB1	627777.1	7565148	4	-5.5	-12.6	2.7
MillMB10A	630772.2	7563698	8	1.8	-0.2	9.2
MillMB10B	630772.2	7563698	11	7.8	6.2	9.9
MillMB11A	631857.9	7562882	2	0.9	-2.5	3.2
MillMB11B	631857.9	7562882	2	2.9	1.5	4.2
MillMB2	627819.4	7563299	4	-11.1	-15.9	-0.1
MillMB3A	630019.1	7562255	2	16.7	8.1	22.2
MillMB3B	630019.1	7562255	2	11.0	6.4	15.9
MillMB4	630485.8	7563384	2	4.4	1.8	6.9
MillMB8B	627205.6	7565983	4	-24.0	-26.5	-17.4
MillMB9A	628476.3	7565513	10	10.7	8.3	12.0
MillMB9B	628476.3	7565513	9	-5.9	-38.4	2.8
MOS_MB01	610570	7562897	2	3.5	3.5	3.5
MOS_MB02	611777	7562388	15	-10.7	-10.7	-10.7
MOS_MB04	613961	7562355	2	-0.6	-0.6	-0.6
MOS_MB05	615206	7563212	2	4.1	4.1	4.1
MOS_MB06	616017	7561336	2	3.0	3.0	3.0
MOS_MB07	615613	7560398	2	-8.2	-8.2	-8.2
MOS_MB08b	615638	7559628	11	-3.8	-3.8	-3.8
MOS_MB09b	618366	7558118	9	-0.1	-0.1	-0.1
MOS_MB11	611617	7558367	15	-5.8	-5.8	-5.8
MOS_MB12	613627	7557429	2	-3.5	-3.5	-3.5
MOS_MB14	615195	7551070	11	-3.9	-3.9	-3.9
MOS_MB16	620083	7547608	11	2.0	2.0	2.0
OBS1	630111	7554627	2	-5.7	-6.9	-5.0
OBS10	627784	7556229	5	-2.6	-3.1	-2.1
OBS11	630313	7556960	2	12.2	11.7	13.1
OBS12	626899	7559552	5	-23.6	-24.6	-22.5
OBS13	626891	7559550	7	-16.8	-16.8	-16.7
OBS14	629680	7560815	2	20.8	20.8	20.9
OBS2	631341	7557693	9	0.3	-0.7	1.2
OBS4	626685	7562094	4	-2.6	-3.2	-2.2
OBS5	626050	7557202	2	-5.1	-6.7	-4.3
OBS6	628887	7556546	5	-11.2	-12.0	-10.4
OBS7	625570	7556820	1	-1.7	-2.1	-1.3
OBS8	631867	7553655	1	2.9	2.6	3.2

ID	Easting	Northing	Layer	Average Residual	Min	Max
OBS9	627800	7556217	6	6.1	5.4	6.7
ODN18MB1	640275	7547943	5	-8.7	-8.8	-8.7
ODN18MB10	639450.5	7554580	10	-15.2	-15.2	-15.2
ODN18MB11	638599.4	7553465	10	-9.8	-9.8	-9.8
ODN18MB12	640277	7547944	5	-0.9	-1.2	-0.6
ODN18MB2	640263	7547944	1	1.5	1.5	1.5
ODN18MB3	639750.5	7551426	5	-11.3	-11.3	-11.3
ODN18MB4	640684.3	7549869	2	-9.7	-10.1	-9.3
ODN18MB6	639943.7	7551802	5	-10.1	-10.1	-10.1
ODN18MB7	640310.3	7554734	2	-4.3	-4.3	-4.3
ODN18MB8	638921.3	7550183	2	-3.5	-3.5	-3.4
ODN18MB9	640088.8	7557236	4	-0.3	-0.3	-0.3
ODN18TB1	640318	7547935	5	-7.7	-7.9	-7.4
ODN18TB2	640303	7547935	1	3.6	3.4	3.8
PDMMB11_01	624187.3	7534394	17	-4.7	-4.7	-4.7
PDMMB12_01	624324.5	7534454	17	-8.3	-8.3	-8.3
PZ00B	632913.9	7529866	2	2.8	2.7	2.9
PZ00C	632984.9	7529934	2	1.8	1.7	1.9
PZ00D	631797.9	7530369	13	5.4	5.1	6.1
PZ01	609954	7560323	18	-2.8	-7.0	-0.8
PZ02	608553	7558420	2	-2.8	-4.9	-1.6
PZ02A	632133.4	7530855	2	11.8	11.3	12.2
PZ02B	632133.4	7530855	15	-2.1	-2.1	-2.0
PZ02C	632133.4	7530855	18	0.3	-6.8	7.4
PZ03-D	609029	7556890	18	-8.8	-11.7	-7.4
PZ03-S	609028	7556894	2	-7.2	-12.0	-2.9
PZ04	610844	7555504	12	-4.0	-5.0	-3.3
PZ04A	630356	7531133	2	15.4	14.2	16.9
PZ04B	630356	7531133	16	14.2	14.0	14.5
PZ04C	630356	7531133	18	13.9	13.7	14.2
PZ05	609030	7554296	18	-16.3	-18.9	-8.8
PZ05A	642440.6	7509401	16	0.0	0.0	0.1
PZ05B	642440.6	7509401	18	-5.1	-5.1	-5.0
PZ06A	639385.5	7513506	14	8.6	8.6	8.7
PZ06B	639385.5	7513506	16	5.4	5.3	5.5
PZ06C	639385.5	7513506	18	-3.9	-4.3	-3.4
PZ06-S	611237	7551854	2	0.7	0.2	1.4

ID	Easting	Northing	Layer	Average Residual	Min	Max
PZ07-D	612578	7550882	12	0.0	-1.5	1.3
PZ07-S	612584	7550881	2	0.2	-0.5	2.0
PZ08A	634760.8	7523250	14	7.1	6.8	7.3
PZ08B	634760.8	7523250	16	2.4	2.3	2.5
PZ08-D	611526	7549891	17	-5.1	-14.2	7.5
PZ08-S	611524	7549887	2	5.4	1.7	6.4
PZ09	614439	7549000	15	-11.9	-25.7	-3.8
PZ09B	633025.7	7527959	16	-0.2	-0.3	-0.2
PZ09C	633025.7	7527959	18	-0.2	-1.0	0.5
PZ10B	634350.2	7524345	16	9.5	8.0	11.0
PZ10C	634350.2	7524345	18	24.8	23.3	26.4
PZ11-D	616904	7547778	14	-7.8	-27.6	2.0
PZ12-D	610834	7557342	13	-3.9	-5.0	-1.3
PZ12-S	610825	7557397	2	-1.0	-1.3	-0.3
R2007	630447.5	7542330	7	-0.8	-0.8	-0.8
R2008	630879	7542573	5	0.0	-0.9	0.2
R2010	631743	7543062	5	-6.3	-7.7	-6.0
R2010R	631730	7543070	5	-6.6	-6.6	-6.6
R2032	630495	7545853	5	4.4	1.2	4.8
R2035	629190	7545103	9	-0.5	-0.8	0.1
R2054	629240	7548107	4	1.6	-3.5	2.8
R2055	628798	7547863	7	3.5	2.3	3.7
R2056	628364.3	7547623	9	6.3	6.3	6.3
S10	642551.8	7546035	2	-3.4	-3.4	-3.4
S11	642455.2	7545332	1	-3.1	-3.1	-3.1
S2	641385.5	7547617	1	-4.7	-4.7	-4.7
S4	641566.7	7546845	1	-8.0	-8.8	-7.2
S5	642239.4	7547332	2	-5.8	-5.8	-5.8
S6	642054.2	7546721	1	-4.1	-4.1	-4.1
S7	641442.7	7545828	2	-7.1	-7.1	-7.1
S8	642339.6	7546343	1	-2.0	-2.1	-1.9
S9	641766.9	7545426	2	-5.8	-5.8	-5.8
W1_MB1	637914	7531373	2	-1.0	-1.0	-1.0
W1_MB2	637916	7531372	5	-0.6	-0.6	-0.5
W1_MB3	637919	7531372	7	-0.6	-0.6	-0.5
W10_MB1	641869	7524259	4	-9.9	-9.9	-9.9
W10_MB2	641869	7524259	7	-18.3	-18.5	-18.0

ID	Easting	Northing	Layer	Average Residual	Min	Max
W10_MB3	641869	7524261	7	-14.5	-14.5	-14.4
W11_MB1	643941	7524860	3	-33.1	-67.0	-15.7
W11_MB2	643943	7524861	5	-13.5	-13.8	-13.3
W12_MB1	643268	7530165	2	-11.3	-11.4	-11.2
W13_MB1	645381	7530927	9	-8.5	-8.5	-8.4
W14_MB1	645373	7528515	2	-4.4	-4.6	-4.2
W15_MB1	649009	7527504	2	5.4	5.4	5.4
W15_MB2	649009	7527504	7	5.4	5.4	5.5
W15_MB3	649009	7527504	7	5.4	5.4	5.6
W2_MB1	637368	7531452	2	-0.4	-0.4	-0.3
W2_MB2	637370	7531452	10	-0.5	-0.5	-0.5
W3_MB1	640470	7529435	2	8.4	7.7	8.8
W3_MB2	640468	7529435	2	-0.4	-0.5	-0.4
W4_MB1	638172	7528735	2	6.6	6.5	6.7
W4_MB2	638169	7528735	9	-0.8	-1.1	-0.7
W5_MB1	638387	7527823	3	-0.5	-0.5	-0.4
W5_MB2	638385	7527820	5	0.5	0.5	0.5
W5_MB3	638384	7527817	7	-1.5	-1.5	-1.4
W6_MB1	637758	7527892	9	-0.5	-1.2	0.1
W6_MB2	637761	7527893	10	0.6	0.5	0.8
W7_MB1	637484	7526145	9	-0.6	-0.6	-0.6
W8_MB1	639306	7523618	10	-3.8	-3.9	-3.7
W9_MB1	640953	7524117	2	-4.5	-4.6	-4.4
W9_MB2	640953	7524119	9	-12.2	-12.4	-11.9
W9_MB3	640952	7524121	9	-11.0	-11.0	-10.9
West-MB1	642872.3	7519929	2	4.4	3.9	5.1
West-MB2	642872.9	7519932	9	6.0	5.6	6.5
WinnetBore	634791	7550023	1	-5.8	-7.1	-5.3

Appendix B:

Calibration Hydrographs

1238-MB1

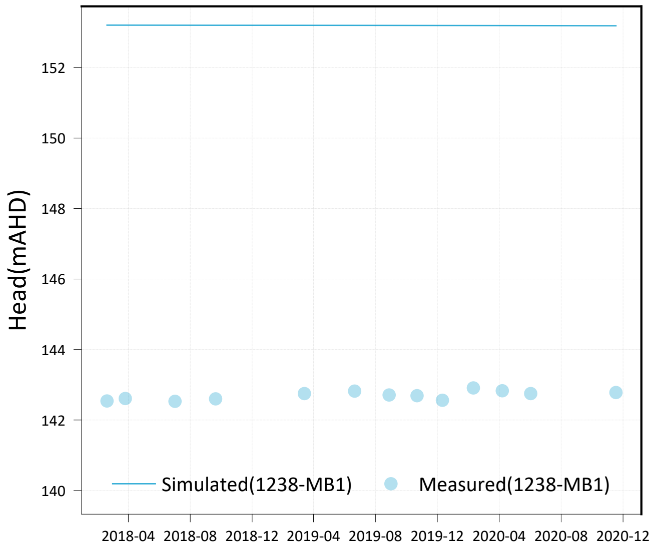

1238-MB2

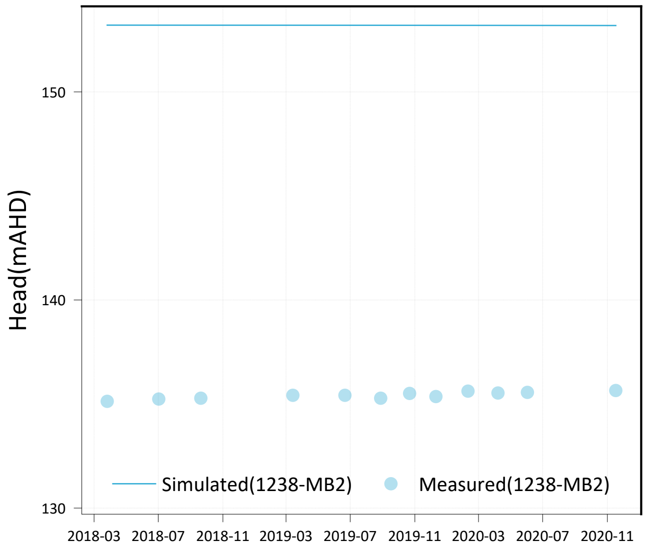

13040180

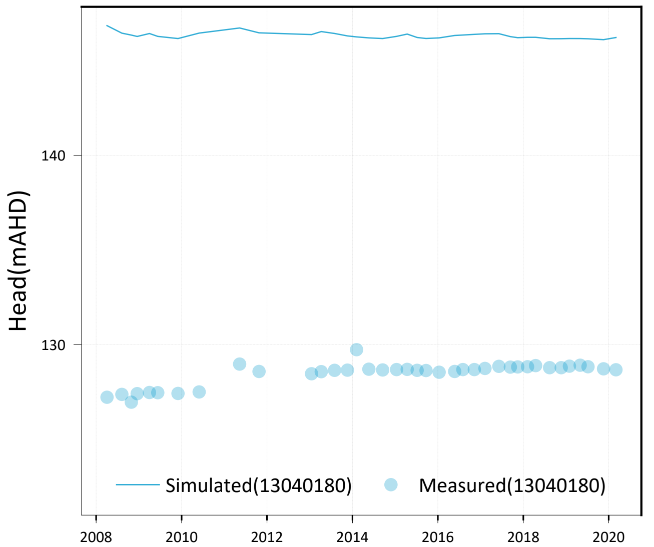

141942

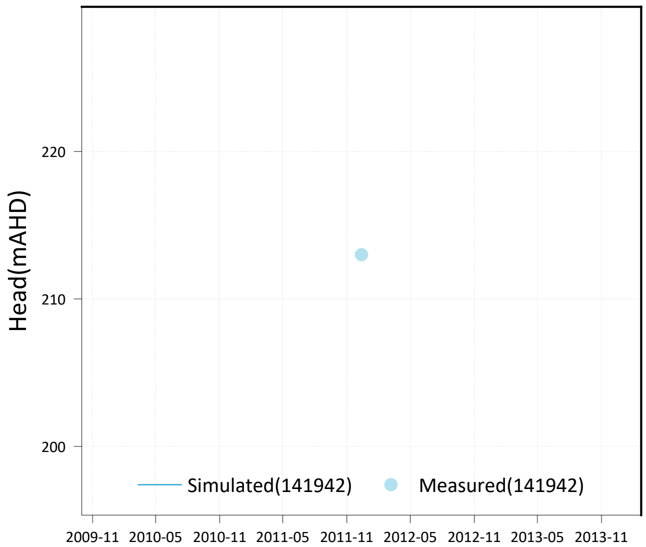

162041

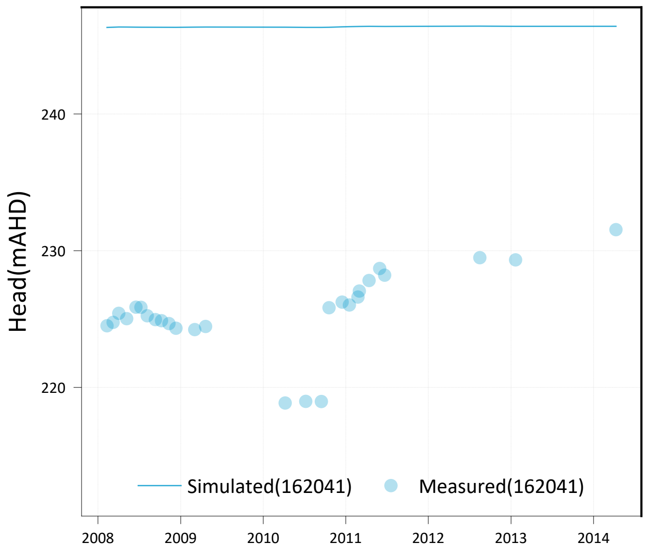

162043

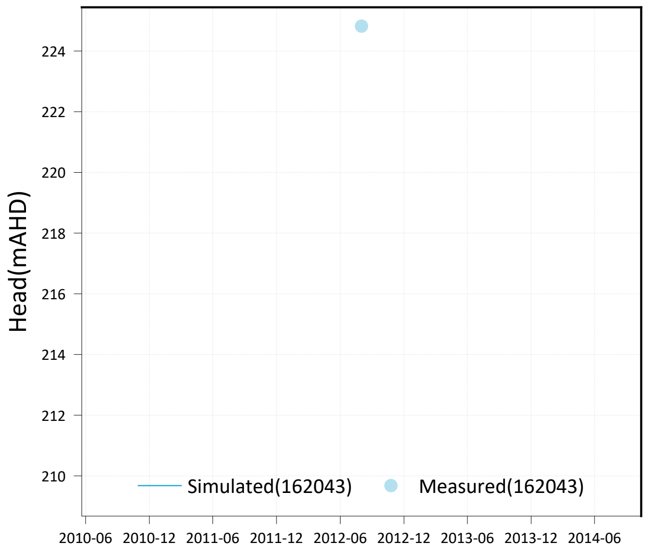

162068

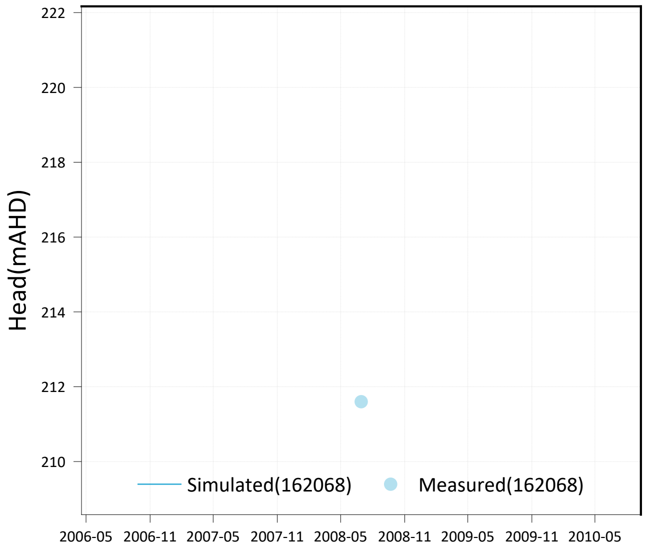

162070

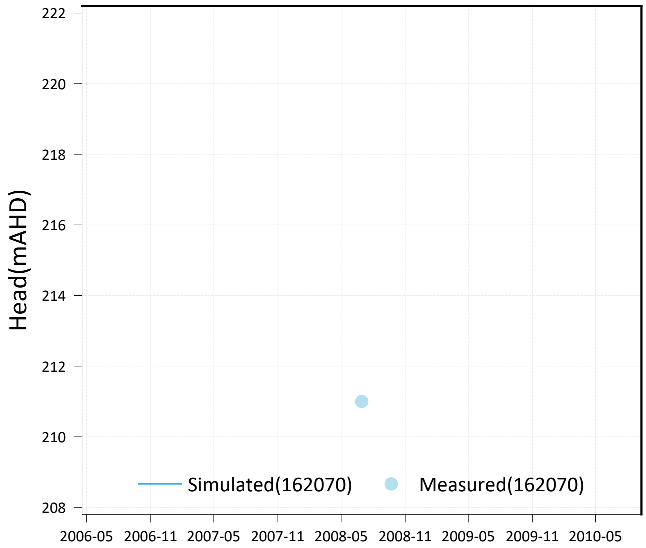

162141

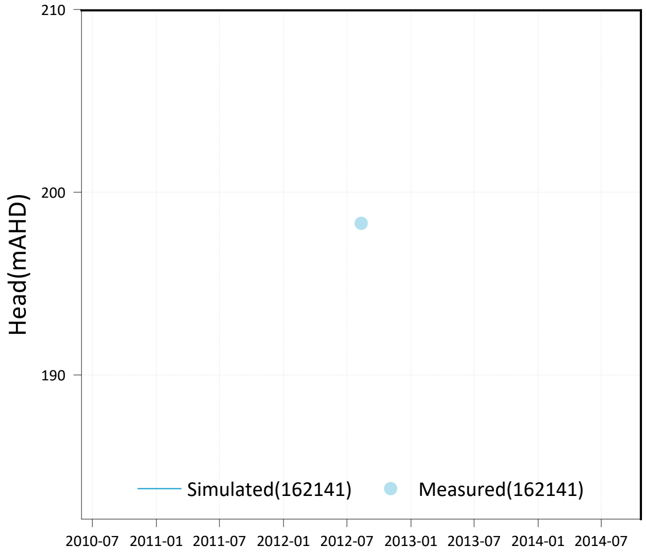

162143

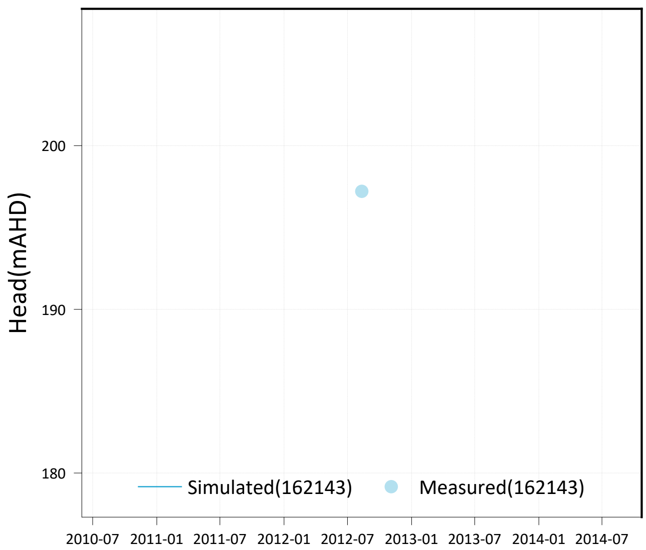

162164

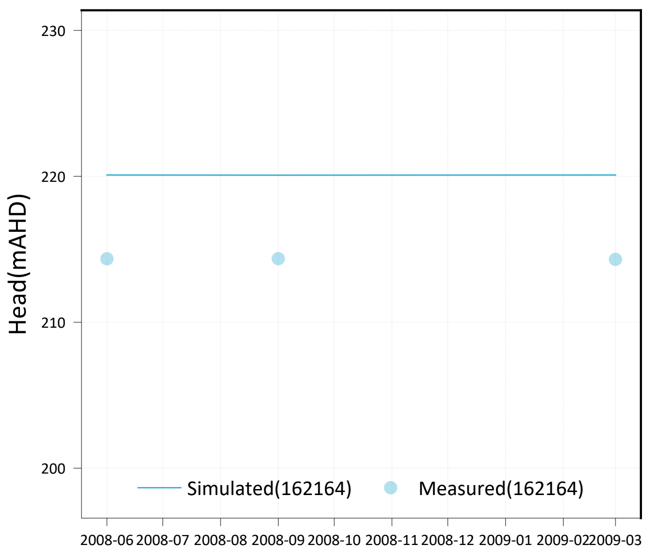

162169

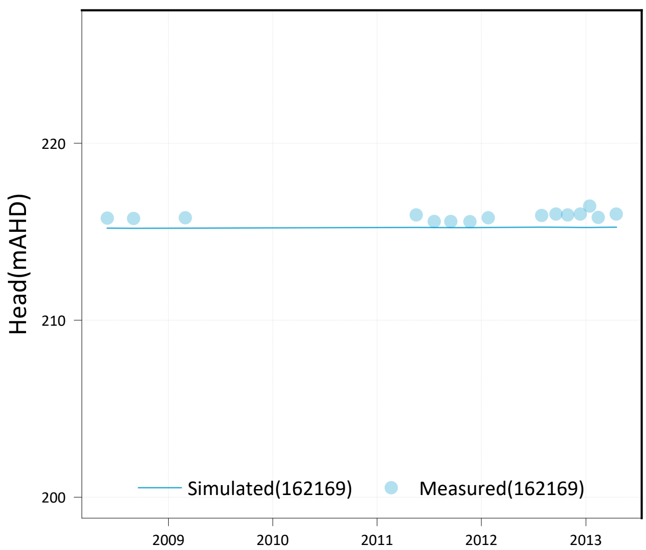

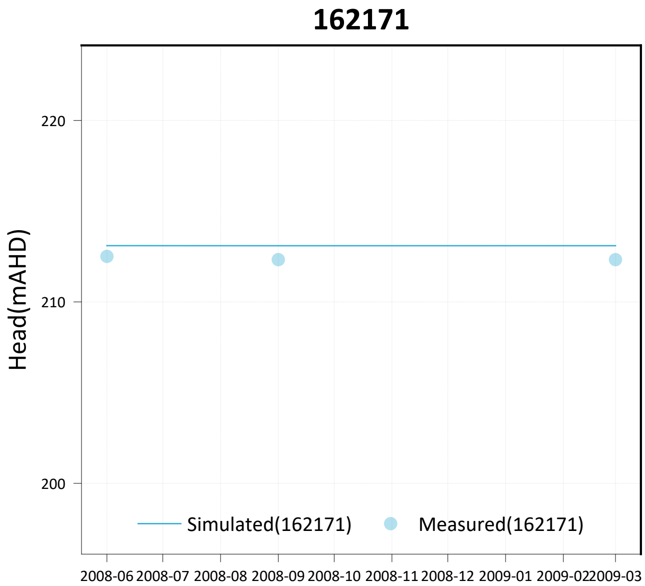
162171
Head(mAHD)
220
210
200
Simulated(162171)
Measured(162171)
2008-06 2008-07 2008-08 2008-09 2008-10 2008-11 2008-12 2009-01 2009-02 2009-03

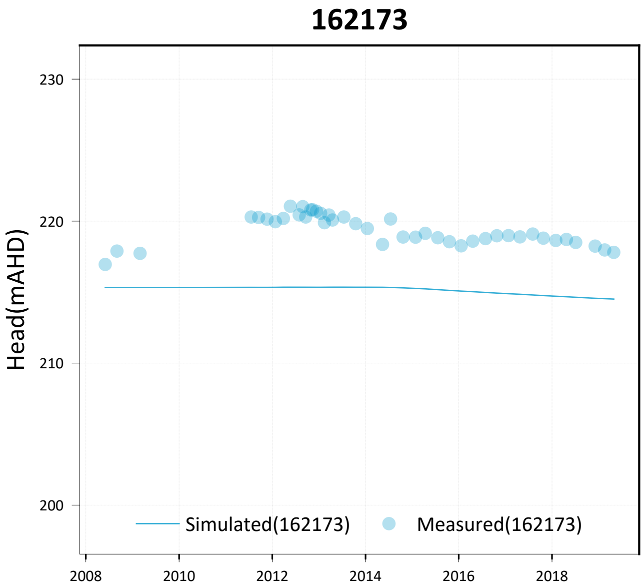
162173
Head(mAHD)
230
220
210
200
Simulated(162173)
Measured(162173)
2008 2010 2012 2014 2016 2018

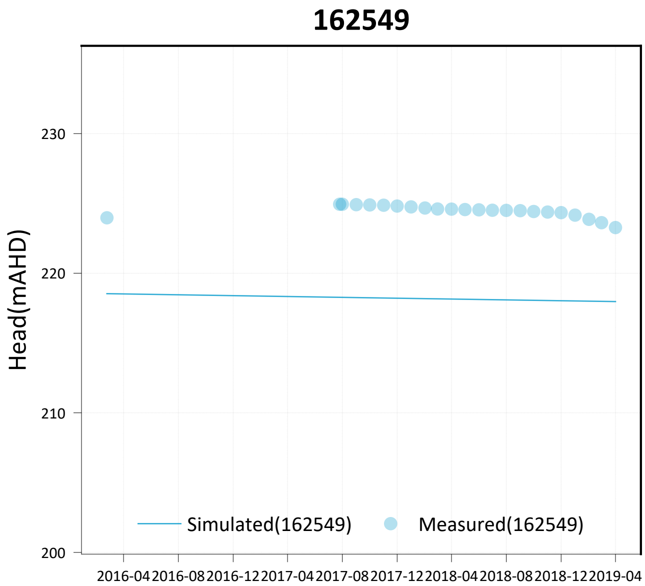
162549
Head(mAHD)
230
220
210
200
Simulated(162549)
Measured(162549)
2016-04 2016-08 2016-12 2017-04 2017-08 2017-12 2018-04 2018-08 2018-12 2019-04

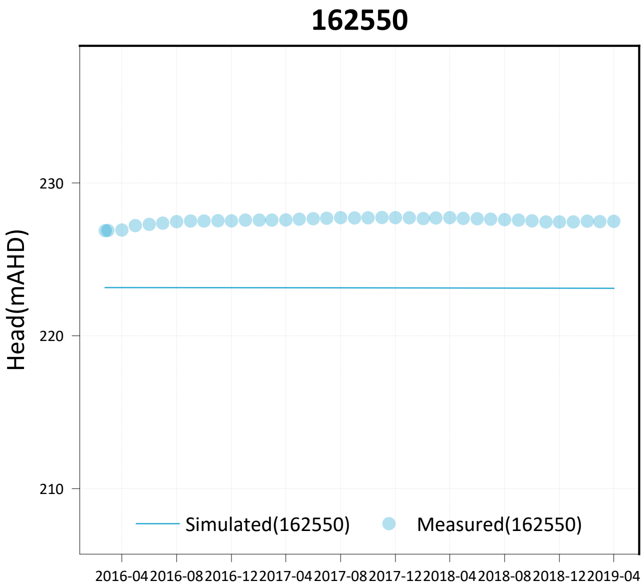
162550
Head(mAHD)
230
220
210
Simulated(162550)
Measured(162550)
2016-04 2016-08 2016-12 2017-04 2017-08 2017-12 2018-04 2018-08 2018-12 2019-04

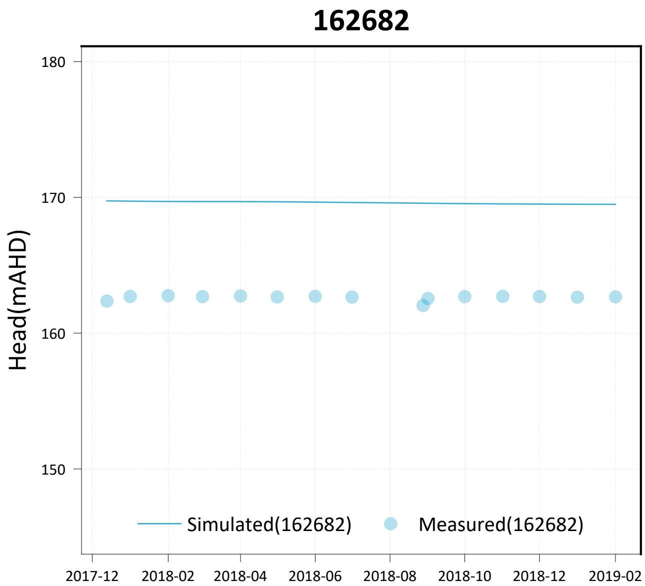
162682
Head(mAHD)
180
170
160
150
Simulated(162682)
Measured(162682)
2017-12 2018-02 2018-04 2018-06 2018-08 2018-10 2018-12 2019-02

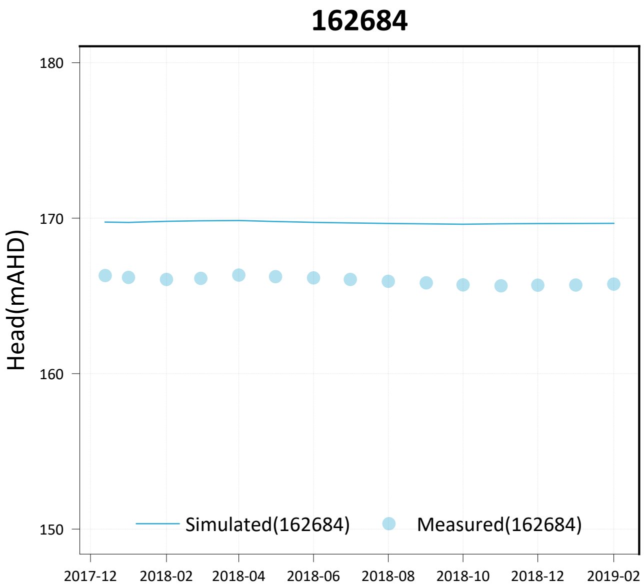
162684
Head(mAHD)
180
170
160
150
Simulated(162684)
Measured(162684)
2017-12 2018-02 2018-04 2018-06 2018-08 2018-10 2018-12 2019-02

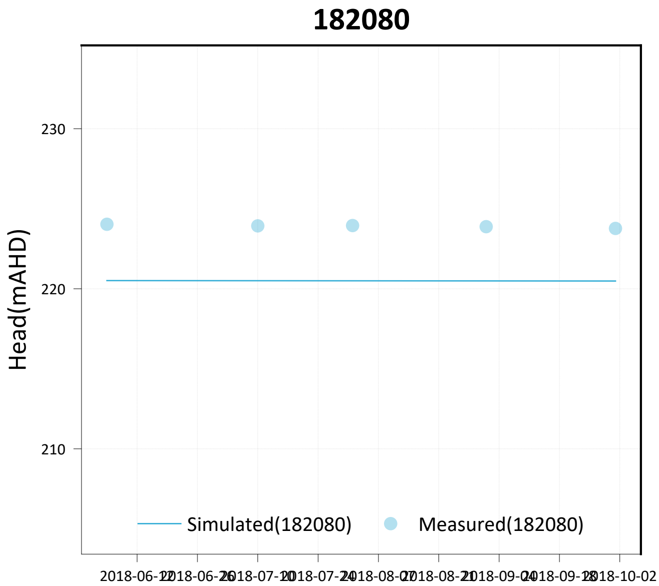

182080
230
220
210
Head(mAHD)
Simulated(182080)
Measured(182080)

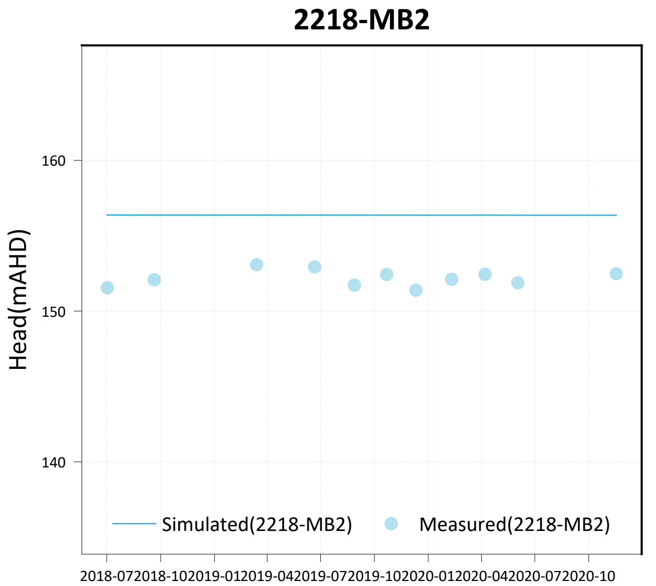

2218-MB2
160
150
140
Head(mAHD)
Simulated(2218-MB2)
Measured(2218-MB2)
2018-07 2018-10 2019-01 2019-04 2019-07 2019-10 2020-01 2020-04 2020-07 2020-10

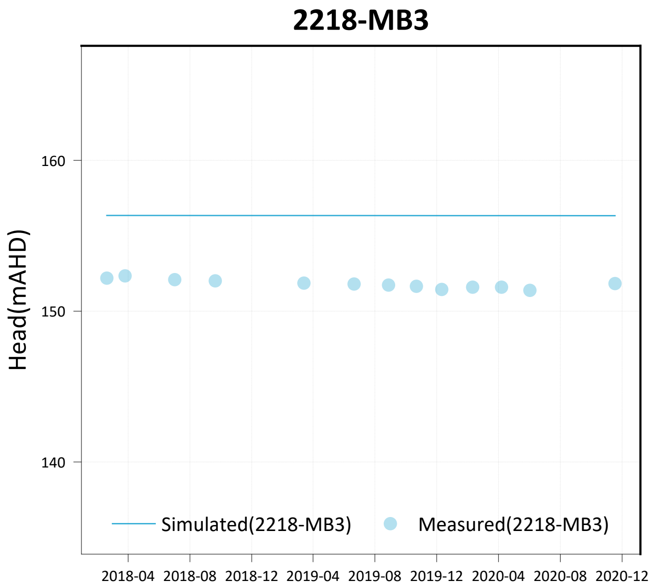

2218-MB3
160
150
140
Head(mAHD)
Simulated(2218-MB3)
Measured(2218-MB3)
2018-04 2018-08 2018-12 2019-04 2019-08 2019-12 2020-04 2020-08 2020-12

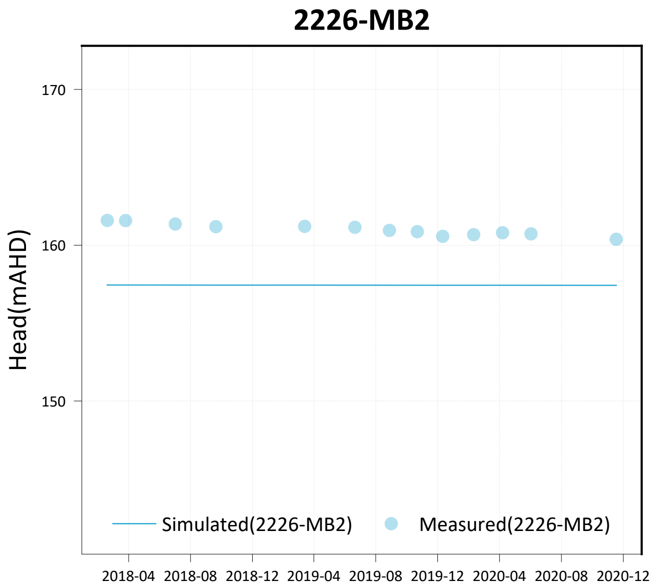

2226-MB2
170
160
150
Head(mAHD)
Simulated(2226-MB2)
Measured(2226-MB2)
2018-04 2018-08 2018-12 2019-04 2019-08 2019-12 2020-04 2020-08 2020-12

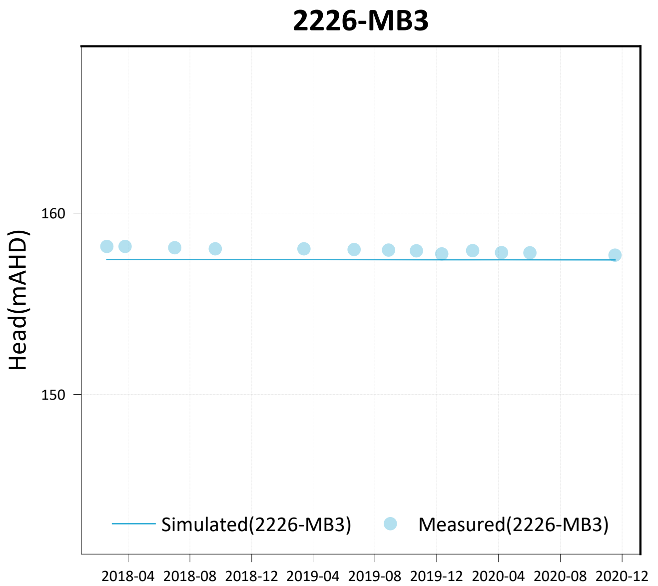

2226-MB3
160
150
Head(mAHD)
Simulated(2226-MB3)
Measured(2226-MB3)
2018-04 2018-08 2018-12 2019-04 2019-08 2019-12 2020-04 2020-08 2020-12

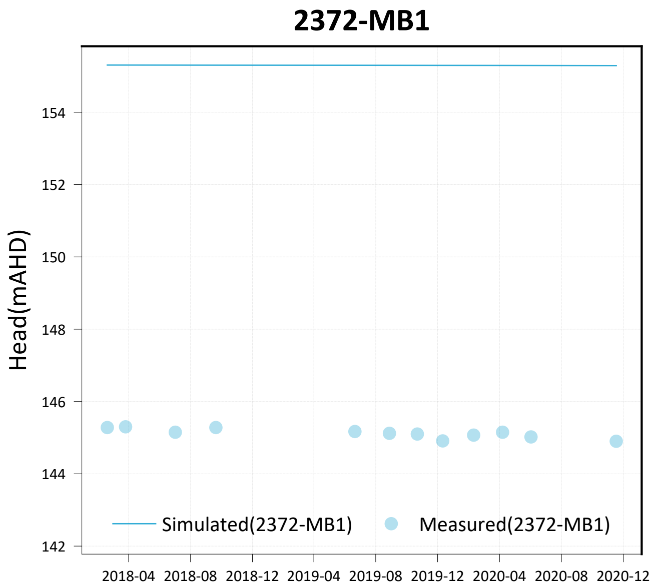

2372-MB1
154
152
150
148
146
144
142
Head(mAHD)
Simulated(2372-MB1)
Measured(2372-MB1)
2018-04 2018-08 2018-12 2019-04 2019-08 2019-12 2020-04 2020-08 2020-12

2372-MB2

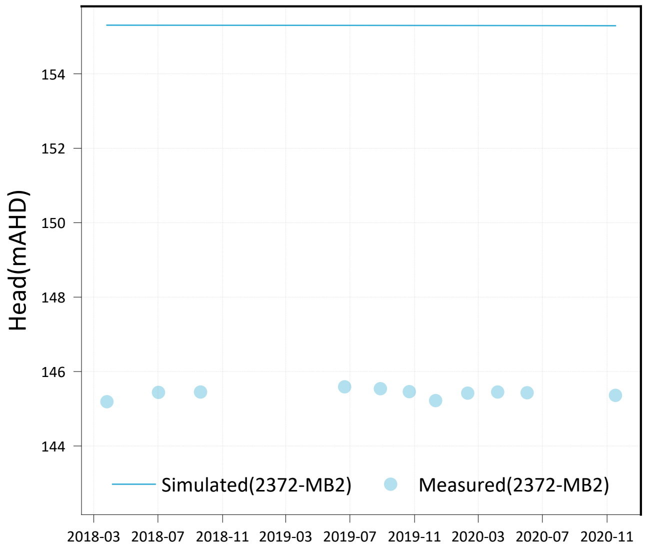

2372-MB3

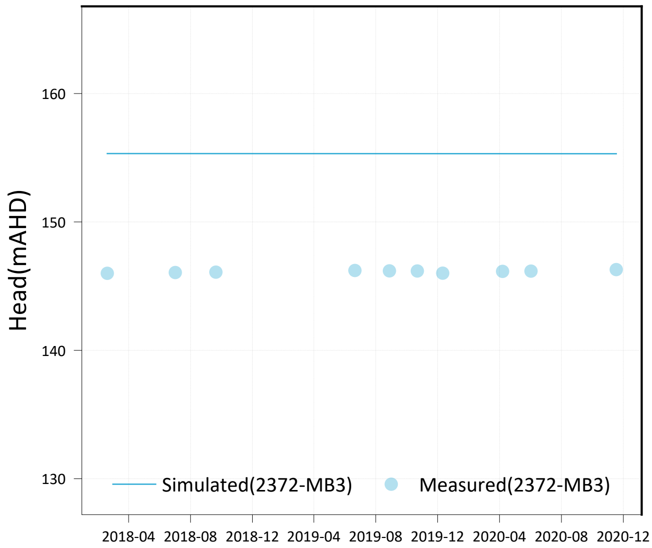

2393-MB1

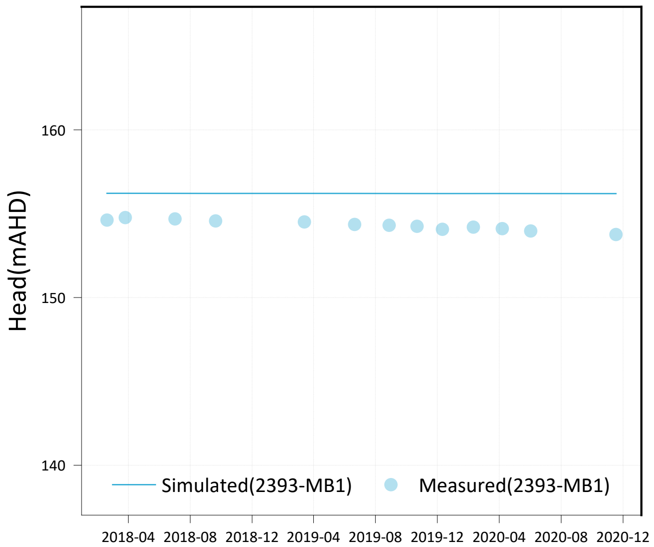

2393-MB2

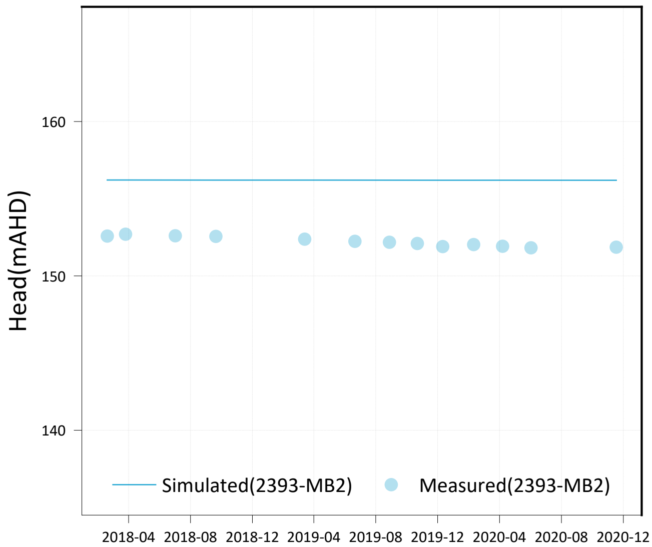

2393-MB3

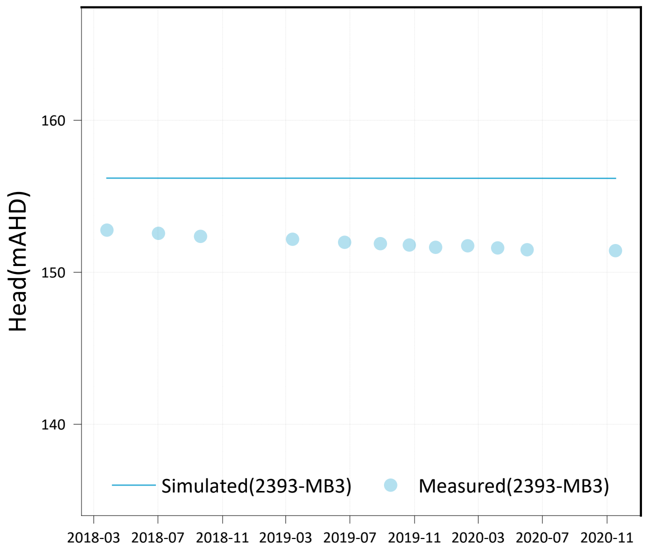

2394-MB1

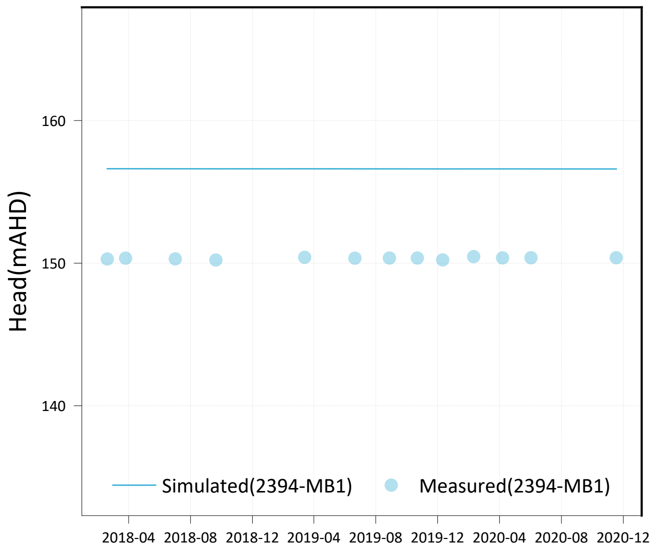

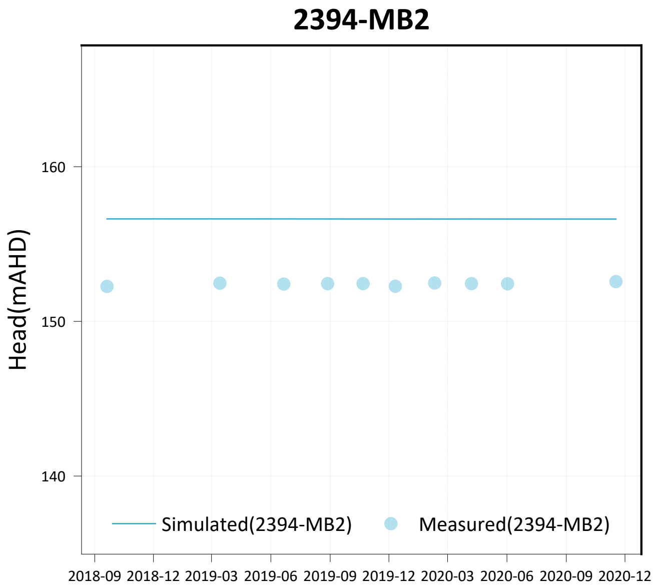
2394-MB2
Head(mAHD)
160
150
140
Simulated(2394-MB2)
Measured(2394-MB2)
2018-09 2018-12 2019-03 2019-06 2019-09 2019-12 2020-03 2020-06 2020-09 2020-12

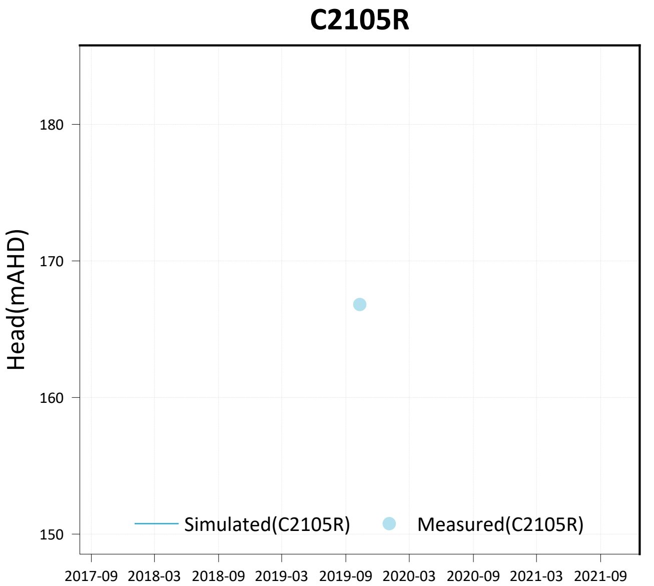
C2105R
Head(mAHD)
180
170
160
150
Simulated(C2105R)
Measured(C2105R)
2017-09 2018-03 2018-09 2019-03 2019-09 2020-03 2020-09 2021-03 2021-09

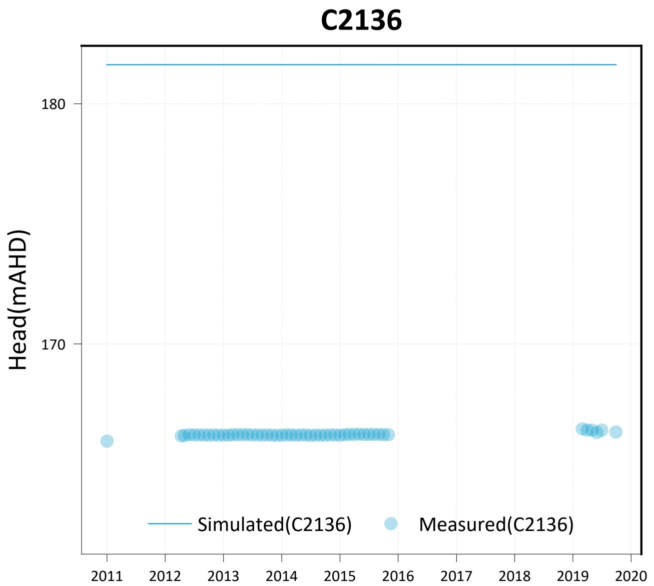
C2136
Head(mAHD)
180
170
Simulated(C2136)
Measured(C2136)
2011 2012 2013 2014 2015 2016 2017 2018 2019 2020

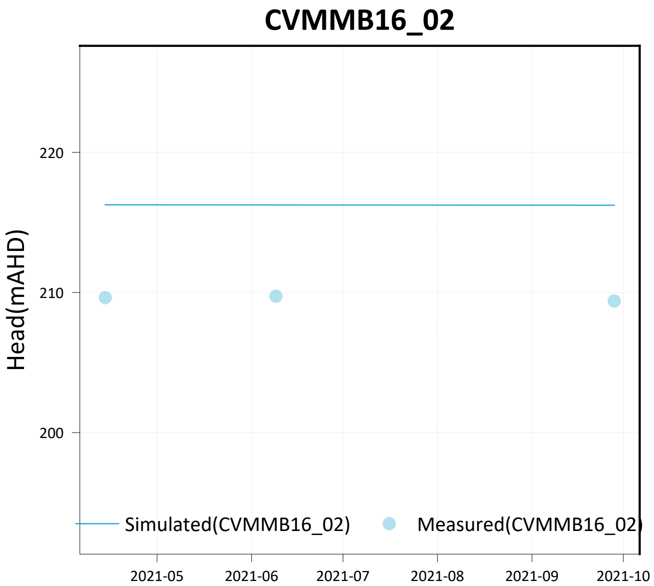
CVMMB16_02
Head(mAHD)
220
210
200
Simulated(CVMMB16_02)
Measured(CVMMB16_02)
2021-05 2021-06 2021-07 2021-08 2021-09 2021-10

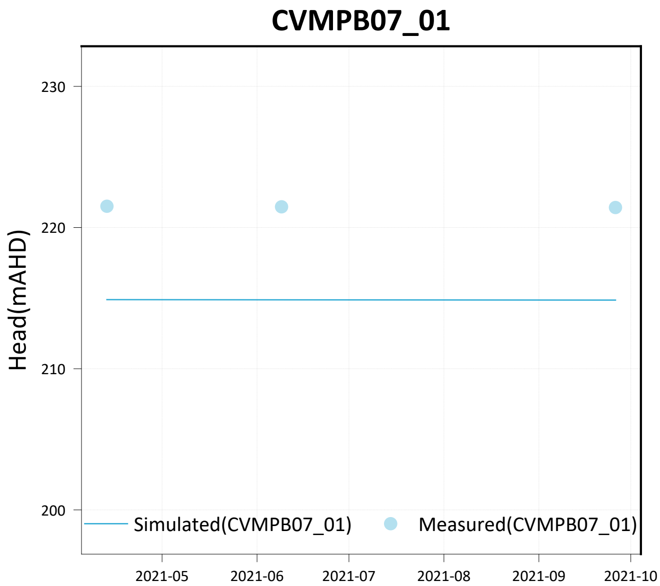
CVMPB07_01
Head(mAHD)
230
220
210
200
Simulated(CVMPB07_01)
Measured(CVMPB07_01)
2021-05 2021-06 2021-07 2021-08 2021-09 2021-10

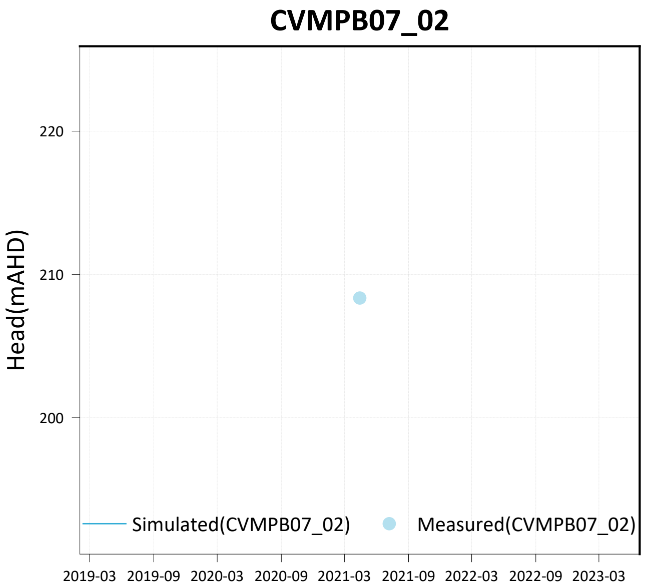
CVMPB07_02
Head(mAHD)
220
210
200
Simulated(CVMPB07_02)
Measured(CVMPB07_02)
2019-03 2019-09 2020-03 2020-09 2021-03 2021-09 2022-03 2022-09 2023-03

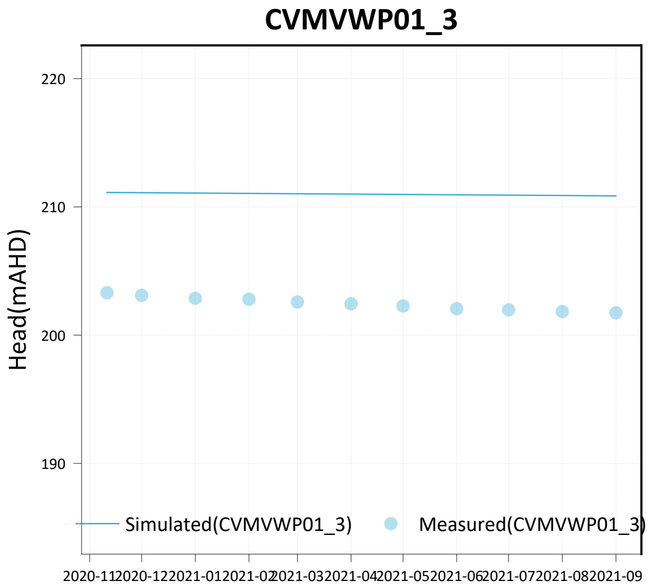
CVMVWP01_3
Head(mAHD)
220
210
200
190
Simulated(CVMVWP01_3)
Measured(CVMVWP01_3)
2020-11
2020-12
2021-01
2021-02
2021-03
2021-04
2021-05
2021-06
2021-07
2021-08
2021-09

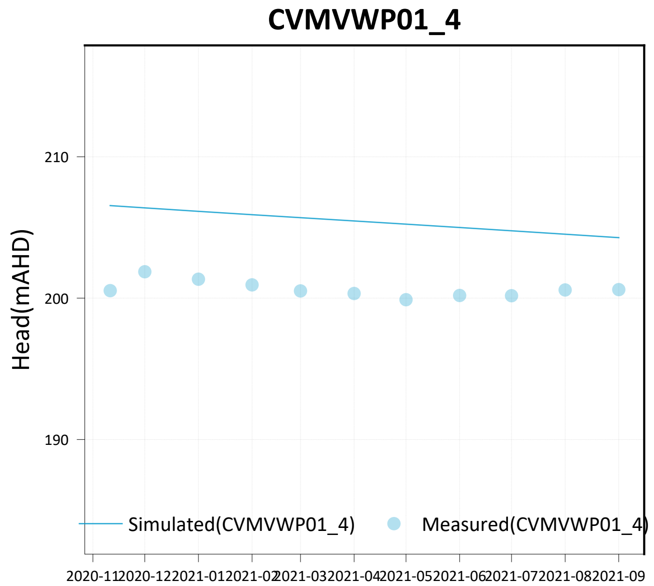
CVMVWP01_4
Head(mAHD)
210
200
190
Simulated(CVMVWP01_4)
Measured(CVMVWP01_4)
2020-11
2020-12
2021-01
2021-02
2021-03
2021-04
2021-05
2021-06
2021-07
2021-08
2021-09

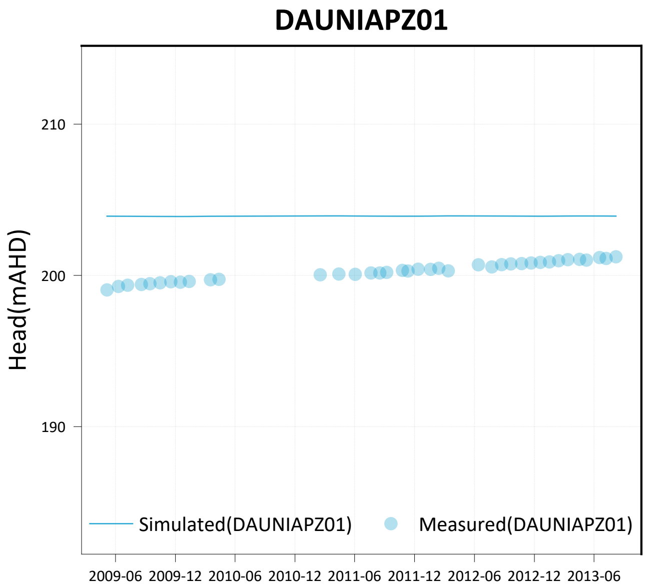
DAUNIAPZ01
Head(mAHD)
210
200
190
Simulated(DAUNIAPZ01)
Measured(DAUNIAPZ01)
2009-06
2009-12
2010-06
2010-12
2011-06
2011-12
2012-06
2012-12
2013-06

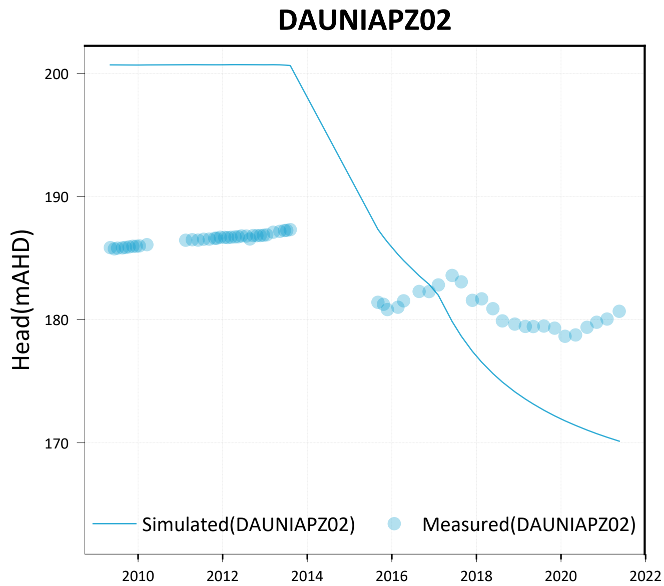
DAUNIAPZ02
Head(mAHD)
200
190
180
170
Simulated(DAUNIAPZ02)
Measured(DAUNIAPZ02)
2010
2012
2014
2016
2018
2020
2022

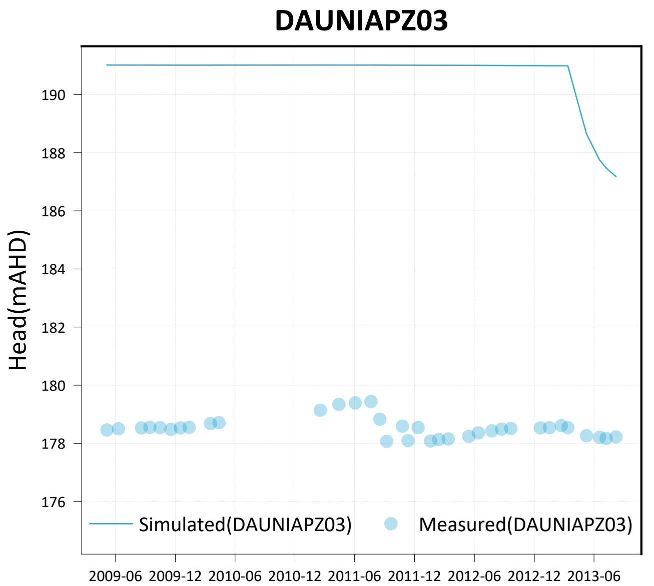
DAUNIAPZ03
Head(mAHD)
190
188
186
184
182
180
178
176
Simulated(DAUNIAPZ03)
Measured(DAUNIAPZ03)
2009-06
2009-12
2010-06
2010-12
2011-06
2011-12
2012-06
2012-12
2013-06

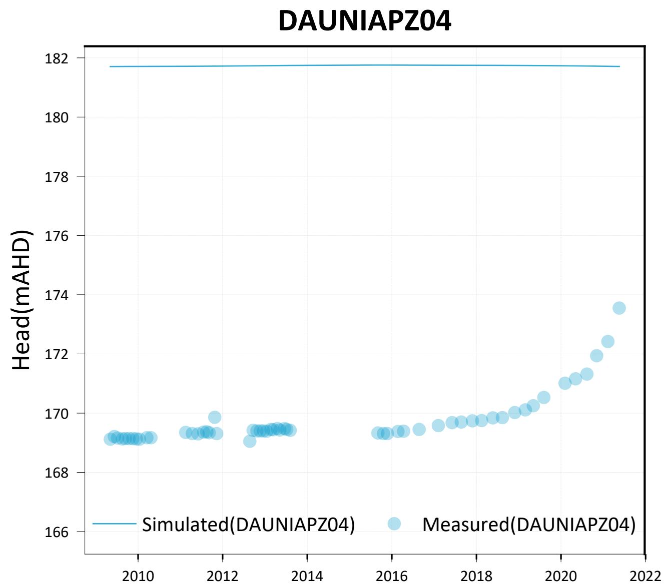
DAUNIAPZ04
Head(mAHD)
182
180
178
176
174
172
170
168
166
Simulated(DAUNIAPZ04)
Measured(DAUNIAPZ04)
2010
2012
2014
2016
2018
2020
2022

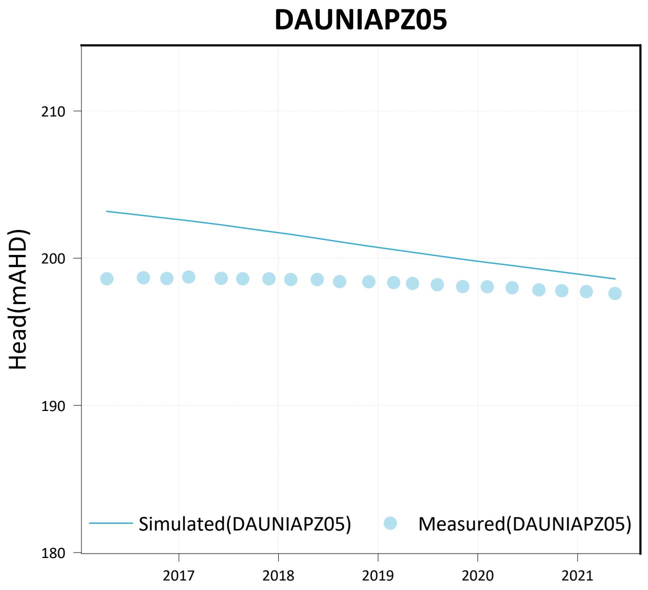
DAUNIAPZ05
Head(mAHD)
Simulated(DAUNIAPZ05)
Measured(DAUNIAPZ05)

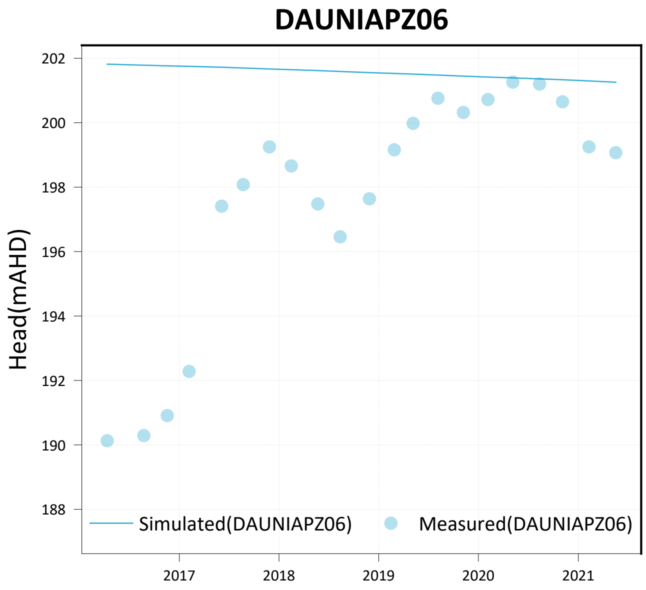
DAUNIAPZ06
Head(mAHD)
Simulated(DAUNIAPZ06)
Measured(DAUNIAPZ06)

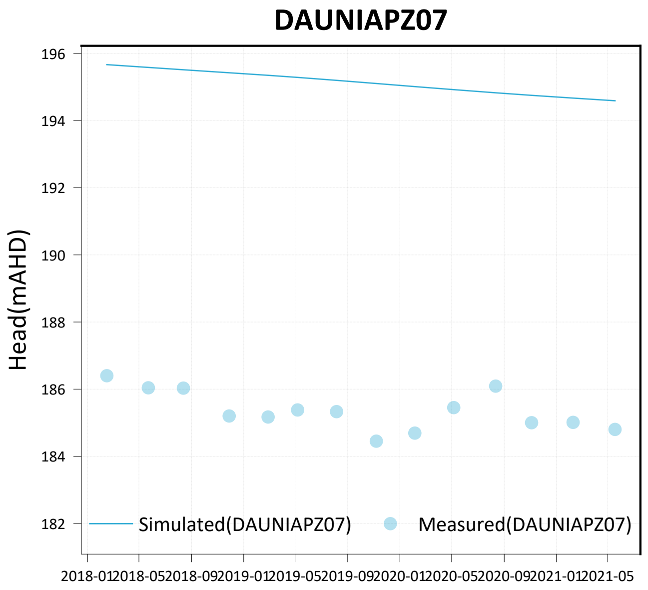
DAUNIAPZ07
Head(mAHD)
Simulated(DAUNIAPZ07)
Measured(DAUNIAPZ07)

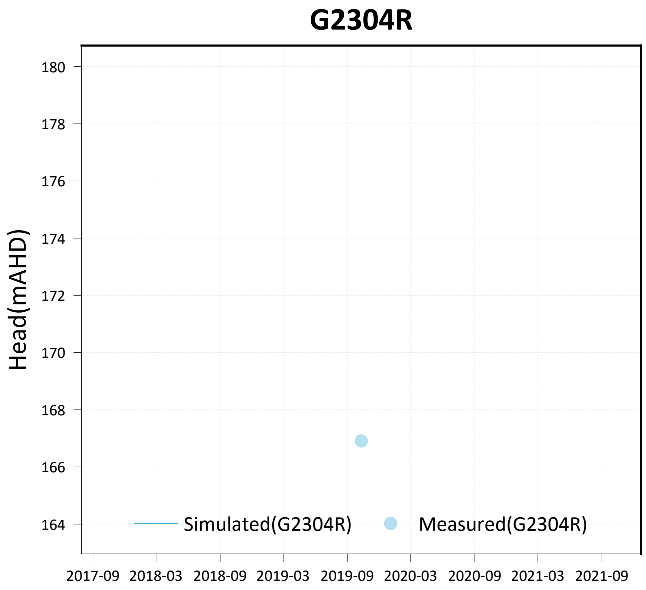
G2304R
Head(mAHD)
Simulated(G2304R)
Measured(G2304R)

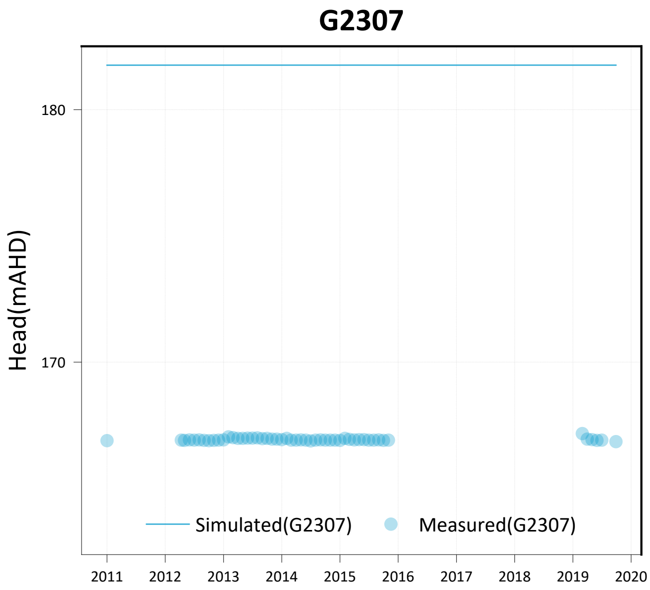
G2307
Head(mAHD)
Simulated(G2307)
Measured(G2307)

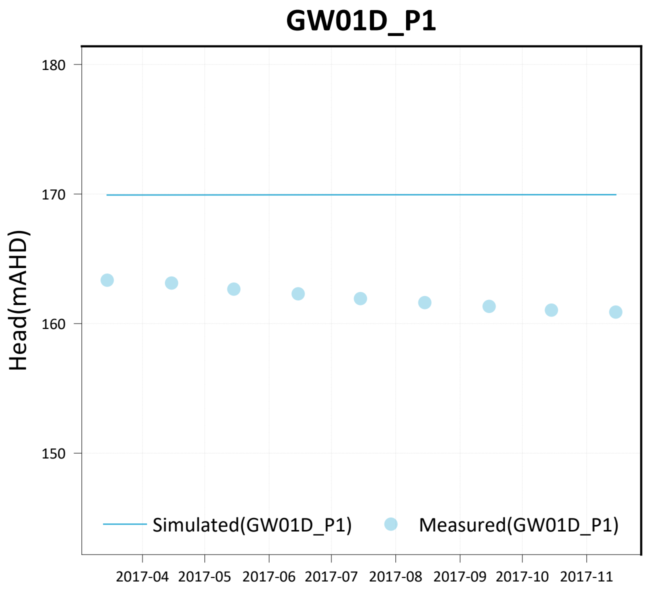
GW01D_P1
Head(mAHD)
Simulated(GW01D_P1)
Measured(GW01D_P1)

GW01D_P2

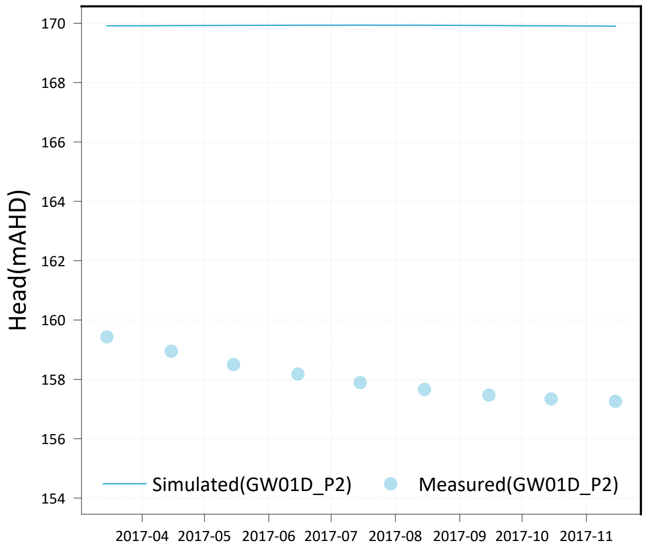

GW01D_P3

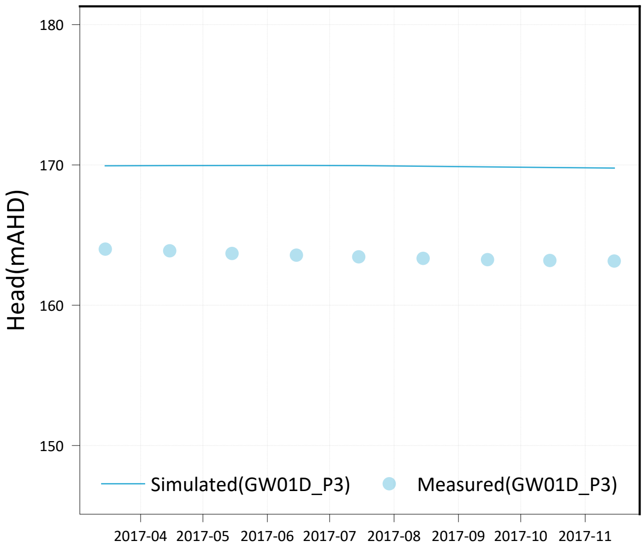

GW01D_P4

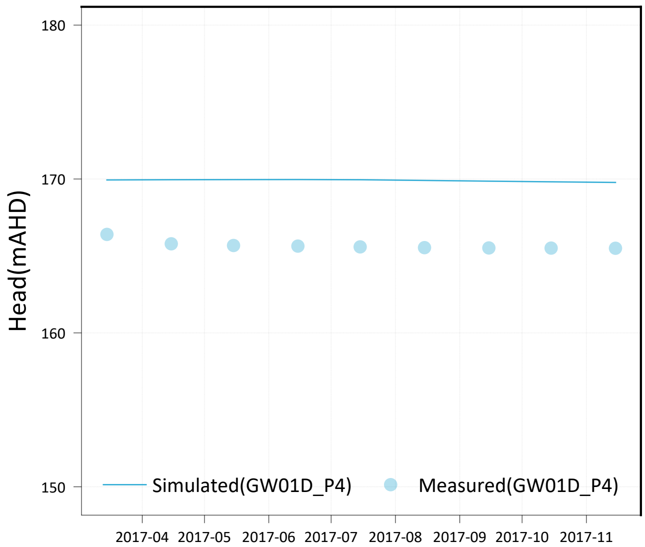

GW01S

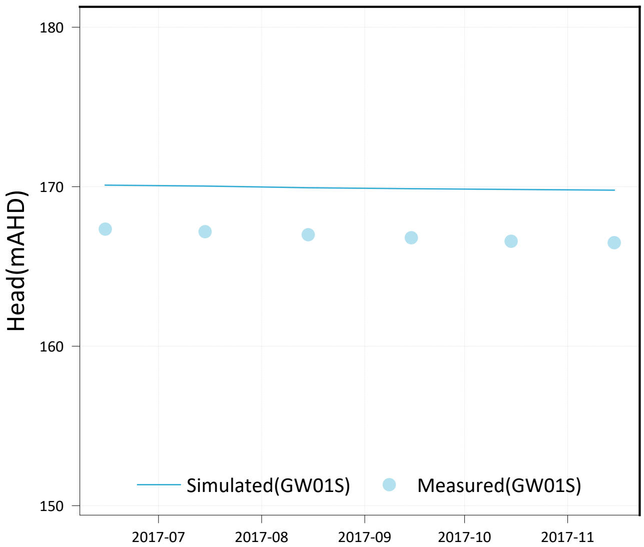

GW02D

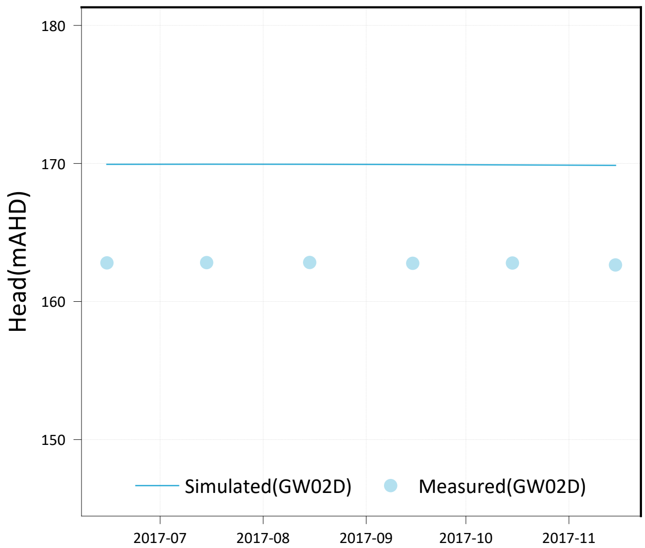

GW02S

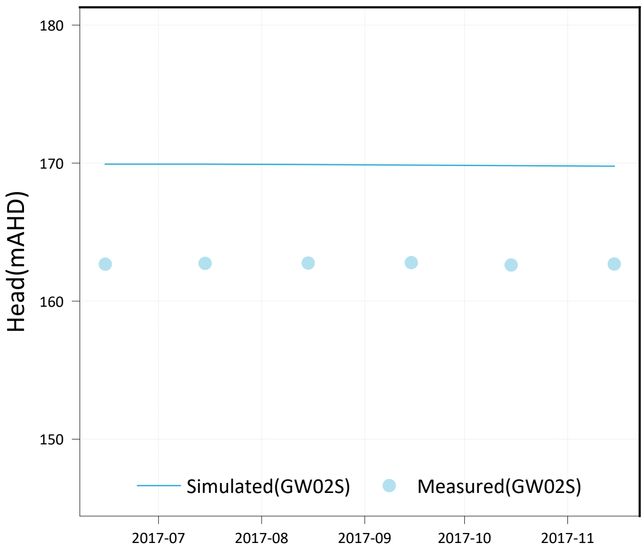

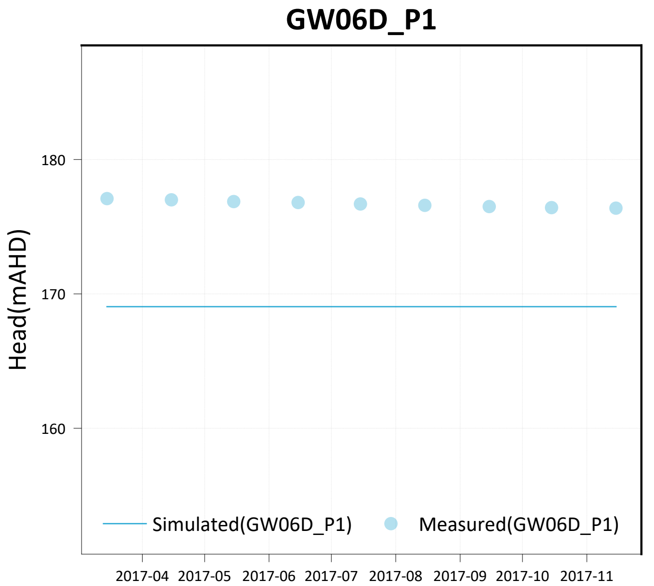
GW06D_P1
Head(mAHD)
180
170
160
Simulated(GW06D_P1)
Measured(GW06D_P1)
2017-04 2017-05 2017-06 2017-07 2017-08 2017-09 2017-10 2017-11

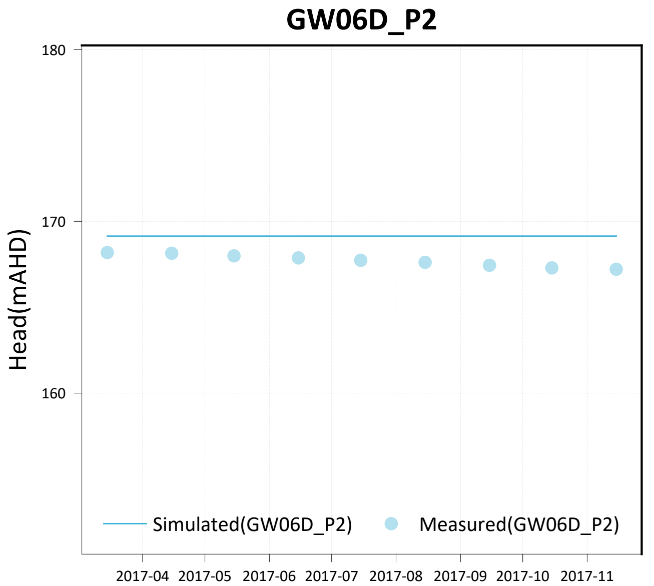
GW06D_P2
Head(mAHD)
180
170
160
Simulated(GW06D_P2)
Measured(GW06D_P2)
2017-04 2017-05 2017-06 2017-07 2017-08 2017-09 2017-10 2017-11

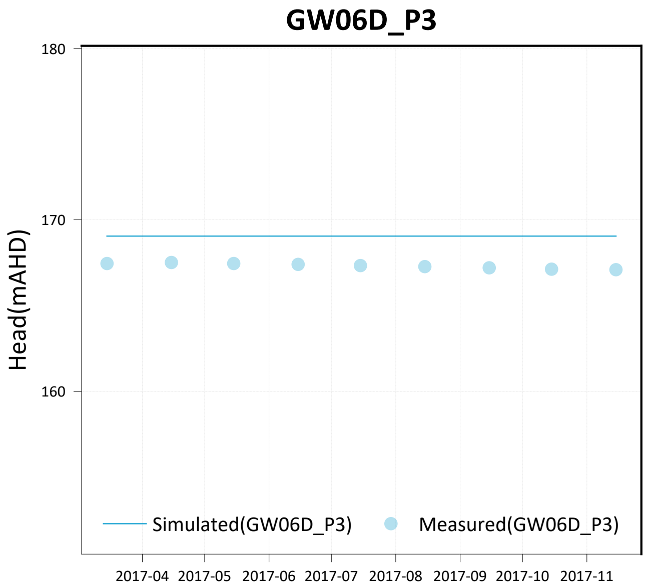
GW06D_P3
Head(mAHD)
180
170
160
Simulated(GW06D_P3)
Measured(GW06D_P3)
2017-04 2017-05 2017-06 2017-07 2017-08 2017-09 2017-10 2017-11

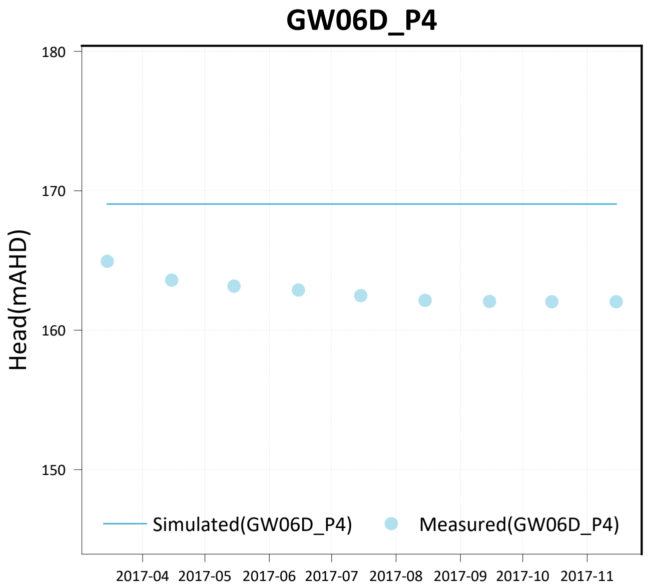
GW06D_P4
Head(mAHD)
180
170
160
150
Simulated(GW06D_P4)
Measured(GW06D_P4)
2017-04 2017-05 2017-06 2017-07 2017-08 2017-09 2017-10 2017-11

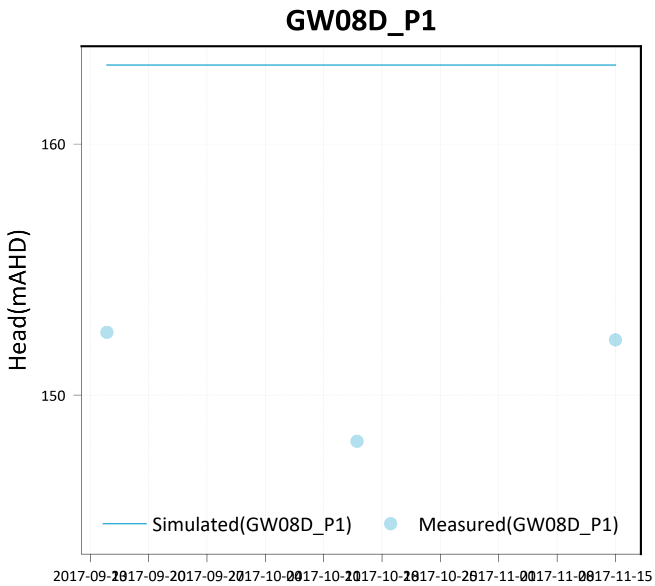
GW08D_P1
Head(mAHD)
160
150
Simulated(GW08D_P1)
Measured(GW08D_P1)
2017-11-15

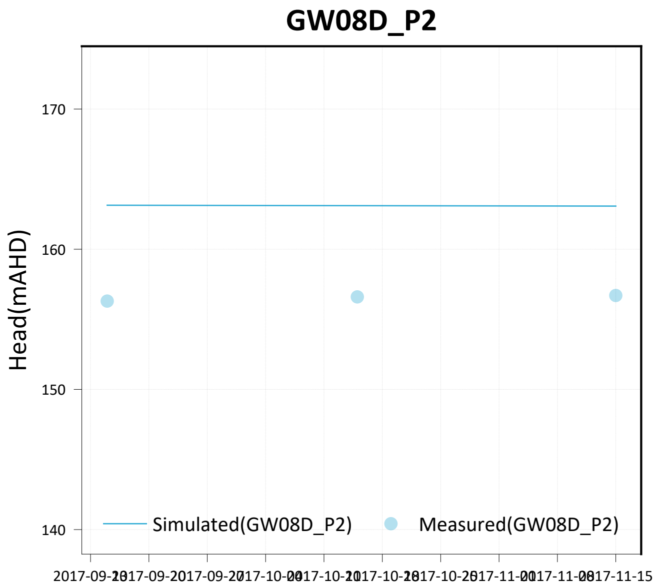
GW08D_P2
Head(mAHD)
170
160
150
140
Simulated(GW08D_P2)
Measured(GW08D_P2)
2017-11-15

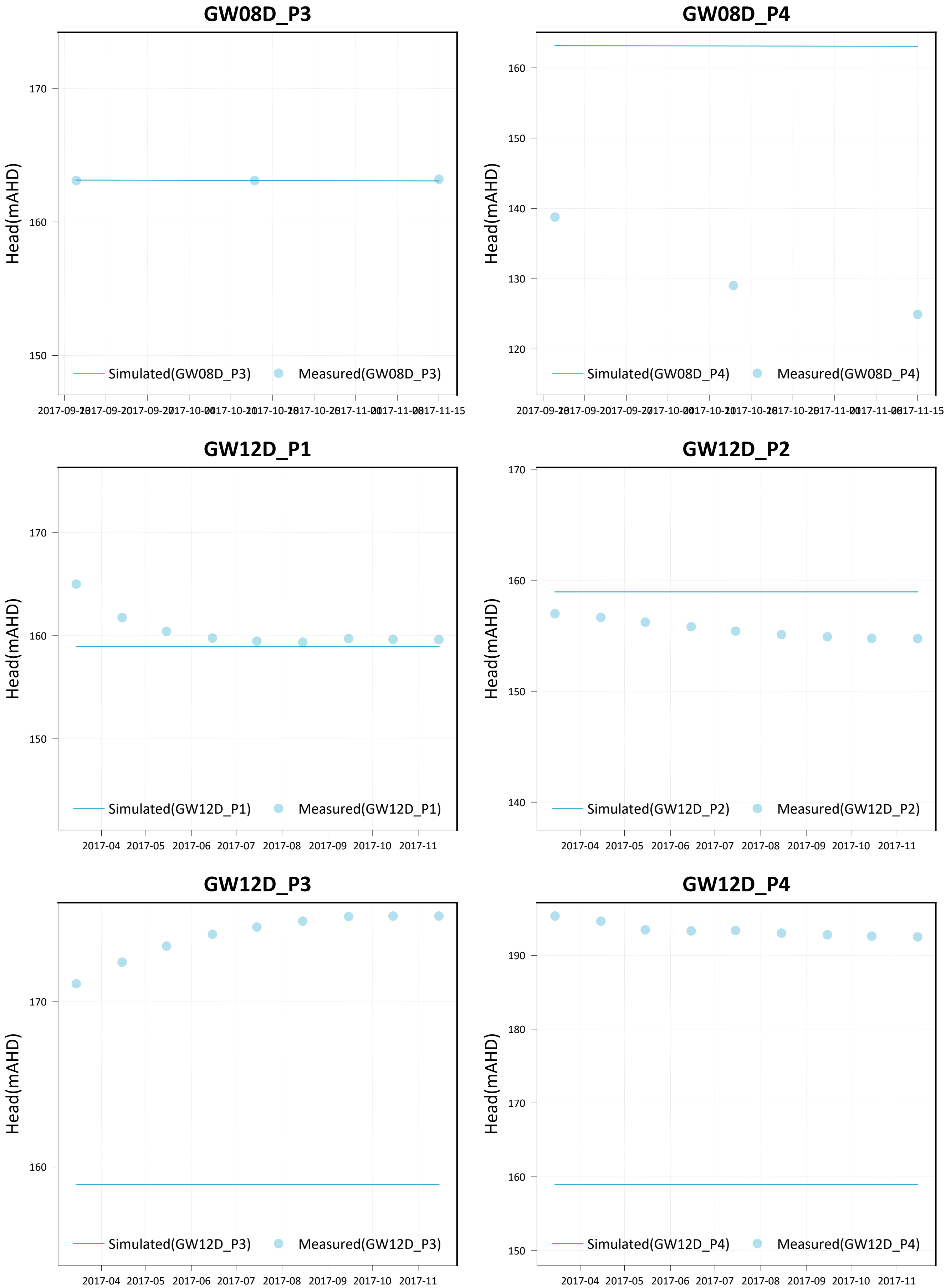

GW08D_P3
Head(mAHD)
Simulated(GW08D_P3)
Measured(GW08D_P3)
GW08D_P4
Simulated(GW08D_P4)
Measured(GW08D_P4)
GW12D_P1
Simulated(GW12D_P1)
Measured(GW12D_P1)
GW12D_P2
Simulated(GW12D_P2)
Measured(GW12D_P2)
GW12D_P3
Simulated(GW12D_P3)
Measured(GW12D_P3)
GW12D_P4
Simulated(GW12D_P4)
Measured(GW12D_P4)
2017-04 2017-05 2017-06 2017-07 2017-08 2017-09 2017-10 2017-11

GW12S

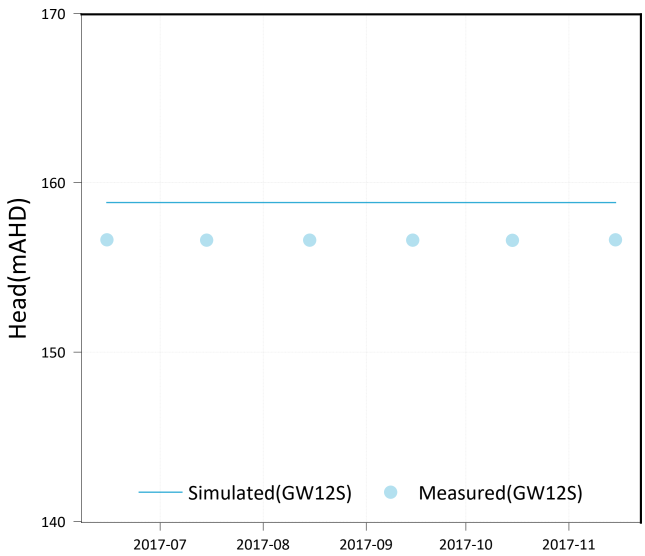

GW16D_P1

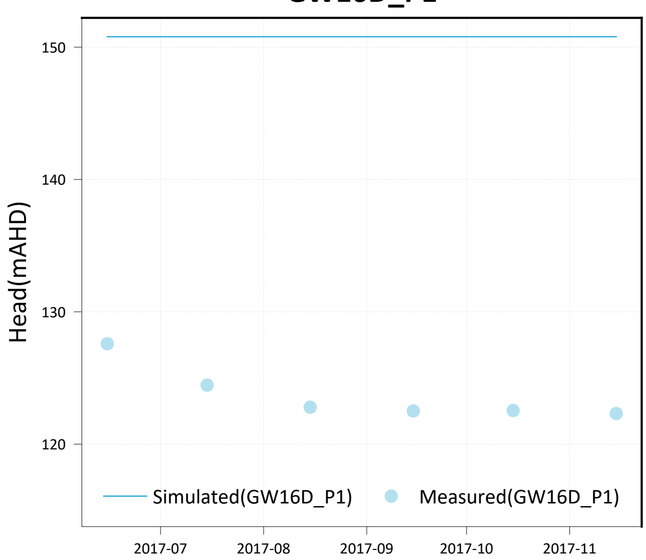

GW16D_P2

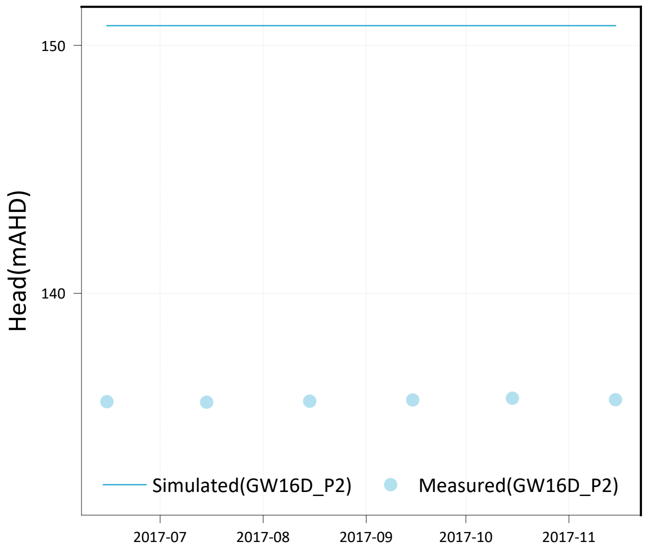

GW16D_P3

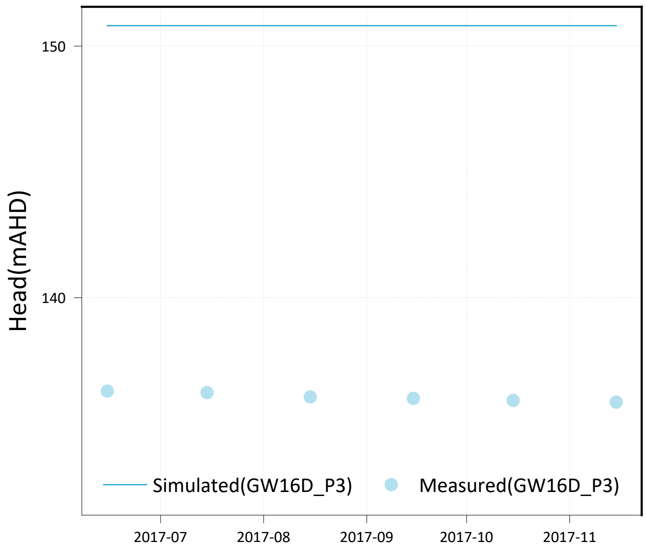

GW16D_P4

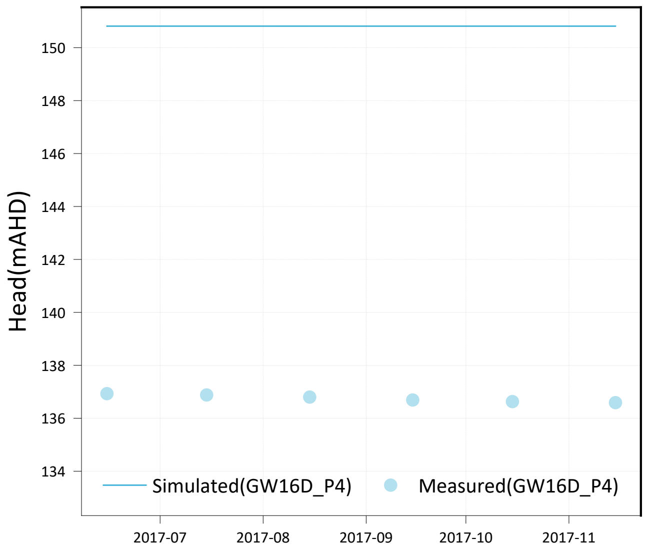

GW18S

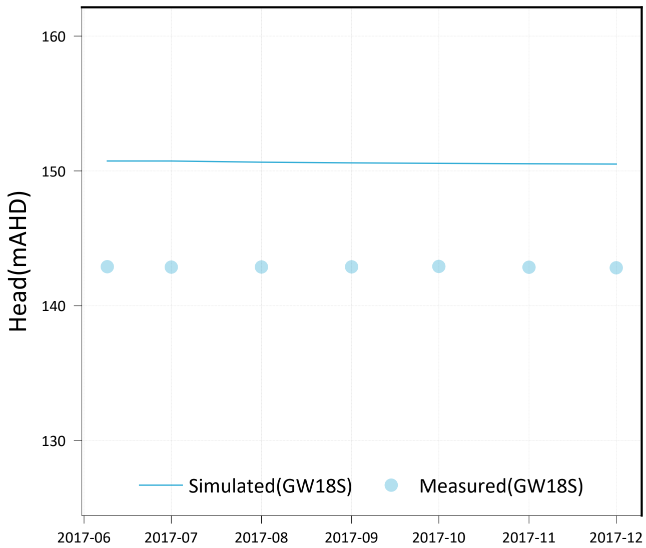

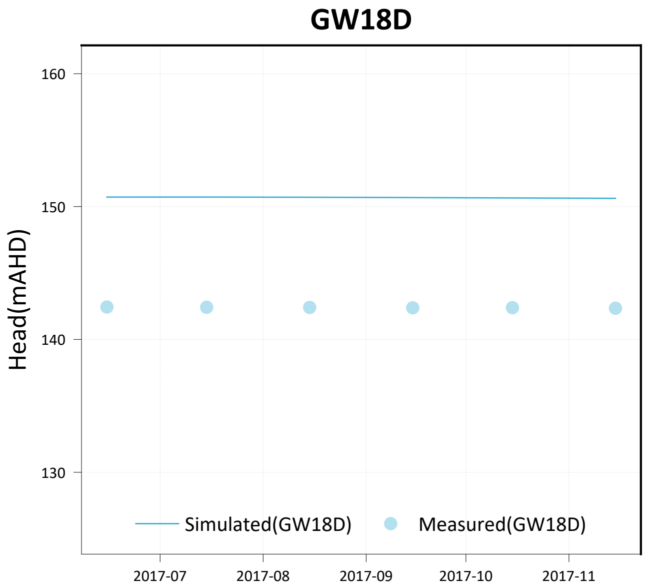
GW18D
160
150
140
130
Head(mAHD)
Simulated(GW18D)
Measured(GW18D)
2017-07
2017-08
2017-09
2017-10
2017-11

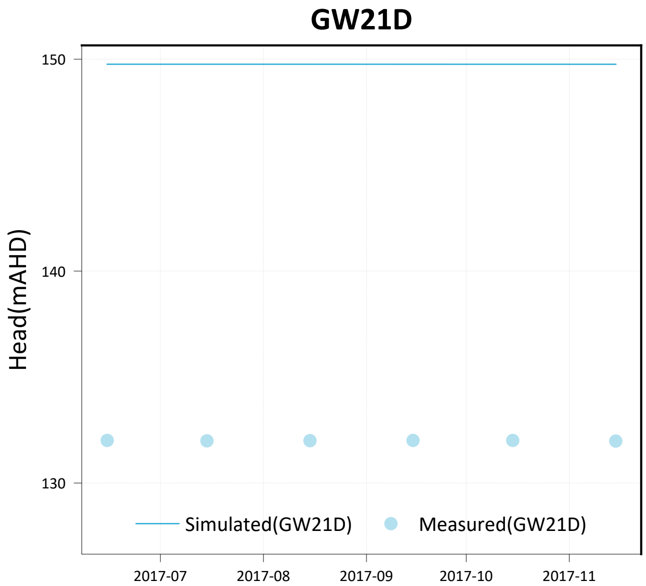
GW21D
150
140
130
Head(mAHD)
Simulated(GW21D)
Measured(GW21D)
2017-07
2017-08
2017-09
2017-10
2017-11

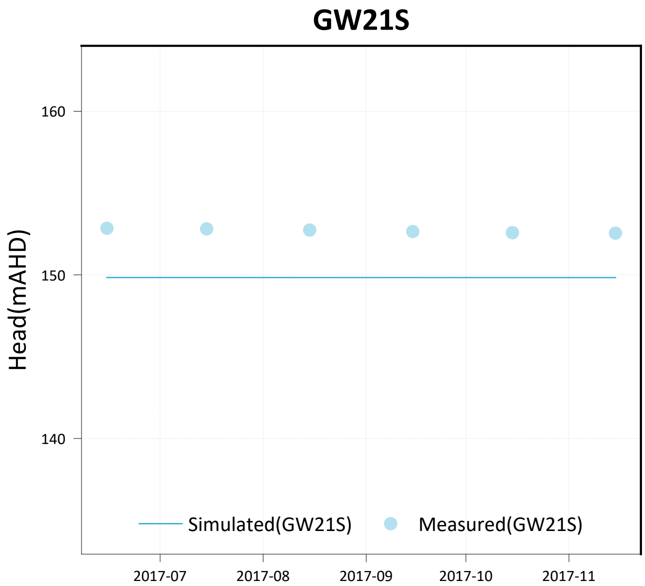
GW21S
160
150
140
Head(mAHD)
Simulated(GW21S)
Measured(GW21S)
2017-07
2017-08
2017-09
2017-10
2017-11

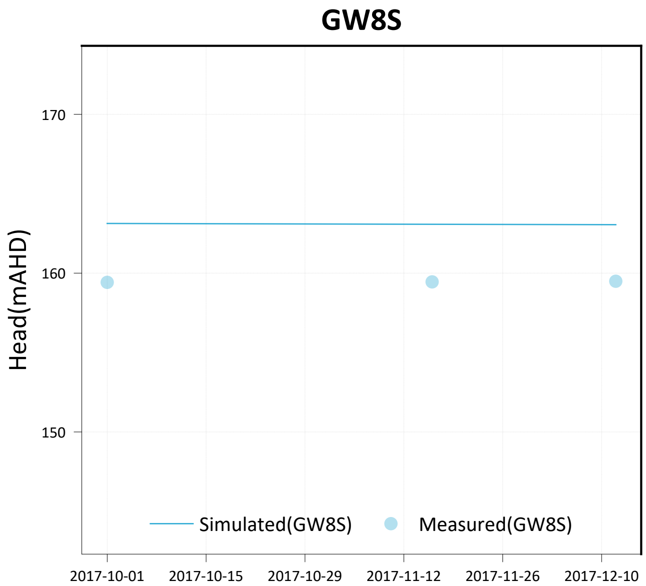
GW8S
170
160
150
Head(mAHD)
Simulated(GW8S)
Measured(GW8S)
2017-10-01
2017-10-15
2017-10-29
2017-11-12
2017-11-26
2017-12-10

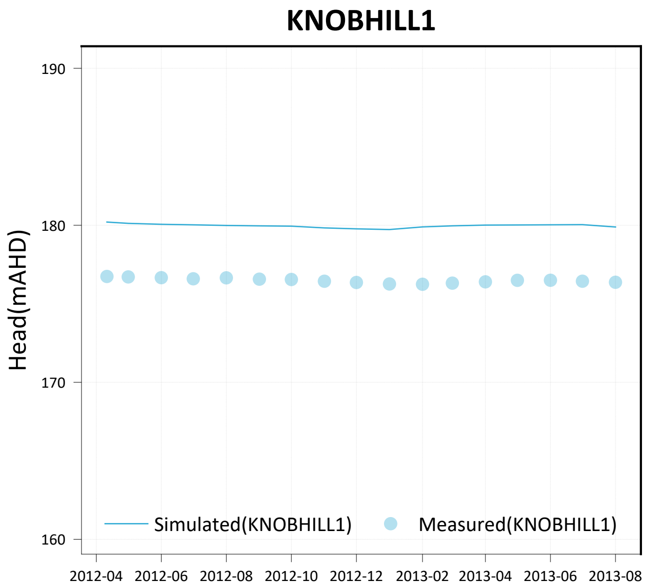
KNOBHILL1
190
180
170
160
Head(mAHD)
Simulated(KNOBHILL1)
Measured(KNOBHILL1)
2012-04
2012-06
2012-08
2012-10
2012-12
2013-02
2013-04
2013-06
2013-08

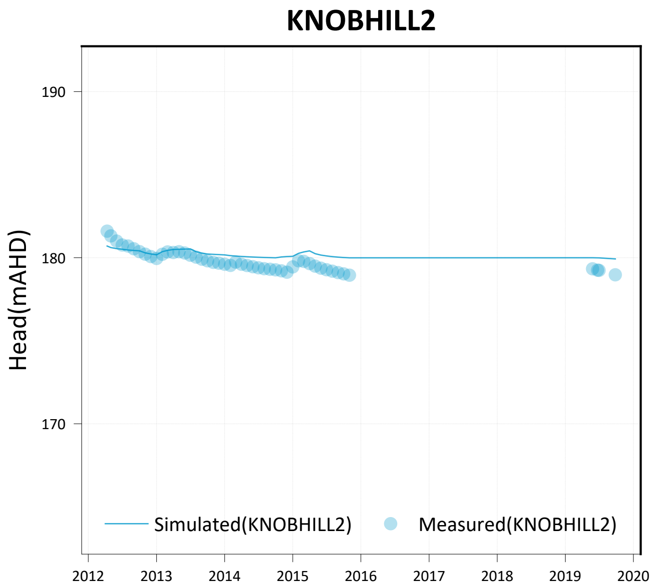
KNOBHILL2
190
180
170
Head(mAHD)
Simulated(KNOBHILL2)
Measured(KNOBHILL2)
2012
2013
2014
2015
2016
2017
2018
2019
2020

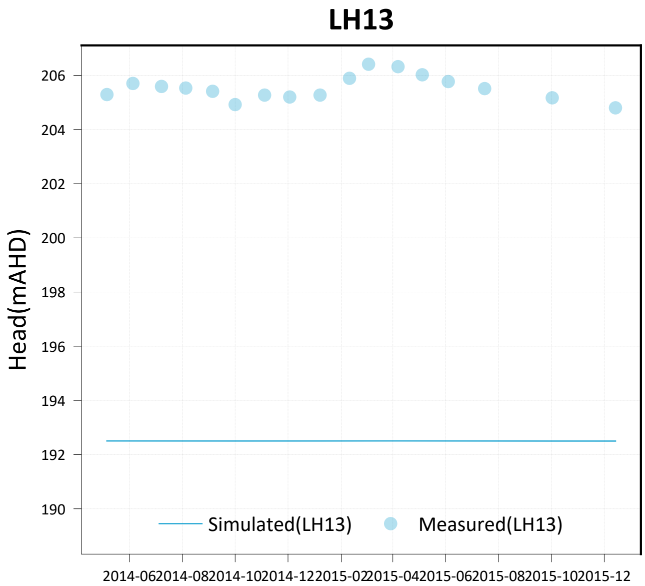
LH13
Head(mAHD)
206
204
202
200
198
196
194
192
190
Simulated(LH13)
Measured(LH13)
2014-06
2014-08
2014-10
2014-12
2015-02
2015-04
2015-06
2015-08
2015-10
2015-12

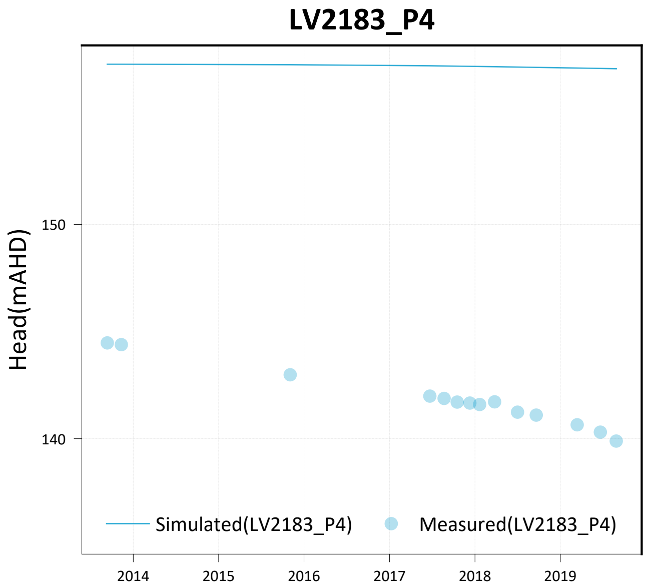
LV2183_P4
Head(mAHD)
150
140
Simulated(LV2183_P4)
Measured(LV2183_P4)
2014
2015
2016
2017
2018
2019

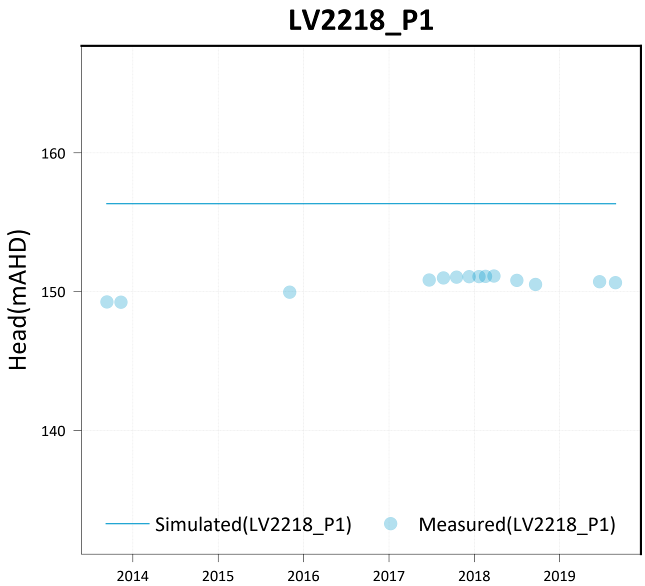
LV2218_P1
Head(mAHD)
160
150
140
Simulated(LV2218_P1)
Measured(LV2218_P1)
2014
2015
2016
2017
2018
2019

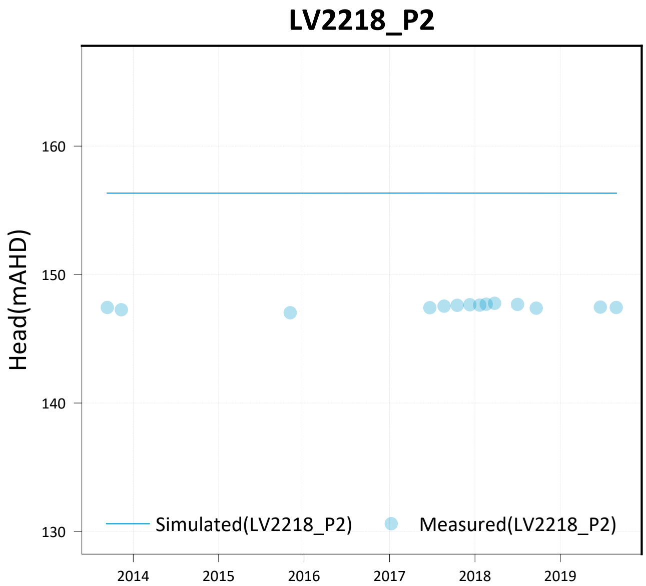
LV2218_P2
Head(mAHD)
160
150
140
130
Simulated(LV2218_P2)
Measured(LV2218_P2)
2014
2015
2016
2017
2018
2019

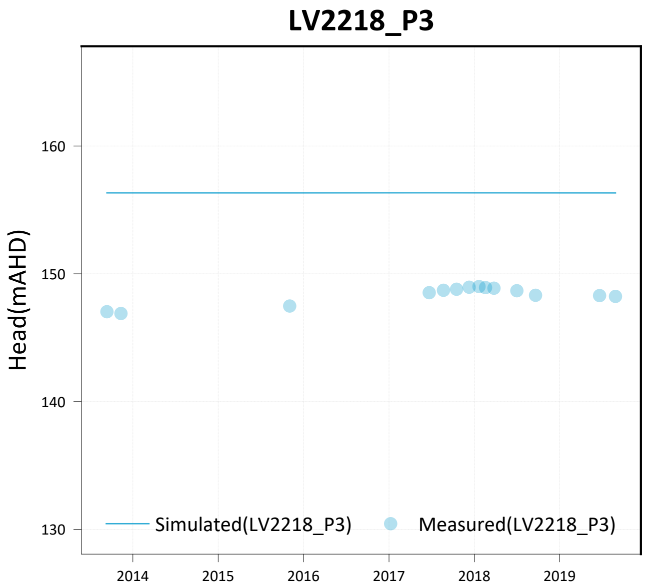
LV2218_P3
Head(mAHD)
160
150
140
130
Simulated(LV2218_P3)
Measured(LV2218_P3)
2014
2015
2016
2017
2018
2019

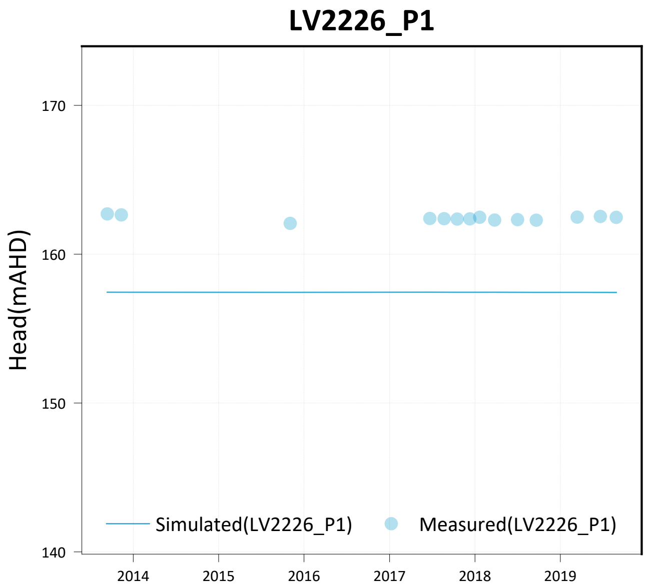
LV2226_P1
Head(mAHD)
170
160
150
140
Simulated(LV2226_P1)
Measured(LV2226_P1)
2014
2015
2016
2017
2018
2019

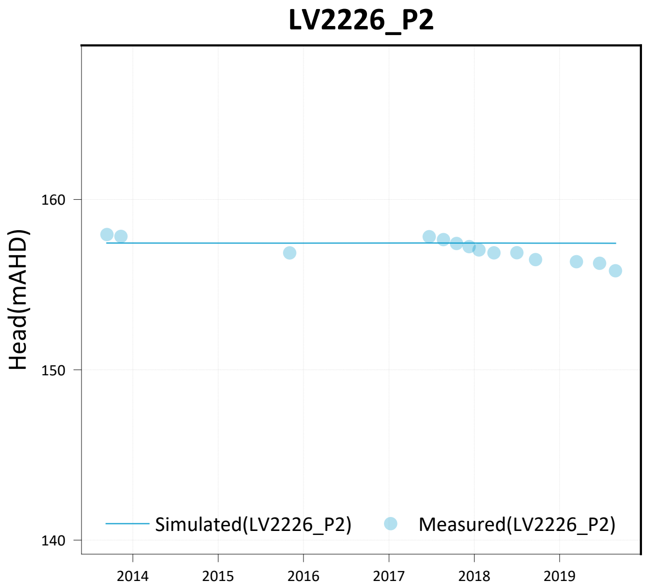
LV2226_P2
Head(mAHD)
160
150
140
2014
2015
2016
2017
2018
2019
Simulated(LV2226_P2)
Measured(LV2226_P2)

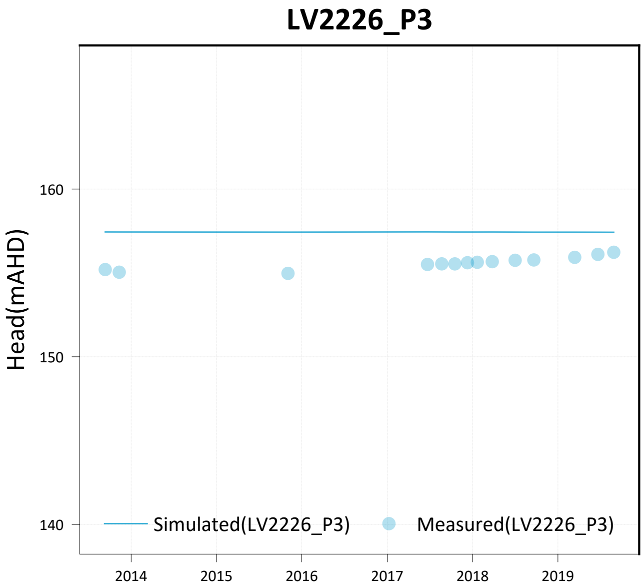
LV2226_P3
Head(mAHD)
160
150
140
2014
2015
2016
2017
2018
2019
Simulated(LV2226_P3)
Measured(LV2226_P3)

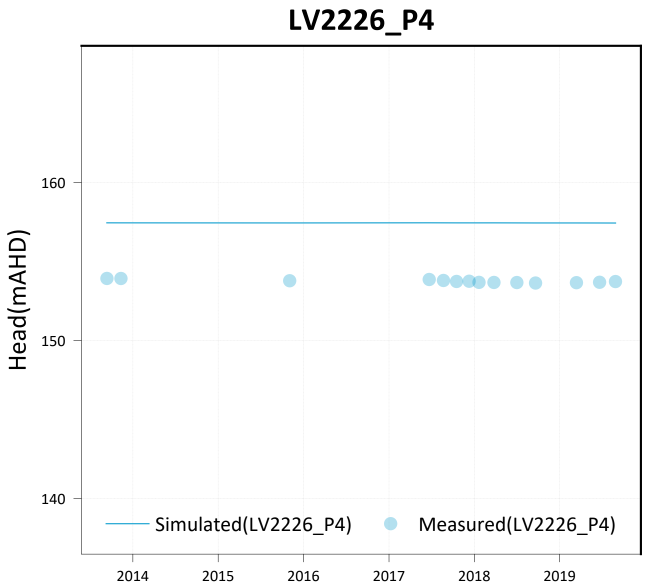
LV2226_P4
Head(mAHD)
160
150
140
2014
2015
2016
2017
2018
2019
Simulated(LV2226_P4)
Measured(LV2226_P4)

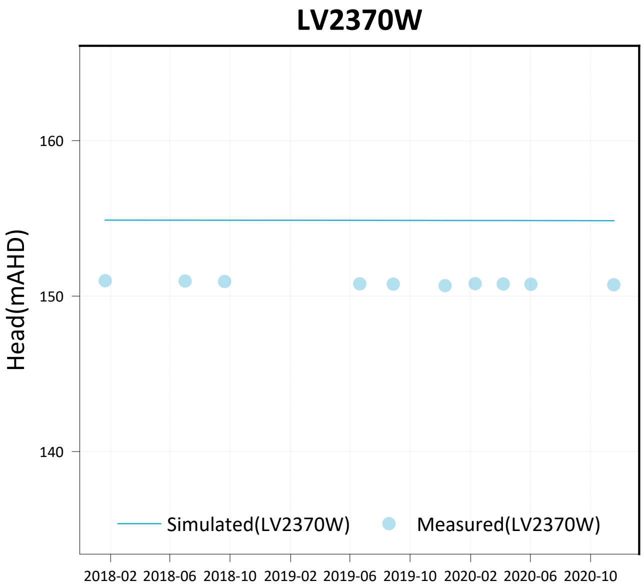
LV2370W
Head(mAHD)
160
150
140
2018-02
2018-06
2018-10
2019-02
2019-06
2019-10
2020-02
2020-06
2020-10
Simulated(LV2370W)
Measured(LV2370W)

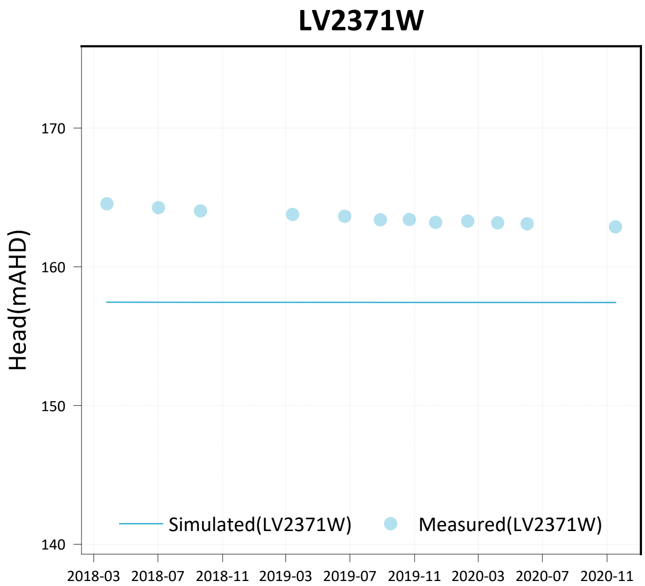
LV2371W
Head(mAHD)
170
160
150
140
2018-03
2018-07
2018-11
2019-03
2019-07
2019-11
2020-03
2020-07
2020-11
Simulated(LV2371W)
Measured(LV2371W)

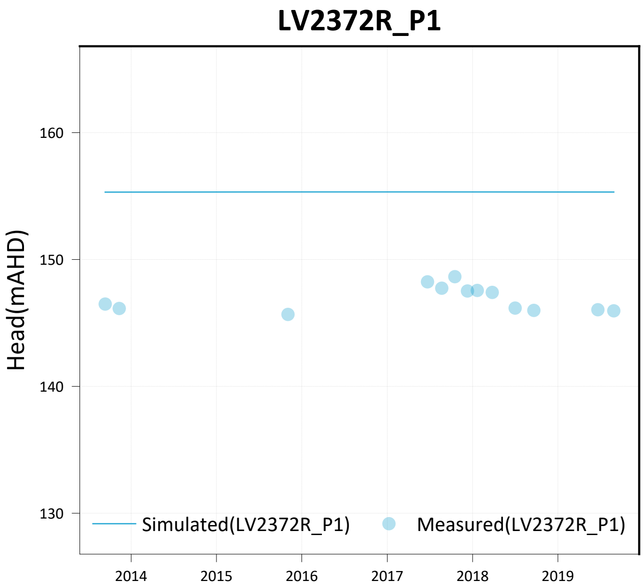
LV2372R_P1
Head(mAHD)
160
150
140
130
2014
2015
2016
2017
2018
2019
Simulated(LV2372R_P1)
Measured(LV2372R_P1)

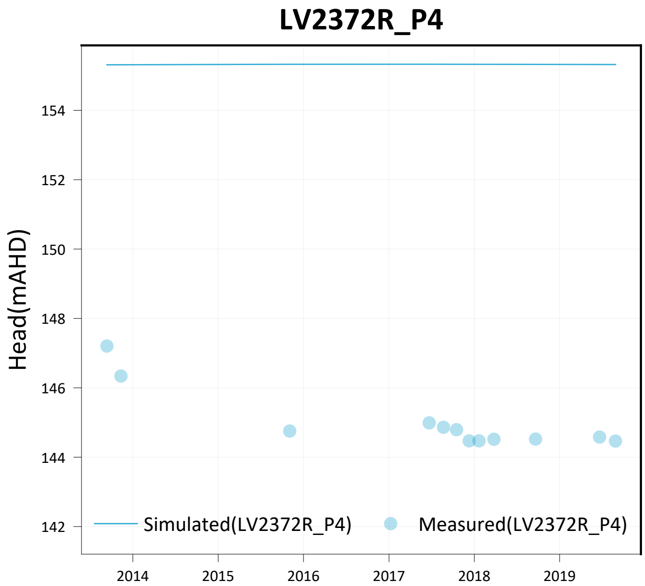
LV2372R_P4
Head(mAHD)
154
152
150
148
146
144
142
2014
2015
2016
2017
2018
2019
Simulated(LV2372R_P4)
Measured(LV2372R_P4)

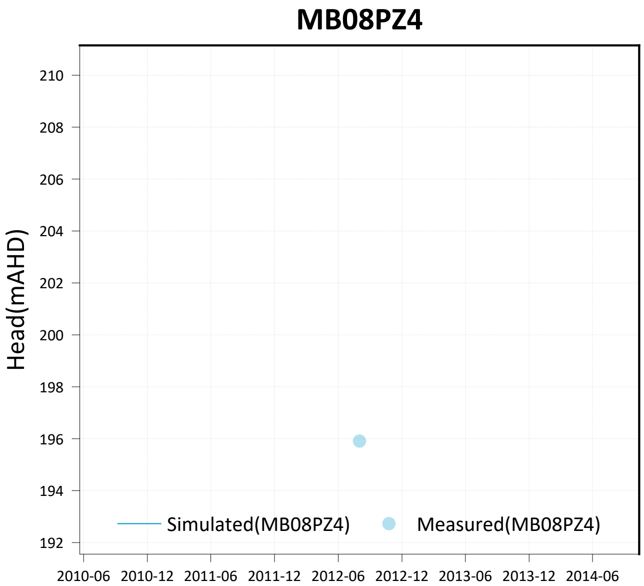
MB08PZ4
Head(mAHD)
210
208
206
204
202
200
198
196
194
192
2010-06
2010-12
2011-06
2011-12
2012-06
2012-12
2013-06
2013-12
2014-06
Simulated(MB08PZ4)
Measured(MB08PZ4)

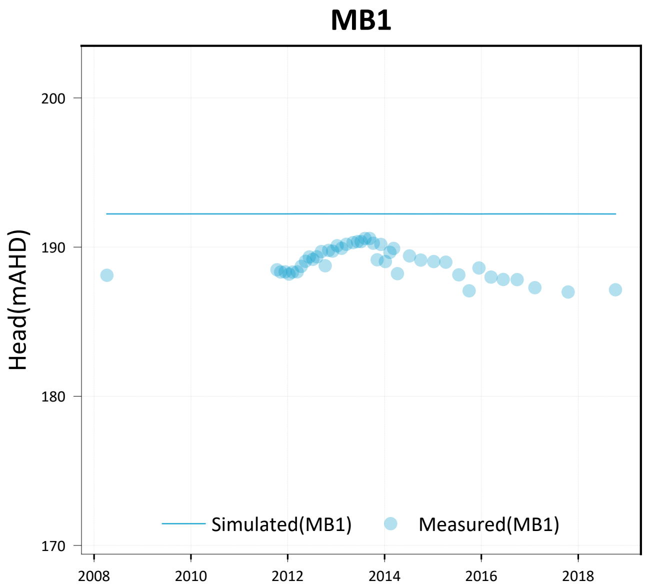
MB1
Head(mAHD)
200
190
180
170
2008
2010
2012
2014
2016
2018
Simulated(MB1)
Measured(MB1)

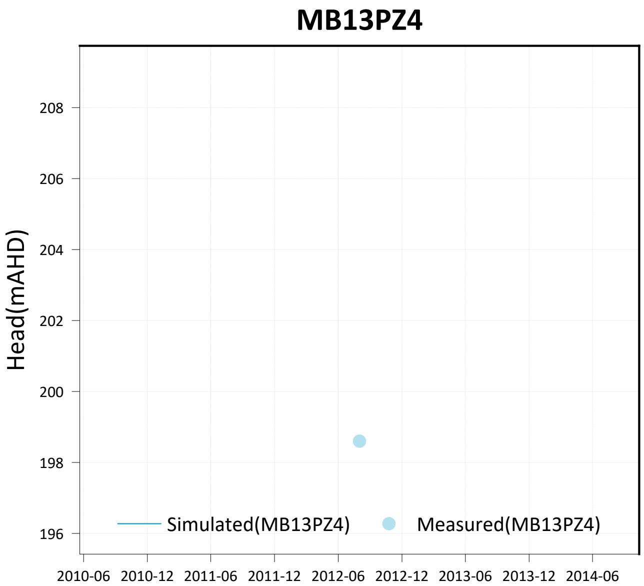
MB13PZ4
Head(mAHD)
208
206
204
202
200
198
196
2010-06
2010-12
2011-06
2011-12
2012-06
2012-12
2013-06
2013-12
2014-06
Simulated(MB13PZ4)
Measured(MB13PZ4)

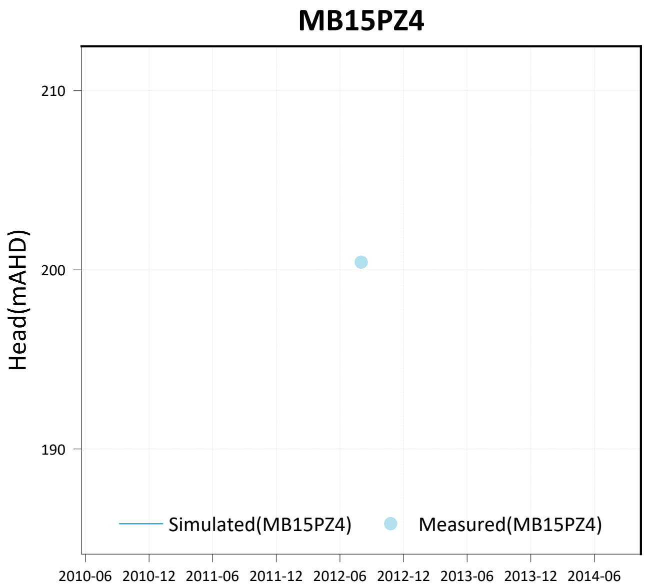
MB15PZ4
Head(mAHD)
210
200
190
2010-06
2010-12
2011-06
2011-12
2012-06
2012-12
2013-06
2013-12
2014-06
Simulated(MB15PZ4)
Measured(MB15PZ4)

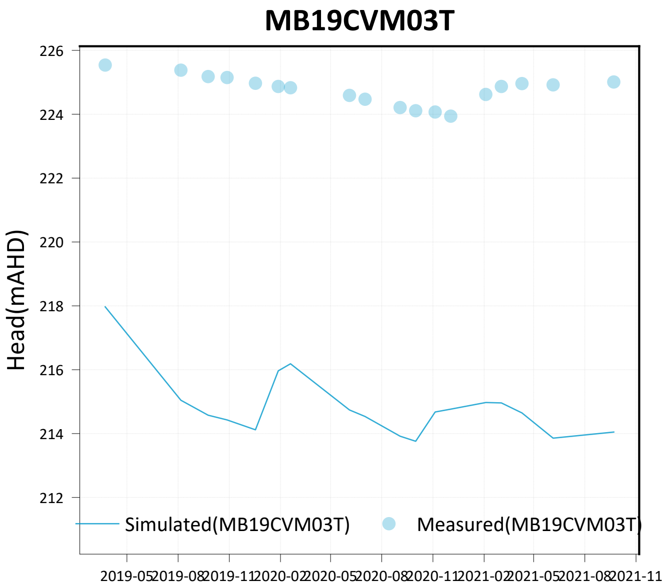
MB19CVM03T
Head(mAHD)
226
224
222
220
218
216
214
212
2019-05
2019-08
2019-11
2020-02
2020-05
2020-08
2020-11
2021-02
2021-05
2021-08
2021-11
Simulated(MB19CVM03T)
Measured(MB19CVM03T)

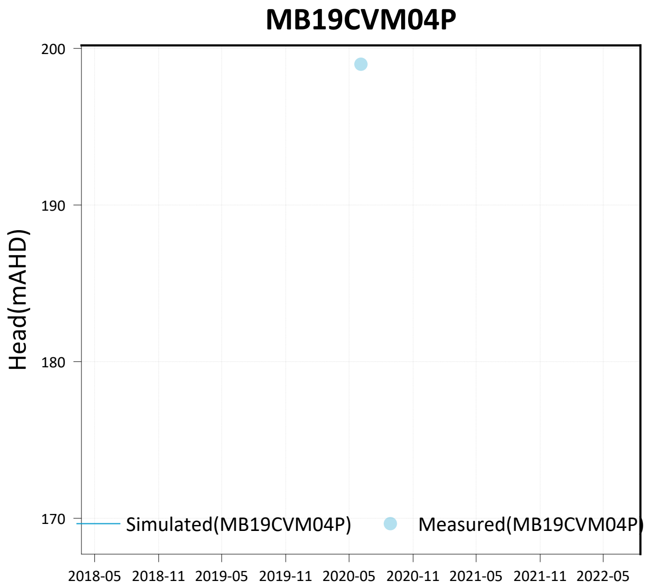
MB19CVM04P
Head(mAHD)
200
190
180
170
Simulated(MB19CVM04P)
Measured(MB19CVM04P)
2018-05 2018-11 2019-05 2019-11 2020-05 2020-11 2021-05 2021-11 2022-05

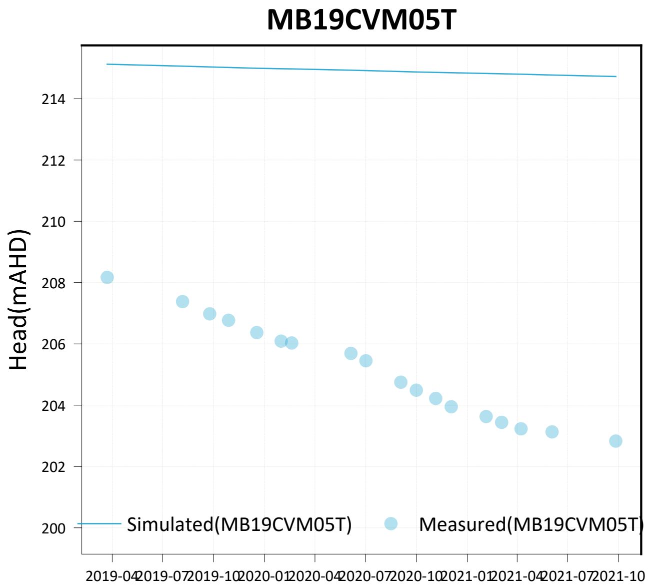
MB19CVM05T
Head(mAHD)
214
212
210
208
206
204
202
200
Simulated(MB19CVM05T)
Measured(MB19CVM05T)
2019-04 2019-07 2019-10 2020-01 2020-04 2020-07 2020-10 2021-01 2021-04 2021-07 2021-10

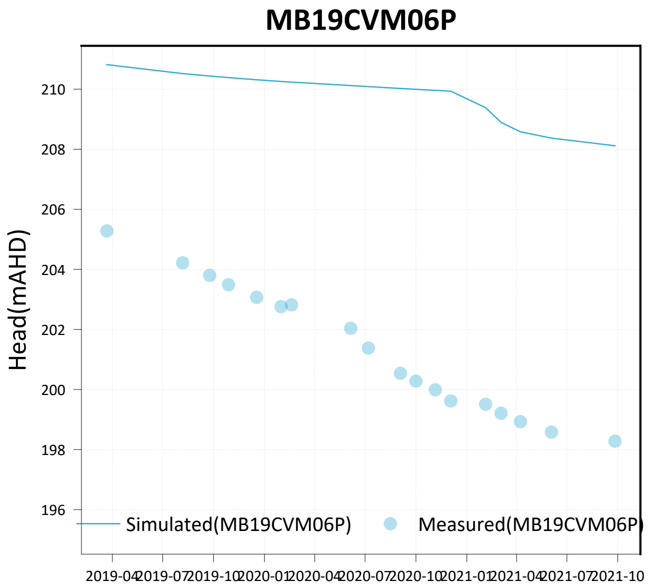
MB19CVM06P
Head(mAHD)
210
208
206
204
202
200
198
196
Simulated(MB19CVM06P)
Measured(MB19CVM06P)
2019-04 2019-07 2019-10 2020-01 2020-04 2020-07 2020-10 2021-01 2021-04 2021-07 2021-10

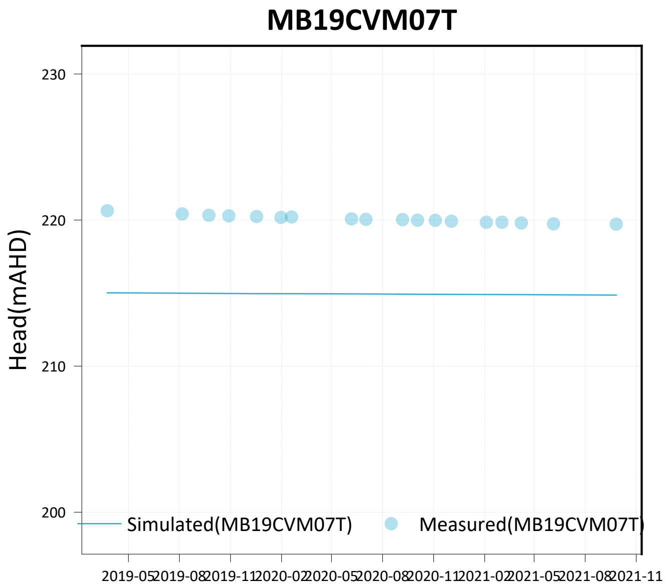
MB19CVM07T
Head(mAHD)
230
220
210
200
Simulated(MB19CVM07T)
Measured(MB19CVM07T)
2019-05 2019-08 2019-11 2020-02 2020-05 2020-08 2020-11 2021-02 2021-05 2021-08 2021-11

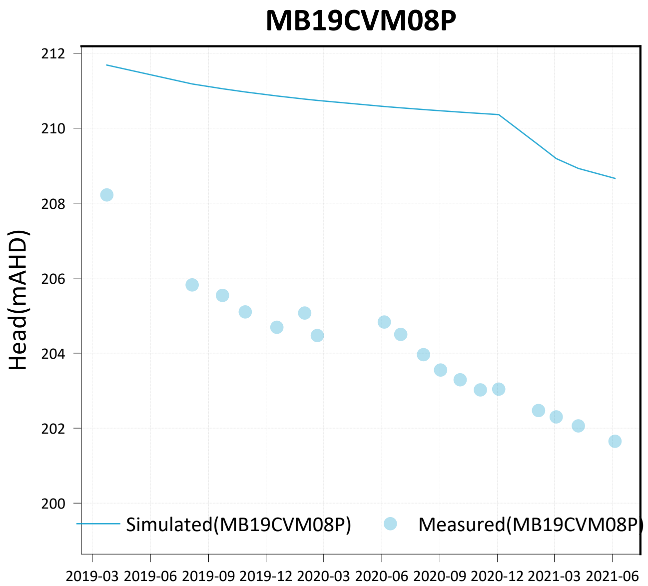
MB19CVM08P
Head(mAHD)
212
210
208
206
204
202
200
Simulated(MB19CVM08P)
Measured(MB19CVM08P)
2019-03 2019-06 2019-09 2019-12 2020-03 2020-06 2020-09 2020-12 2021-03 2021-06

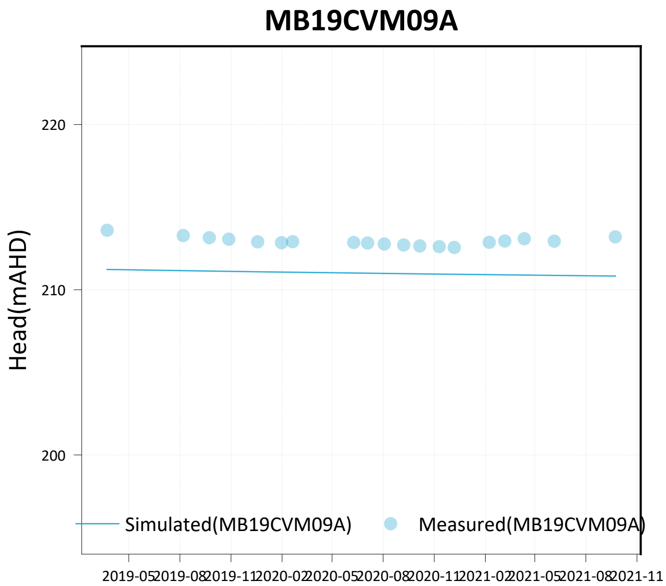
MB19CVM09A
Head(mAHD)
220
210
200
Simulated(MB19CVM09A)
Measured(MB19CVM09A)
2019-05 2019-08 2019-11 2020-02 2020-05 2020-08 2020-11 2021-02 2021-05 2021-08 2021-11

MB19CVM10P

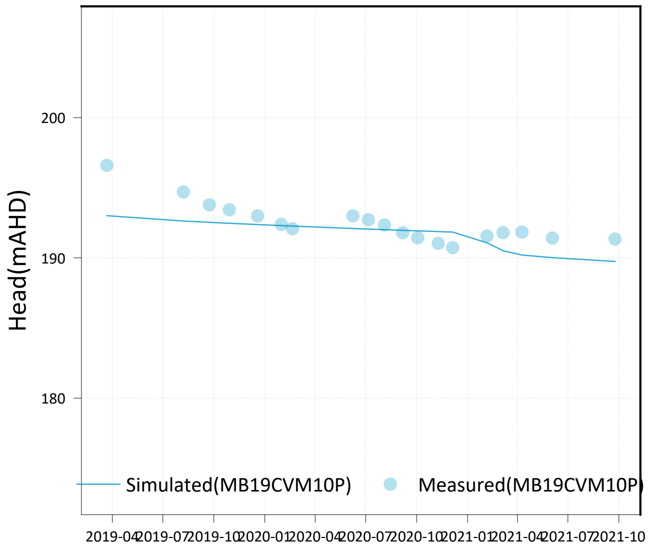

MB19SRM02T

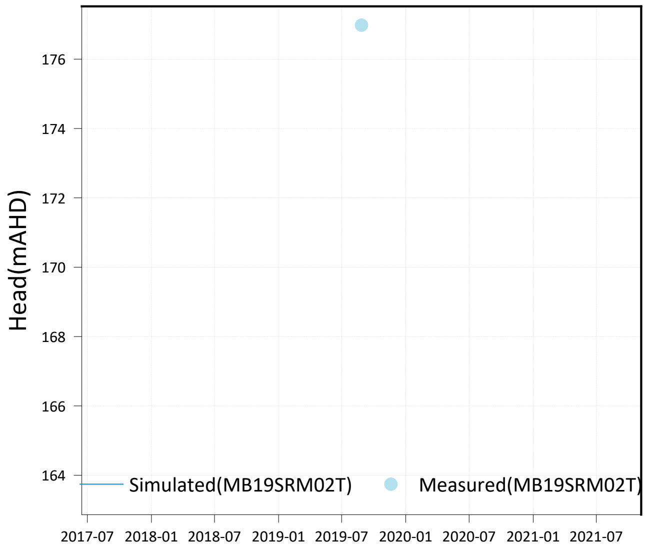

MB19SRM03P

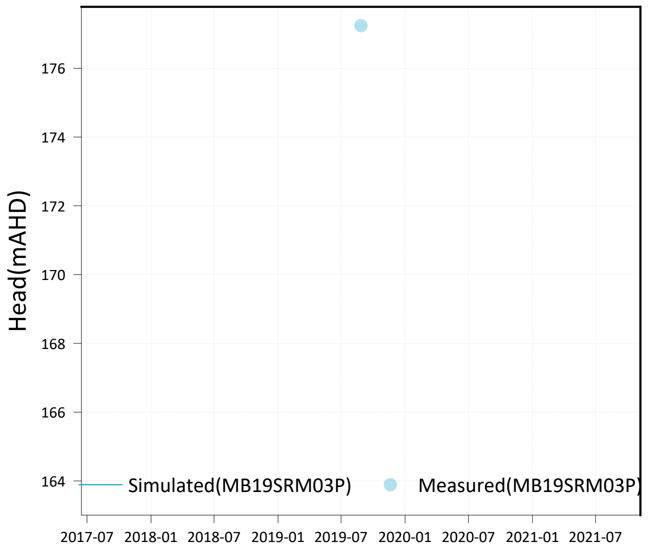

MB19SRM04P

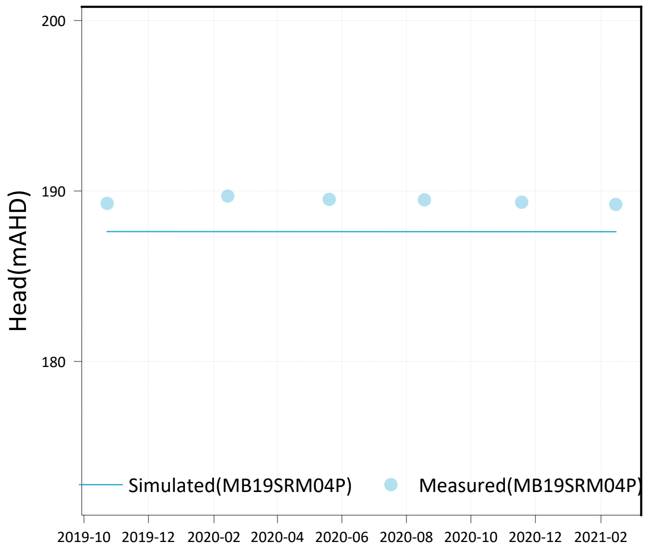

MB2

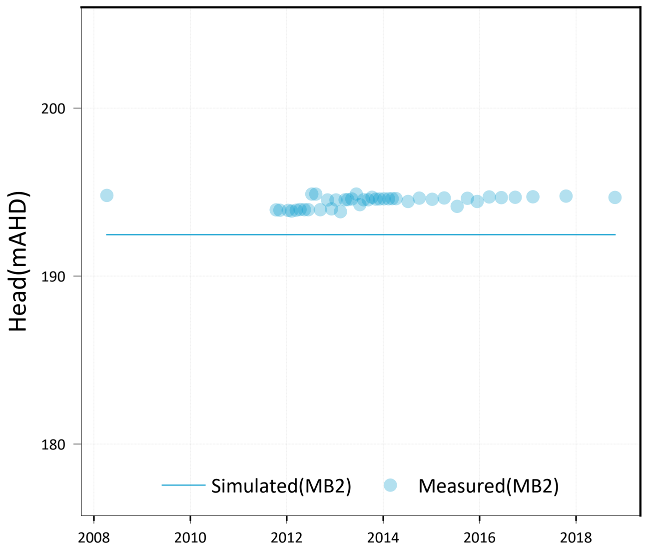

MB20CVM04T

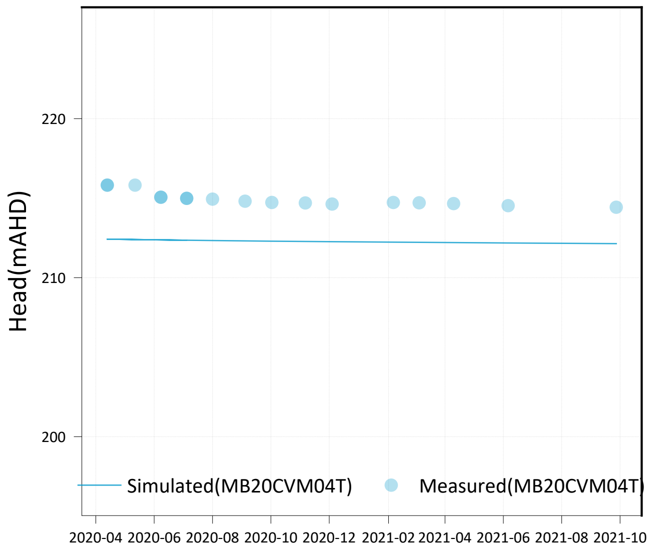

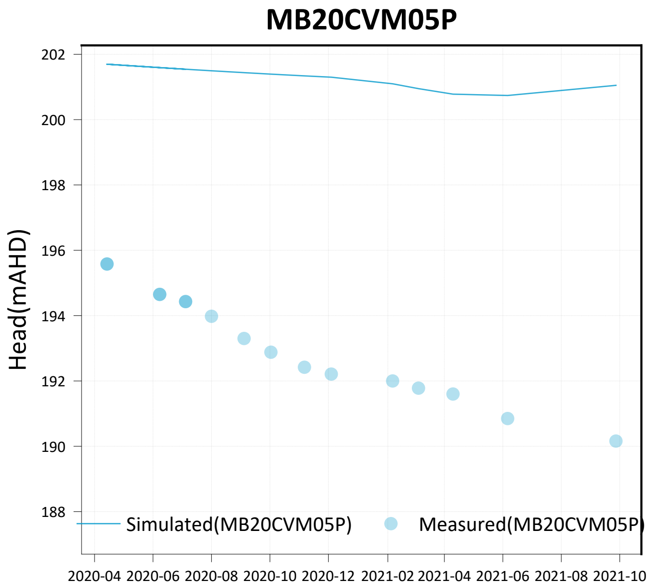
MB20CVM05P
Head(mAHD)
202
200
198
196
194
192
190
188
2020-04 2020-06 2020-08 2020-10 2020-12 2021-02 2021-04 2021-06 2021-08 2021-10
Simulated(MB20CVM05P)
Measured(MB20CVM05P)

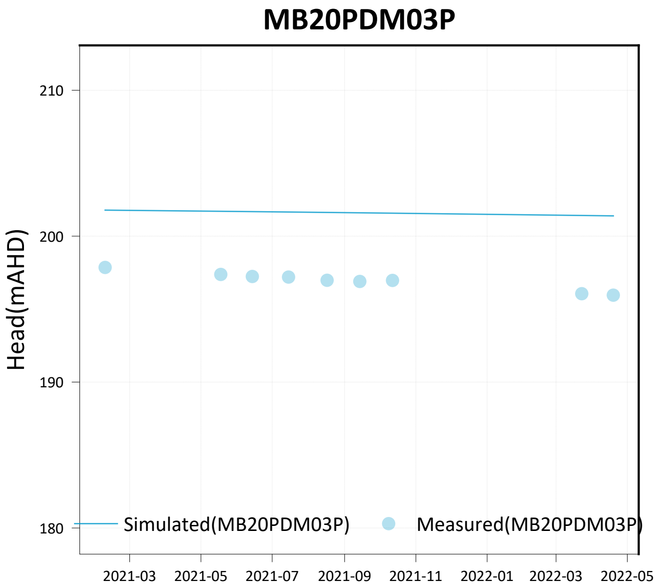
MB20PDM03P
Head(mAHD)
210
200
190
180
2021-03 2021-05 2021-07 2021-09 2021-11 2022-01 2022-03 2022-05
Simulated(MB20PDM03P)
Measured(MB20PDM03P)

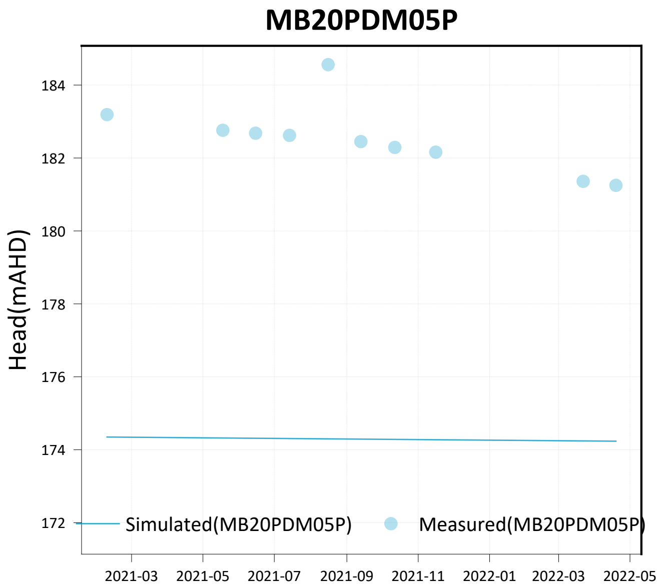
MB20PDM05P
Head(mAHD)
184
182
180
178
176
174
172
2021-03 2021-05 2021-07 2021-09 2021-11 2022-01 2022-03 2022-05
Simulated(MB20PDM05P)
Measured(MB20PDM05P)

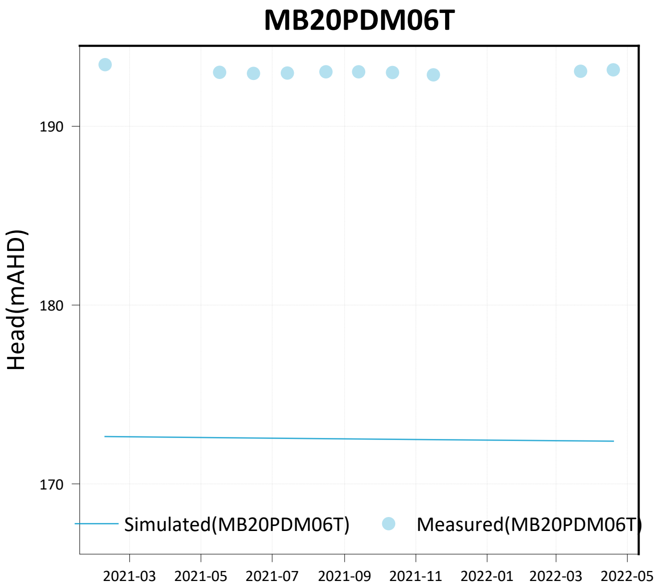
MB20PDM06T
Head(mAHD)
190
180
170
2021-03 2021-05 2021-07 2021-09 2021-11 2022-01 2022-03 2022-05
Simulated(MB20PDM06T)
Measured(MB20PDM06T)

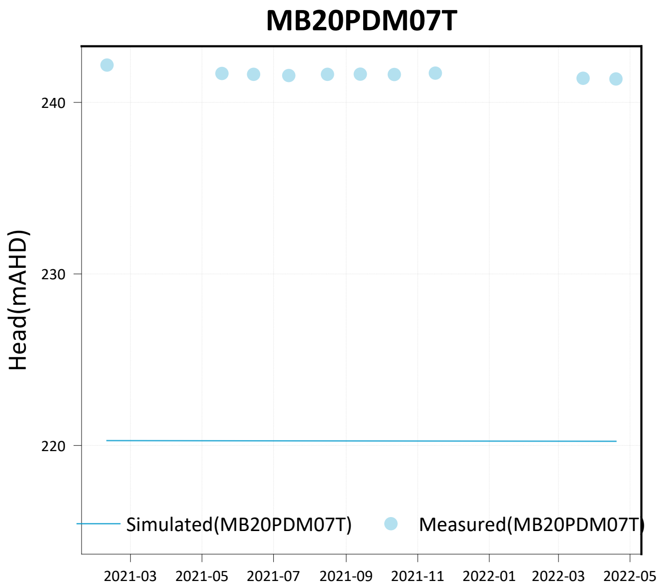
MB20PDM07T
Head(mAHD)
240
230
220
2021-03 2021-05 2021-07 2021-09 2021-11 2022-01 2022-03 2022-05
Simulated(MB20PDM07T)
Measured(MB20PDM07T)

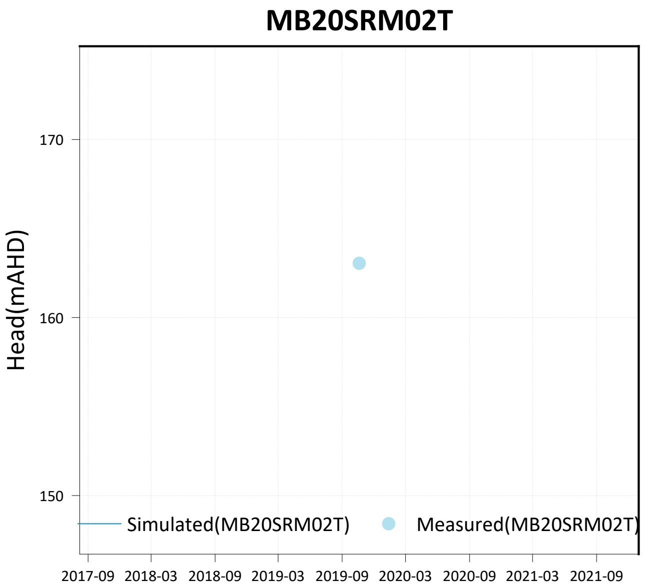
MB20SRM02T
Head(mAHD)
170
160
150
2017-09 2018-03 2018-09 2019-03 2019-09 2020-03 2020-09 2021-03 2021-09
Simulated(MB20SRM02T)
Measured(MB20SRM02T)

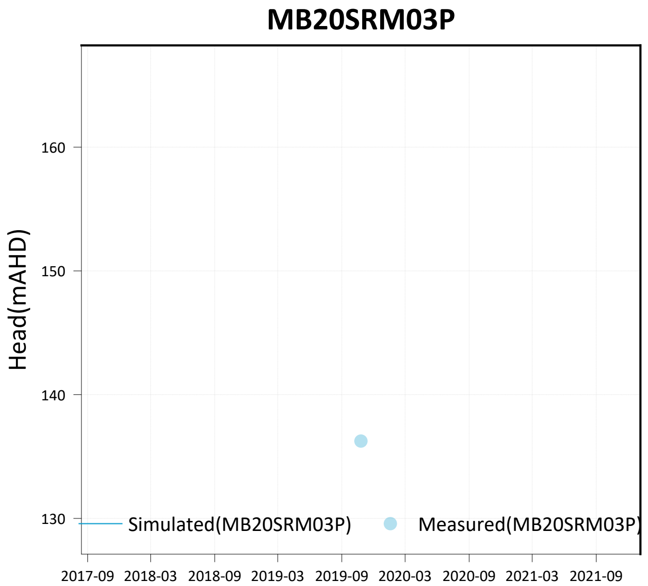
MB20SRM03P
Head(mAHD)
160
150
140
130
Simulated(MB20SRM03P)
Measured(MB20SRM03P)
2017-09
2018-03
2018-09
2019-03
2019-09
2020-03
2020-09
2021-03
2021-09

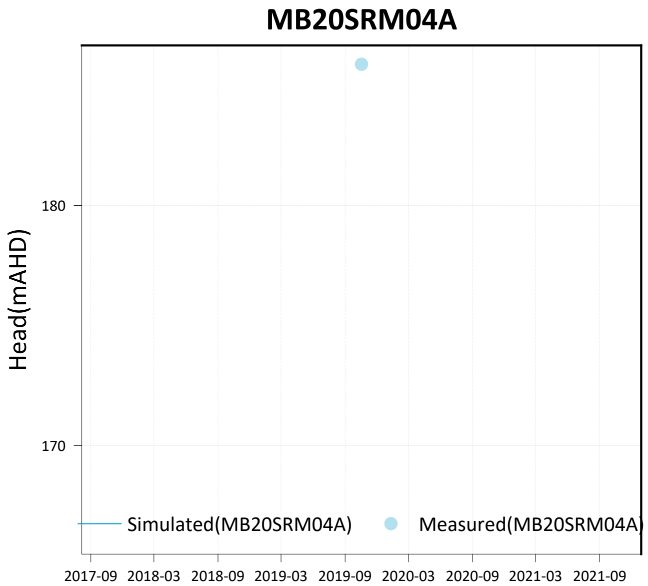
MB20SRM04A
Head(mAHD)
180
170
Simulated(MB20SRM04A)
Measured(MB20SRM04A)
2017-09
2018-03
2018-09
2019-03
2019-09
2020-03
2020-09
2021-03
2021-09

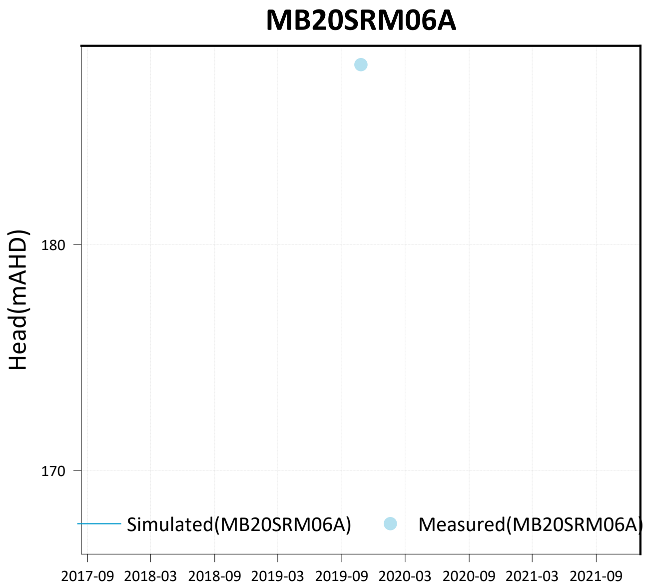
MB20SRM06A
Head(mAHD)
180
170
Simulated(MB20SRM06A)
Measured(MB20SRM06A)
2017-09
2018-03
2018-09
2019-03
2019-09
2020-03
2020-09
2021-03
2021-09

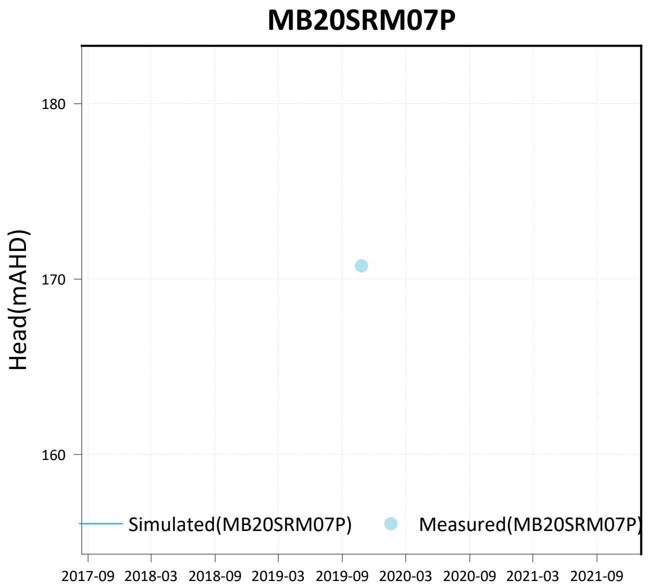
MB20SRM07P
Head(mAHD)
180
170
160
Simulated(MB20SRM07P)
Measured(MB20SRM07P)
2017-09
2018-03
2018-09
2019-03
2019-09
2020-03
2020-09
2021-03
2021-09

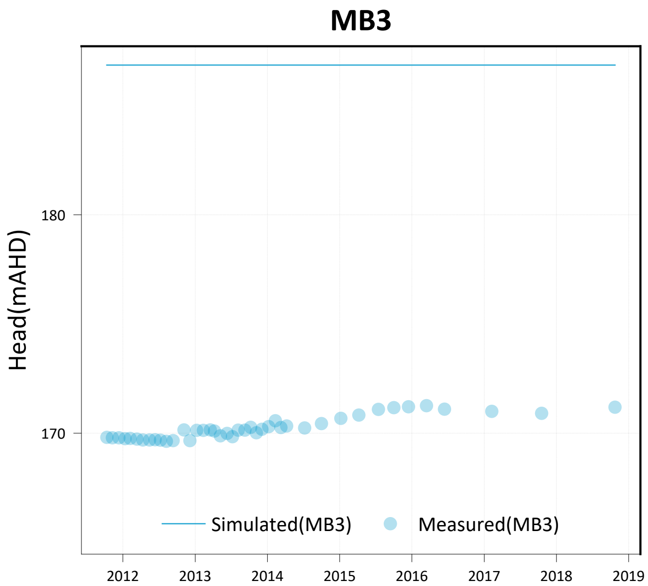
MB3
Head(mAHD)
180
170
Simulated(MB3)
Measured(MB3)
2012
2013
2014
2015
2016
2017
2018
2019

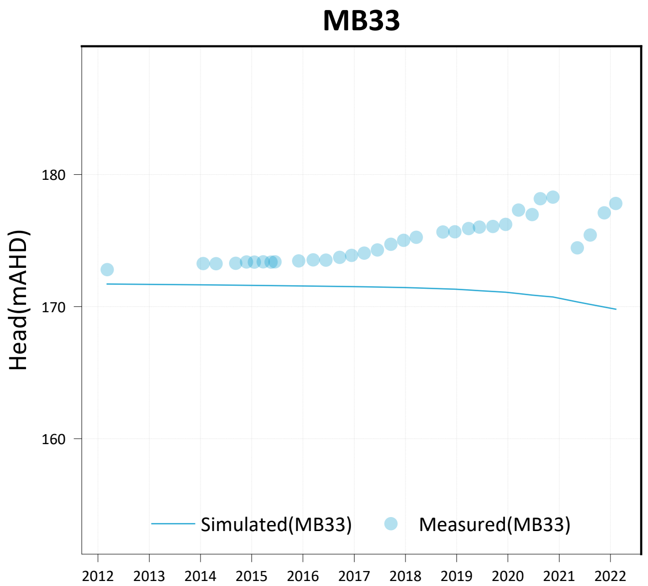
MB33
Head(mAHD)
180
170
160
Simulated(MB33)
Measured(MB33)
2012
2013
2014
2015
2016
2017
2018
2019
2020
2021
2022

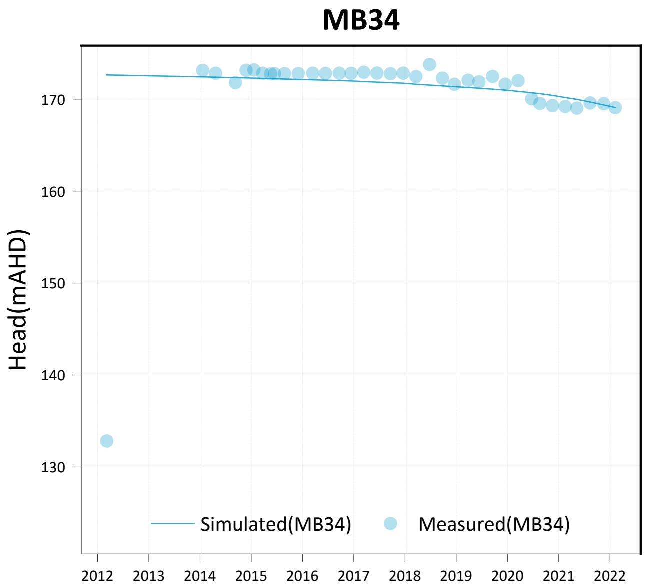
MB34
Head(mAHD)
Simulated(MB34)
Measured(MB34)

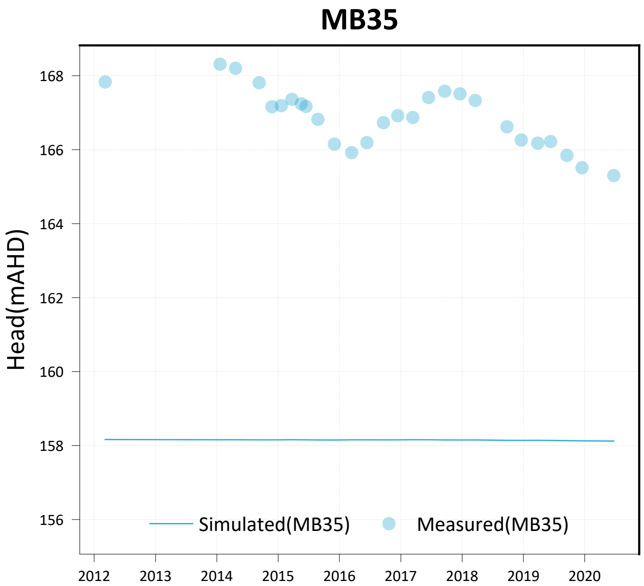
MB35
Head(mAHD)
Simulated(MB35)
Measured(MB35)

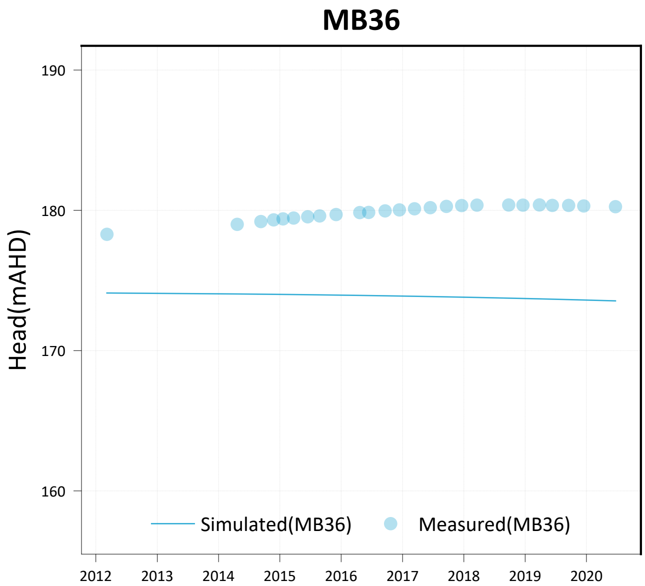
MB36
Head(mAHD)
Simulated(MB36)
Measured(MB36)

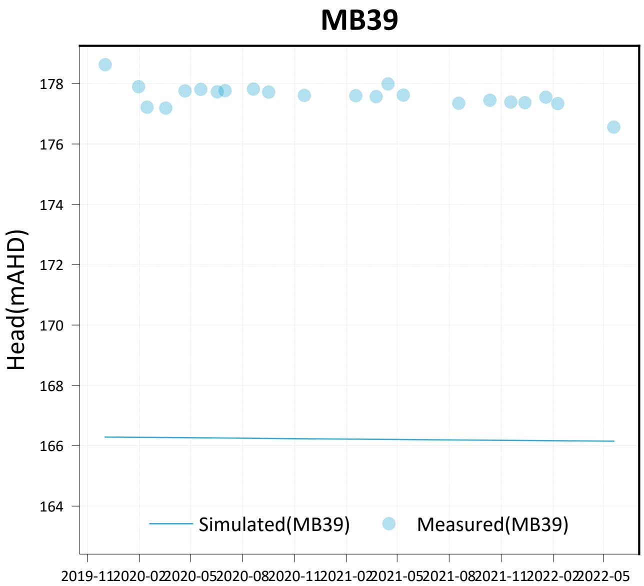
MB39
Head(mAHD)
Simulated(MB39)
Measured(MB39)

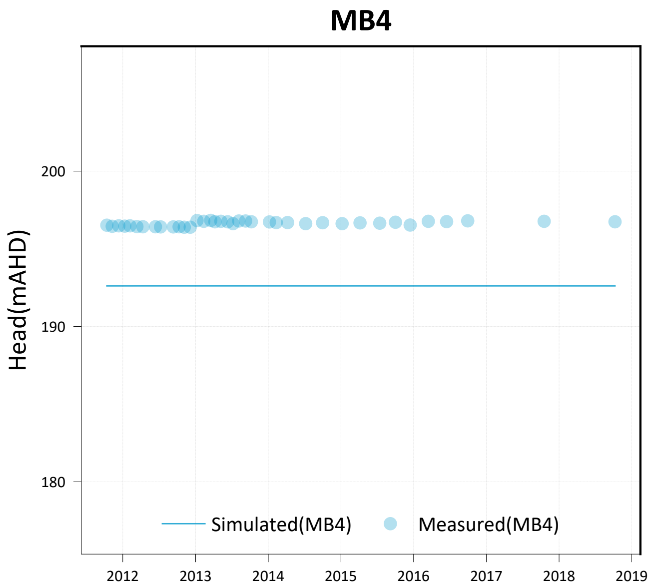
MB4
Head(mAHD)
Simulated(MB4)
Measured(MB4)

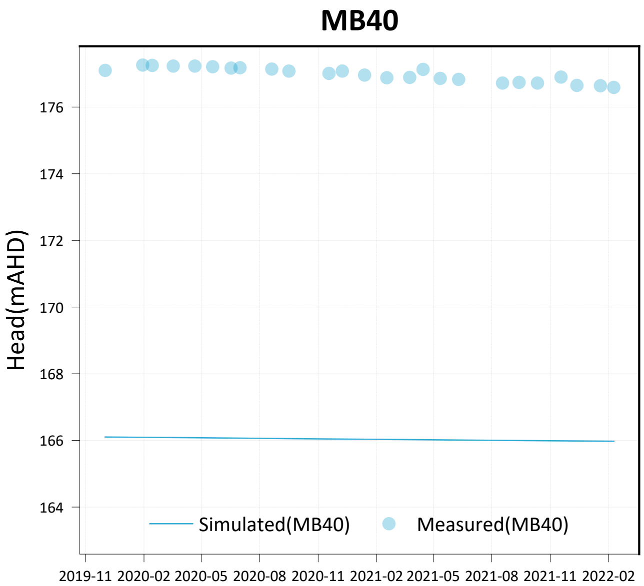
MB40
Head(mAHD)
Simulated(MB40)
Measured(MB40)

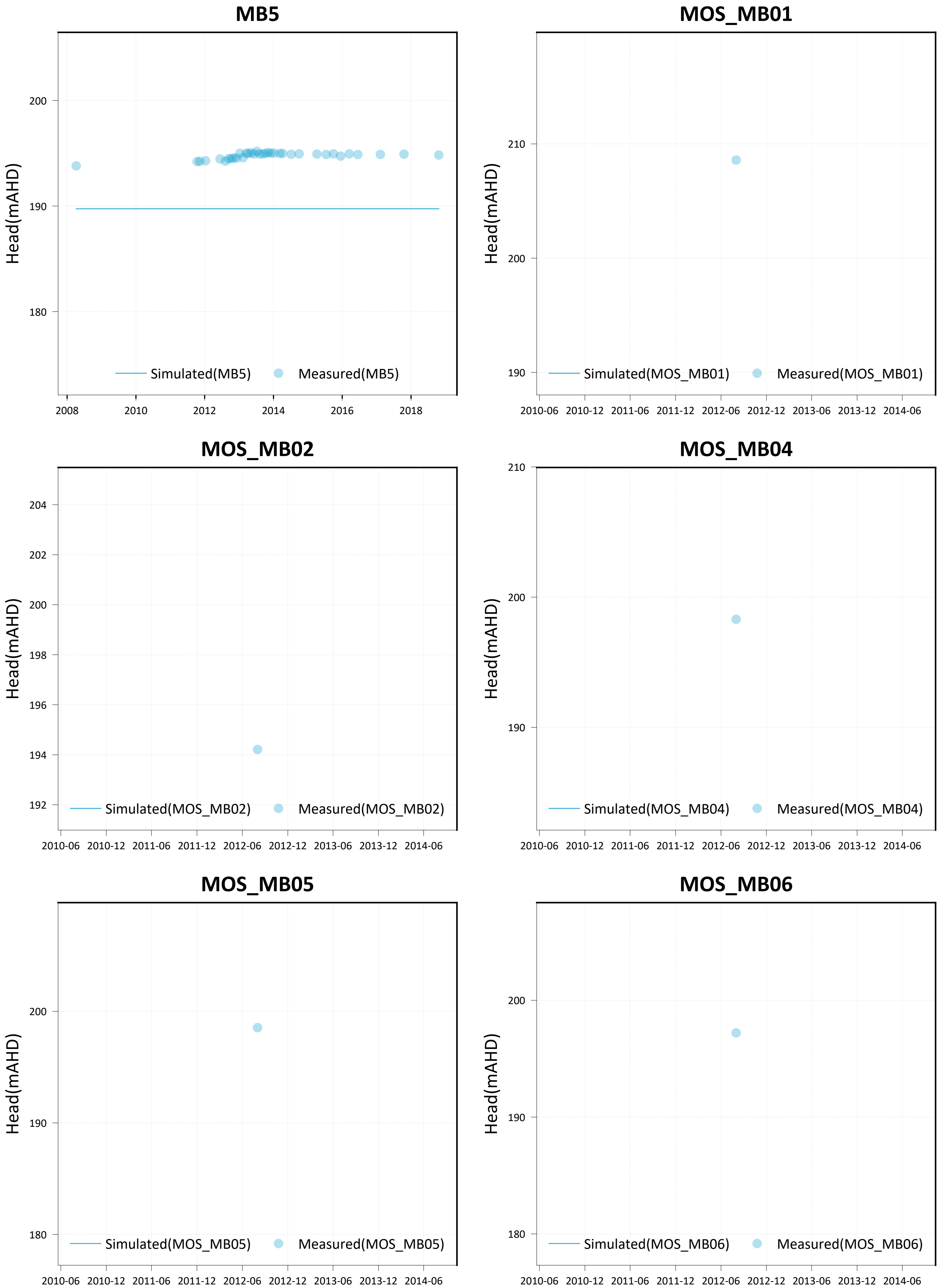
MB5
Head(mAHD)
200
190
180
2008
2010
2012
2014
2016
2018
Simulated(MB5)
Measured(MB5)
MOS_MB01
210
200
190
Simulated(MOS_MB01)
Measured(MOS_MB01)
2010-06
2010-12
2011-06
2011-12
2012-06
2012-12
2013-06
2013-12
2014-06
MOS_MB02
204
202
200
198
196
194
192
Simulated(MOS_MB02)
Measured(MOS_MB02)
MOS_MB04
Simulated(MOS_MB04)
Measured(MOS_MB04)
MOS_MB05
Simulated(MOS_MB05)
Measured(MOS_MB05)
MOS_MB06
Simulated(MOS_MB06)
Measured(MOS_MB06)

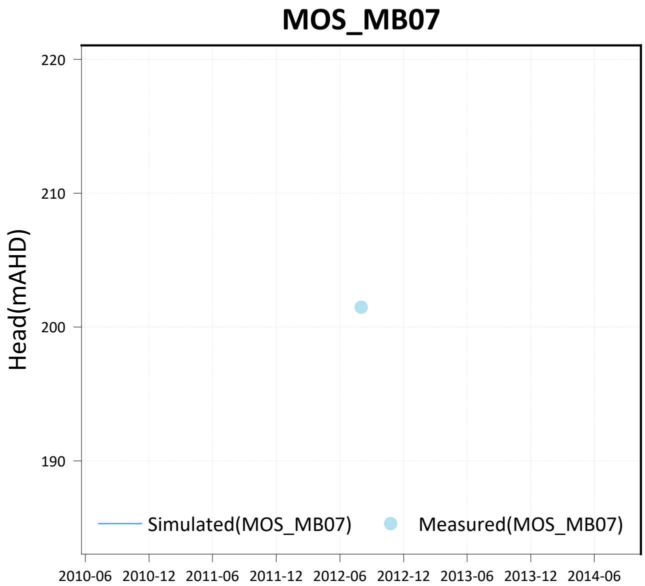
MOS_MB07
220
210
200
190
Head(mAHD)
Simulated(MOS_MB07)
Measured(MOS_MB07)
2010-06 2010-12 2011-06 2011-12 2012-06 2012-12 2013-06 2013-12 2014-06

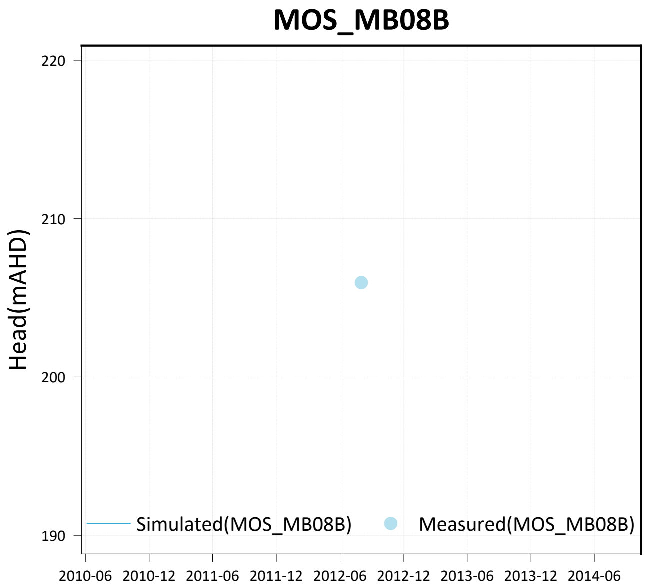
MOS_MB08B
220
210
200
190
Head(mAHD)
Simulated(MOS_MB08B)
Measured(MOS_MB08B)
2010-06 2010-12 2011-06 2011-12 2012-06 2012-12 2013-06 2013-12 2014-06

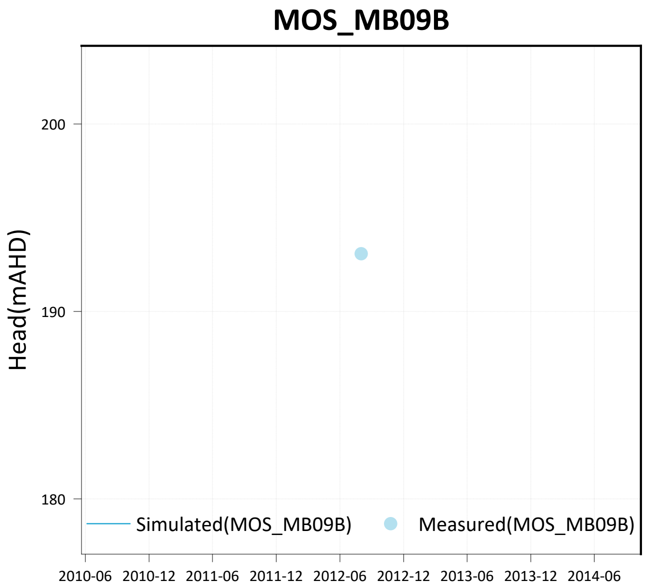
MOS_MB09B
200
190
180
Head(mAHD)
Simulated(MOS_MB09B)
Measured(MOS_MB09B)
2010-06 2010-12 2011-06 2011-12 2012-06 2012-12 2013-06 2013-12 2014-06

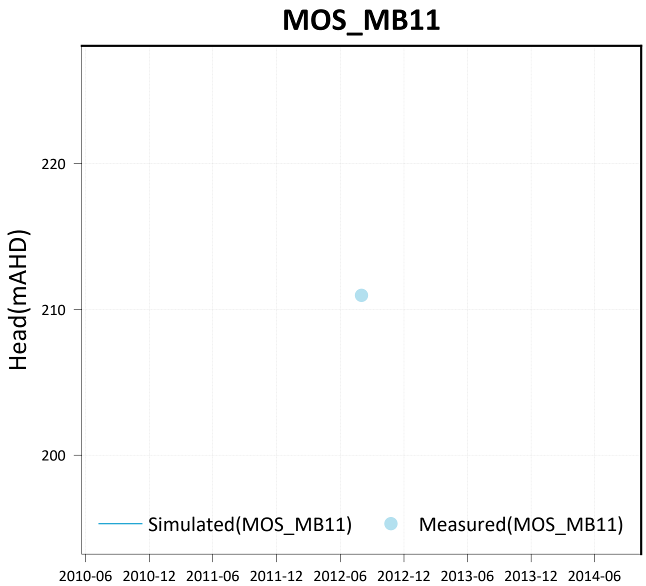
MOS_MB11
220
210
200
Head(mAHD)
Simulated(MOS_MB11)
Measured(MOS_MB11)
2010-06 2010-12 2011-06 2011-12 2012-06 2012-12 2013-06 2013-12 2014-06

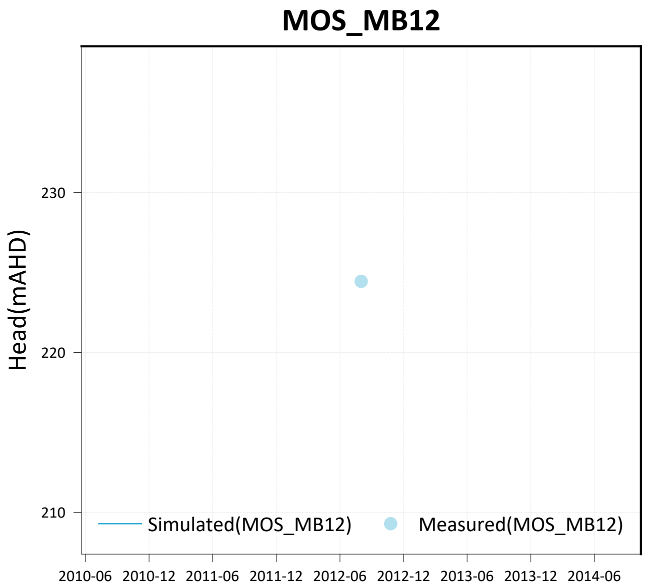
MOS_MB12
230
220
210
Head(mAHD)
Simulated(MOS_MB12)
Measured(MOS_MB12)
2010-06 2010-12 2011-06 2011-12 2012-06 2012-12 2013-06 2013-12 2014-06

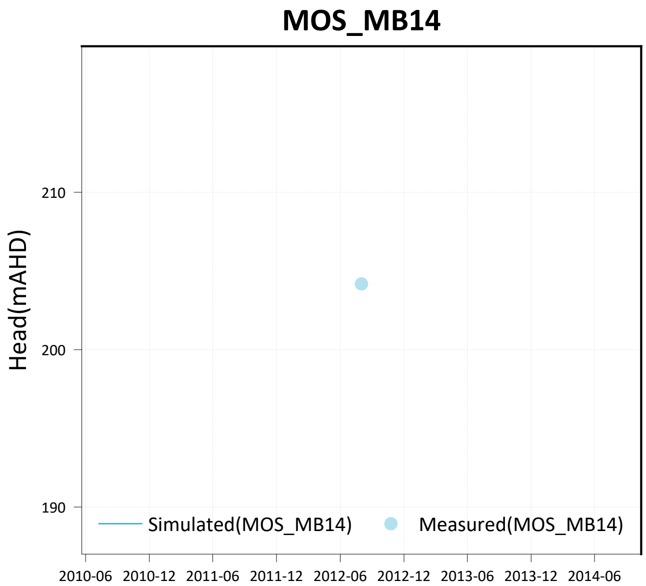
MOS_MB14
210
200
190
Head(mAHD)
Simulated(MOS_MB14)
Measured(MOS_MB14)
2010-06 2010-12 2011-06 2011-12 2012-06 2012-12 2013-06 2013-12 2014-06

MOS_MB16

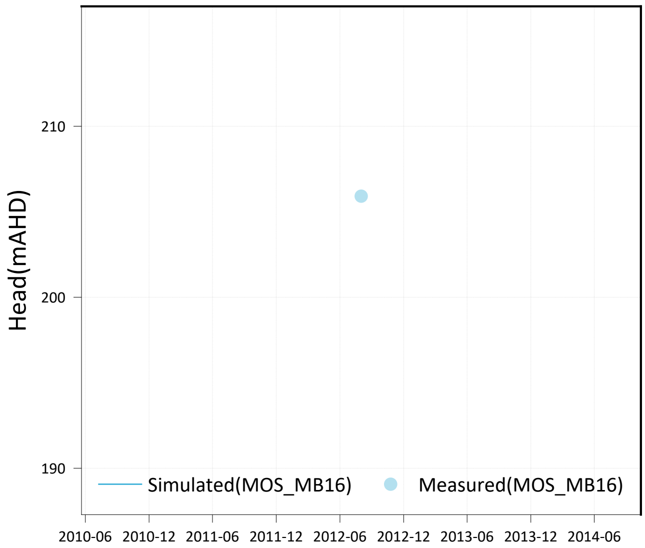

MILLMB1

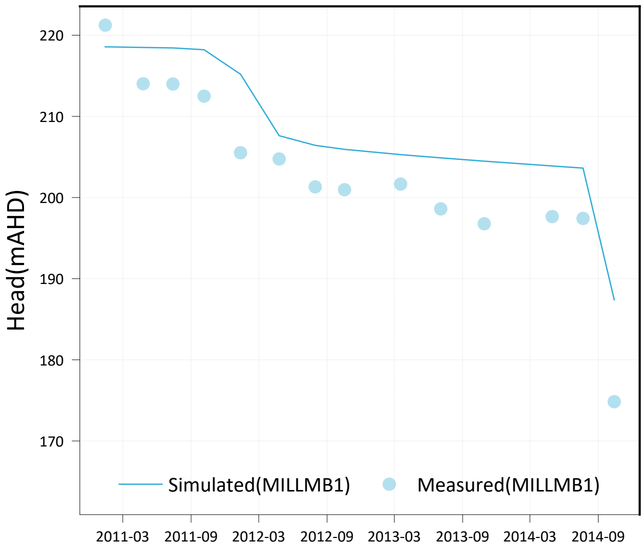

MILLMB10A

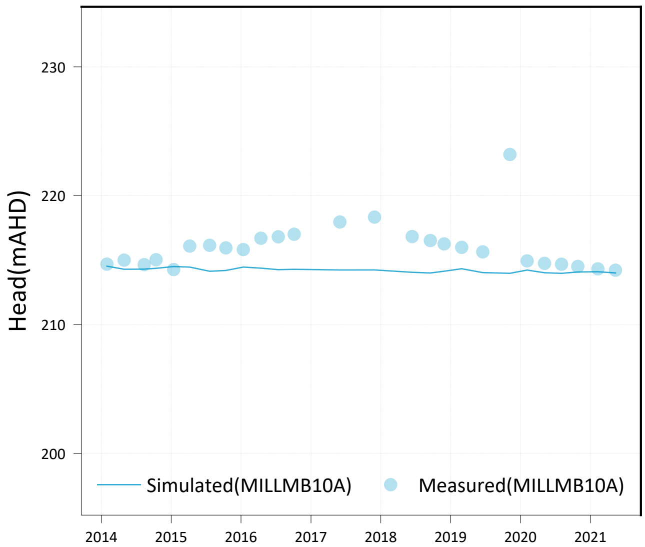

MILLMB10B

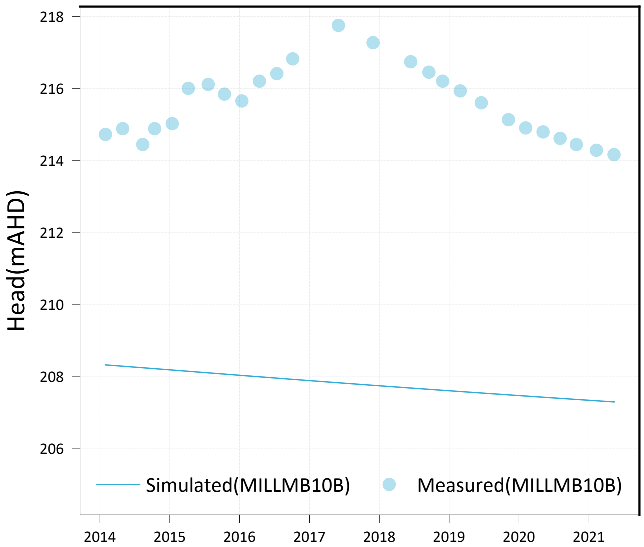

MILLMB11A

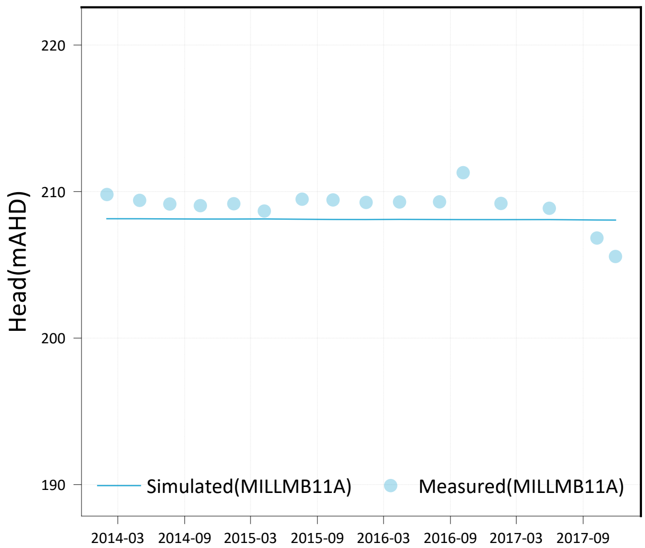

MILLMB11B

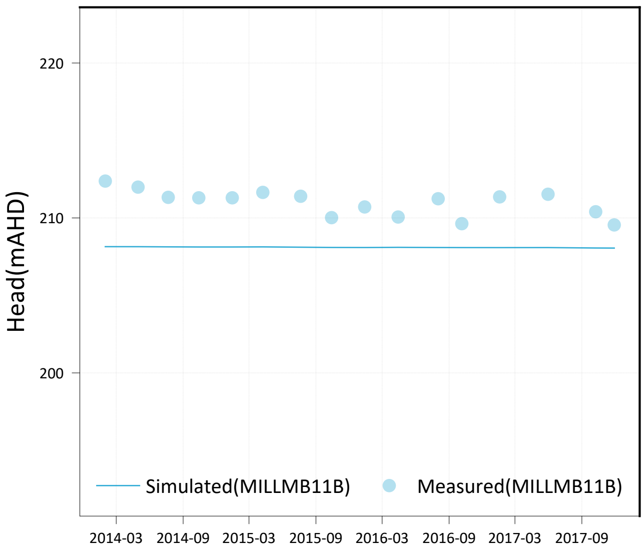

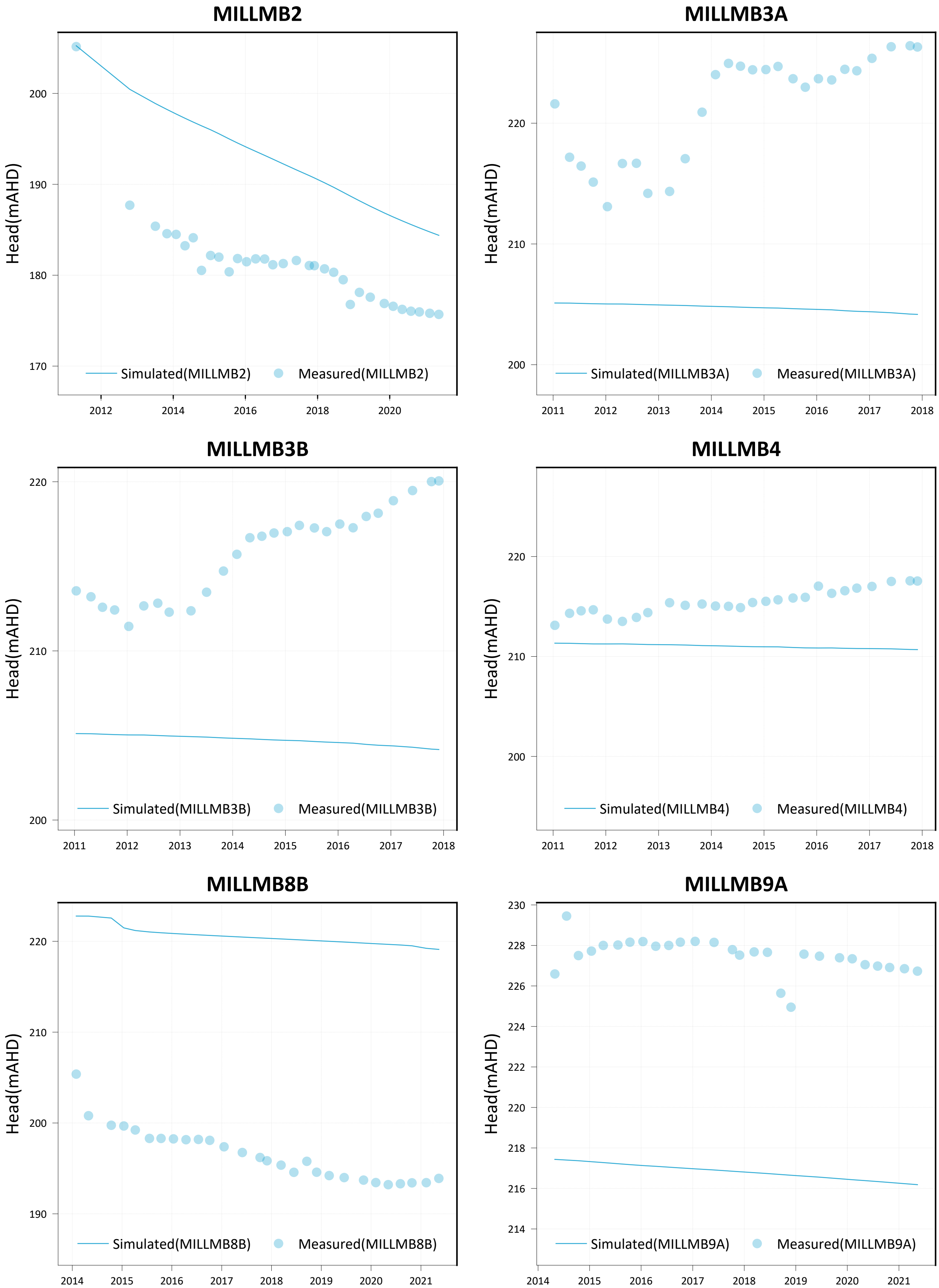
MILLMB2
Head(mAHD)
200
190
180
170
Simulated(MILLMB2)
Measured(MILLMB2)
2012
2014
2016
2018
2020
MILLMB3A
Head(mAHD)
220
210
200
Simulated(MILLMB3A)
Measured(MILLMB3A)
2011
2012
2013
2014
2015
2016
2017
2018
MILLMB3B
Head(mAHD)
220
210
200
Simulated(MILLMB3B)
Measured(MILLMB3B)
2011
2012
2013
2014
2015
2016
2017
2018
MILLMB4
Head(mAHD)
220
210
200
Simulated(MILLMB4)
Measured(MILLMB4)
2011
2012
2013
2014
2015
2016
2017
2018
MILLMB8B
Head(mAHD)
220
210
200
190
Simulated(MILLMB8B)
Measured(MILLMB8B)
2014
2015
2016
2017
2018
2019
2020
2021
MILLMB9A
Head(mAHD)
230
228
226
224
222
220
218
216
214
Simulated(MILLMB9A)
Measured(MILLMB9A)
2014
2015
2016
2017
2018
2019
2020
2021

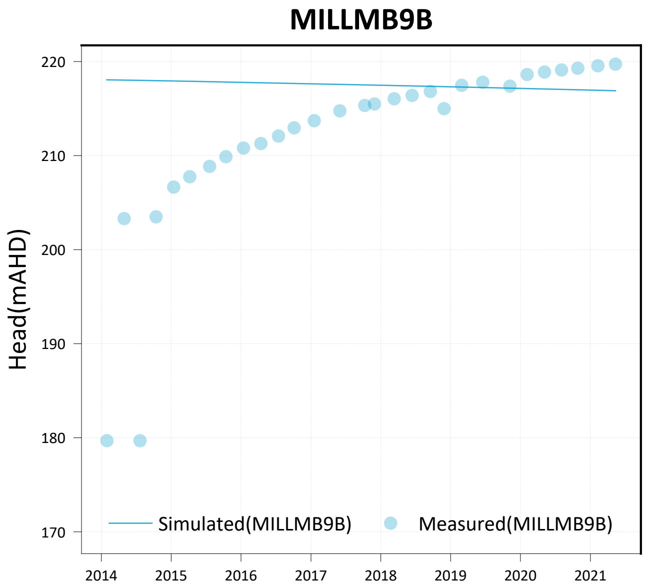
MILLMB9B
Head(mAHD)
220
210
200
190
180
170
Simulated(MILLMB9B)
Measured(MILLMB9B)
2014
2015
2016
2017
2018
2019
2020
2021

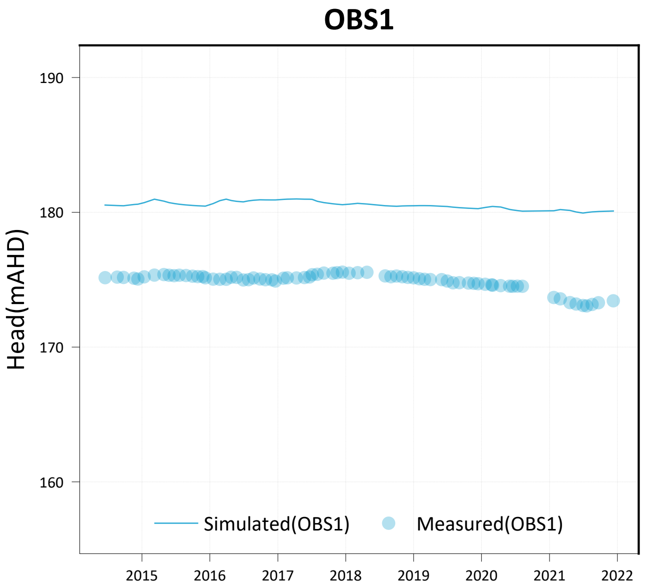
OBS1
Head(mAHD)
190
180
170
160
Simulated(OBS1)
Measured(OBS1)
2015
2016
2017
2018
2019
2020
2021
2022

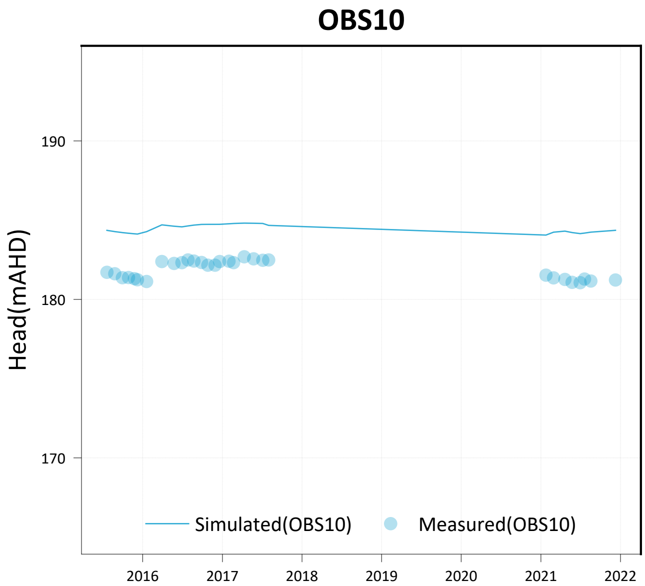
OBS10
Head(mAHD)
190
180
170
Simulated(OBS10)
Measured(OBS10)
2016
2017
2018
2019
2020
2021
2022

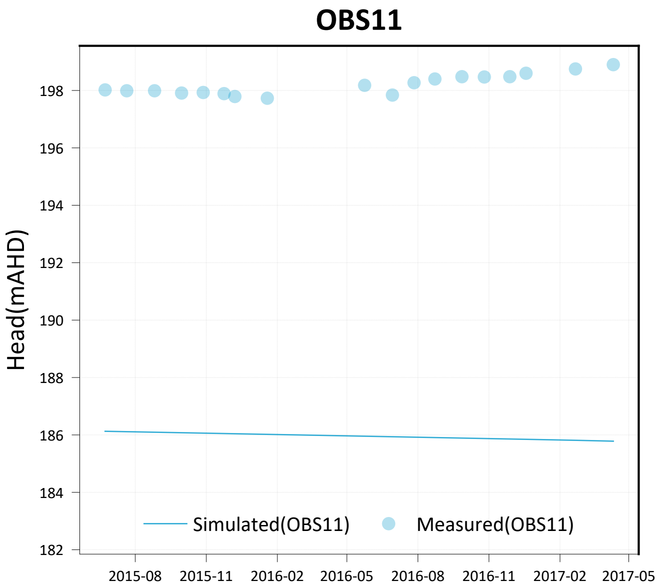
OBS11
Head(mAHD)
198
196
194
192
190
188
186
184
182
Simulated(OBS11)
Measured(OBS11)
2015-08
2015-11
2016-02
2016-05
2016-08
2016-11
2017-02
2017-05

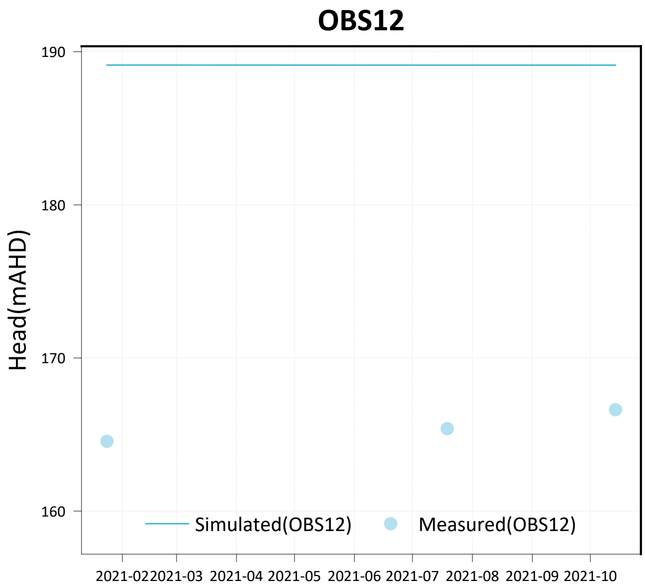
OBS12
Head(mAHD)
190
180
170
160
Simulated(OBS12)
Measured(OBS12)
2021-02
2021-03
2021-04
2021-05
2021-06
2021-07
2021-08
2021-09
2021-10

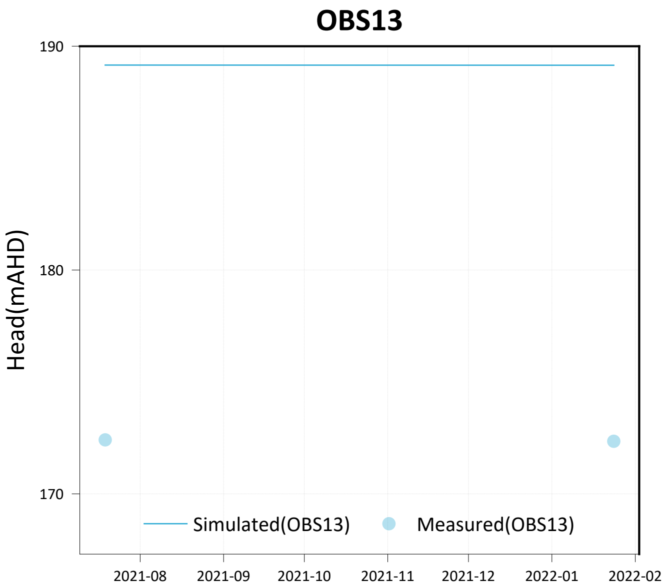
OBS13
Head(mAHD)
190
180
170
Simulated(OBS13)
Measured(OBS13)
2021-08
2021-09
2021-10
2021-11
2021-12
2022-01
2022-02

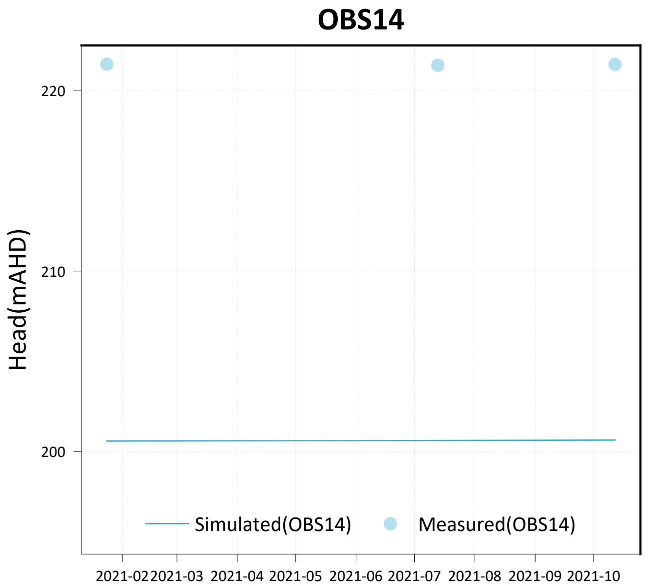
OBS14
Head(mAHD)
220
210
200
Simulated(OBS14)
Measured(OBS14)
2021-02 2021-03 2021-04 2021-05 2021-06 2021-07 2021-08 2021-09 2021-10

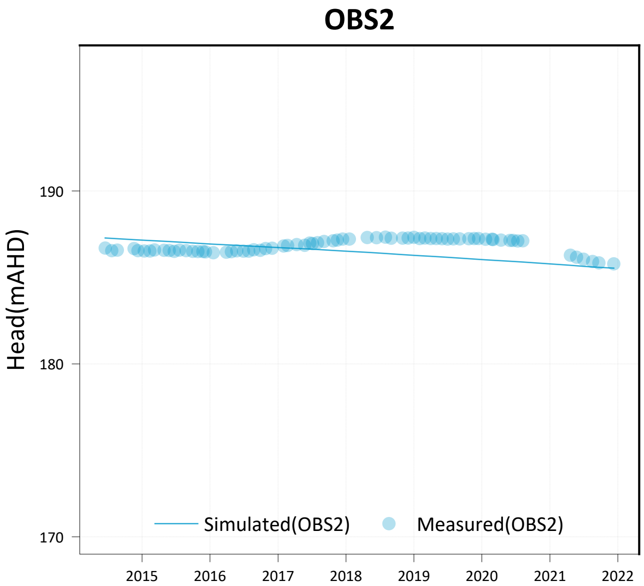
OBS2
Head(mAHD)
190
180
170
Simulated(OBS2)
Measured(OBS2)
2015 2016 2017 2018 2019 2020 2021 2022

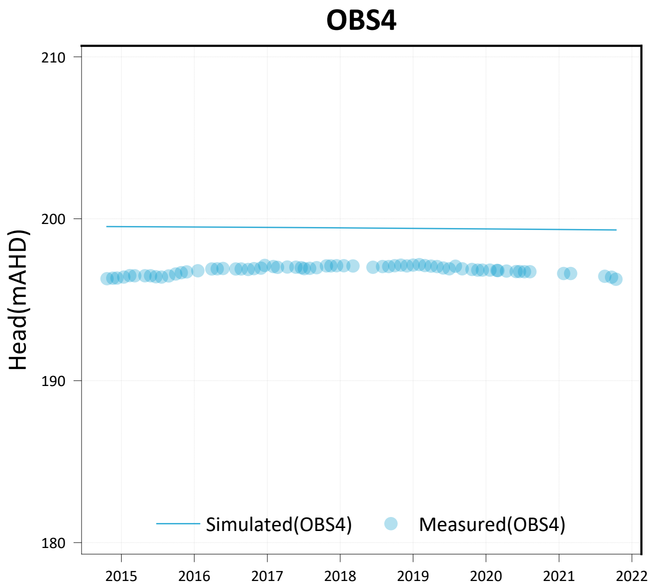
OBS4
Head(mAHD)
210
200
190
180
Simulated(OBS4)
Measured(OBS4)
2015 2016 2017 2018 2019 2020 2021 2022

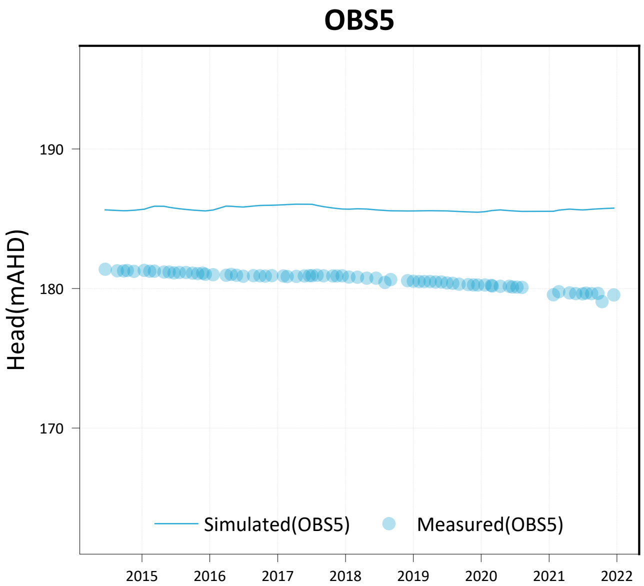
OBS5
Head(mAHD)
190
180
170
Simulated(OBS5)
Measured(OBS5)
2015 2016 2017 2018 2019 2020 2021 2022

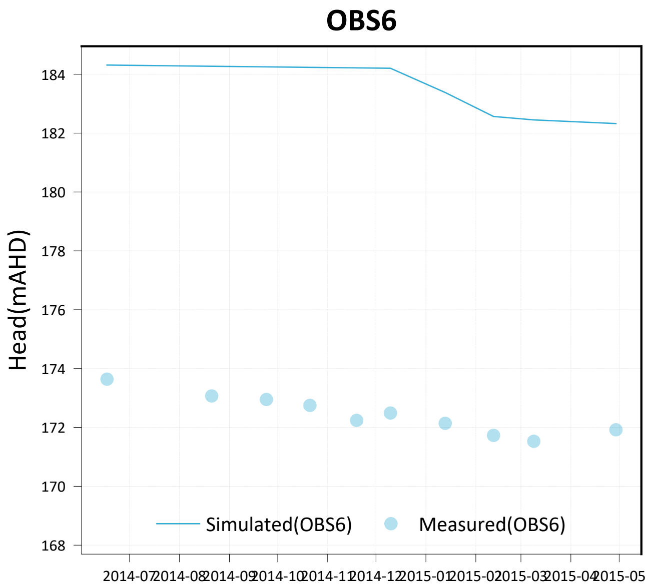
OBS6
Head(mAHD)
184
182
180
178
176
174
172
170
168
Simulated(OBS6)
Measured(OBS6)
2014-07 2014-08 2014-09 2014-10 2014-11 2014-12 2015-01 2015-02 2015-03 2015-04 2015-05

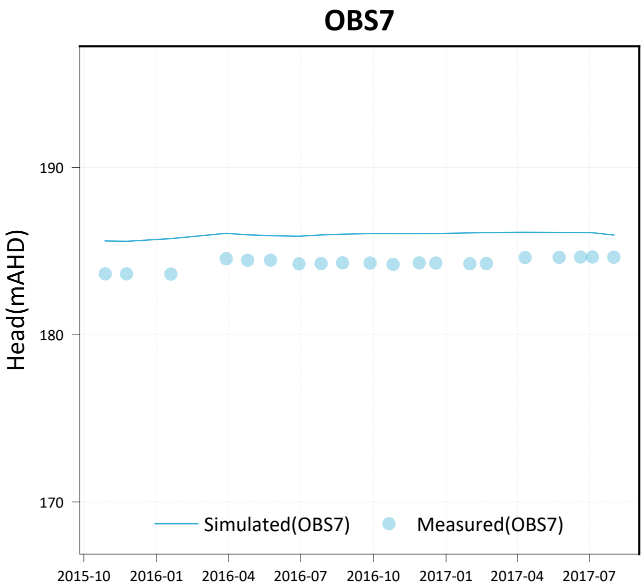
OBS7
Head(mAHD)
190
180
170
Simulated(OBS7)
Measured(OBS7)
2015-10 2016-01 2016-04 2016-07 2016-10 2017-01 2017-04 2017-07

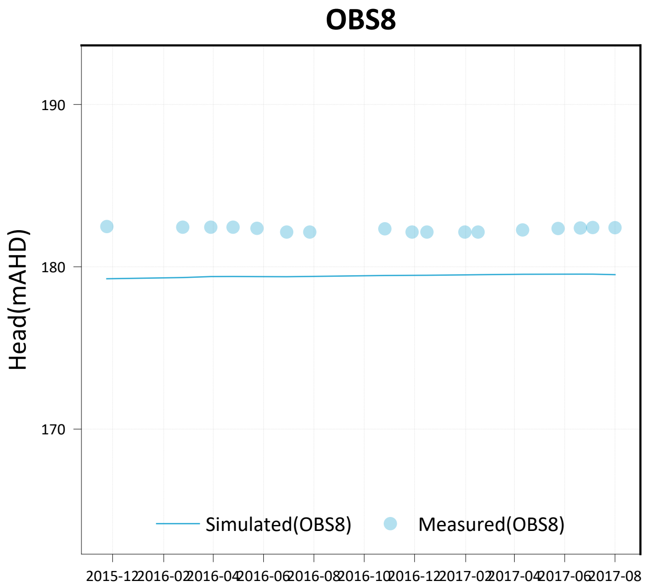

OBS8
Head(mAHD)
190
180
170
Simulated(OBS8)
Measured(OBS8)
2015-12
2016-02
2016-04
2016-06
2016-08
2016-10
2016-12
2017-02
2017-04
2017-06
2017-08

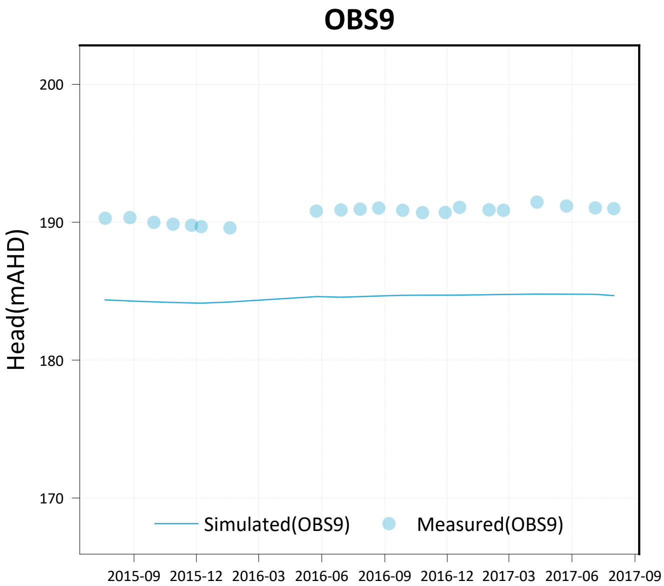

OBS9
Head(mAHD)
200
190
180
170
Simulated(OBS9)
Measured(OBS9)
2015-09
2015-12
2016-03
2016-06
2016-09
2016-12
2017-03
2017-06
2017-09

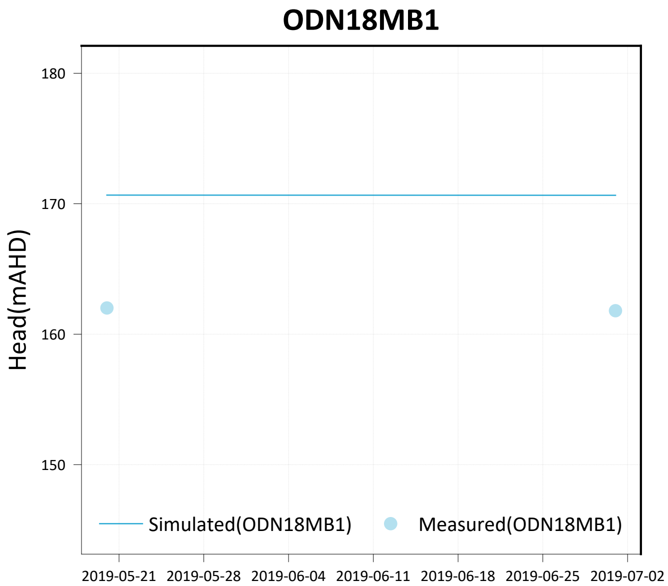

ODN18MB1
Head(mAHD)
180
170
160
150
Simulated(ODN18MB1)
Measured(ODN18MB1)
2019-05-21
2019-05-28
2019-06-04
2019-06-11
2019-06-18
2019-06-25
2019-07-02

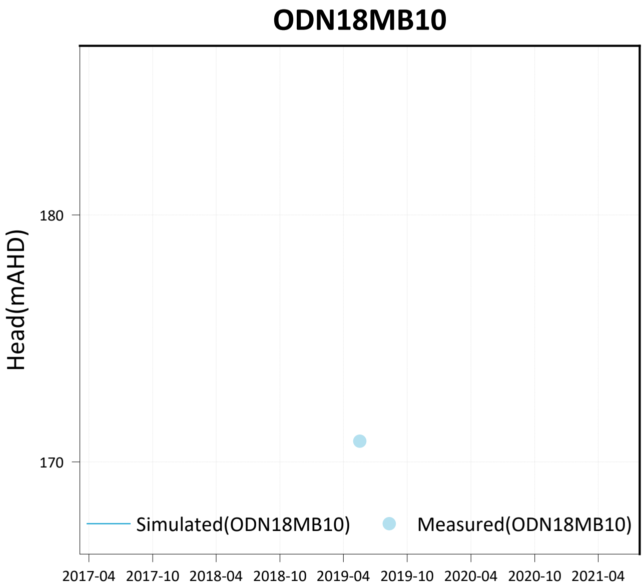

ODN18MB10
Head(mAHD)
180
170
Simulated(ODN18MB10)
Measured(ODN18MB10)
2017-04
2017-10
2018-04
2018-10
2019-04
2019-10
2020-04
2020-10
2021-04

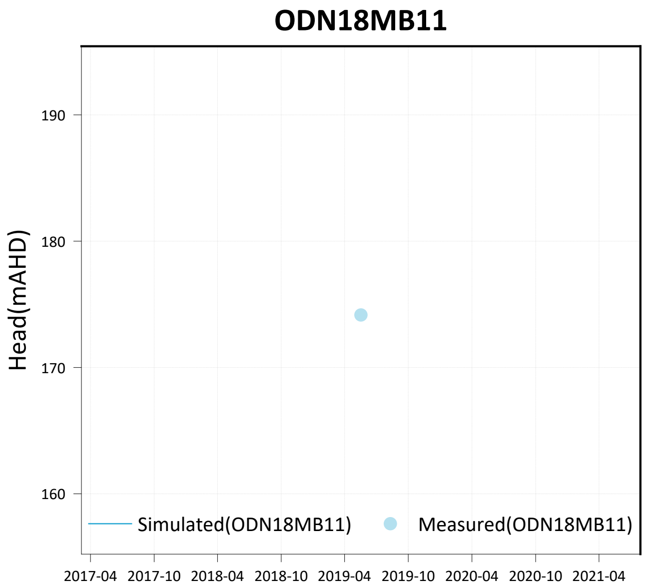

ODN18MB11
Head(mAHD)
190
180
170
160
Simulated(ODN18MB11)
Measured(ODN18MB11)
2017-04
2017-10
2018-04
2018-10
2019-04
2019-10
2020-04
2020-10
2021-04

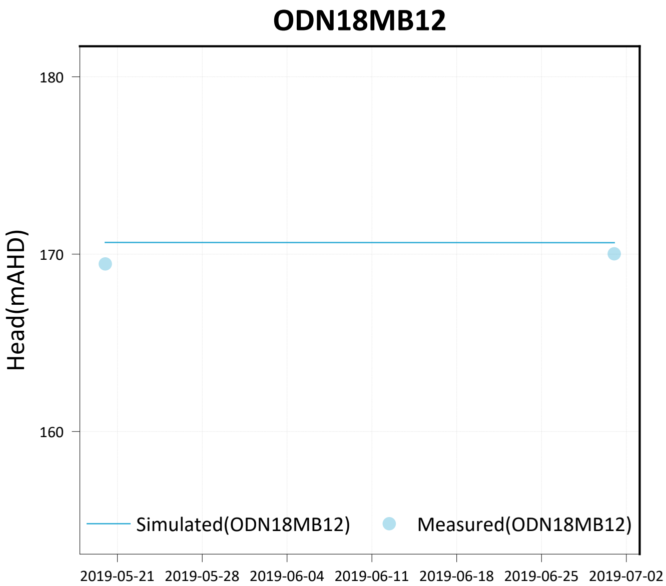

ODN18MB12
Head(mAHD)
180
170
160
Simulated(ODN18MB12)
Measured(ODN18MB12)
2019-05-21
2019-05-28
2019-06-04
2019-06-11
2019-06-18
2019-06-25
2019-07-02

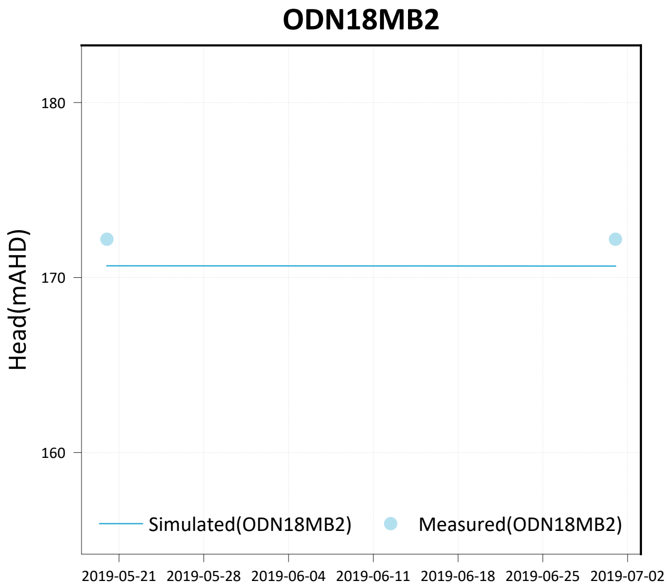
ODN18MB2
Head(mAHD)
180
170
160
Simulated(ODN18MB2)
Measured(ODN18MB2)
2019-05-21
2019-05-28
2019-06-04
2019-06-11
2019-06-18
2019-06-25
2019-07-02

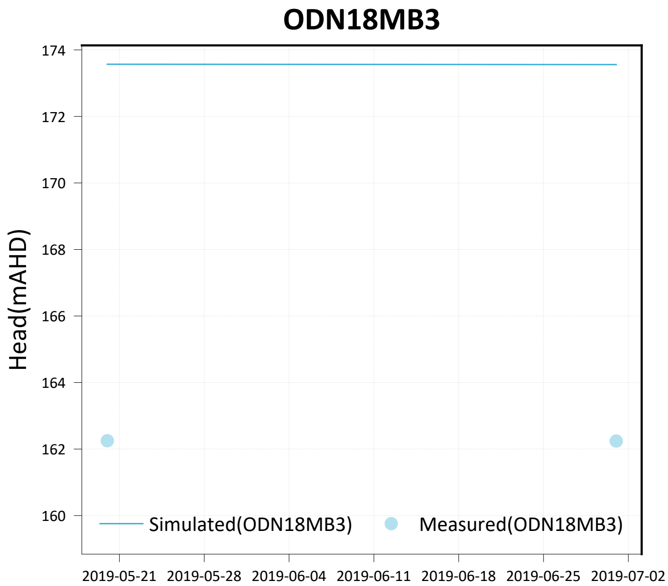
ODN18MB3
Head(mAHD)
174
172
170
168
166
164
162
160
Simulated(ODN18MB3)
Measured(ODN18MB3)
2019-05-21
2019-05-28
2019-06-04
2019-06-11
2019-06-18
2019-06-25
2019-07-02

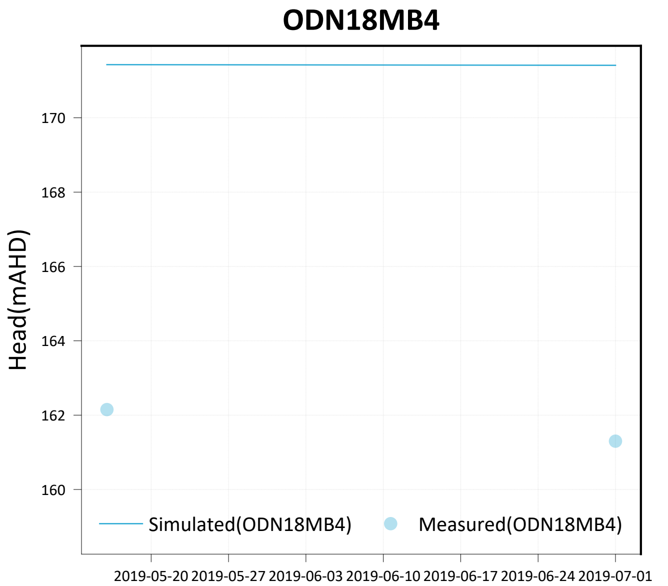
ODN18MB4
Head(mAHD)
170
168
166
164
162
160
Simulated(ODN18MB4)
Measured(ODN18MB4)
2019-05-20
2019-05-27
2019-06-03
2019-06-10
2019-06-17
2019-06-24
2019-07-01

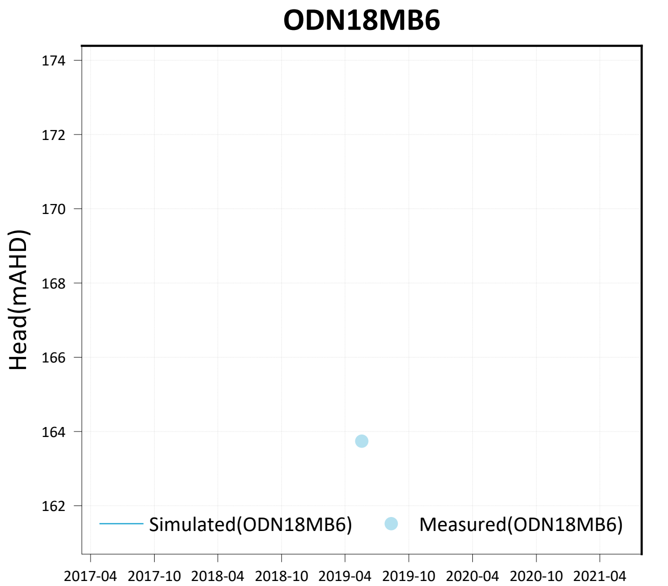
ODN18MB6
Head(mAHD)
174
172
170
168
166
164
162
Simulated(ODN18MB6)
Measured(ODN18MB6)
2017-04
2017-10
2018-04
2018-10
2019-04
2019-10
2020-04
2020-10
2021-04

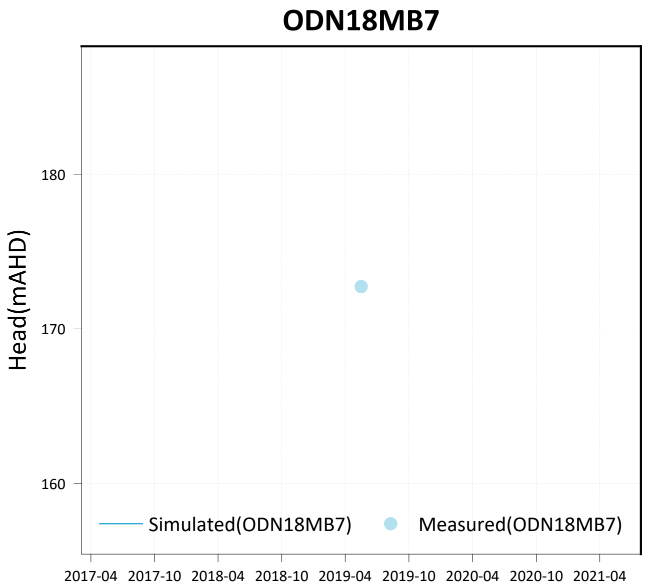
ODN18MB7
Head(mAHD)
180
170
160
Simulated(ODN18MB7)
Measured(ODN18MB7)
2017-04
2017-10
2018-04
2018-10
2019-04
2019-10
2020-04
2020-10
2021-04

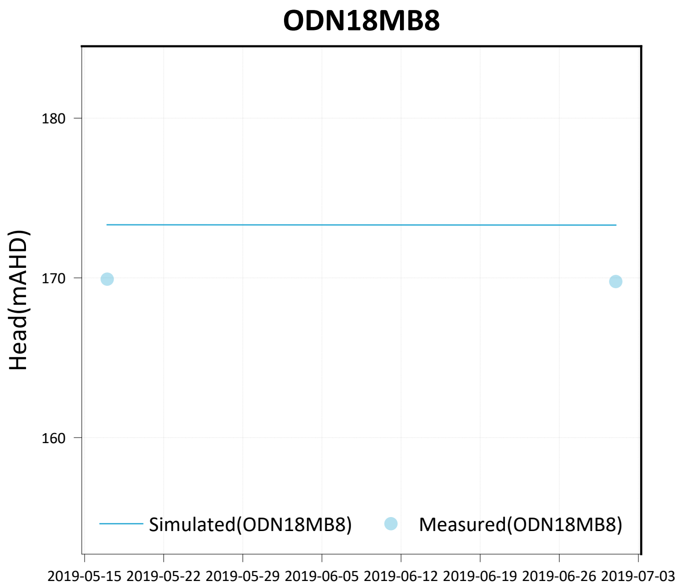
ODN18MB8
Head(mAHD)
180
170
160
Simulated(ODN18MB8)
Measured(ODN18MB8)
2019-05-15
2019-05-22
2019-05-29
2019-06-05
2019-06-12
2019-06-19
2019-06-26
2019-07-03

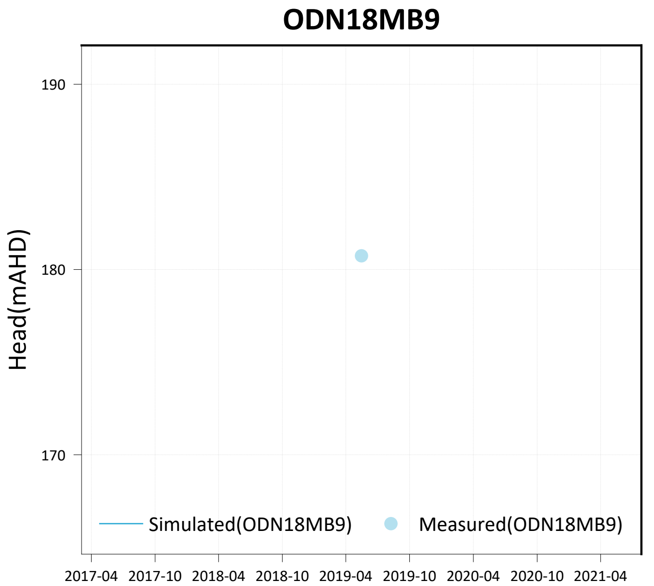
ODN18MB9
Head(mAHD)
190
180
170
Simulated(ODN18MB9)
Measured(ODN18MB9)
2017-04 2017-10 2018-04 2018-10 2019-04 2019-10 2020-04 2020-10 2021-04

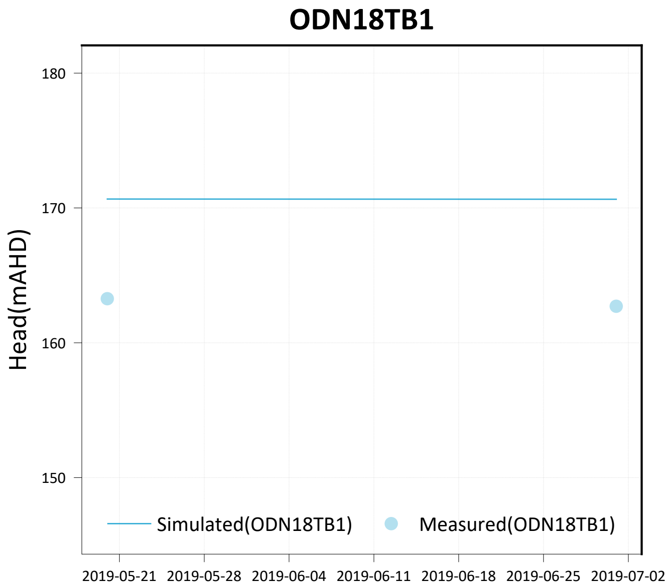
ODN18TB1
Head(mAHD)
180
170
160
150
Simulated(ODN18TB1)
Measured(ODN18TB1)
2019-05-21 2019-05-28 2019-06-04 2019-06-11 2019-06-18 2019-06-25 2019-07-02

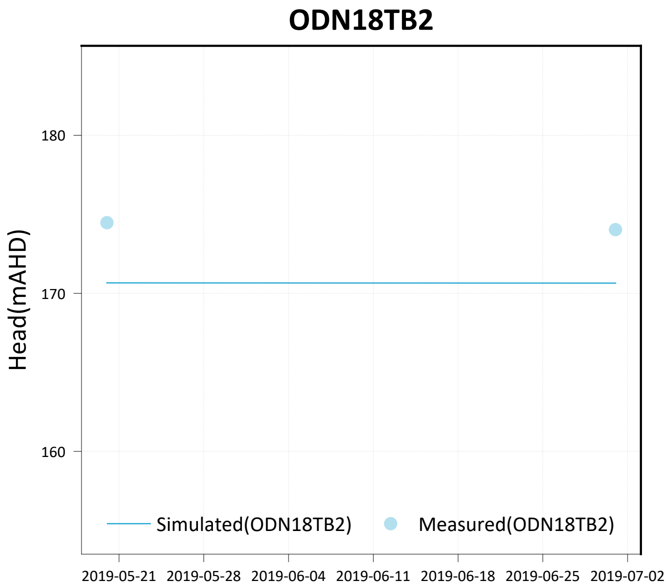
ODN18TB2
Head(mAHD)
180
170
160
Simulated(ODN18TB2)
Measured(ODN18TB2)
2019-05-21 2019-05-28 2019-06-04 2019-06-11 2019-06-18 2019-06-25 2019-07-02

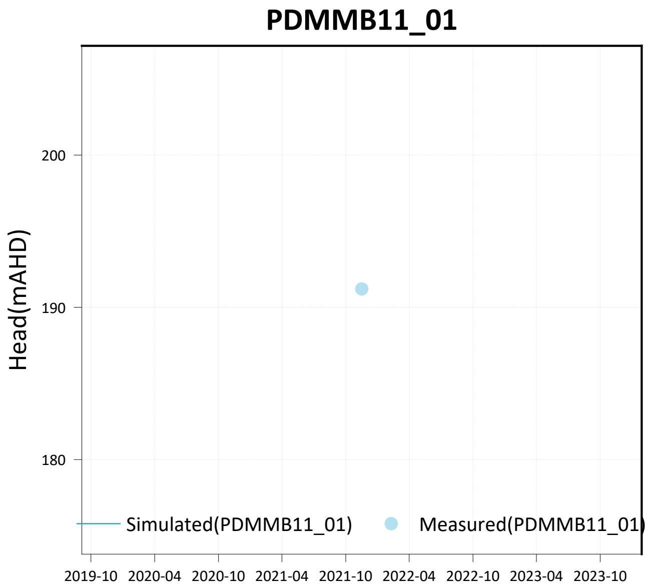
PDMMB11_01
Head(mAHD)
200
190
180
Simulated(PDMMB11_01)
Measured(PDMMB11_01)
2019-10 2020-04 2020-10 2021-04 2021-10 2022-04 2022-10 2023-04 2023-10

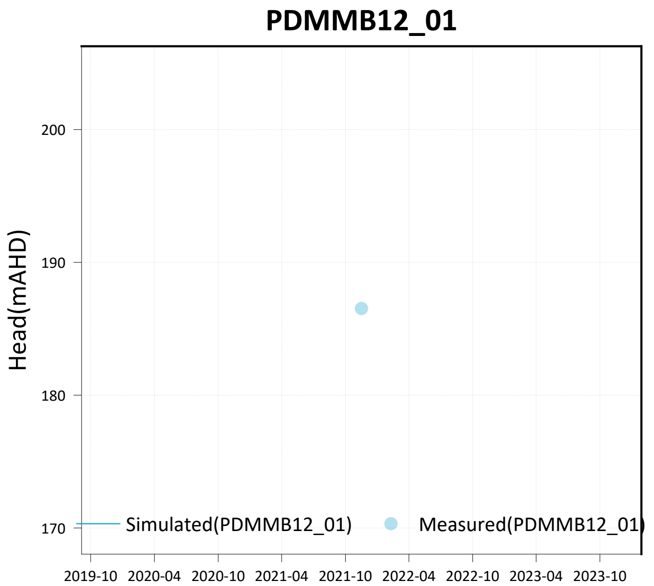
PDMMB12_01
Head(mAHD)
200
190
180
170
Simulated(PDMMB12_01)
Measured(PDMMB12_01)
2019-10 2020-04 2020-10 2021-04 2021-10 2022-04 2022-10 2023-04 2023-10

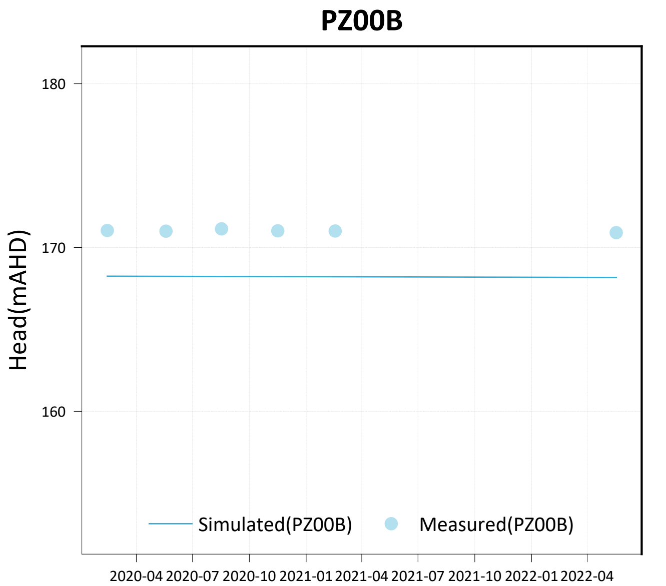
PZ00B
Head(mAHD)
180
170
160
Simulated(PZ00B)
Measured(PZ00B)
2020-04 2020-07 2020-10 2021-01 2021-04 2021-07 2021-10 2022-01 2022-04

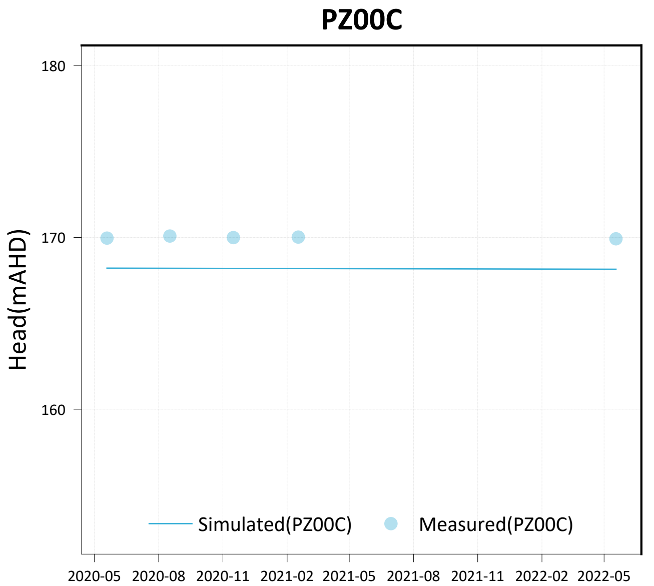
PZ00C
Head(mAHD)
180
170
160
Simulated(PZ00C)
Measured(PZ00C)
2020-05
2020-08
2020-11
2021-02
2021-05
2021-08
2021-11
2022-02
2022-05

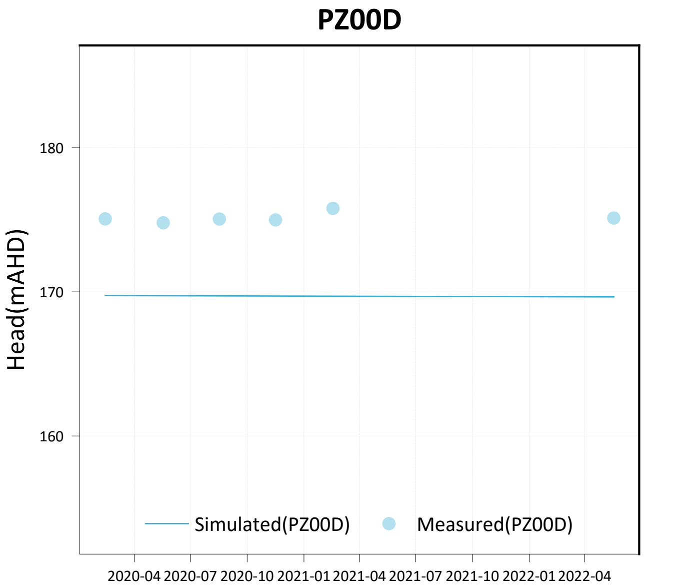
PZ00D
Head(mAHD)
180
170
160
Simulated(PZ00D)
Measured(PZ00D)
2020-04
2020-07
2020-10
2021-01
2021-04
2021-07
2021-10
2022-01
2022-04

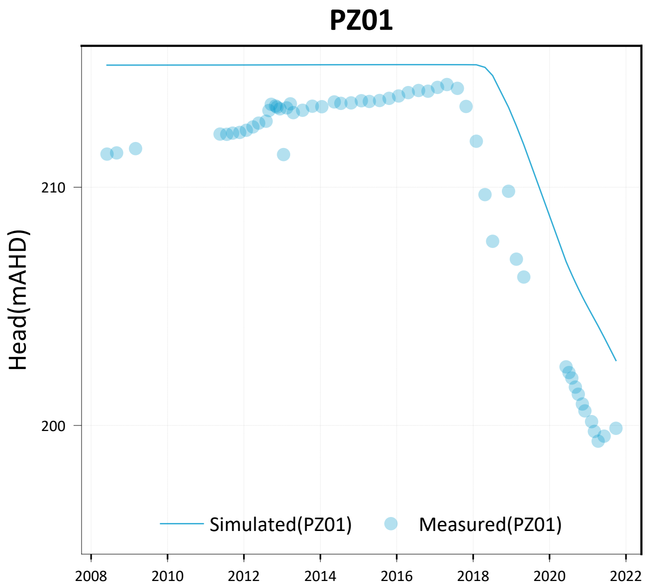
PZ01
Head(mAHD)
210
200
Simulated(PZ01)
Measured(PZ01)
2008
2010
2012
2014
2016
2018
2020
2022

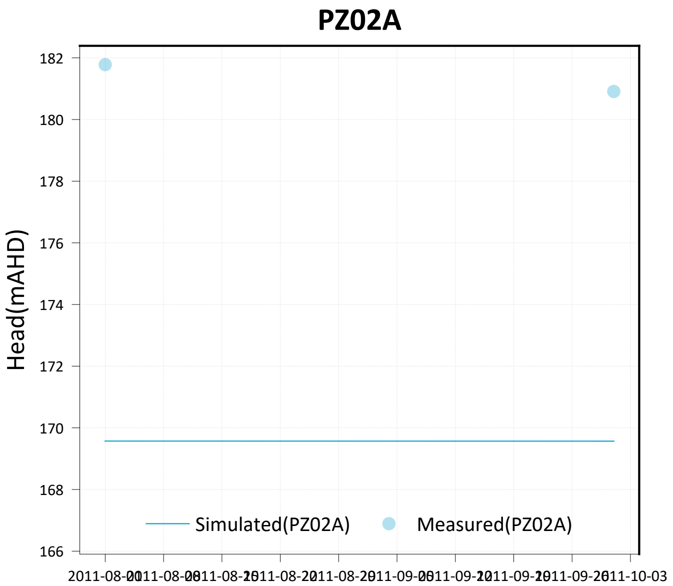
PZ02A
Head(mAHD)
182
180
178
176
174
172
170
168
166
Simulated(PZ02A)
Measured(PZ02A)
2011-10-03

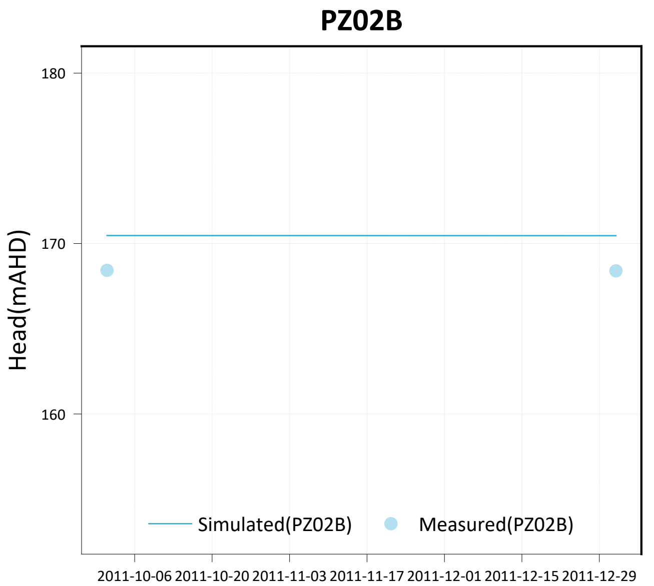
PZ02B
Head(mAHD)
180
170
160
Simulated(PZ02B)
Measured(PZ02B)
2011-10-06
2011-10-20
2011-11-03
2011-11-17
2011-12-01
2011-12-15
2011-12-29

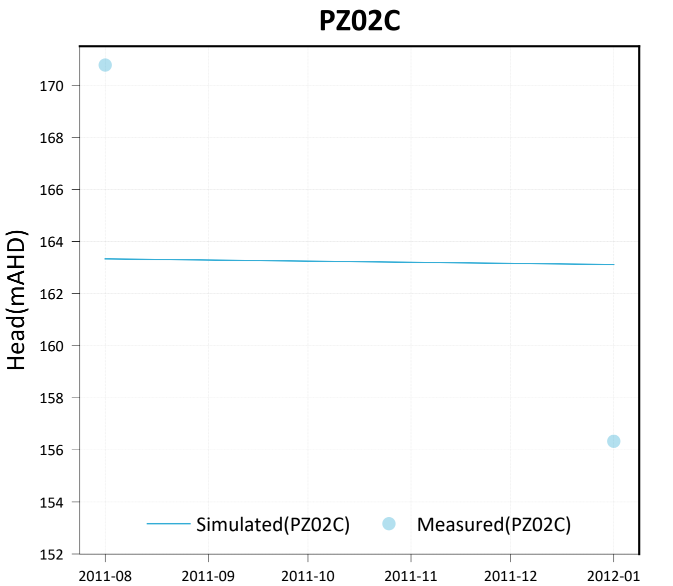
PZ02C
Head(mAHD)
170
168
166
164
162
160
158
156
154
152
Simulated(PZ02C)
Measured(PZ02C)
2011-08
2011-09
2011-10
2011-11
2011-12
2012-01

PZ03-D

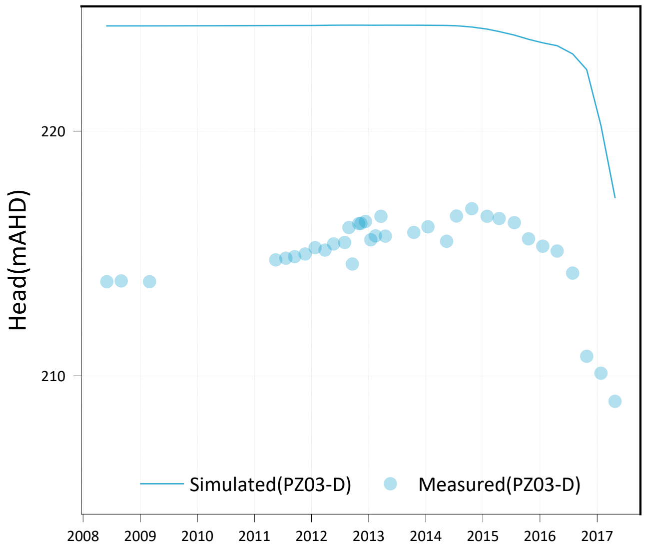

PZ04

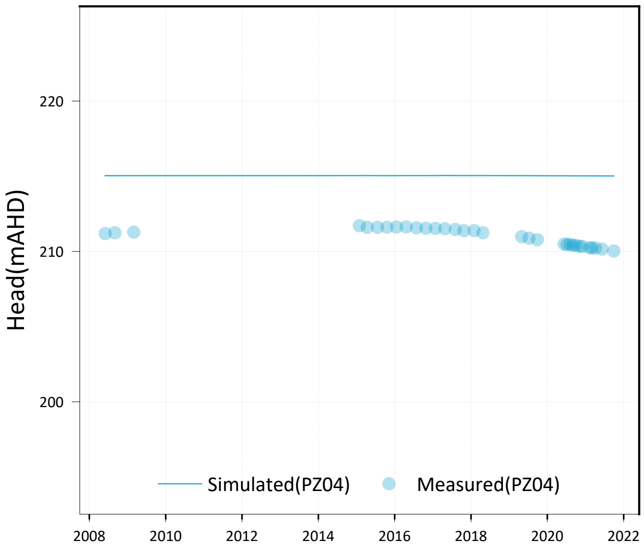

PZ04A

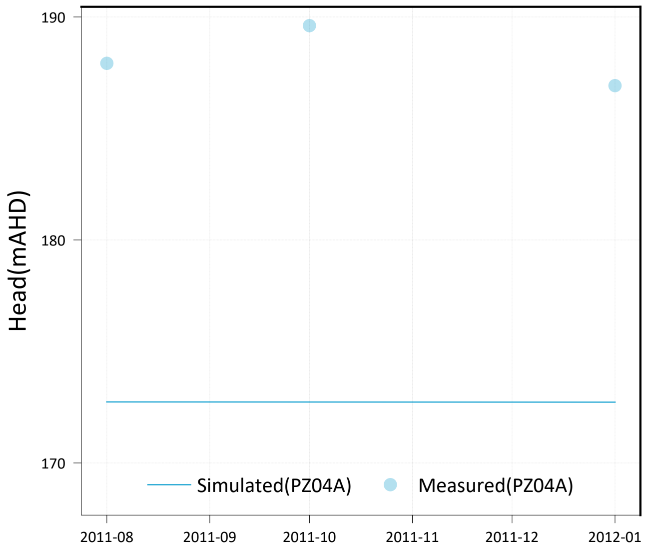

PZ04B

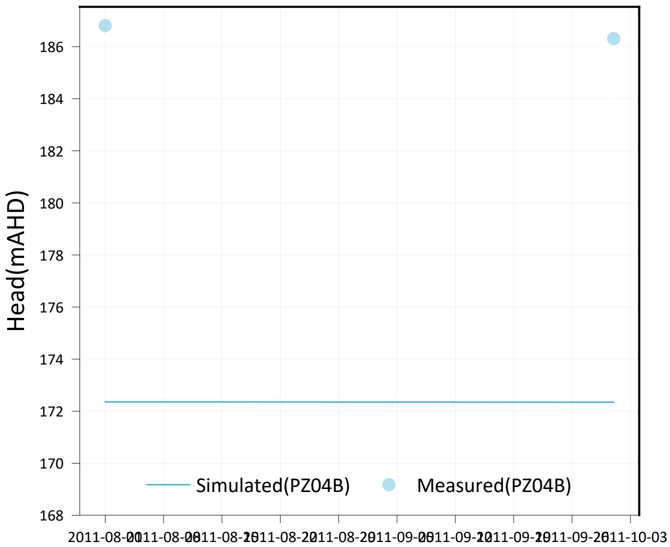

PZ04C

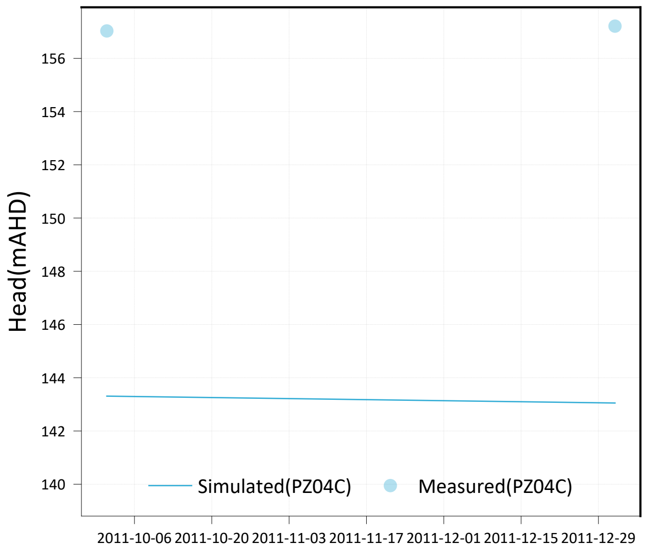

PZ05

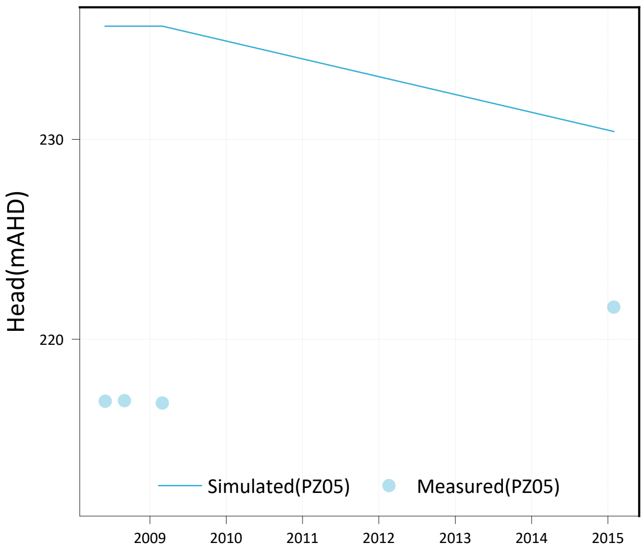

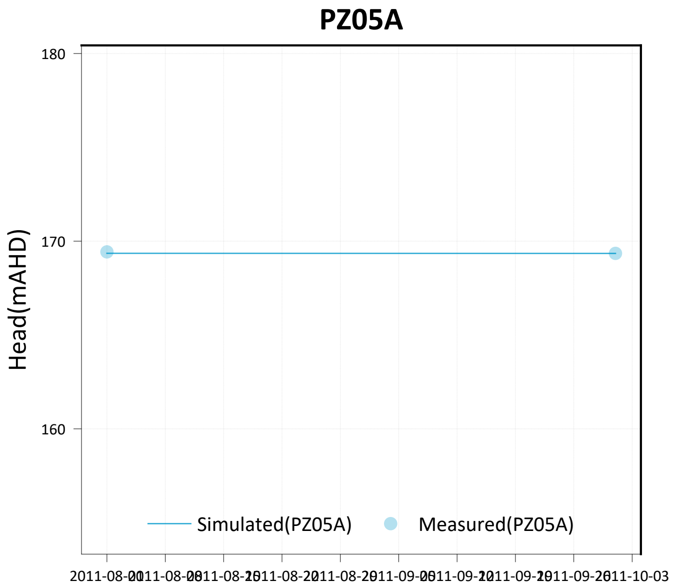
PZ05A
180
170
160
Head(mAHD)
Simulated(PZ05A)
Measured(PZ05A)
2011-10-03

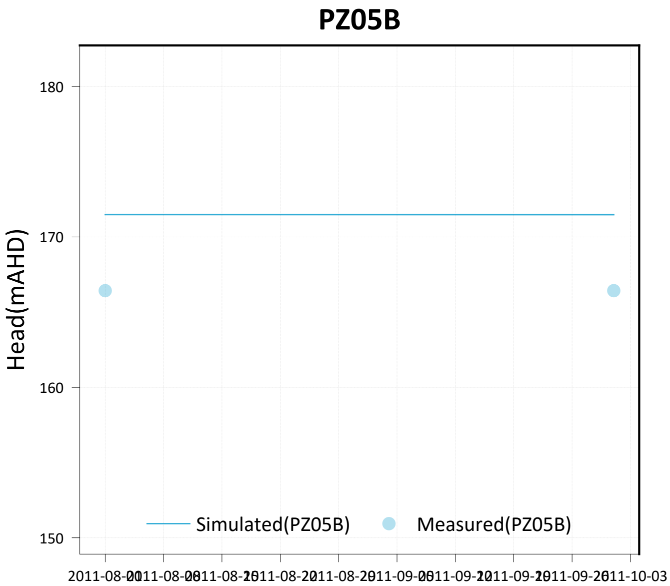
PZ05B
180
170
160
150
Head(mAHD)
Simulated(PZ05B)
Measured(PZ05B)
2011-10-03

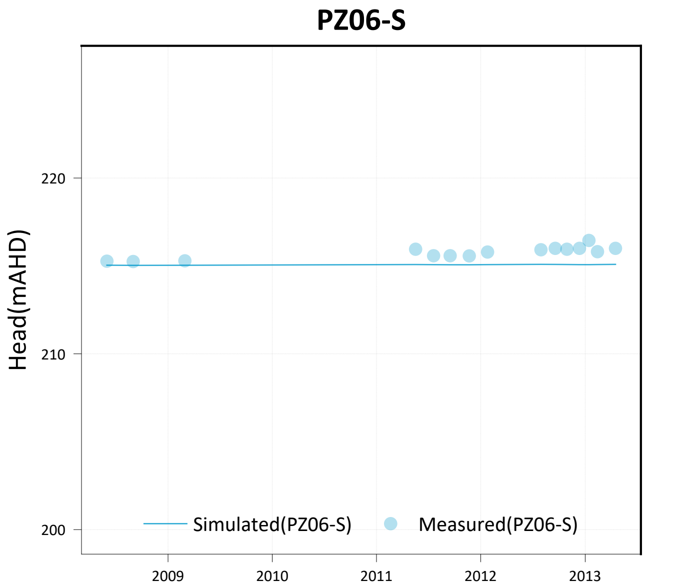
PZ06-S
220
210
200
Head(mAHD)
Simulated(PZ06-S)
Measured(PZ06-S)
2009
2010
2011
2012
2013

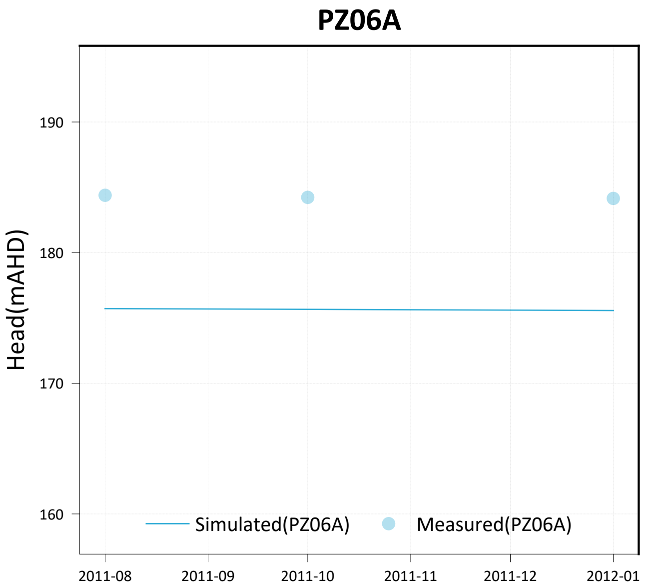
PZ06A
190
180
170
160
Head(mAHD)
Simulated(PZ06A)
Measured(PZ06A)
2011-08
2011-09
2011-10
2011-11
2011-12
2012-01

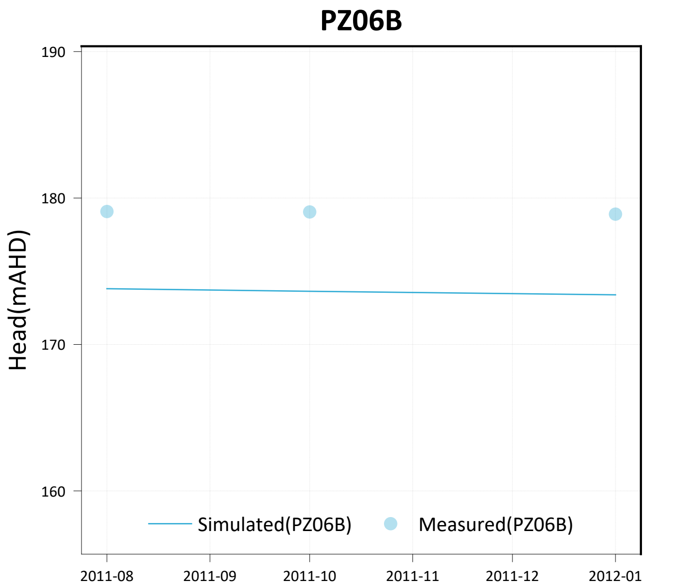
PZ06B
190
180
170
160
Head(mAHD)
Simulated(PZ06B)
Measured(PZ06B)
2011-08
2011-09
2011-10
2011-11
2011-12
2012-01

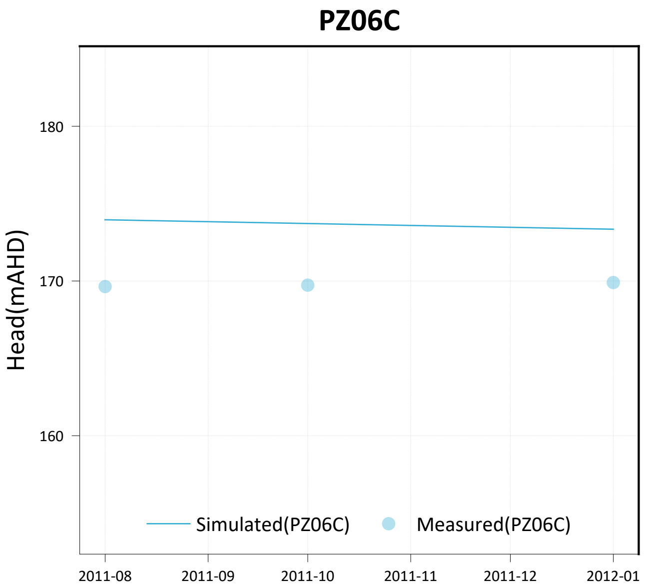
PZ06C
180
170
160
Head(mAHD)
Simulated(PZ06C)
Measured(PZ06C)
2011-08
2011-09
2011-10
2011-11
2011-12
2012-01

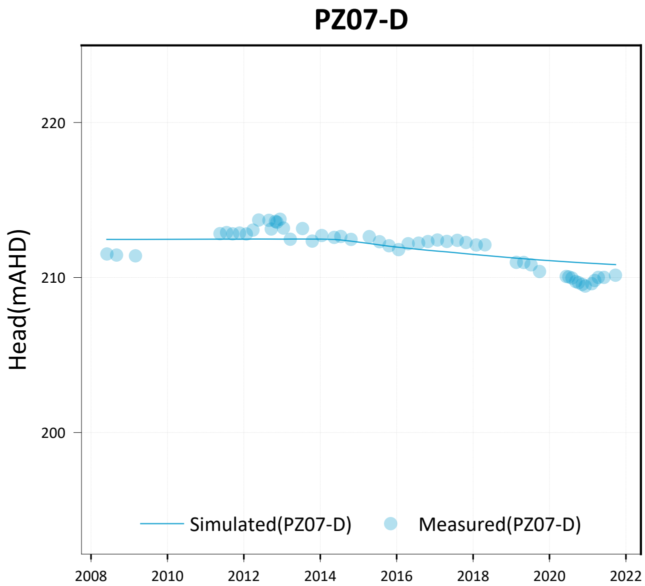
PZ07-D
Head(mAHD)
220
210
200
Simulated(PZ07-D)
Measured(PZ07-D)
2008
2010
2012
2014
2016
2018
2020
2022

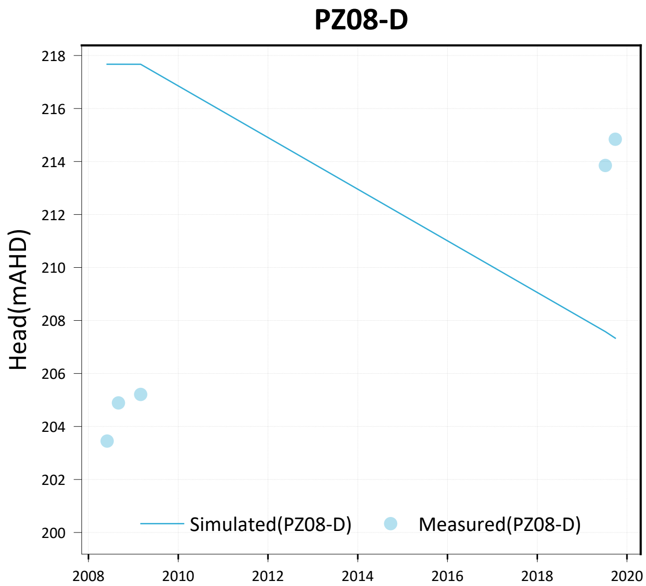
PZ08-D
Head(mAHD)
218
216
214
212
210
208
206
204
202
200
Simulated(PZ08-D)
Measured(PZ08-D)
2008
2010
2012
2014
2016
2018
2020

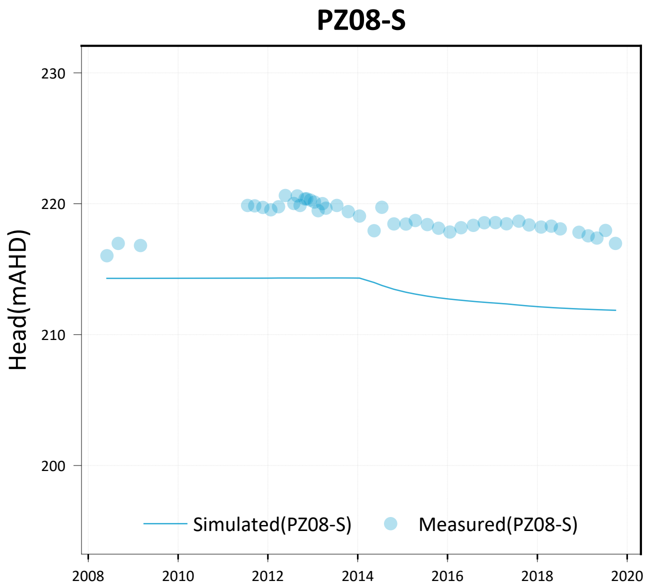
PZ08-S
Head(mAHD)
230
220
210
200
Simulated(PZ08-S)
Measured(PZ08-S)
2008
2010
2012
2014
2016
2018
2020

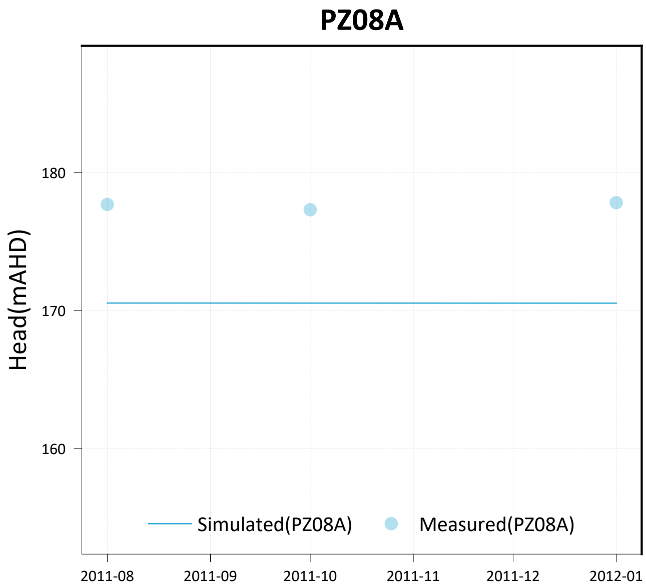
PZ08A
Head(mAHD)
180
170
160
Simulated(PZ08A)
Measured(PZ08A)
2011-08
2011-09
2011-10
2011-11
2011-12
2012-01

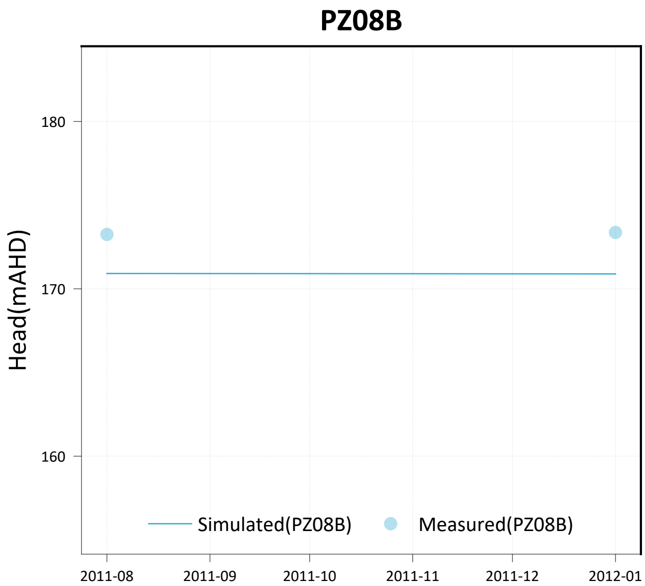
PZ08B
Head(mAHD)
180
170
160
Simulated(PZ08B)
Measured(PZ08B)
2011-08
2011-09
2011-10
2011-11
2011-12
2012-01

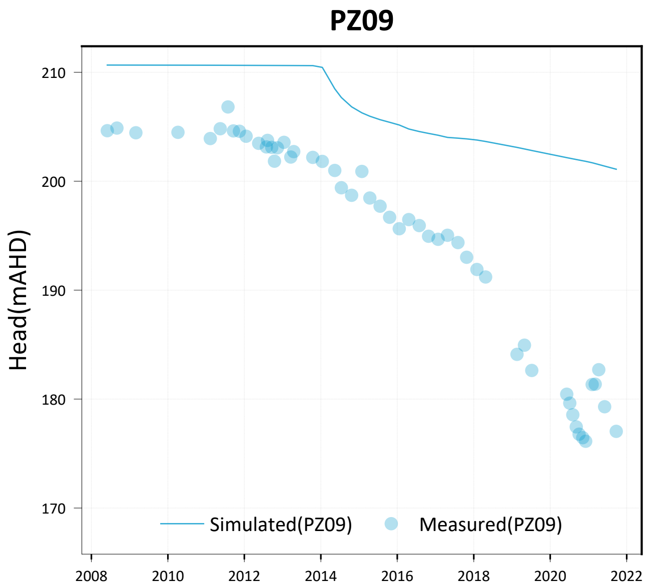
PZ09
Head(mAHD)
210
200
190
180
170
Simulated(PZ09)
Measured(PZ09)
2008
2010
2012
2014
2016
2018
2020
2022

PZ09B

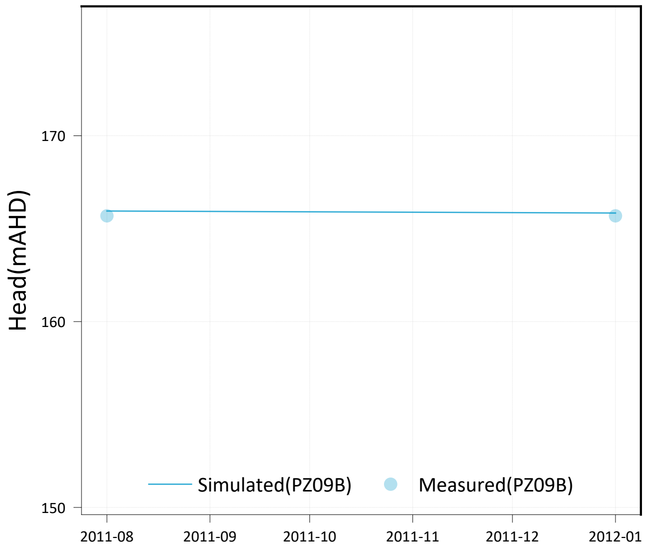

PZ09C

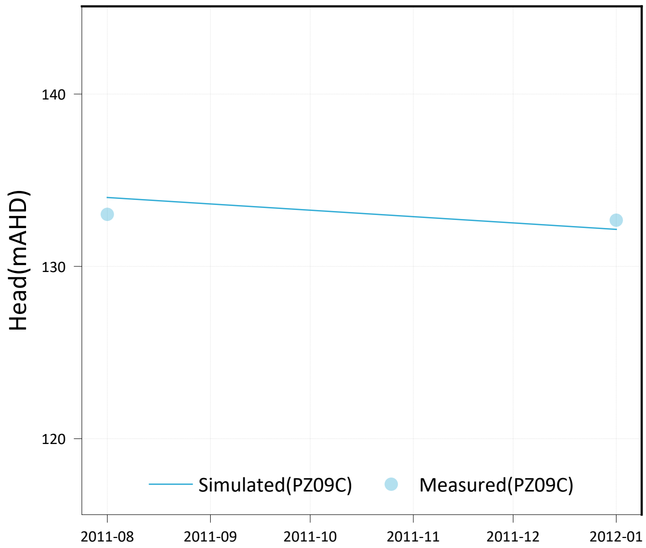

PZ10B

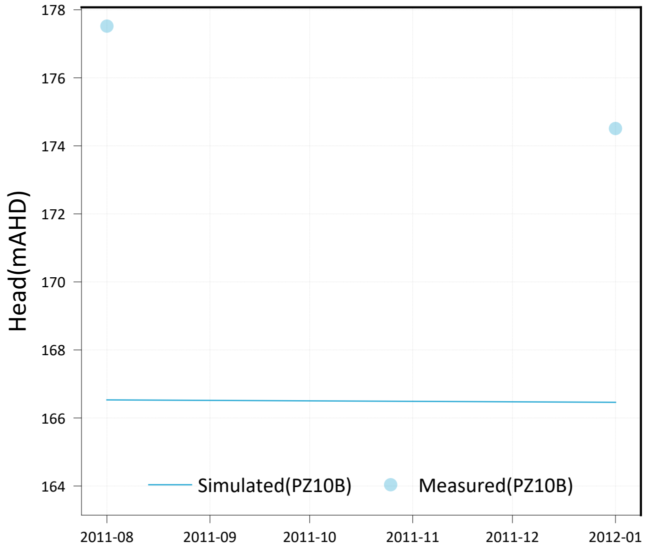

PZ10C

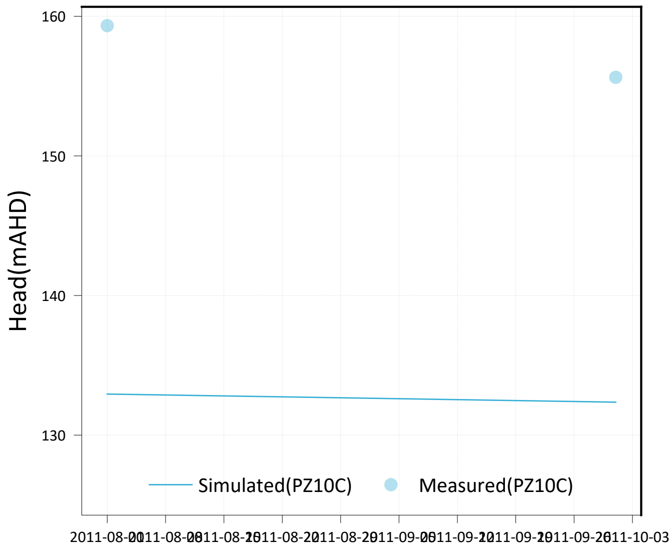

PZ11-D

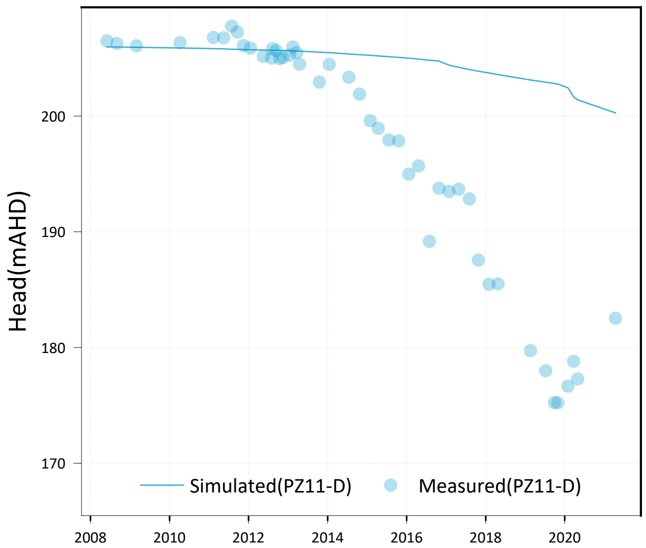

PZ12-D

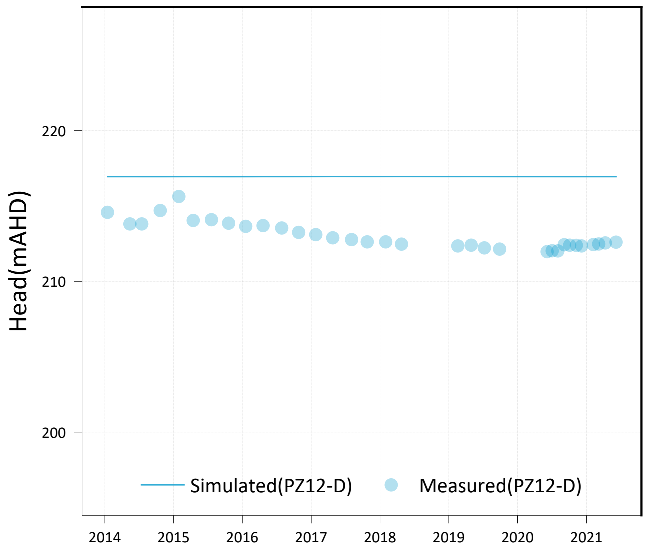

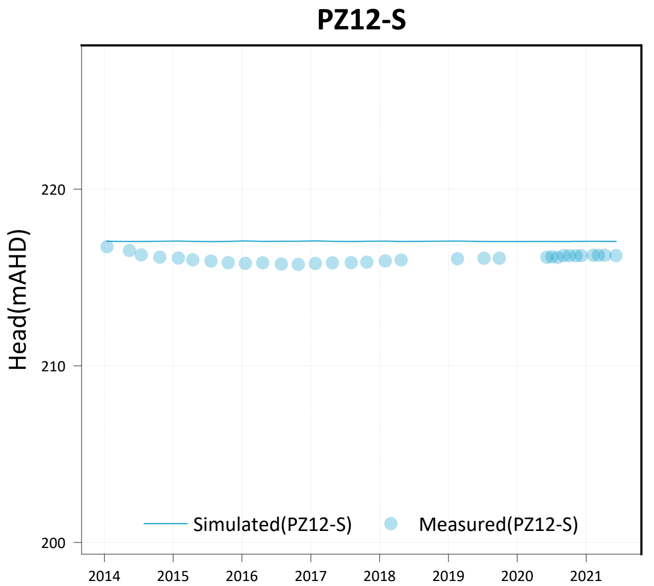
PZ12-S
Head(mAHD)
220
210
200
2014
2015
2016
2017
2018
2019
2020
2021
Simulated(PZ12-S)
Measured(PZ12-S)

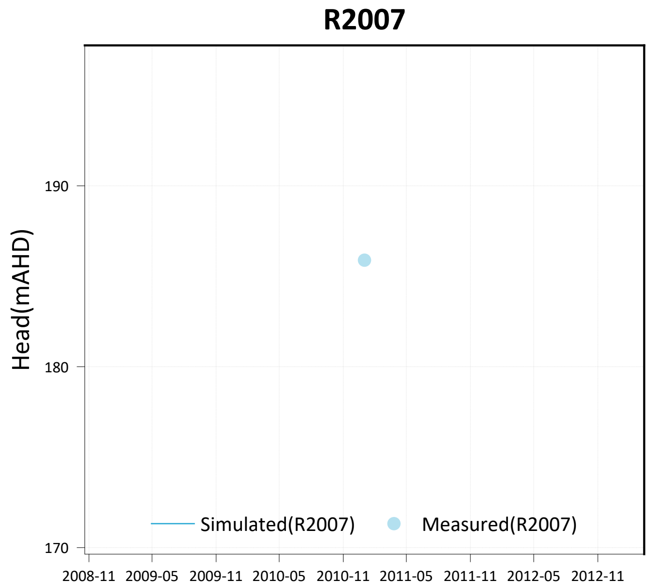
R2007
Head(mAHD)
190
180
170
2008-11
2009-05
2009-11
2010-05
2010-11
2011-05
2011-11
2012-05
2012-11
Simulated(R2007)
Measured(R2007)

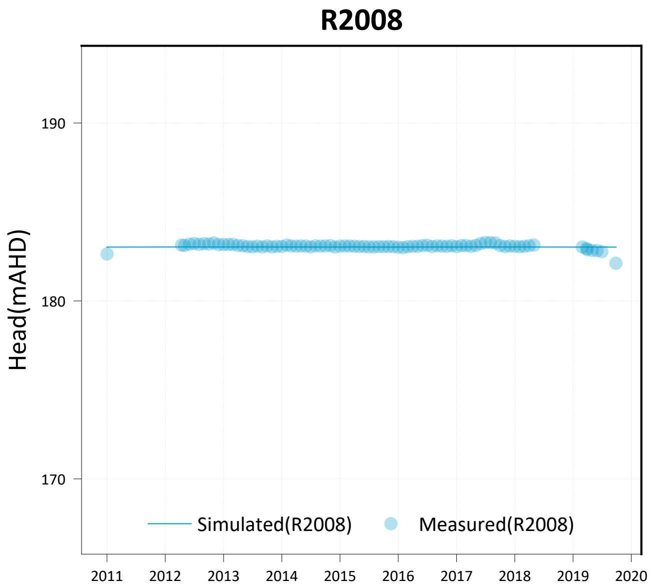
R2008
Head(mAHD)
190
180
170
2011
2012
2013
2014
2015
2016
2017
2018
2019
2020
Simulated(R2008)
Measured(R2008)

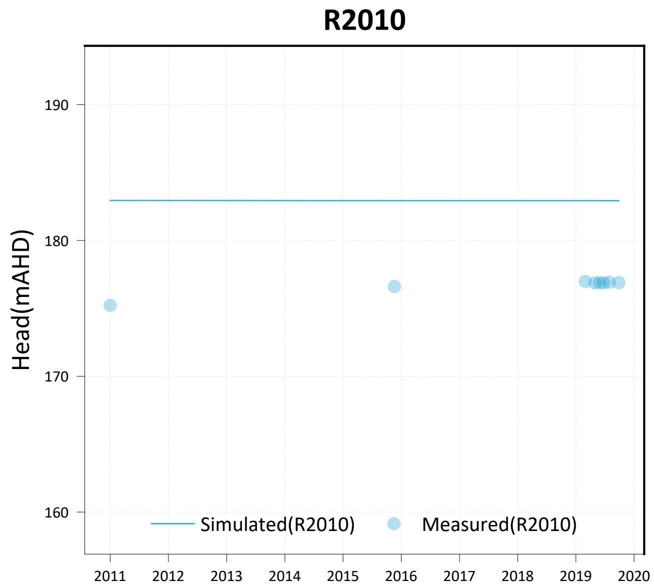
R2010
Head(mAHD)
190
180
170
160
2011
2012
2013
2014
2015
2016
2017
2018
2019
2020
Simulated(R2010)
Measured(R2010)

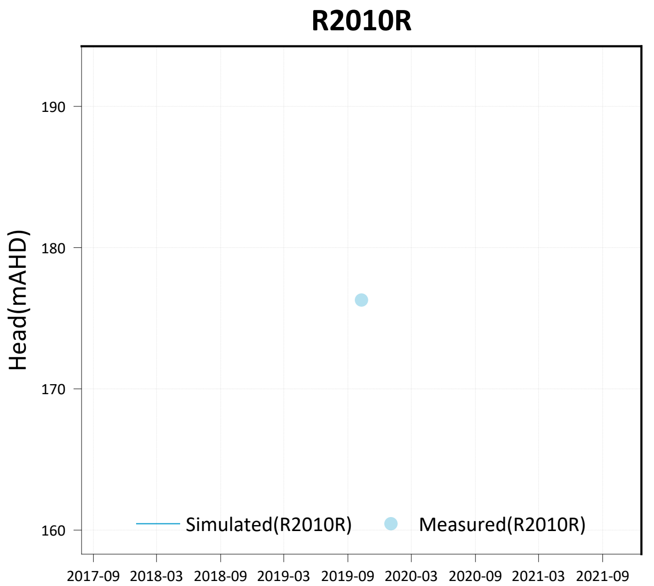
R2010R
Head(mAHD)
190
180
170
160
2017-09
2018-03
2018-09
2019-03
2019-09
2020-03
2020-09
2021-03
2021-09
Simulated(R2010R)
Measured(R2010R)

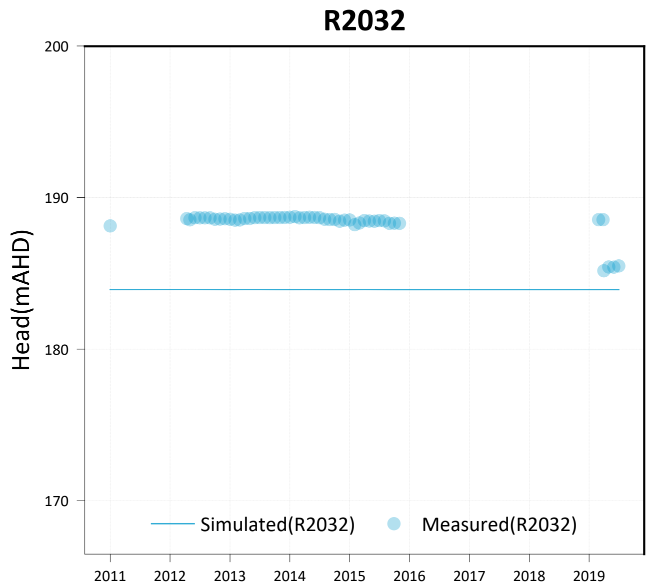
R2032
Head(mAHD)
200
190
180
170
2011
2012
2013
2014
2015
2016
2017
2018
2019
Simulated(R2032)
Measured(R2032)

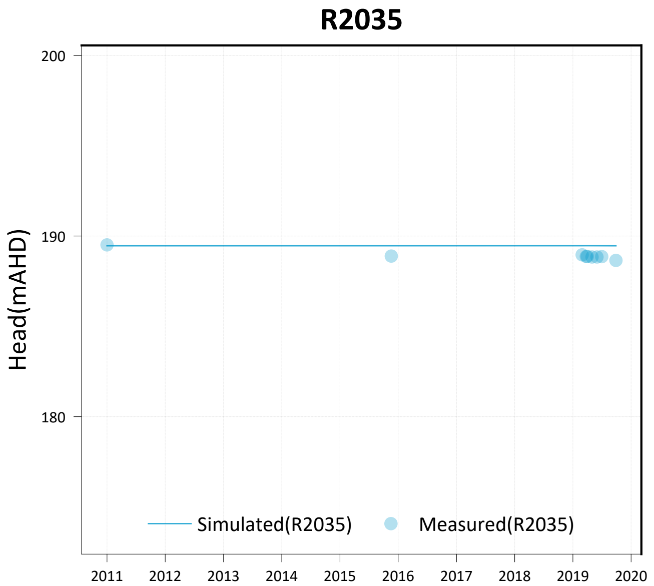
R2035
Head(mAHD)
200
190
180
Simulated(R2035)
Measured(R2035)
2011
2012
2013
2014
2015
2016
2017
2018
2019
2020

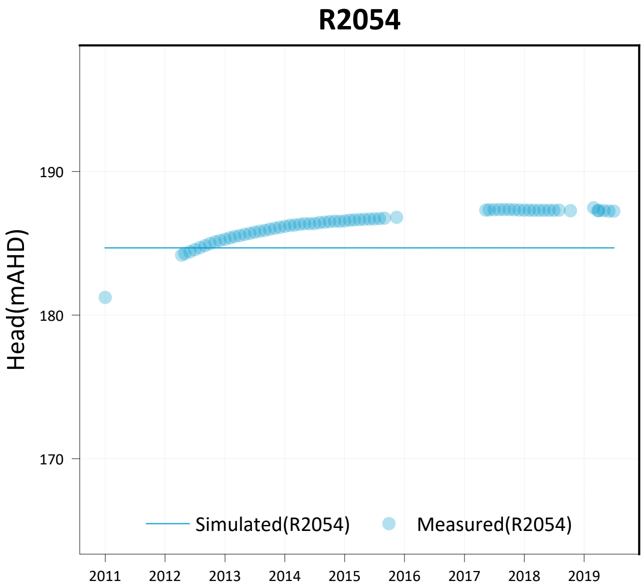
R2054
Head(mAHD)
190
180
170
Simulated(R2054)
Measured(R2054)
2011
2012
2013
2014
2015
2016
2017
2018
2019

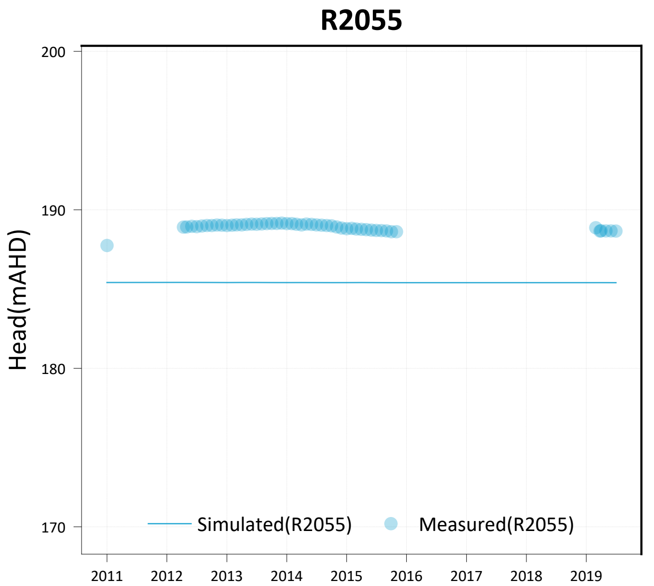
R2055
Head(mAHD)
200
190
180
170
Simulated(R2055)
Measured(R2055)
2011
2012
2013
2014
2015
2016
2017
2018
2019

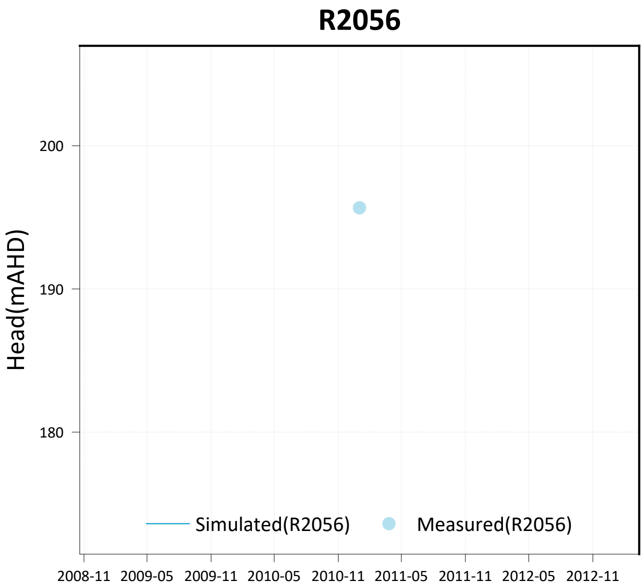
R2056
Head(mAHD)
200
190
180
Simulated(R2056)
Measured(R2056)
2008-11
2009-05
2009-11
2010-05
2010-11
2011-05
2011-11
2012-05
2012-11

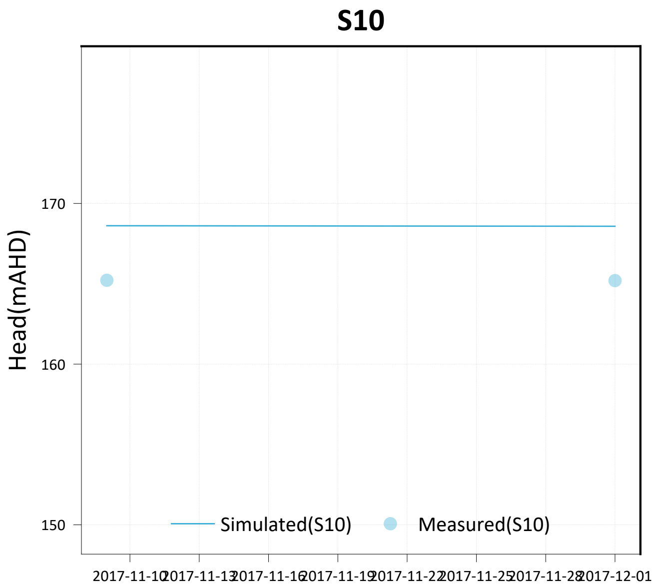
S10
Head(mAHD)
170
160
150
Simulated(S10)
Measured(S10)
2017-11-10
2017-11-13
2017-11-16
2017-11-19
2017-11-22
2017-11-25
2017-11-28
2017-12-01

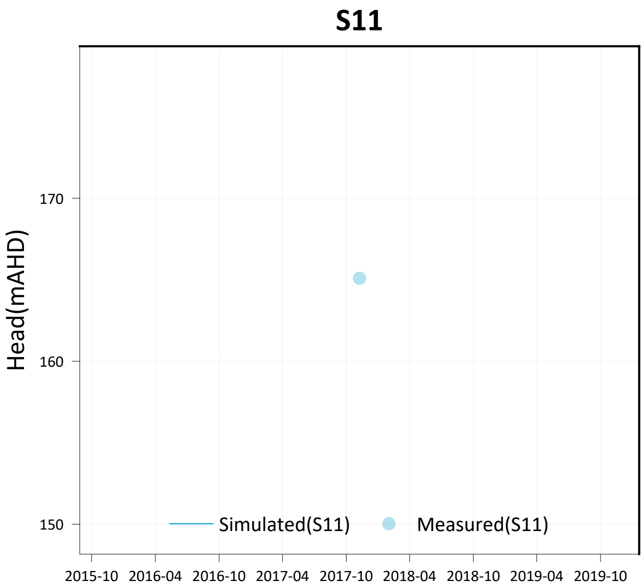
S11
Head(mAHD)
170
160
150
Simulated(S11)
Measured(S11)
2015-10
2016-04
2016-10
2017-04
2017-10
2018-04
2018-10
2019-04
2019-10

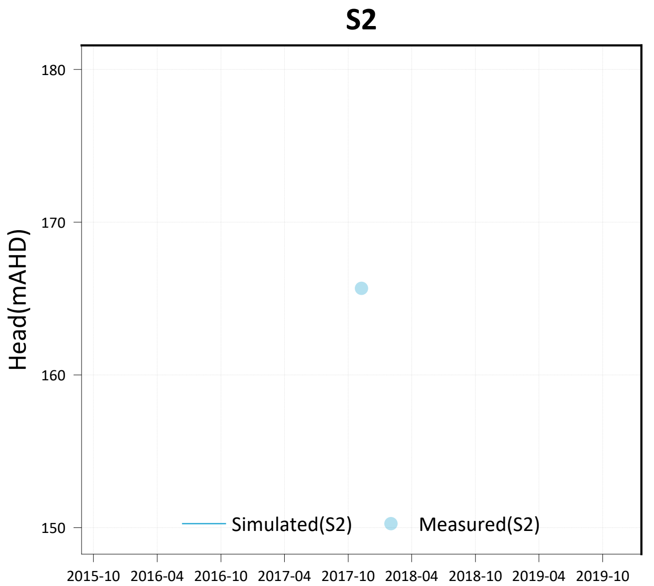
S2
Head(mAHD)
180
170
160
150
Simulated(S2)
Measured(S2)
2015-10
2016-04
2016-10
2017-04
2017-10
2018-04
2018-10
2019-04
2019-10

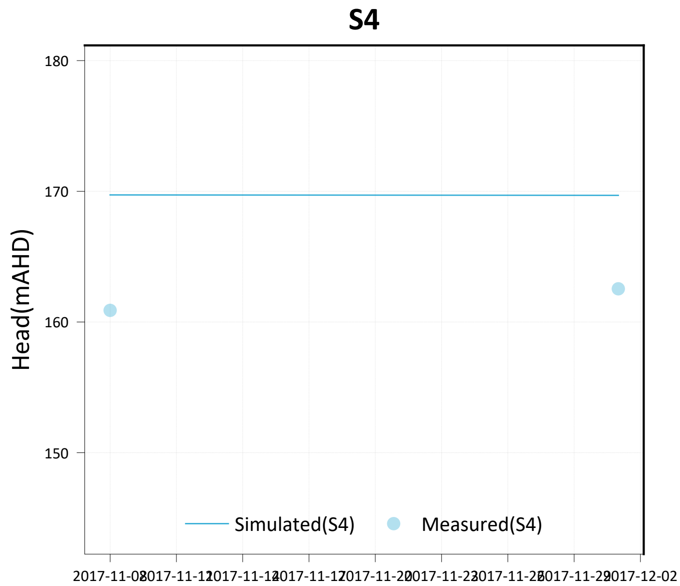
S4
Head(mAHD)
180
170
160
150
Simulated(S4)
Measured(S4)
2017-12-02

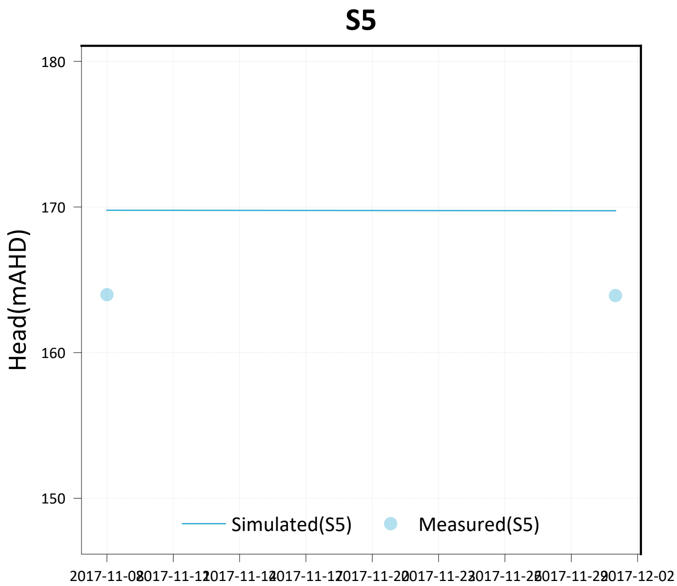
S5
Head(mAHD)
180
170
160
150
Simulated(S5)
Measured(S5)
2017-12-02

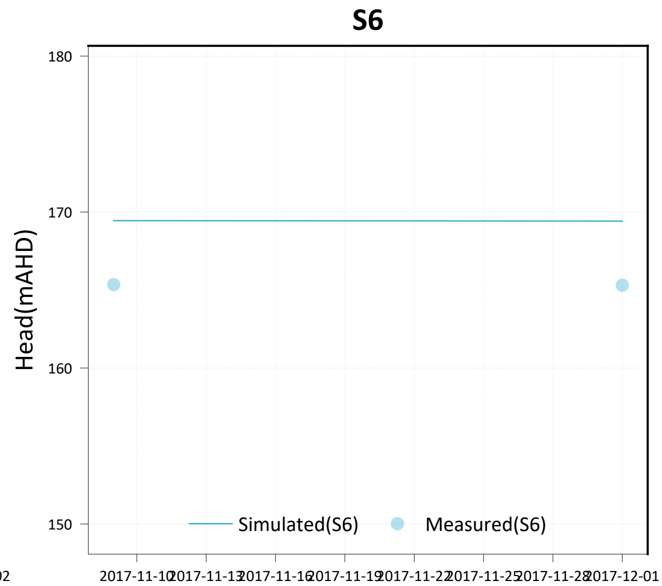
S6
Head(mAHD)
180
170
160
150
Simulated(S6)
Measured(S6)
2017-12-01

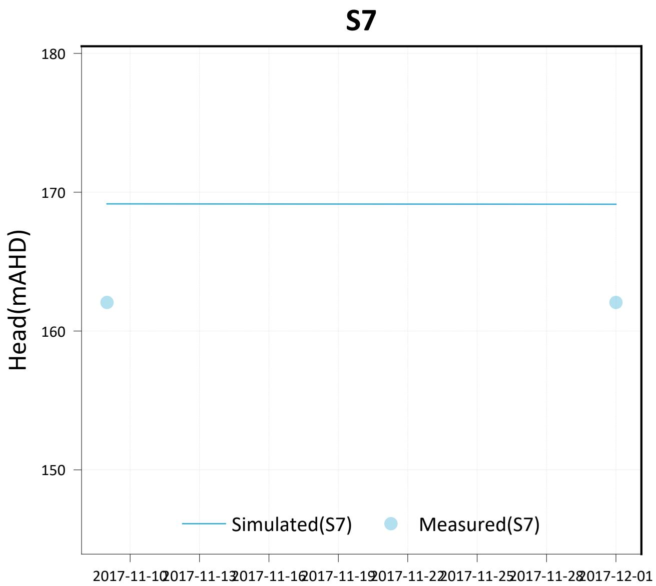
S7
Head(mAHD)
180
170
160
150
Simulated(S7)
Measured(S7)
2017-12-01

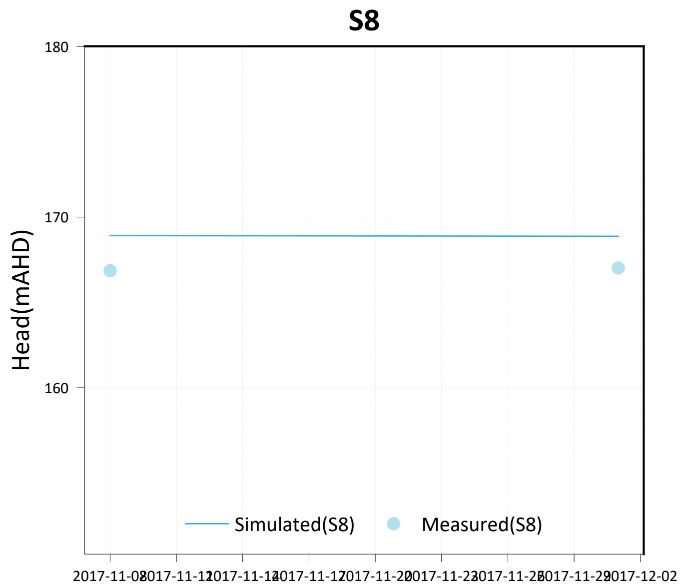
S8
Head(mAHD)
180
170
160
Simulated(S8)
Measured(S8)
2017-12-02

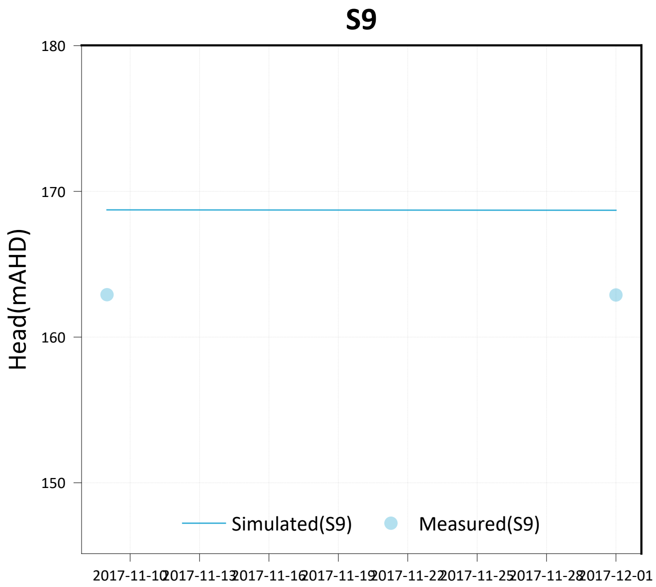
S9
Head(mAHD)
180
170
160
150
Simulated(S9)
Measured(S9)
2017-11-10
2017-11-13
2017-11-16
2017-11-19
2017-11-22
2017-11-25
2017-11-28
2017-12-01

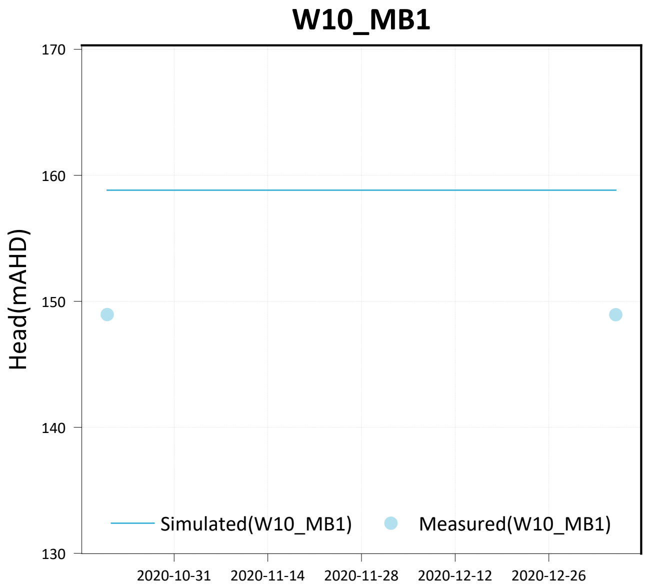
W10_MB1
Head(mAHD)
170
160
150
140
130
Simulated(W10_MB1)
Measured(W10_MB1)
2020-10-31
2020-11-14
2020-11-28
2020-12-12
2020-12-26

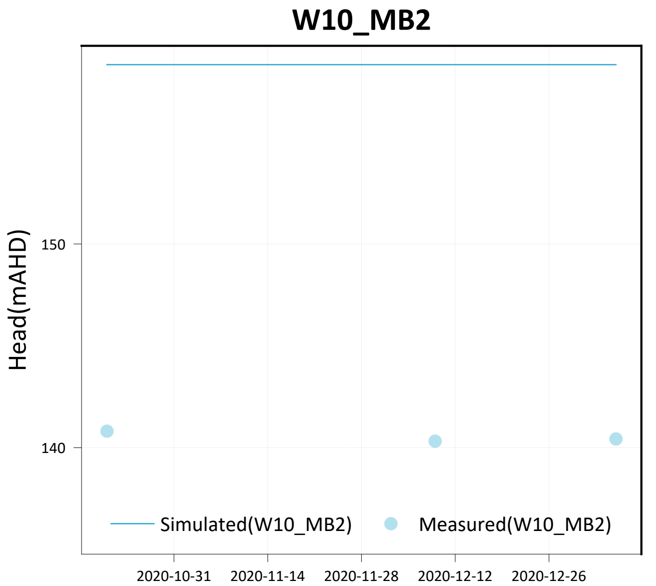
W10_MB2
Head(mAHD)
150
140
Simulated(W10_MB2)
Measured(W10_MB2)
2020-10-31
2020-11-14
2020-11-28
2020-12-12
2020-12-26

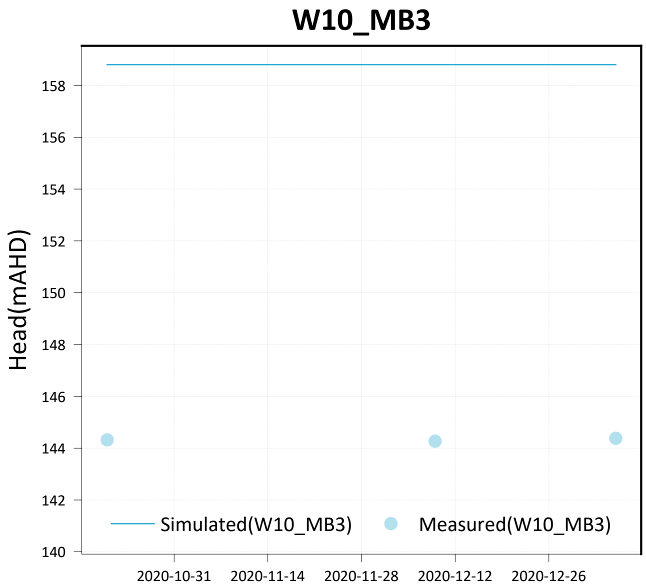
W10_MB3
Head(mAHD)
158
156
154
152
150
148
146
144
142
140
Simulated(W10_MB3)
Measured(W10_MB3)
2020-10-31
2020-11-14
2020-11-28
2020-12-12
2020-12-26

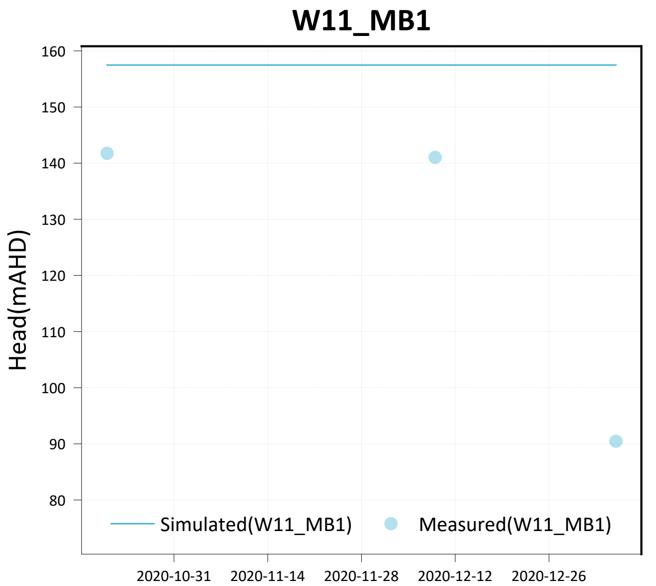
W11_MB1
Head(mAHD)
160
150
140
130
120
110
100
90
80
Simulated(W11_MB1)
Measured(W11_MB1)
2020-10-31
2020-11-14
2020-11-28
2020-12-12
2020-12-26

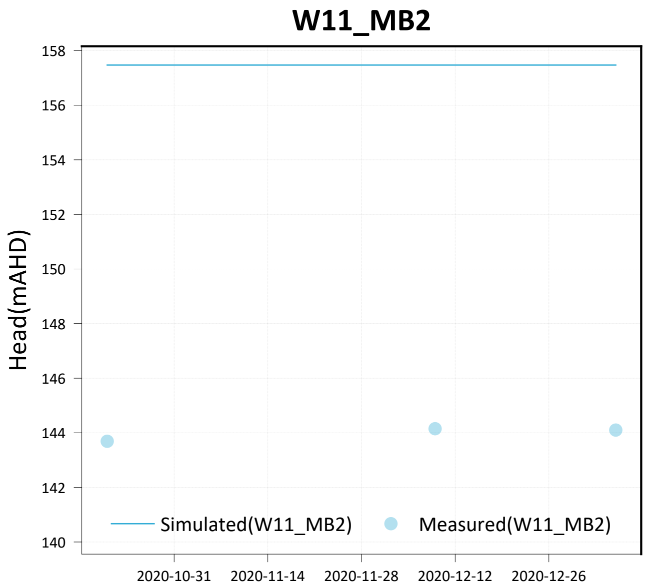
W11_MB2
Head(mAHD)
158
156
154
152
150
148
146
144
142
140
Simulated(W11_MB2)
Measured(W11_MB2)
2020-10-31
2020-11-14
2020-11-28
2020-12-12
2020-12-26

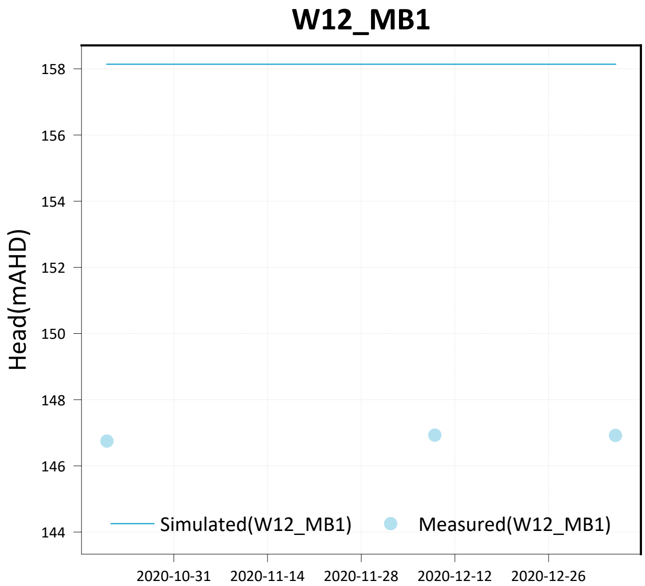
W12_MB1
Head(mAHD)
158
156
154
152
150
148
146
144
Simulated(W12_MB1)
Measured(W12_MB1)
2020-10-31
2020-11-14
2020-11-28
2020-12-12
2020-12-26

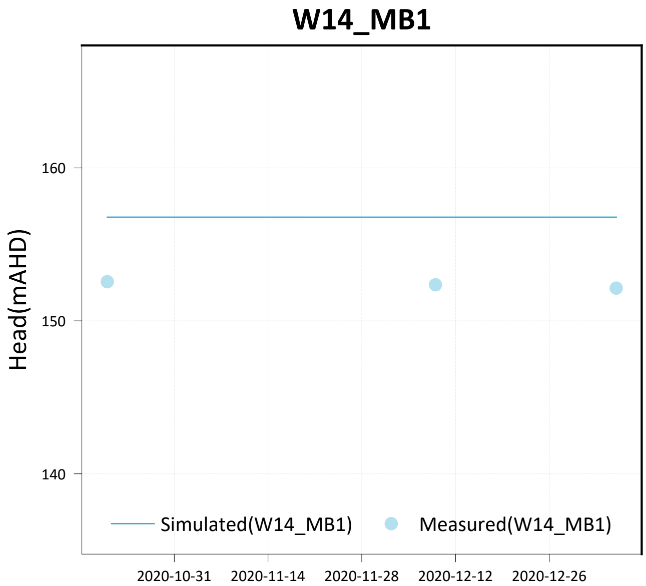
W14_MB1
Head(mAHD)
160
150
140
Simulated(W14_MB1)
Measured(W14_MB1)
2020-10-31
2020-11-14
2020-11-28
2020-12-12
2020-12-26

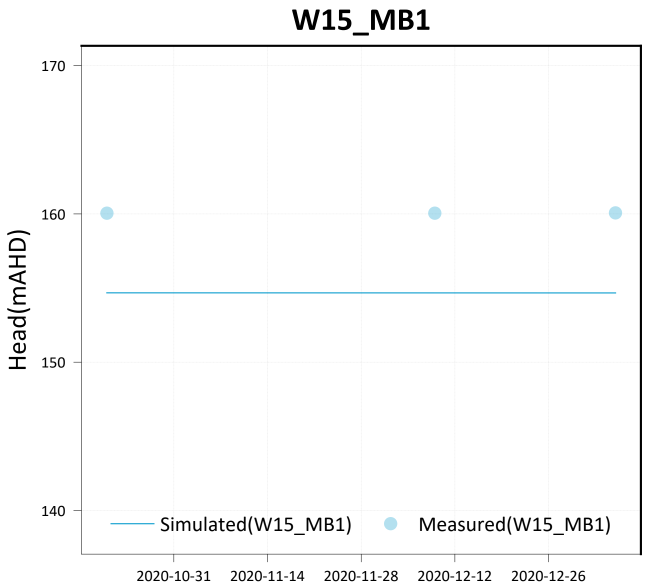
W15_MB1
Head(mAHD)
170
160
150
140
Simulated(W15_MB1)
Measured(W15_MB1)
2020-10-31
2020-11-14
2020-11-28
2020-12-12
2020-12-26

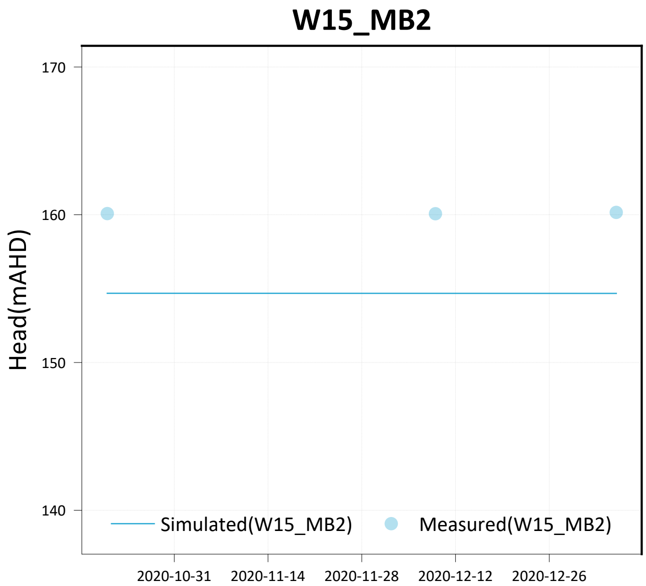
W15_MB2
Head(mAHD)
170
160
150
140
Simulated(W15_MB2)
Measured(W15_MB2)
2020-10-31
2020-11-14
2020-11-28
2020-12-12
2020-12-26

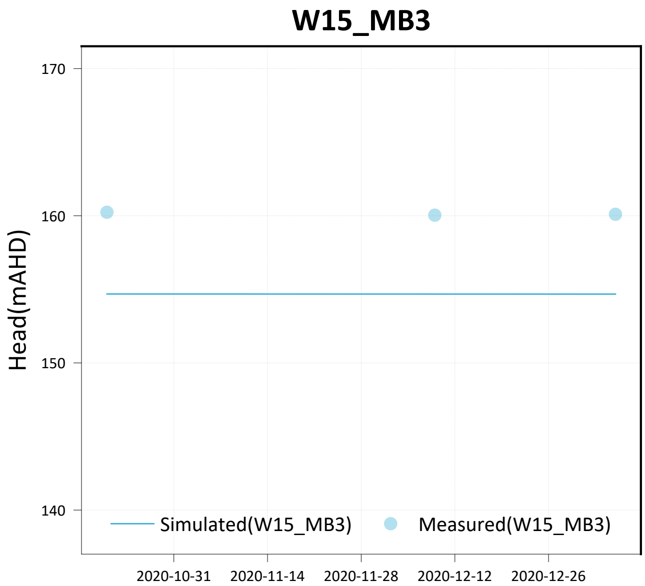
W15_MB3
Head(mAHD)
170
160
150
140
Simulated(W15_MB3)
Measured(W15_MB3)
2020-10-31
2020-11-14
2020-11-28
2020-12-12
2020-12-26

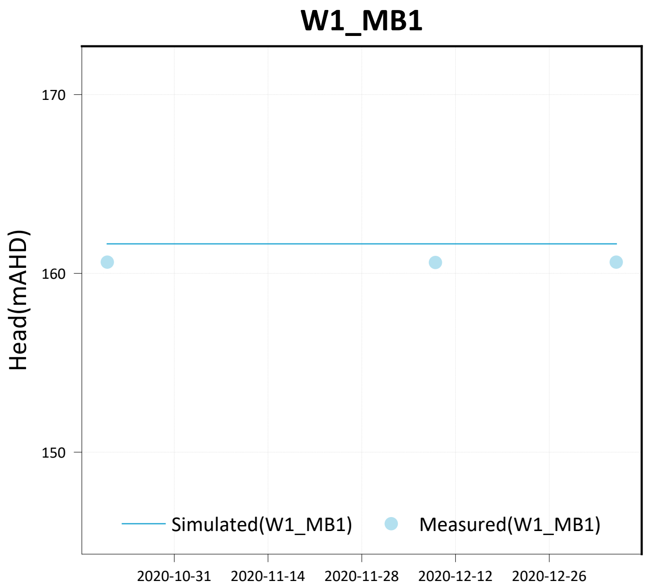
W1_MB1
Head(mAHD)
170
160
150
Simulated(W1_MB1)
Measured(W1_MB1)
2020-10-31
2020-11-14
2020-11-28
2020-12-12
2020-12-26

W1_MB2

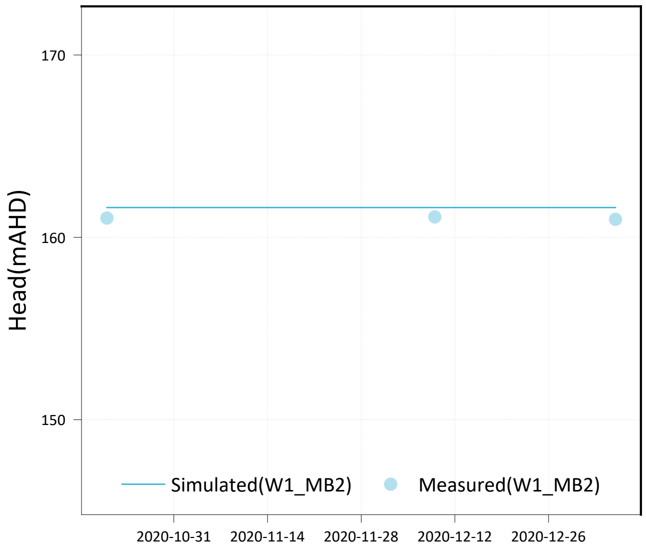

W1_MB3

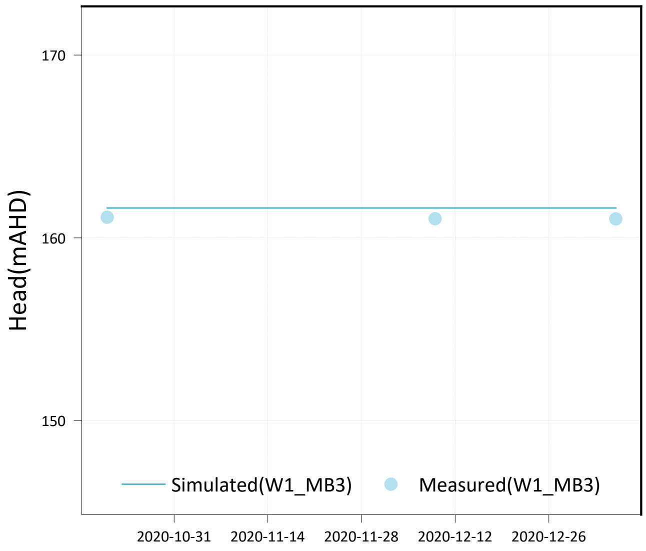

W2_MB1

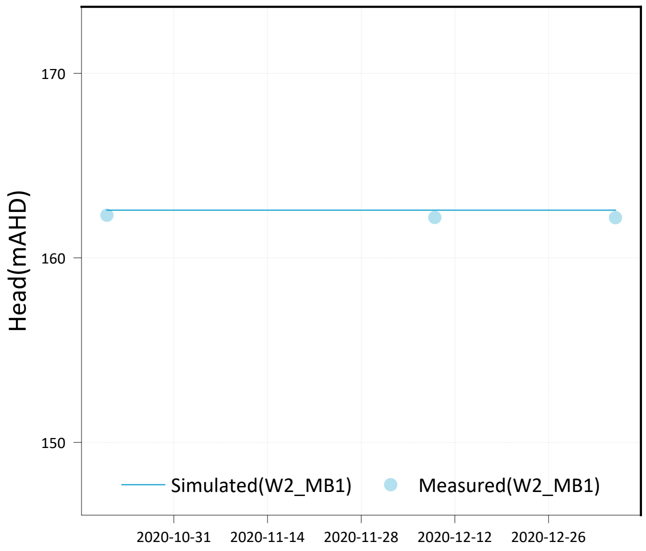

W2_MB2

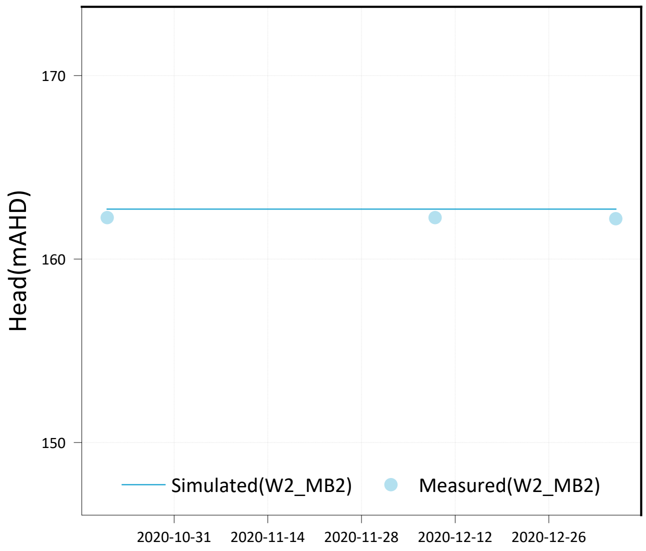

W3_MB1

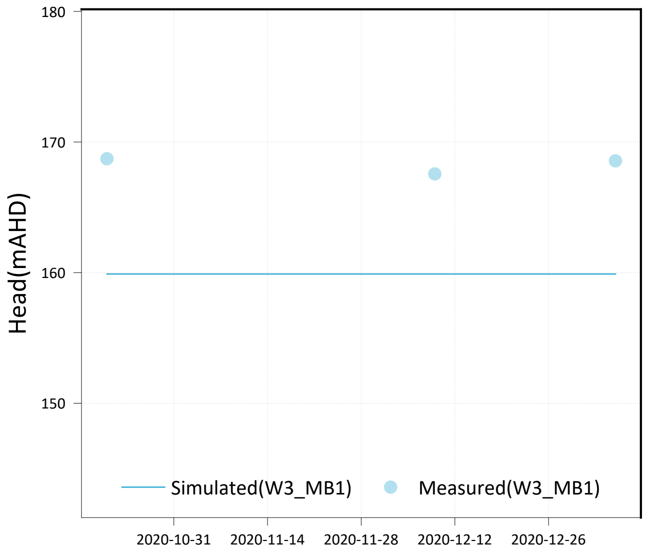

W3_MB2

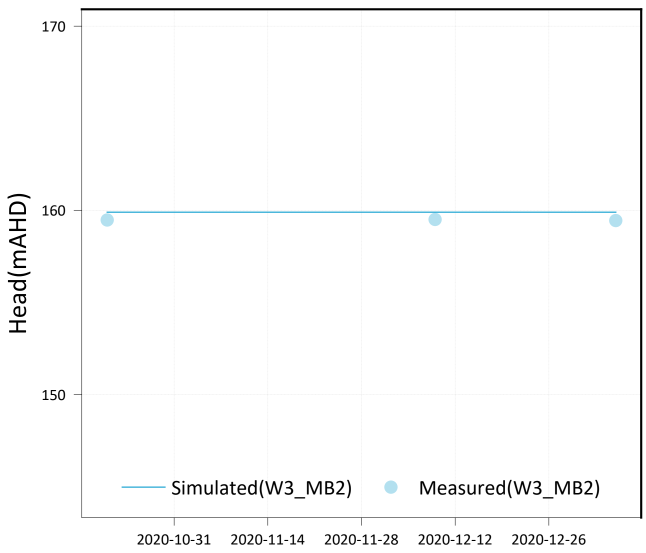

W4_MB1

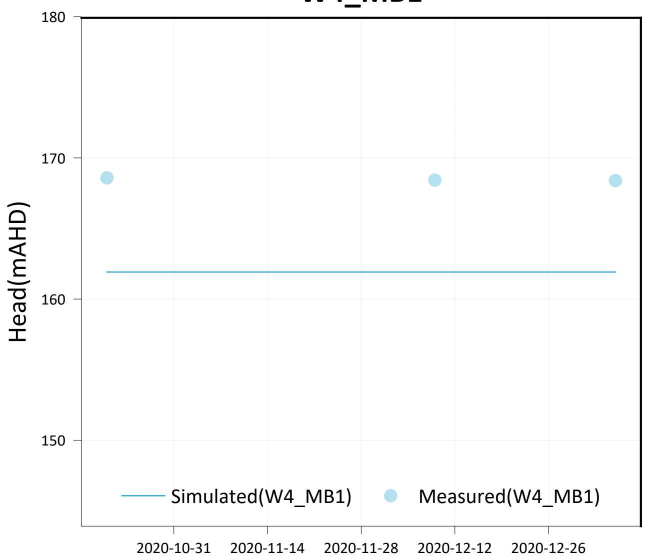

W4_MB2

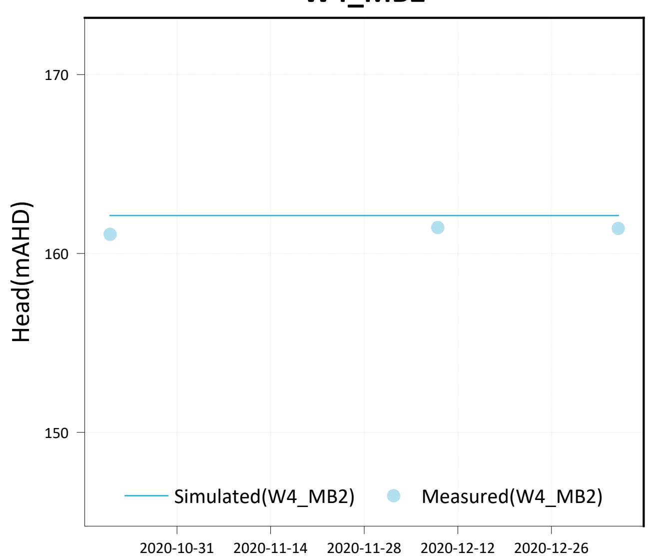

W5_MB1

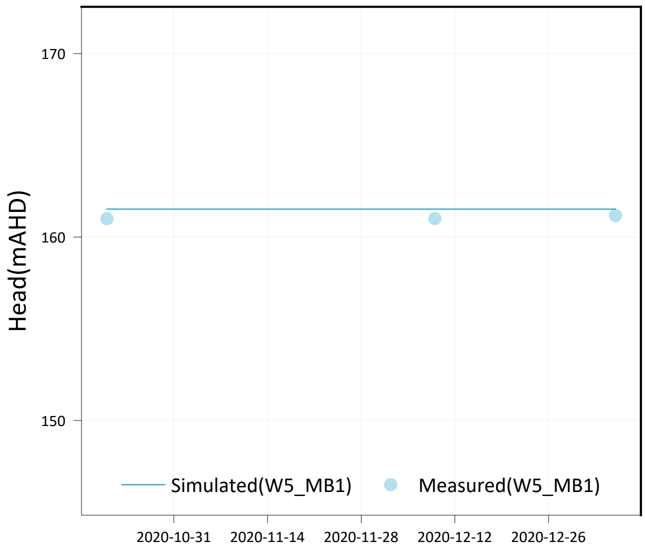

W5_MB2

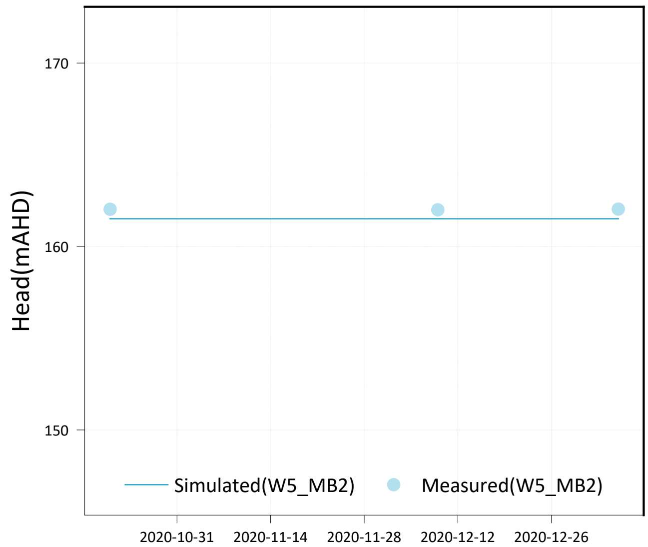

W5_MB3

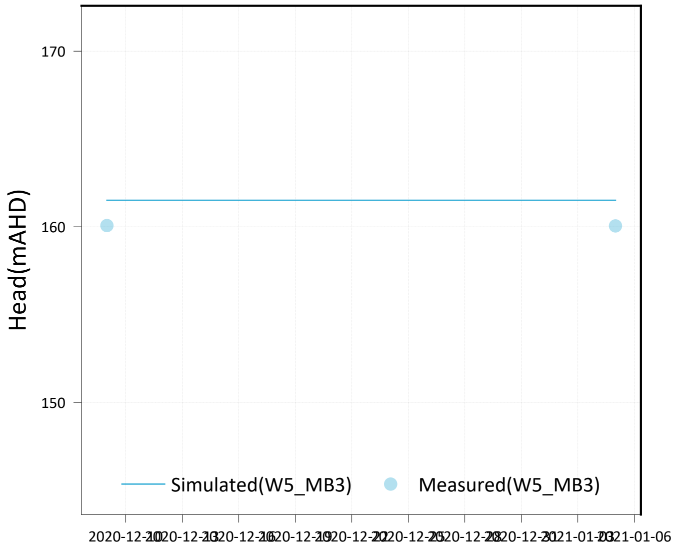

W6_MB1

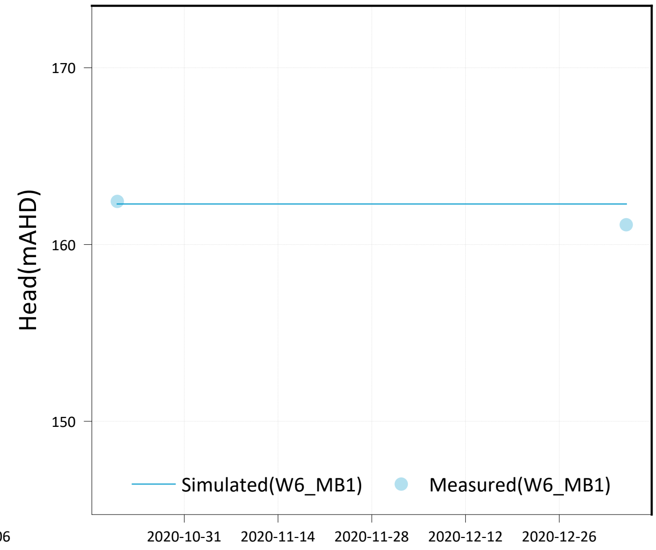

W6_MB2

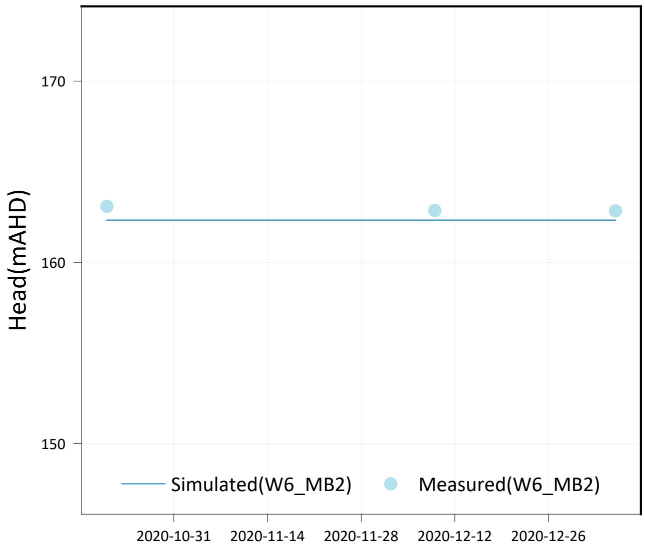

W7_MB1

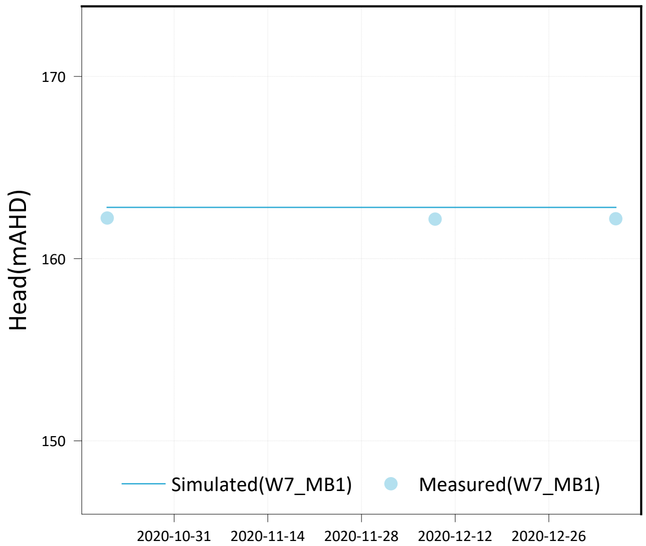

W8_MB1

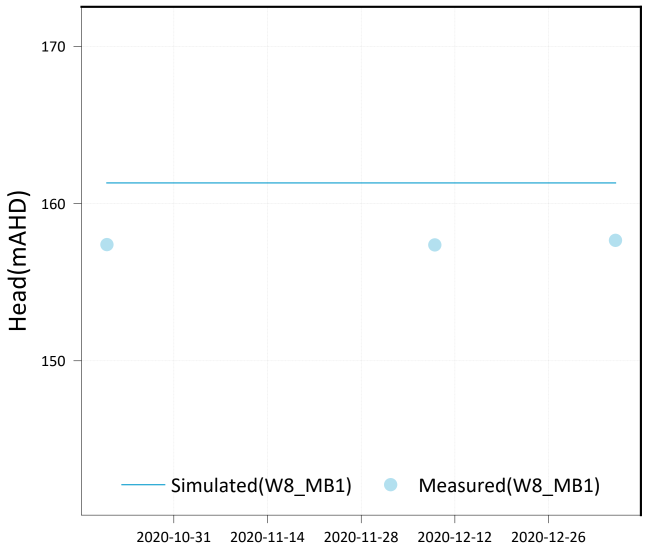

W9_MB1

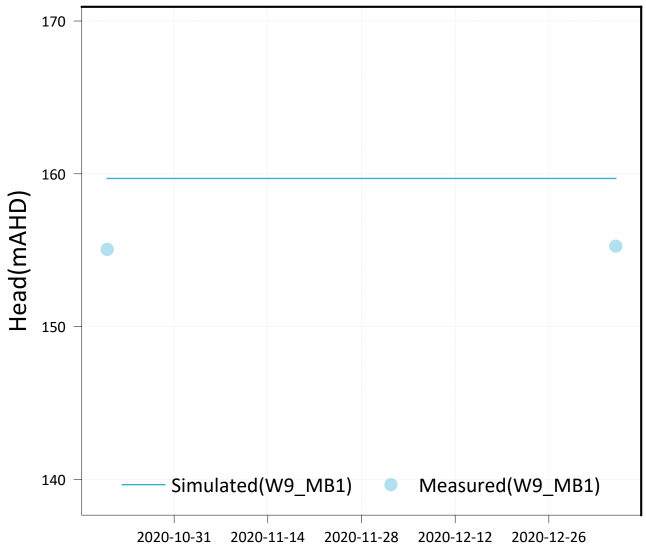

WEST-MB1

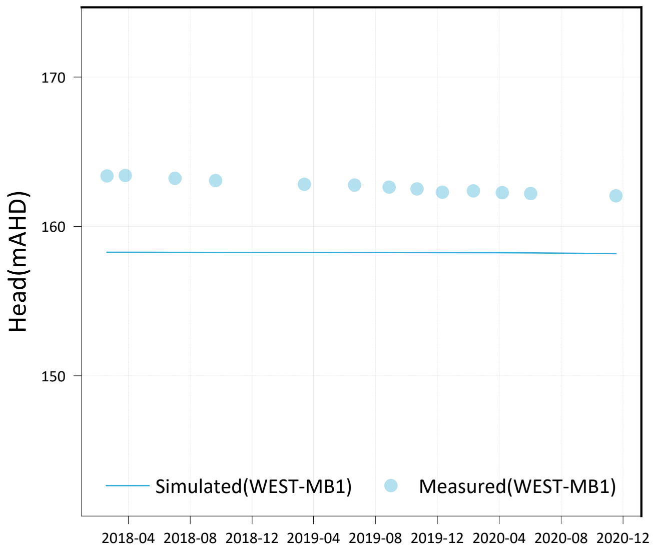

WEST-MB2

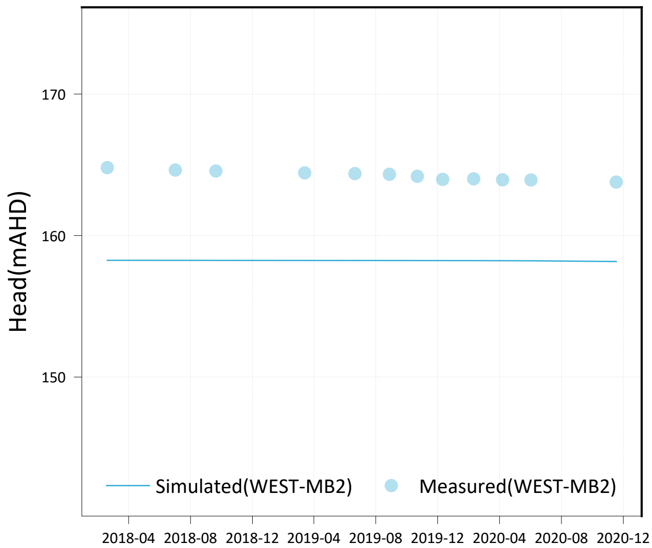

WINNETBORE

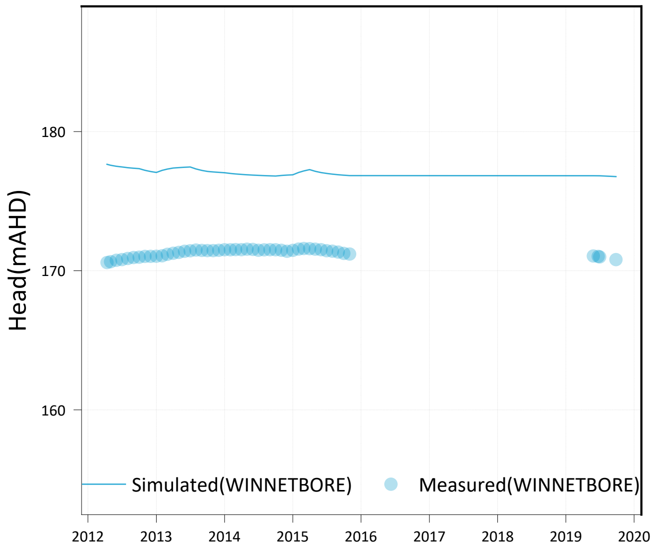

Head(mAHD)
180
170
160
Simulated(WINNETBORE)
Measured(WINNETBORE)
2012
2013
2014
2015
2016
2017
2018
2019
2020

Appendix C:

Hydraulic Parameters and Recharge Zone Distribution

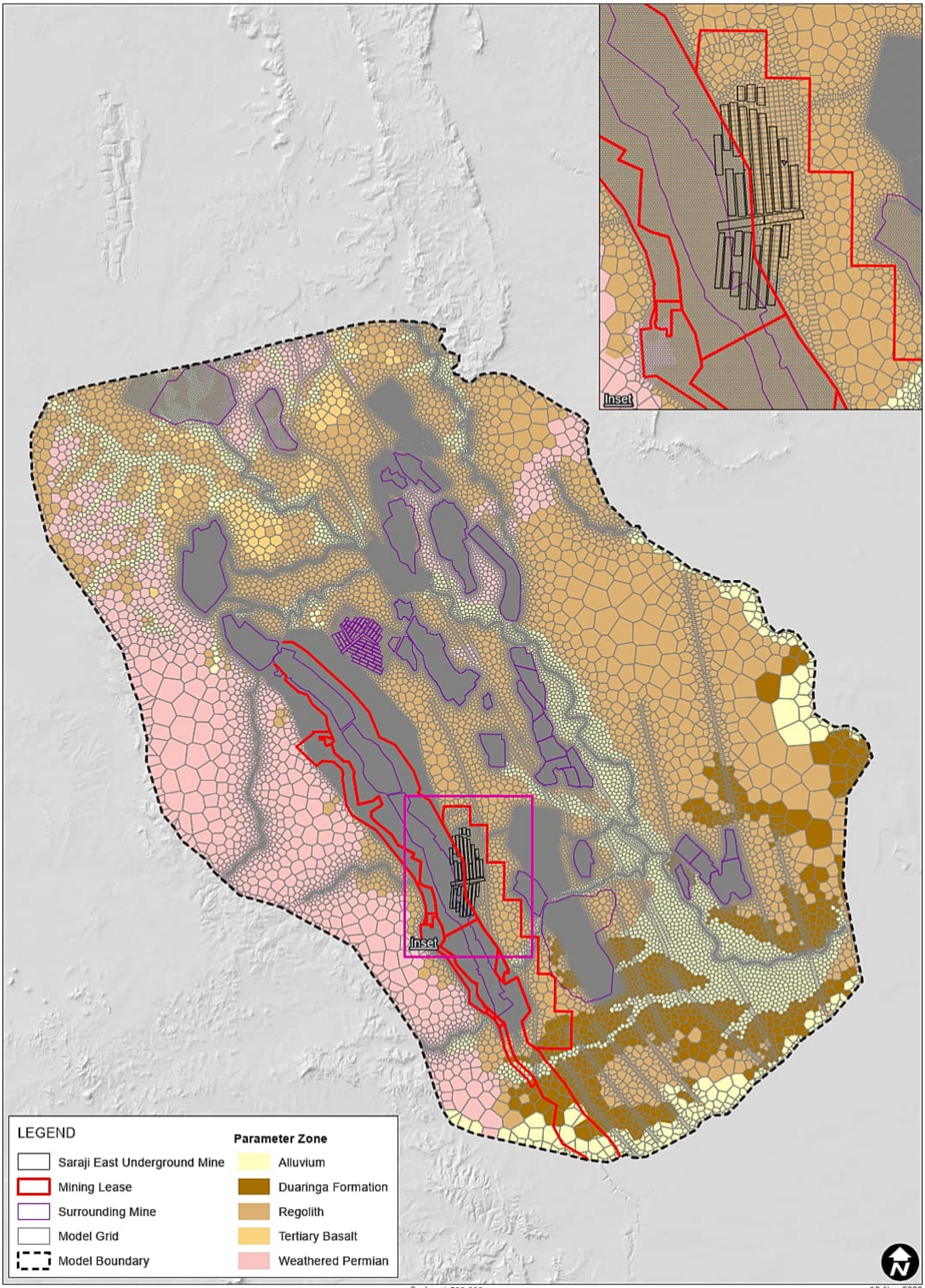

Scale: 1:500,000
GDA 1994 MGA Zone 55

18-Nov-2022
620.31025

Sheet Size : A4

SLR
www.slrconsultingaustralia.com

0 5 10 15 20 km

Hydraulic Parameter Zone Distribution Layer 2

FIGURE C-2

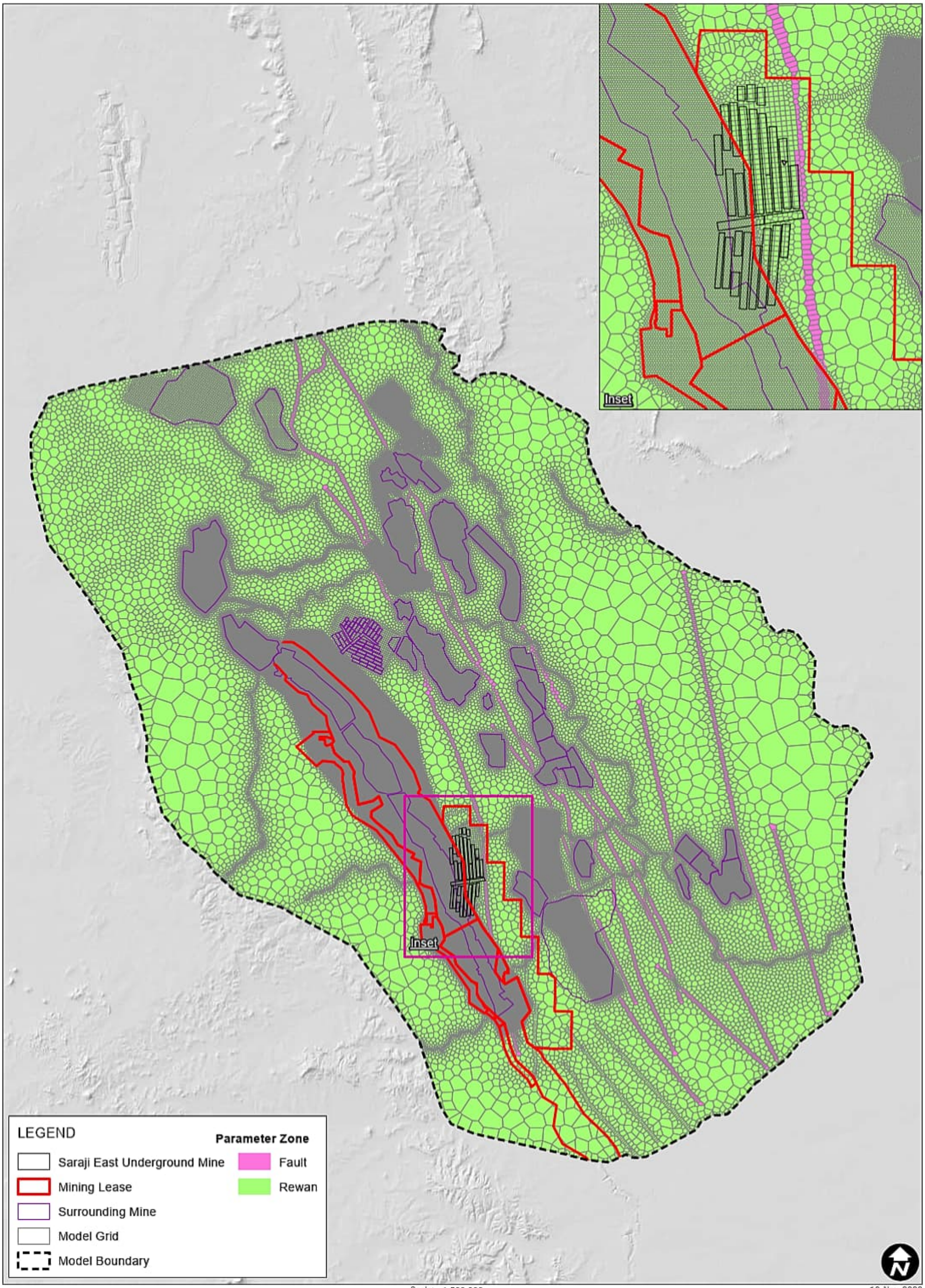

H:\Projects-SLR\620-BNE\620-BNE\620.31025.00000 Saraji East GW Modelling\03 SLR Data\01 CADGIS\GIS\620031025 C-3 Hydraulic Zone L3.mxd

Scale: 1:500,000
GDA 1994 MGA Zone 55

18-Nov-2022
620.31025

Sheet Size : A4

SLR
www.slrconsultingaustralia.com

0 5 10 15 20 km

Hydraulic Parameter Zone Distribution Layer 3

FIGURE C-3

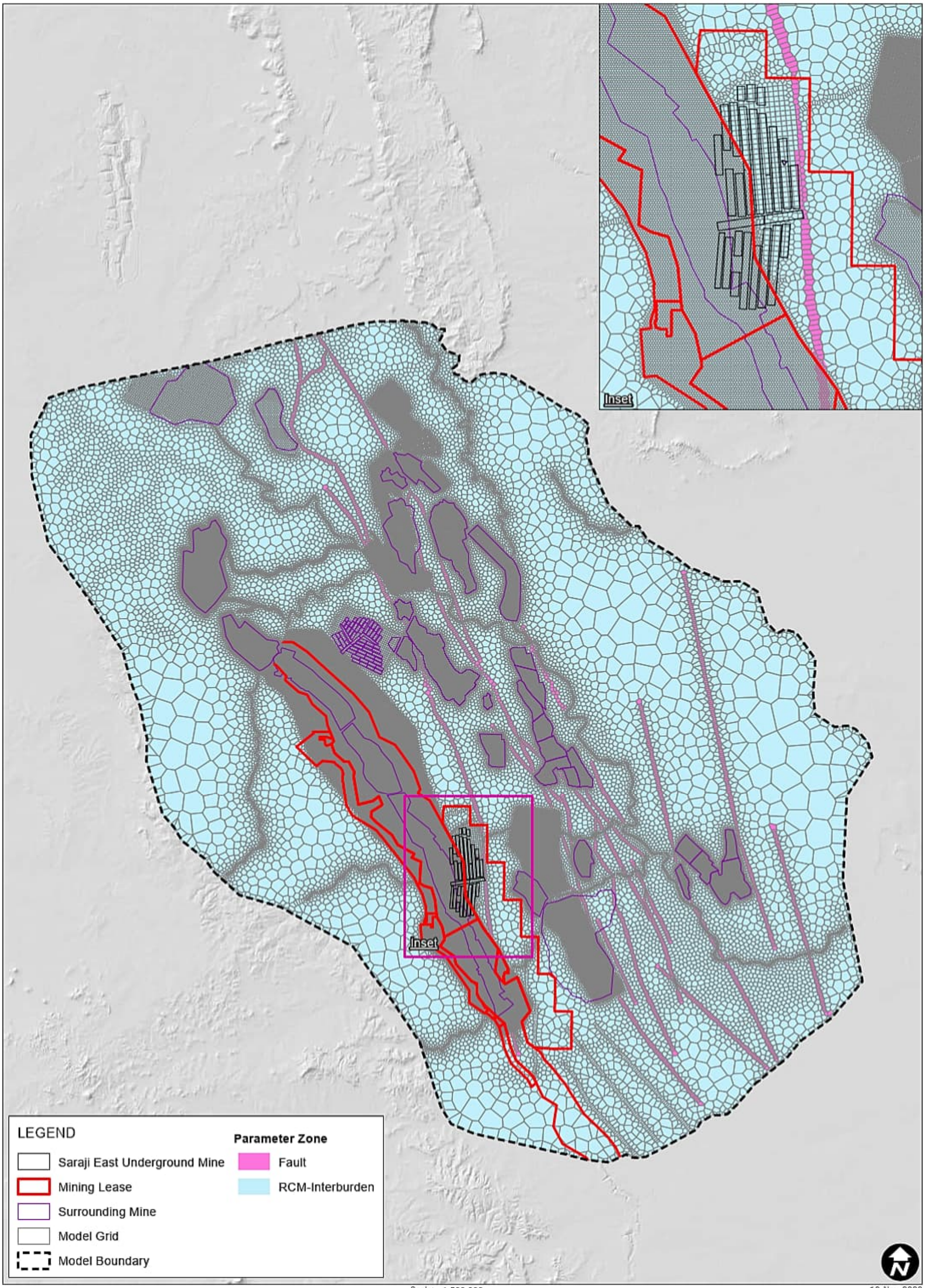

H:\Projects-SLR\620-BNE\620-BNE\620.31025.00000 Saraji East GW Modelling\03 SLR Data\01 CADGIS\GIS\6203102S C-4 Hydraulic Zone L4.mxd

Scale: 1:500,000
GDA 1994 MGA Zone 55

18-Nov-2022
620.31025

Sheet Size : A4

0 5 10 15 20 km

SLR
www.slrconsultingaustralia.com

Hydraulic Parameter Zone Distribution Layer 4

FIGURE C-4

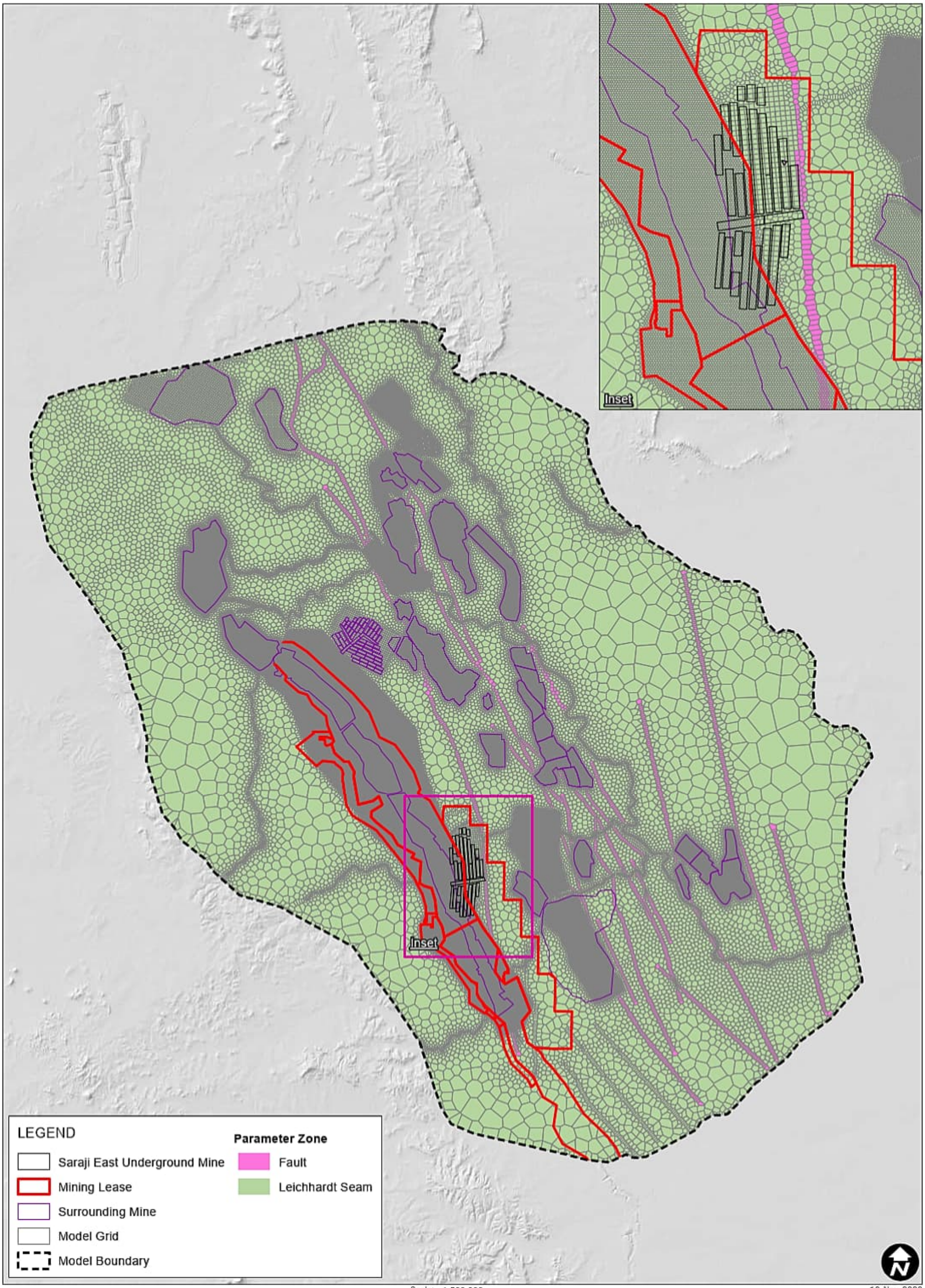

H:\Projects-SLR\620-BNE\620-BNE\620.31025.00000 Saraji East GW Modelling\03 SLR Data\01 CADGIS\GIS\62031025 C-5 Hydraulic Zone L5.mxd

Scale: 1:500,000
GDA 1994 MGA Zone 55

18-Nov-2022
620.31025

Sheet Size : A4

0 5 10 15 20 km

SLR
www.slrconsultingaustralia.com

Hydraulic Parameter Zone Distribution Layer 5

FIGURE C-5

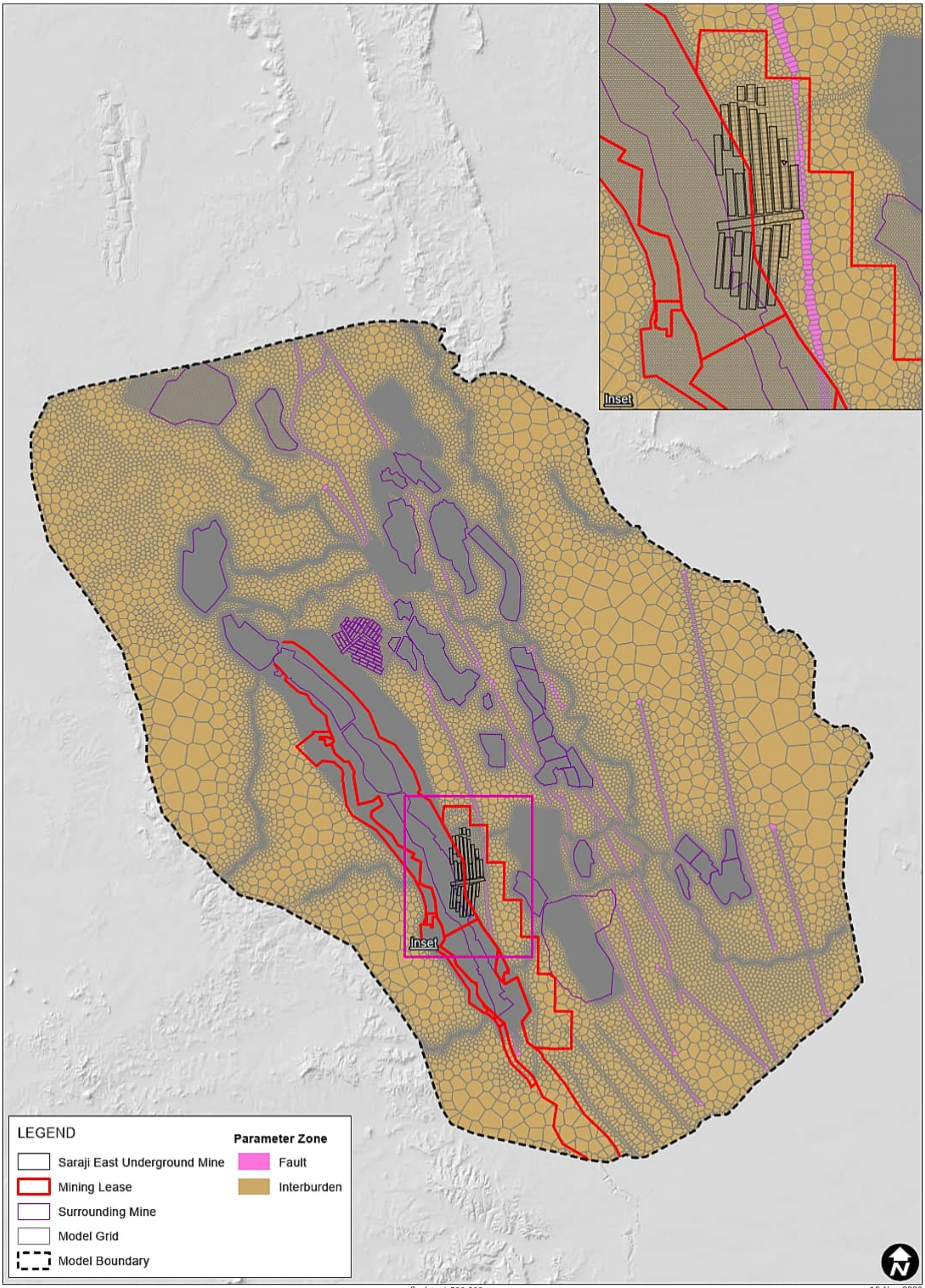

Sheet Size : A4

SLR
www.slrconsultingaustralia.com

0 5 10 15 20 km

Hydraulic Parameter Zone Distribution Layer 6

FIGURE C-6

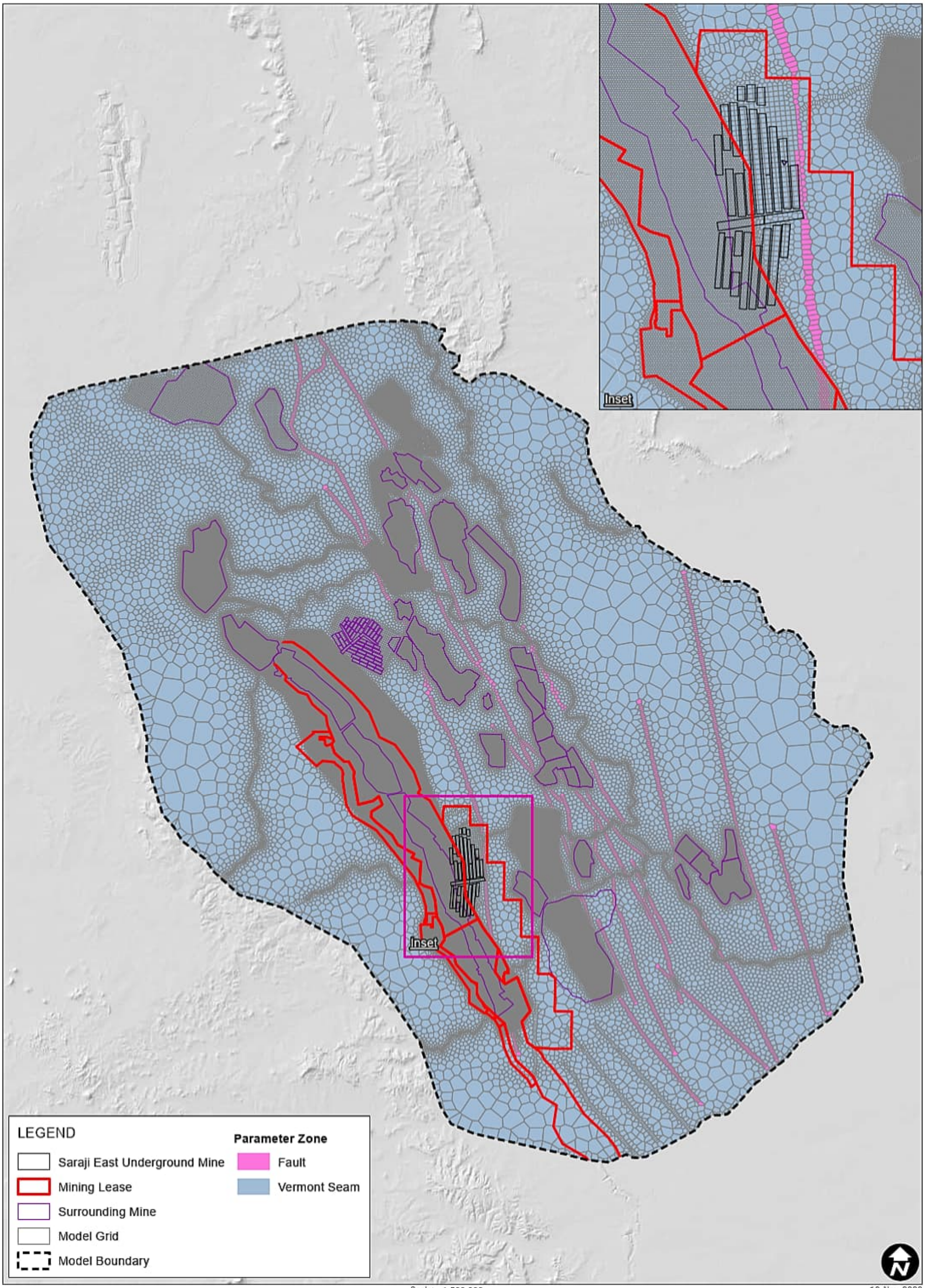

Scale: 1:500,000
GDA 1994 MGA Zone 55

18-Nov-2022
620.31025

Sheet Size : A4

SLR
www.slrconsultingaustralia.com

0 5 10 15 20 km

Hydraulic Parameter Zone Distribution Layer 7

FIGURE C-7

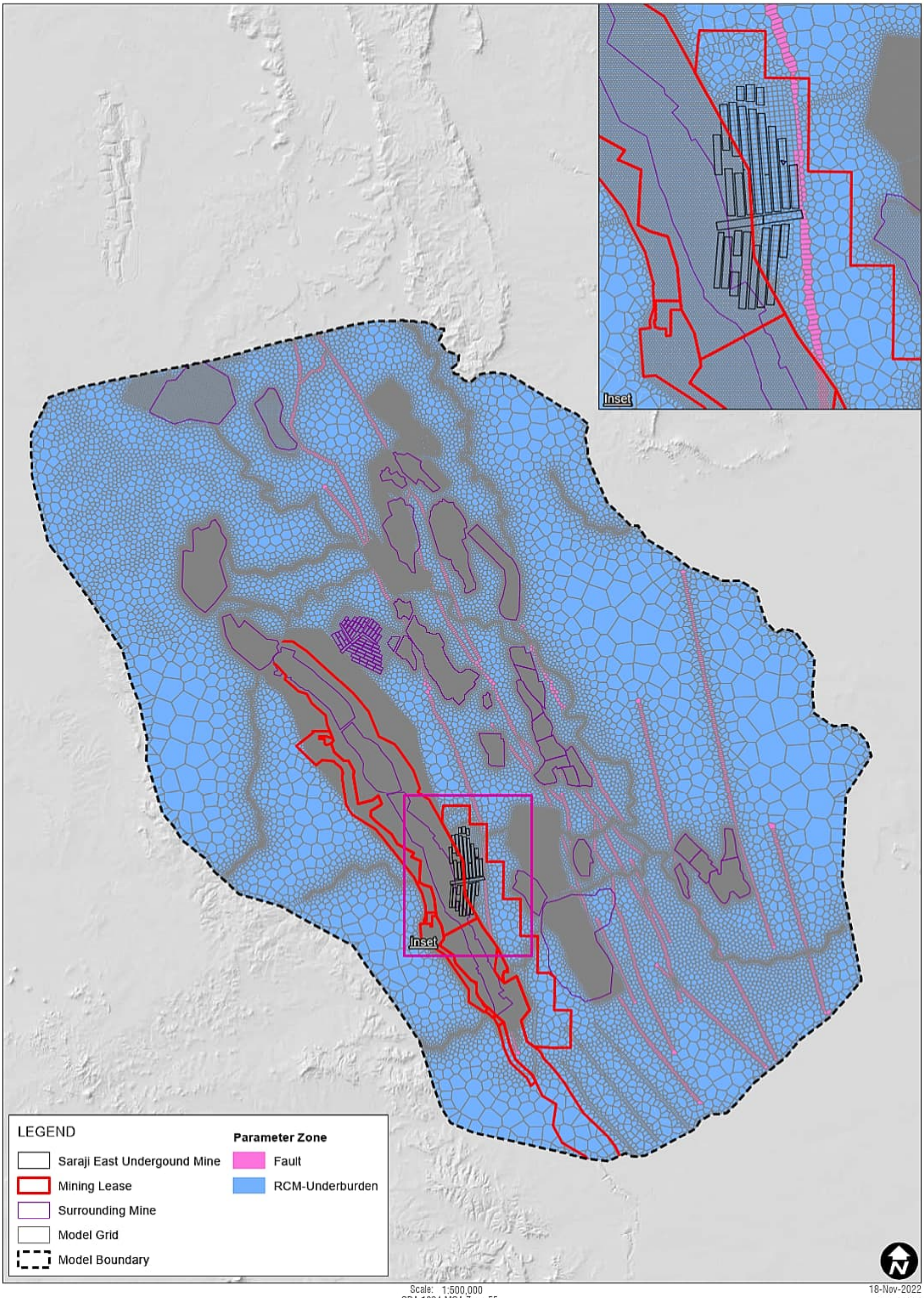

Scale: 1:500,000
GDA 1994 MGA Zone 55

18-Nov-2022
620.31025

Sheet Size : A4

0 5 10 15 20 km

SLR
www.slrconsultingaustralia.com

Hydraulic Parameter Zone Distribution Layer 8

FIGURE C-8

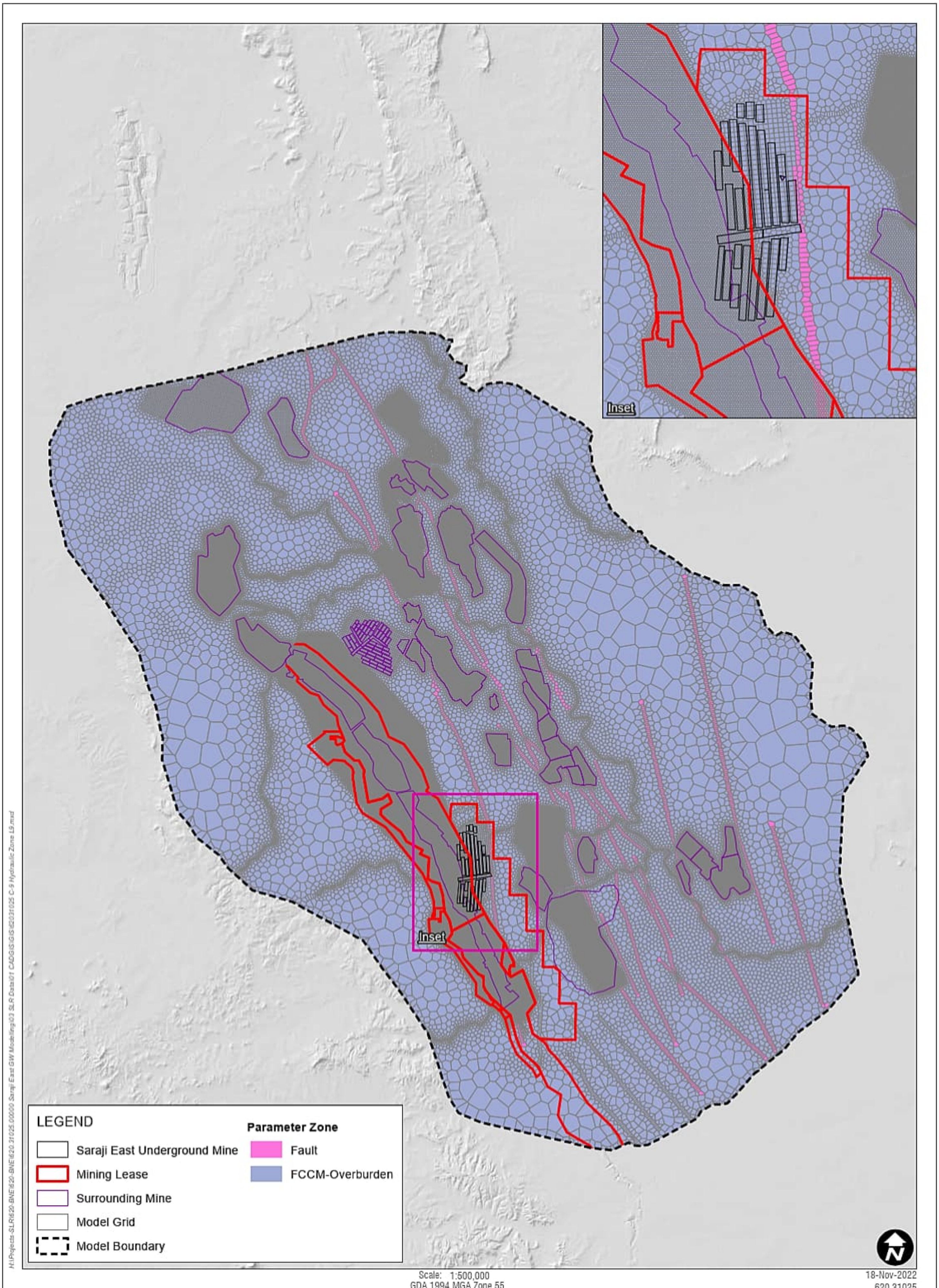

Sheet Size : A4

SLR
www.slrconsultingaustralia.com

Hydraulic Parameter Zone Distribution Layer 9

FIGURE C-9

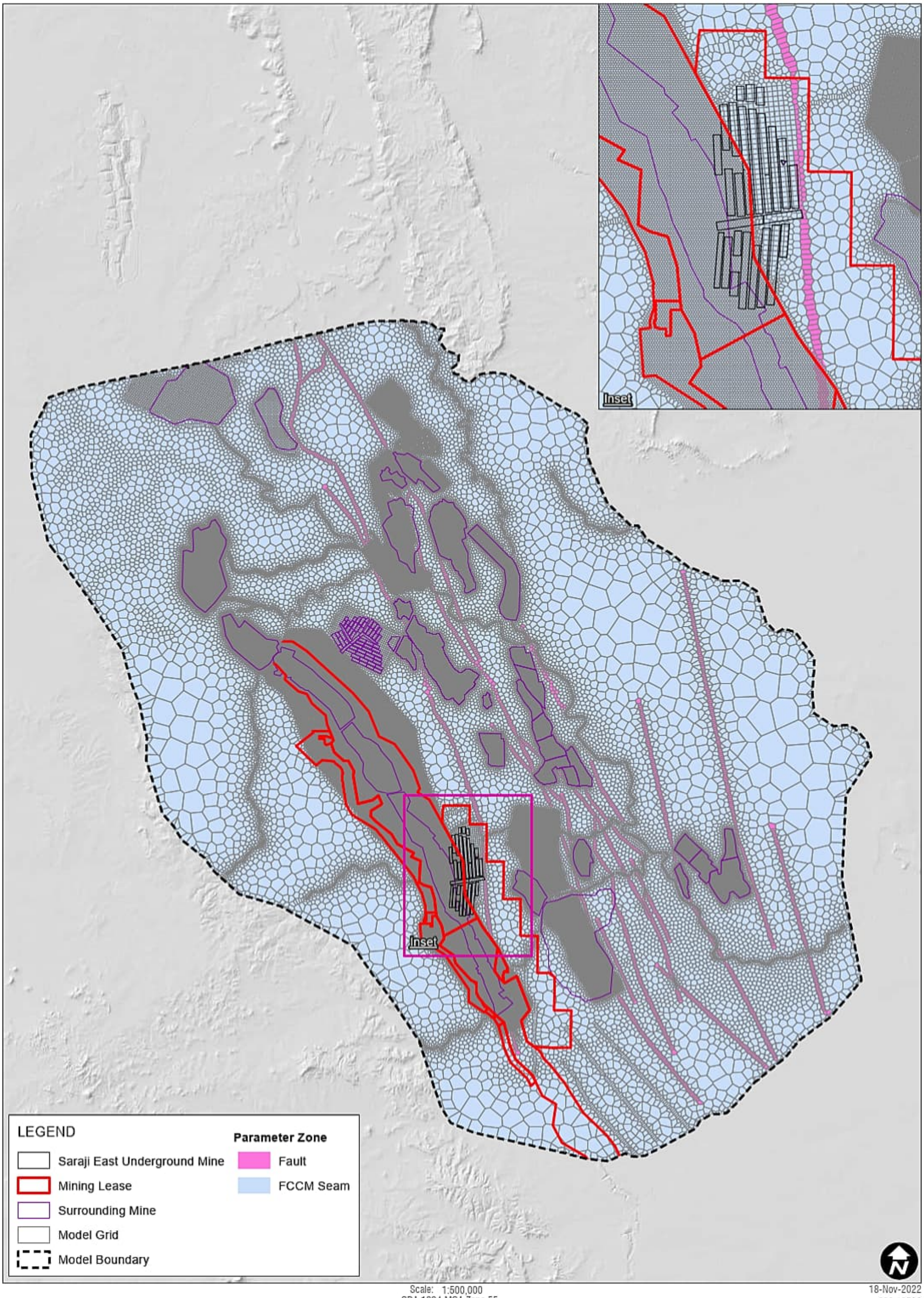

Scale: 1:500,000
GDA 1994 MGA Zone 55

18-Nov-2022
620.13593

Sheet Size : A4

SLR
www.slrconsultingaustralia.com

0 5 10 15 20 km

Hydraulic Parameter Zone Distribution Layer 10

FIGURE C-10

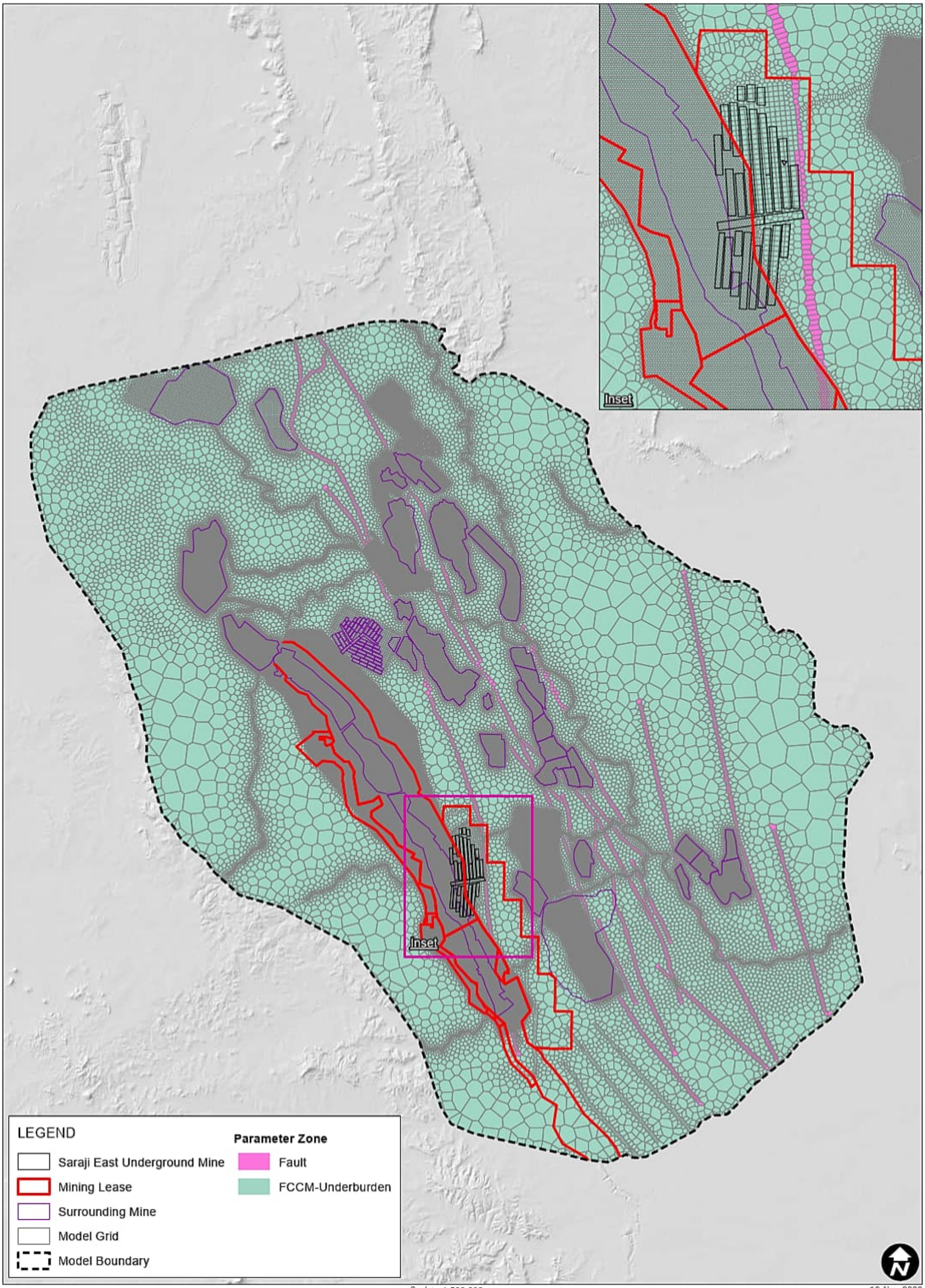

Scale: 1:500,000
GDA 1994 MGA Zone 55

18-Nov-2022
620.31025

Sheet Size : A4

SLR
www.slrconsultingaustralia.com

0 5 10 15 20 km

Hydraulic Parameter Zone Distribution Layer 11

FIGURE C-11

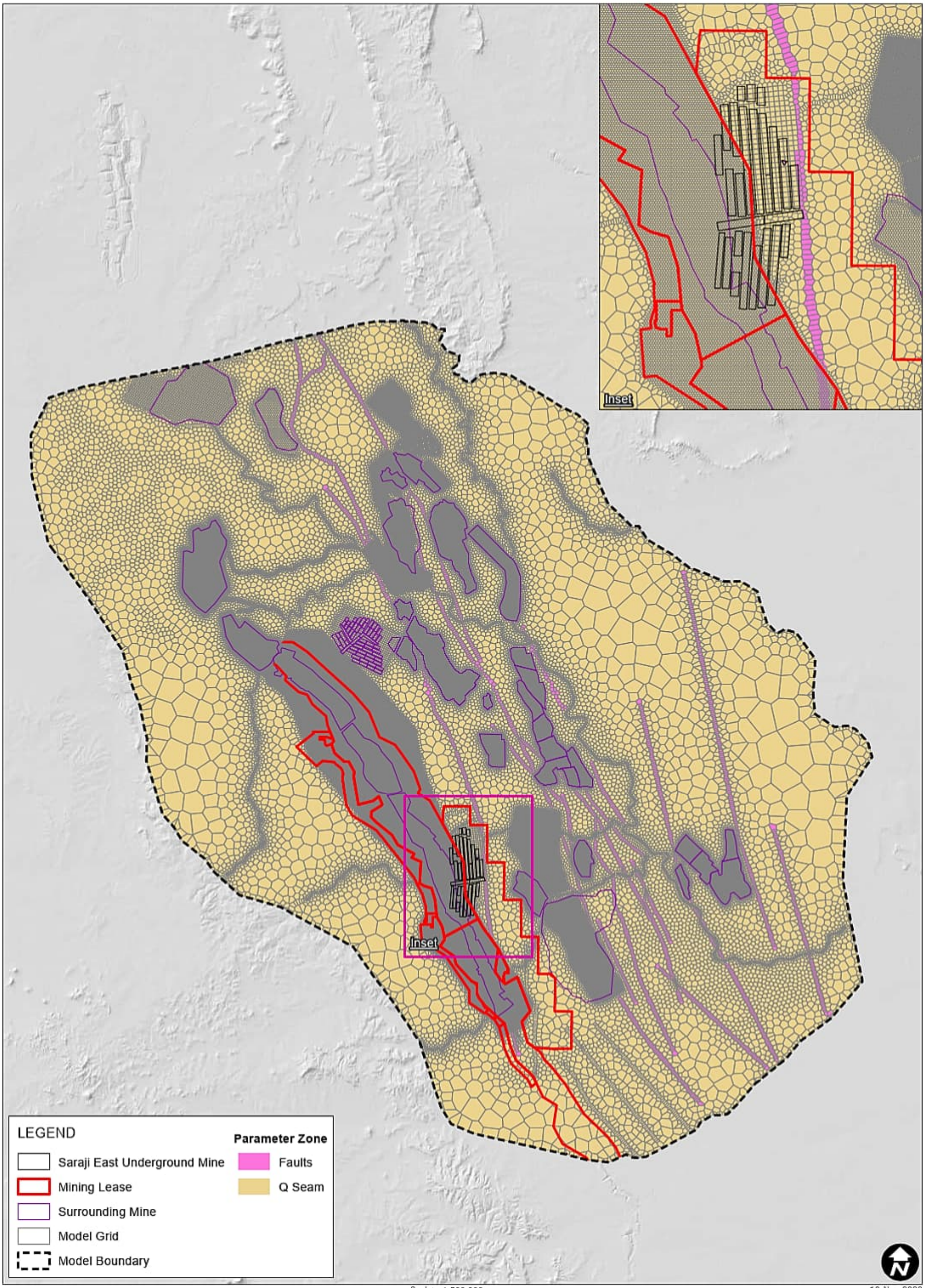

Scale: 1:500,000
GDA 1994 MGA Zone 55

18-Nov-2022
620.31025

Sheet Size : A4

0 5 10 15 20 km

SLR
www.slrconsultingaustralia.com

Hydraulic Parameter Zone Distribution Layer 12

FIGURE C-12

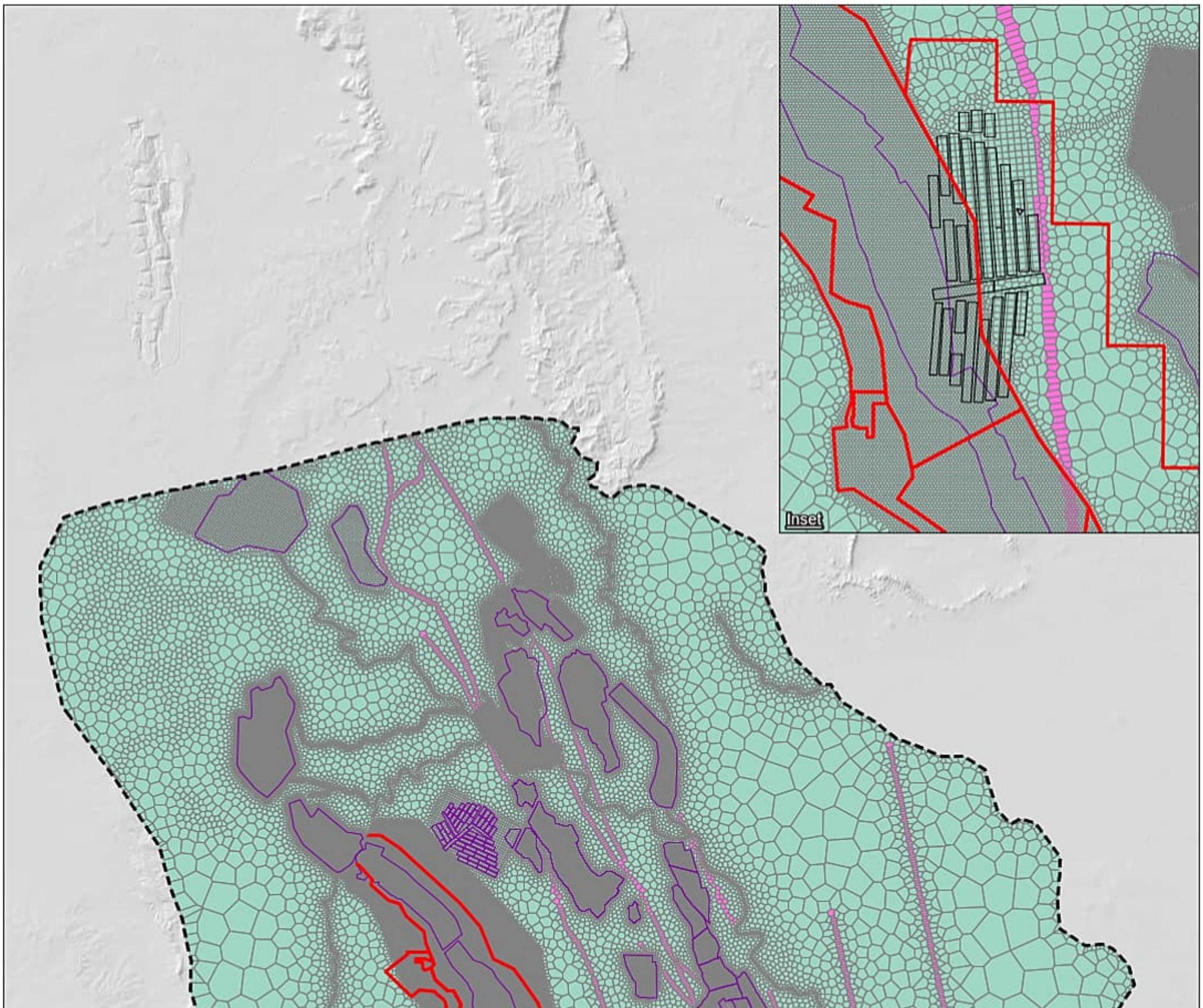

Scale: 1:500,000
GDA 1994 MGA Zone 55

18-Nov-2022
620.31025

Sheet Size : A4

SLR
www.slrconsultingaustralia.com

Hydraulic Parameter Zone Distribution Layer 13

FIGURE C-13

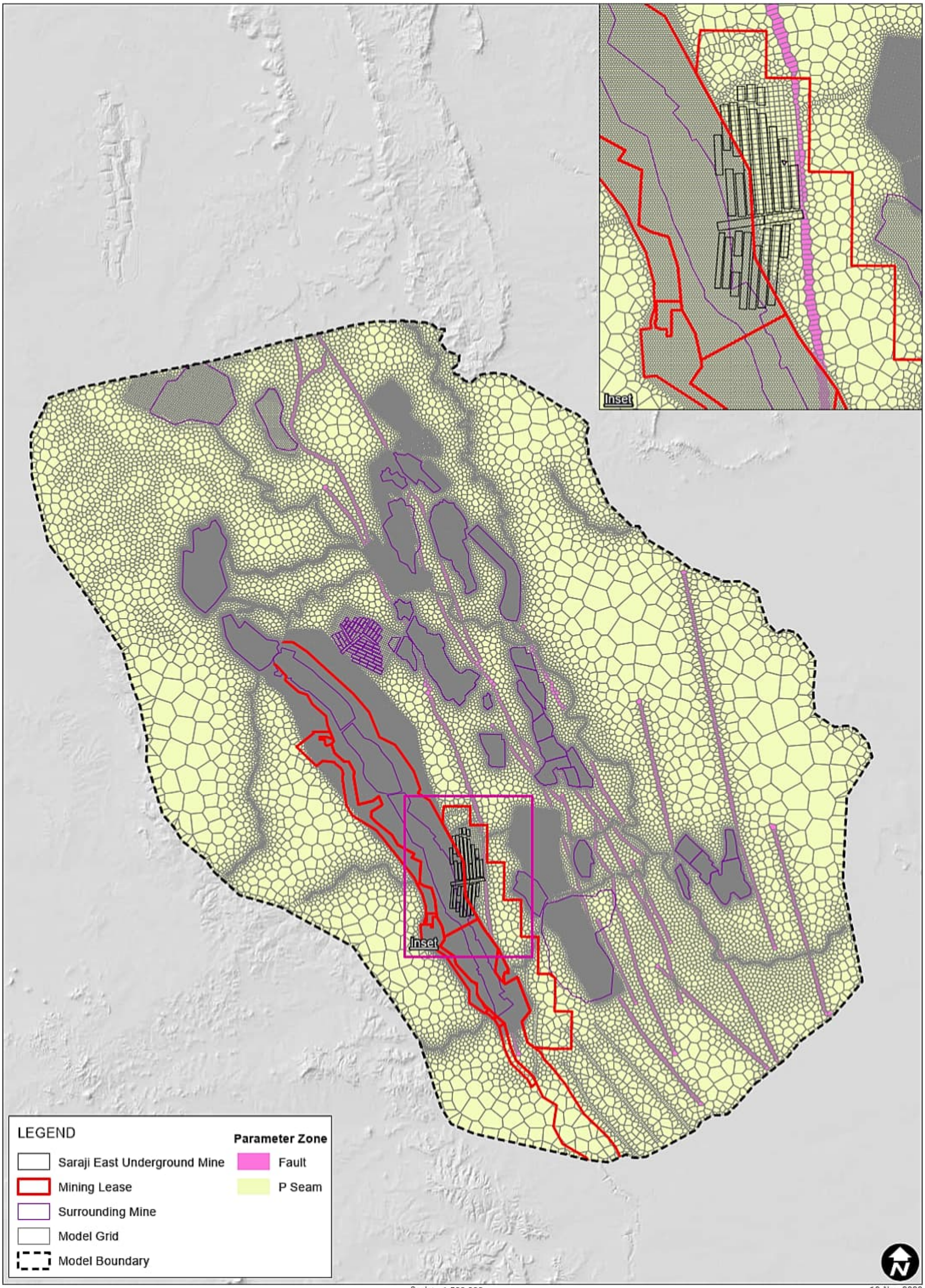

Scale: 1:500,000
GDA 1994 MGA Zone 55

18-Nov-2022
620.31025

Sheet Size : A4

SLR
www.slrconsultingaustralia.com

0 5 10 15 20 km

Hydraulic Parameter Zone Distribution Layer 14

FIGURE C-14

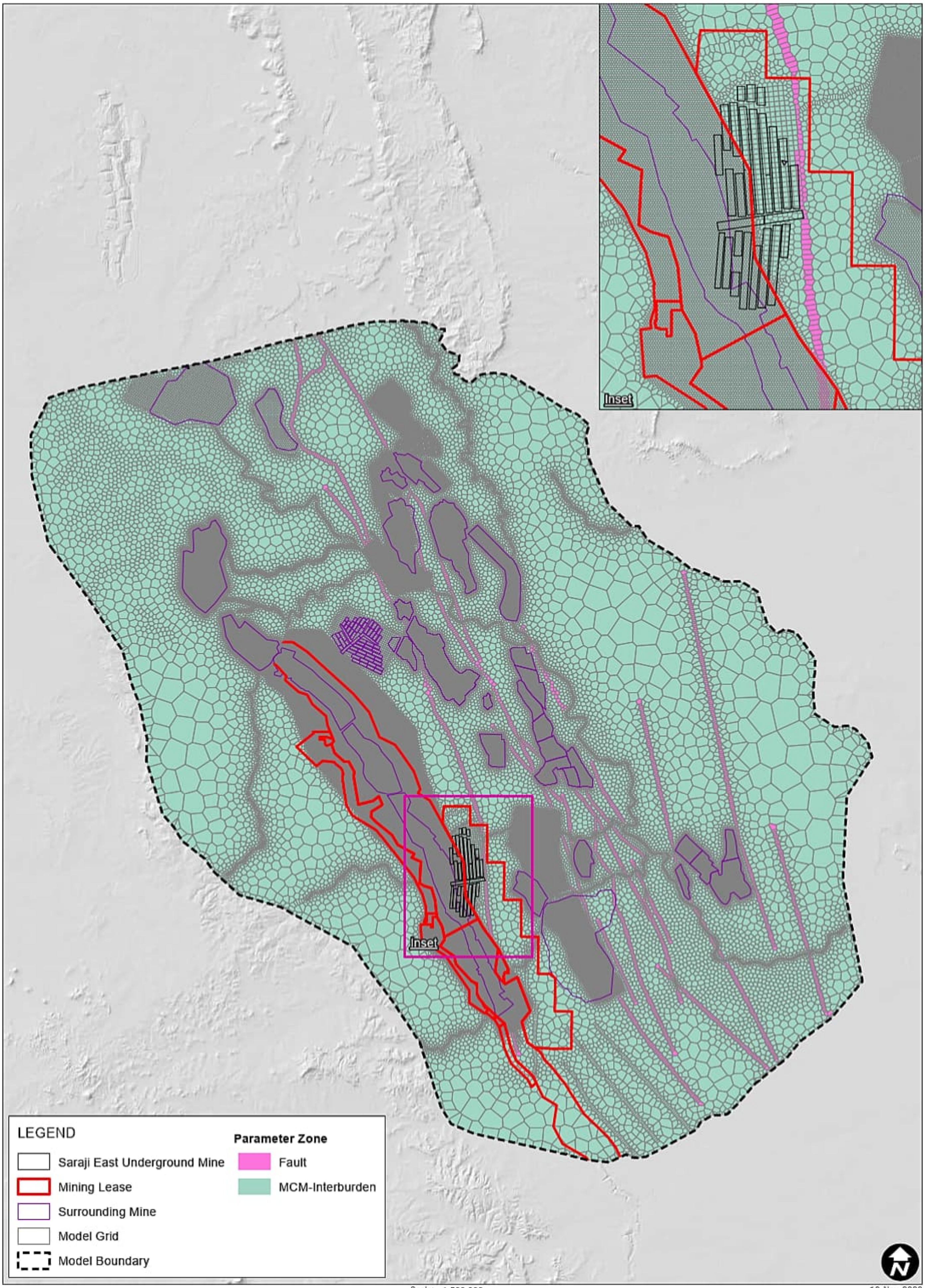

Scale: 1:500,000
GDA 1994 MGA Zone 55

18-Nov-2022
620.31025

Sheet Size : A4

0 5 10 15 20 km

www.slrconsultingaustralia.com

Hydraulic Parameter Zone Distribution Layer 15

FIGURE C-15

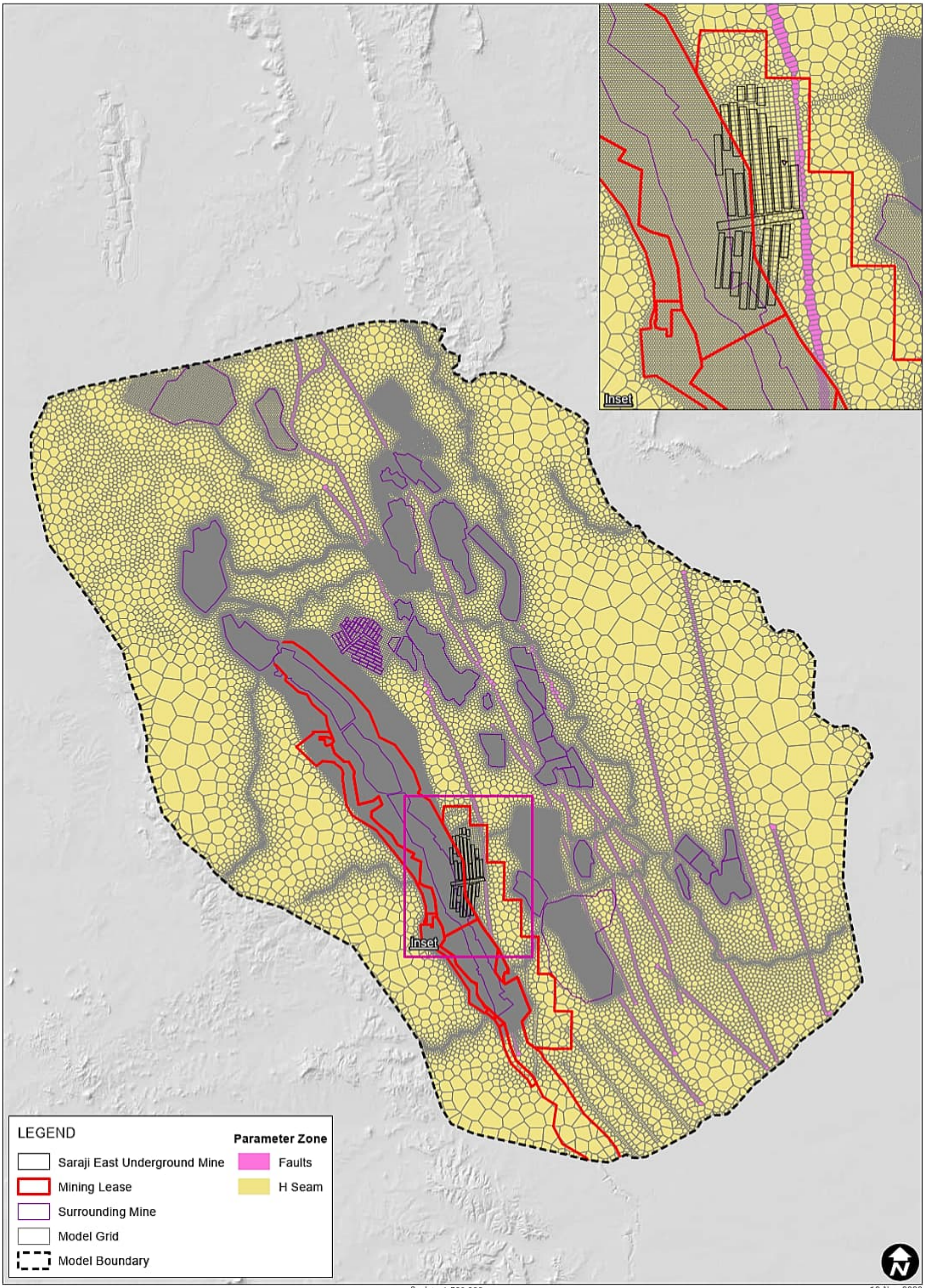

Sheet Size : A4

SLR
www.slrconsultingaustralia.com

Hydraulic Parameter Zone Distribution Layer 16

FIGURE C-16

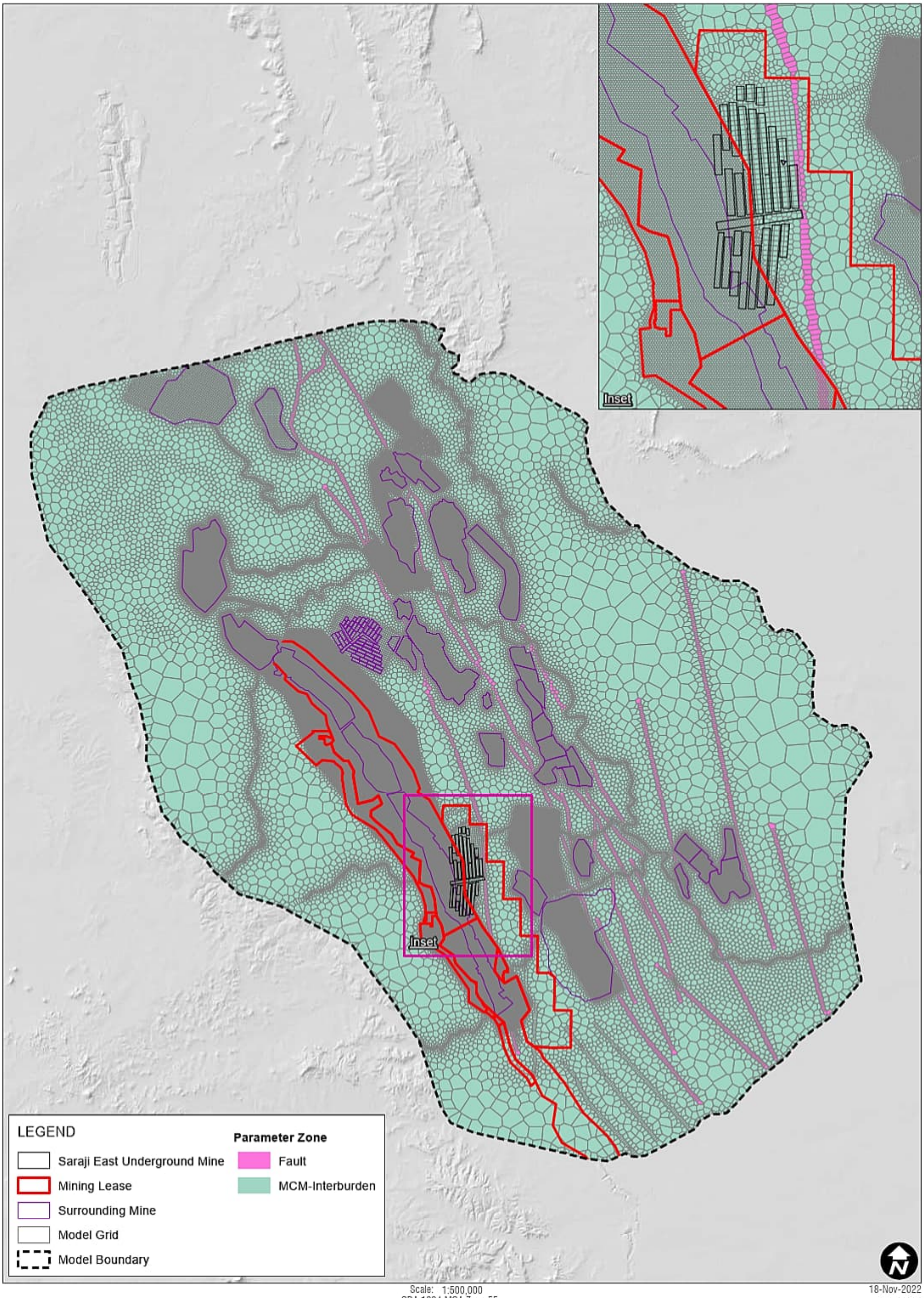

www.slrconsultingaustralia.com

Hydraulic Parameter Zone Distribution Layer 17

FIGURE C-17

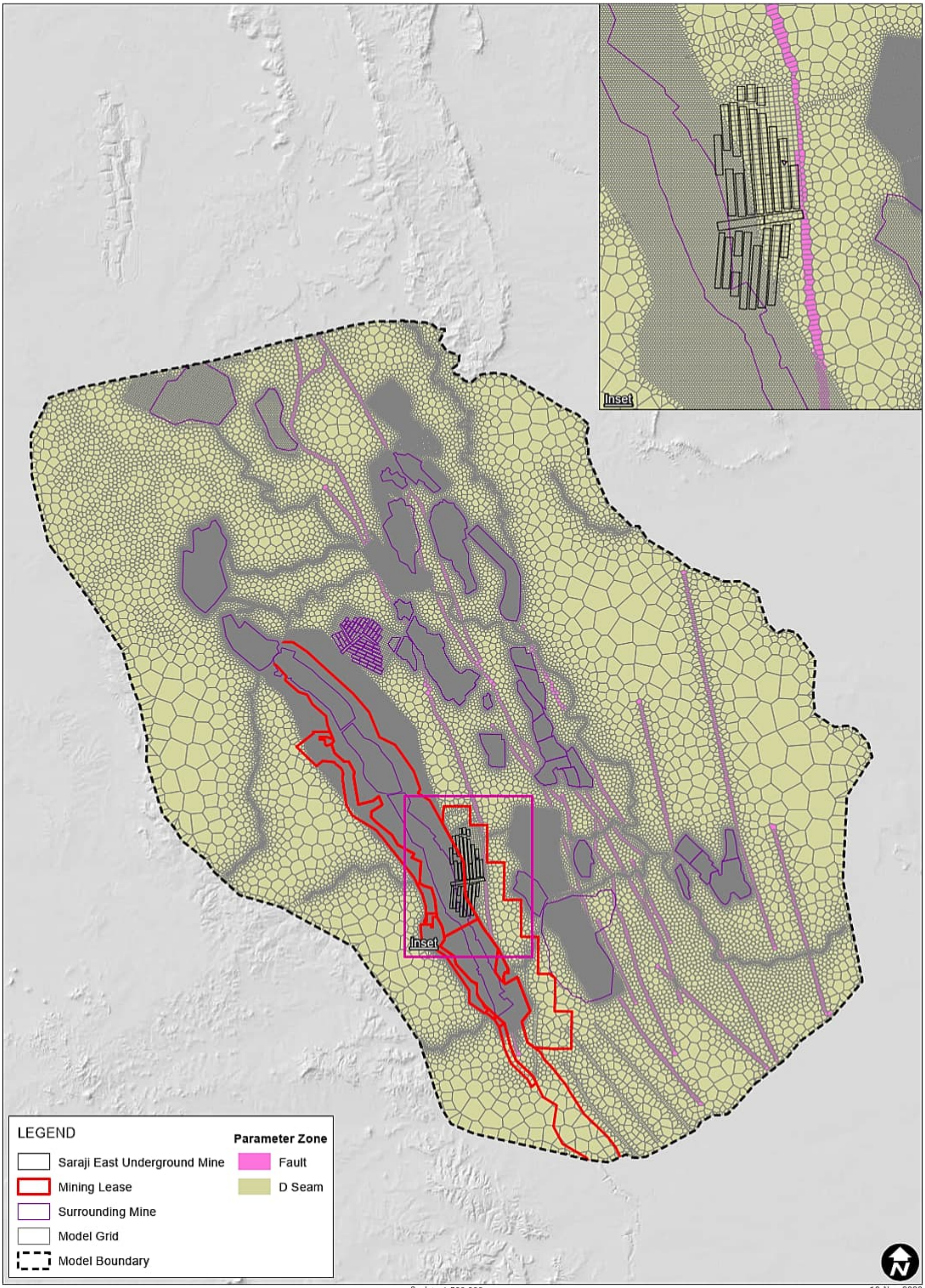

Scale: 1:500,000
GDA 1994 MGA Zone 55

18-Nov-2022
620.31025

Sheet Size : A4

SLR
www.slrconsultingaustralia.com

0 5 10 15 20 km

Hydraulic Parameter Zone Distribution Layer 18

FIGURE C-18

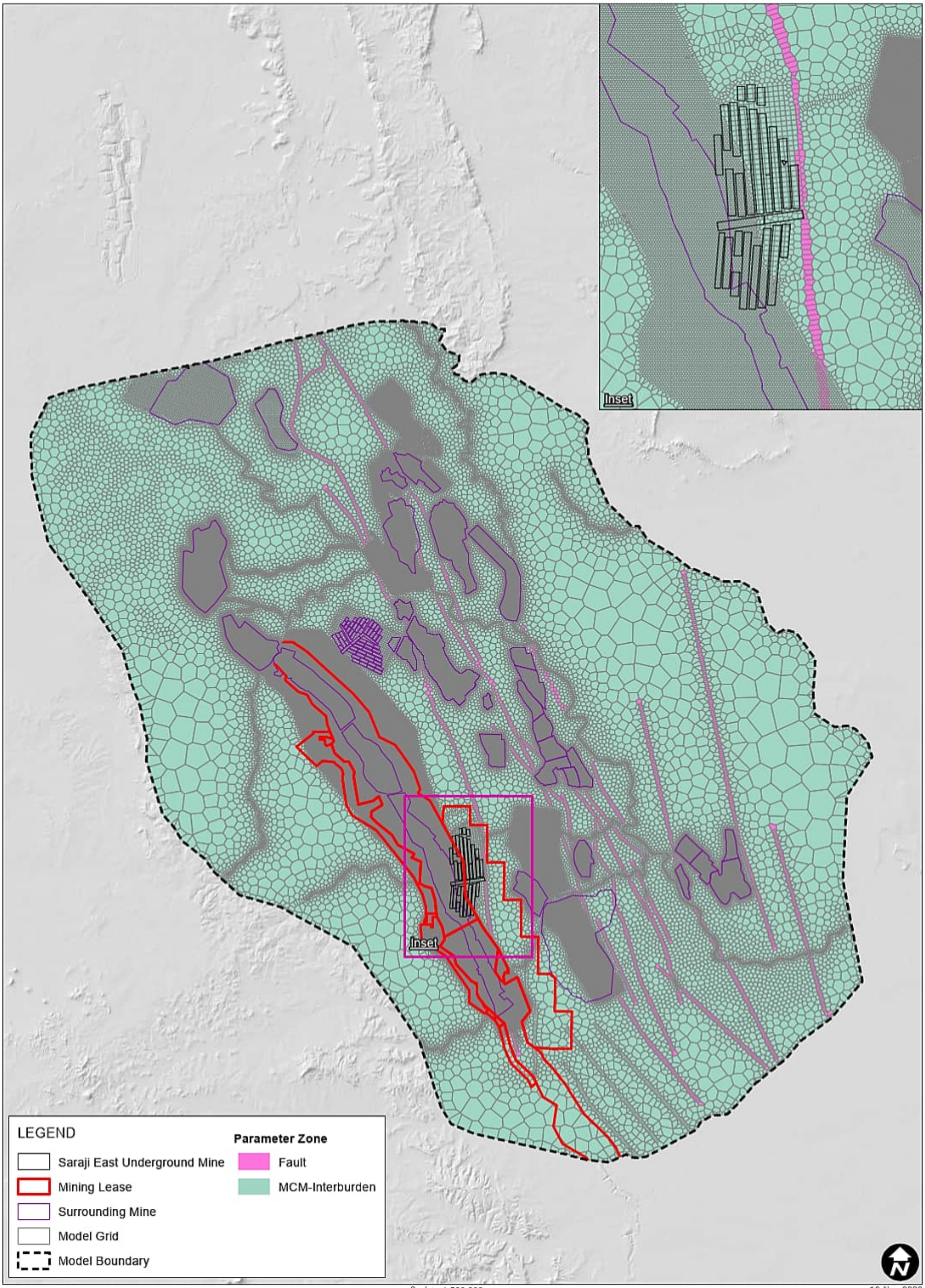

Scale: 1:500,000
GDA 1994 MGA Zone 55

18-Nov-2022
620.31025

Sheet Size : A4

SLR
www.slrconsultingaustralia.com

0 5 10 15 20 km

Hydraulic Parameter Zone Distribution Layer 19

FIGURE C-19

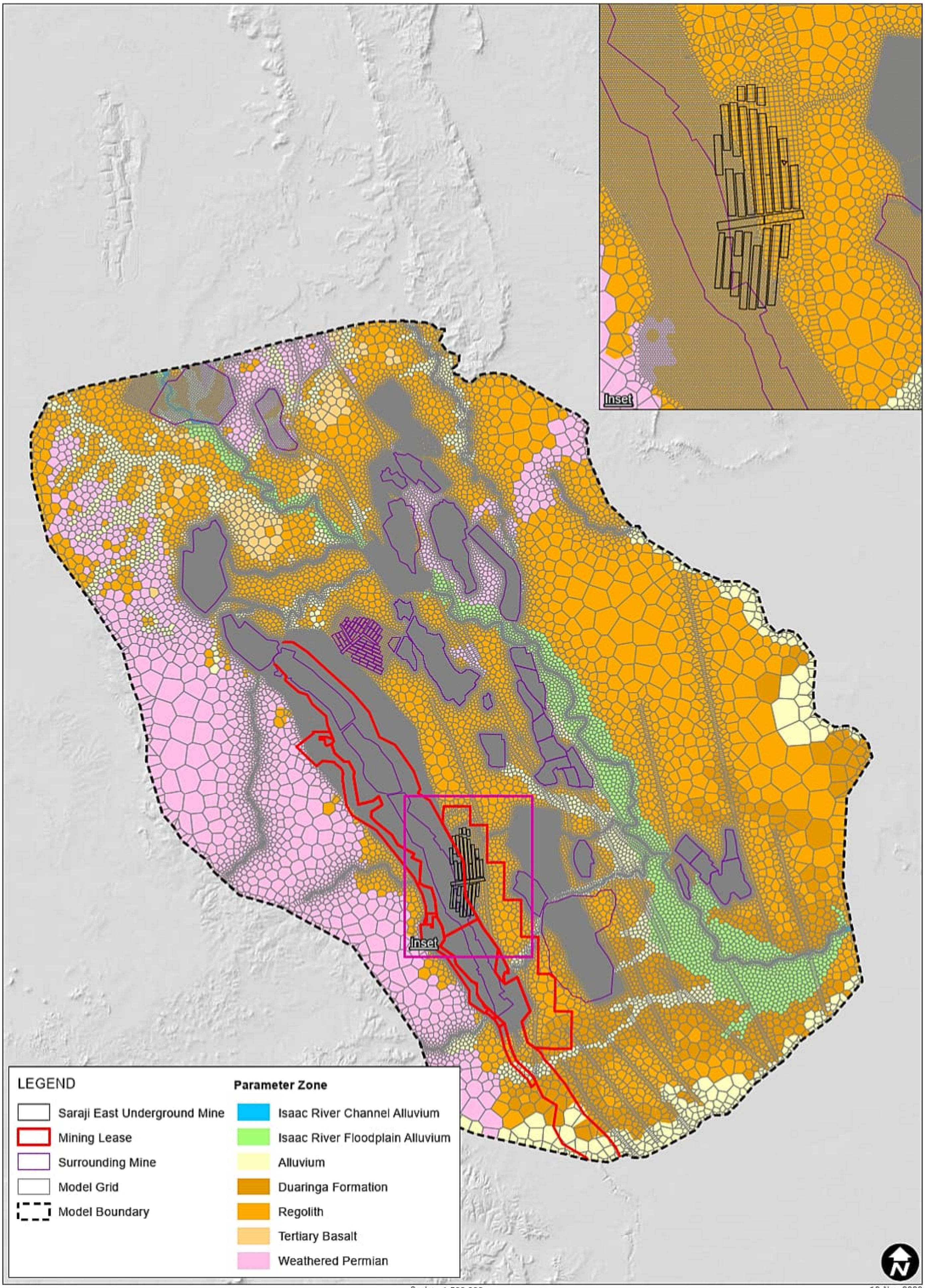

Scale: 1:500,000
GDA 1994 MGA Zone 55

18-Nov-2022
620.31025

Sheet Size : A4

0 5 10 15 20 km

SLR
www.slrconsultingaustralia.com

Recharge Zone Distribution

FIGURE C-20

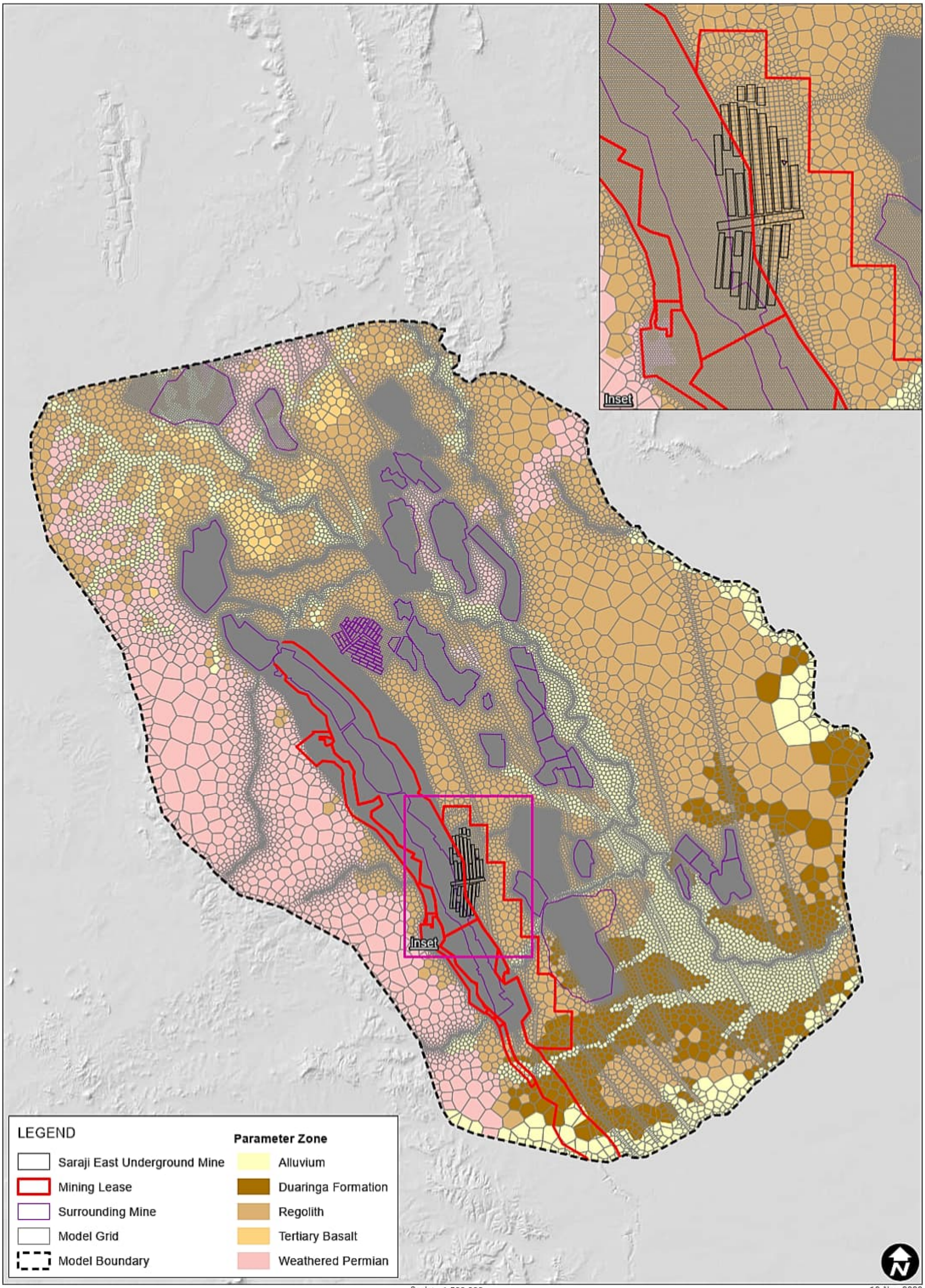

Scale: 1:500,000
GDA 1994 MGA Zone 55

18-Nov-2022
620.13593

Sheet Size : A4

0 5 10 15 20 km

SLR
www.slrconsultingaustralia.com

Hydraulic Parameter Zone Distribution Layer 1

FIGURE C-1

Appendix D:

Stress Periods and Simulated Active Mine Timings

Calibration Period	Interval	Stress Period	Date (from)	Date (to)	Moorvale South (OC)	CVM (OC)	Peak Downs (OC)	Saraji (OC)	Saraji (UG)	Grosvenor (UG)	Poitrel (OC)	Winchester South (OC)	Daunia (OC)	Millennium (OC)	Isaac Plains (OC)	Olive Downs (OC)	Eagle Downs (UG)	Lake Vermont (OC)	Lake Vermont North (OC)
Steady-state		1	Steady-state																
Warm-up	20 Years	2	Transient Warm up					x			x			x					
Calibration	Quarterly	3	01-01-2008	01-04-2008				x			x			x	x				
	Quarterly	4	01-04-2008	01-07-2008				x			x			x	x				
	Quarterly	5	02-07-2008	01-10-2008				x			x			x	x				
	Quarterly	6	01-10-2008	31-12-2008				x			x			x	x				
	Quarterly	7	31-12-2008	01-04-2009				x			x			x	x			x	
	Quarterly	8	02-04-2009	02-07-2009				x			x			x	x			x	
	Quarterly	9	02-07-2009	01-10-2009				x			x			x	x			x	
	Quarterly	10	01-10-2009	31-12-2009				x			x			x	x			x	
	Quarterly	11	01-01-2010	02-04-2010			x	x			x			x	x			x	
	Quarterly	12	02-04-2010	02-07-2010			x	x			x			x	x			x	
	Quarterly	13	02-07-2010	01-10-2010			x	x			x			x	x			x	
	Quarterly	14	01-10-2010	31-12-2010			x	x			x			x	x			x	
	Quarterly	15	01-01-2011	02-04-2011			x	x			x			x	x			x	
	Quarterly	16	02-04-2011	02-07-2011			x	x			x			x	x			x	
	Quarterly	17	02-07-2011	01-10-2011			x	x			x			x	x			x	
	Quarterly	18	02-10-2011	01-01-2012			x	x			x			x	x			x	
	Quarterly	19	01-01-2012	01-04-2012			x	x			x			x	x			x	
	Quarterly	20	01-04-2012	01-07-2012			x	x			x			x	x			x	
	Quarterly	21	02-07-2012	01-10-2012			x	x			x			x	x			x	
	Quarterly	22	01-10-2012	31-12-2012			x	x			x			x	x			x	
	Quarterly	23	31-12-2012	01-04-2013		x	x	x			x		x	x	x			x	
	Quarterly	24	02-04-2013	02-07-2013		x	x	x			x		x	x	x			x	

Calibration Period	Interval	Stress Period	Date (from)	Date (to)	Moorvale South (OC)	CVM (OC)	Peak Downs (OC)	Saraji (OC)	Saraji (UG)	Grosvenor (UG)	Poitrel (OC)	Winchester South (OC)	Daunia (OC)	Millennium (OC)	Isaac Plains (OC)	Olive Downs (OC)	Eagle Downs (UG)	Lake Vermont (OC)	Lake Vermont North (OC)
	Quarterly	25	02-07-2013	01-10-2013		x	x	x			x		x	x	x			x	
	Quarterly	26	01-10-2013	31-12-2013		x	x	x			x		x	x	x			x	
	Quarterly	27	01-01-2014	02-04-2014		x	x	x			x		x	x	x			x	
	Quarterly	28	02-04-2014	02-07-2014		x	x	x			x		x	x	x			x	
	Quarterly	29	02-07-2014	01-10-2014		x	x	x			x		x	x	x			x	
	Quarterly	30	01-10-2014	31-12-2014		x	x	x			x		x	x	x			x	
	Quarterly	31	01-01-2015	02-04-2015		x	x	x			x		x	x	x			x	
	Quarterly	32	02-04-2015	02-07-2015		x	x	x			x		x	x	x			x	
	Quarterly	33	02-07-2015	01-10-2015		x	x	x			x		x	x	x			x	
	Quarterly	34	02-10-2015	01-01-2016		x	x	x			x		x	x	x			x	
	Quarterly	35	01-01-2016	01-04-2016		x	x	x		x	x		x	x	x			x	
	Quarterly	36	01-04-2016	01-07-2016		x	x	x		x	x		x	x	x			x	
	Quarterly	37	02-07-2016	01-10-2016		x	x	x		x	x		x	x	x			x	
	Quarterly	38	01-10-2016	31-12-2016		x	x	x		x	x		x	x	x			x	
	Quarterly	39	31-12-2016	01-04-2017		x	x	x		x	x		x	x	x			x	
	Quarterly	40	02-04-2017	02-07-2017		x	x	x		x	x		x	x	x			x	
	Quarterly	41	02-07-2017	01-10-2017		x	x	x		x	x		x	x	x			x	
	Quarterly	42	01-10-2017	31-12-2017		x	x	x		x	x		x	x	x			x	
	Quarterly	43	31-12-2017	01-04-2018		x	x	x		x	x		x	x	x			x	
	Quarterly	44	01-04-2018	01-07-2018		x	x	x		x	x		x	x				x	
	Quarterly	45	01-07-2018	30-09-2018		x	x	x		x	x		x	x				x	
	Quarterly	46	30-09-2018	31-12-2018		x	x	x		x	x		x	x				x	
	Quarterly	47	31-12-2018	01-04-2019		x	x	x		x	x		x	x				x	
	Quarterly	48	01-04-2019	01-07-2019		x	x	x		x	x		x	x				x	
	Quarterly	49	01-07-2019	01-10-2019		x	x	x		x	x		x	x				x	
	Quarterly	50	01-10-2019	31-12-2019		x	x	x		x	x		x	x				x	

Calibration Period	Interval	Stress Period	Date (from)	Date (to)	Moorvale South (OC)	CVM (OC)	Peak Downs (OC)	Saraji (OC)	Saraji (UG)	Grosvenor (UG)	Poitrel (OC)	Winchester South (OC)	Daunia (OC)	Millennium (OC)	Isaac Plains (OC)	Olive Downs (OC)	Eagle Downs (UG)	Lake Vermont (OC)	Lake Vermont North (OC)
	Quarterly	51	31-12-2019	31-03-2020		x	x	x		x	x		x	x				x	
	Quarterly	52	31-03-2020	30-06-2020		x	x	x		x	x		x	x				x	x
	Quarterly	53	30-06-2020	30-09-2020	x	x	x	x		x	x		x	x				x	x
	Quarterly	54	30-09-2020	31-12-2020	x	x	x	x		x	x		x	x		x		x	x
	Quarterly	55	01-01-2021	01-04-2021	x	x	x	x		x	x		x	x		x		x	x
	Quarterly	56	02-04-2021	01-07-2021	x	x	x	x		x	x		x	x		x		x	x
	Quarterly	57	02-07-2021	30-09-2021	x	x	x	x		x	x		x	x		x		x	x
	Quarterly	58	01-10-2021	31-12-2021	x	x	x	x		x	x		x	x		x		x	x
Predictive	Annual	59	30-12-2021	30-12-2022	x	x	x	x	x	x	x		x	x		x		x	x
	Annual	60	30-12-2022	30-12-2023	x	x	x	x	x	x	x		x	x		x		x	x
	Annual	61	30-12-2023	29-12-2024	x	x	x	x	x	x	x	x	x	x		x		x	x
	Annual	62	29-12-2024	30-12-2025	x	x	x	x	x	x	x	x	x	x		x		x	x
	Annual	63	30-12-2025	30-12-2026	x	x	x	x	x	x	x	x	x	x		x		x	x
	Annual	64	30-12-2026	30-12-2027	x	x	x	x	x	x	x	x	x	x		x			x
	Annual	65	30-12-2027	29-12-2028		x	x	x	x	x		x	x			x	x		x
	Annual	66	29-12-2028	30-12-2029		x	x	x	x	x		x	x			x	x		x
	Annual	67	30-12-2029	30-12-2030		x	x	x	x	x		x	x			x	x		x
	Annual	68	30-12-2030	30-12-2031		x	x	x	x	x		x	x			x	x		x
	Annual	69	30-12-2031	29-12-2032		x	x		x	x		x	x			x	x		x
	Annual	70	29-12-2032	30-12-2033		x	x		x	x		x	x			x	x		x
	Annual	71	30-12-2033	30-12-2034		x	x		x	x		x	x			x	x		x
	Annual	72	30-12-2034	30-12-2035		x	x		x	x		x	x			x	x		x
	Annual	73	30-12-2035	29-12-2036		x	x		x	x		x	x			x	x		x
	Annual	74	29-12-2036	30-12-2037		x	x		x	x		x	x			x	x		x
	Annual	75	30-12-2037	30-12-2038		x	x		x	x		x	x			x	x		x
	Annual	76	30-12-2038	30-12-2039		x	x		x	x		x				x	x		x

Calibration Period	Interval	Stress Period	Date (from)	Date (to)	Moorvale South (OC)	CVM (OC)	Peak Downs (OC)	Saraji (OC)	Saraji (UG)	Grosvenor (UG)	Poitrel (OC)	Winchester South (OC)	Daunia (OC)	Millennium (OC)	Isaac Plains (OC)	Olive Downs (OC)	Eagle Downs (UG)	Lake Vermont (OC)	Lake Vermont North (OC)
	Annual	77	30-12-2039	29-12-2040		x	x		x	x		x				x	x		x
	Annual	78	29-12-2040	30-12-2041		x	x		x	x		x				x	x		x
	Annual	79	30-12-2041	30-12-2042		x	x		x	x		x				x	x		x
	Annual	80	01-01-2043	31-12-2043		x	x		x	x		x				x	x		x
	Annual	81	01-01-2044	30-12-2044		x	x		x	x		x				x	x		x
	Annual	82	31-12-2044	31-12-2045		x	x			x		x				x	x		x
	Annual	83	01-01-2046	31-12-2046		x	x			x		x				x	x		x
	Annual	84	01-01-2047	31-12-2047		x	x			x		x				x	x		x
	Annual	85	01-01-2048	30-12-2048		x	x			x		x				x	x		x
	Annual	86	31-12-2048	31-12-2049		x	x					x				x	x		x
	Annual	87	01-01-2050	31-12-2050		x	x					x				x	x		x
	Annual	88	01-01-2051	31-12-2051		x	x					x				x	x		x
	Annual	89	01-01-2052	30-12-2052			x					x				x	x		x
	Annual	90	31-12-2052	31-12-2053			x									x	x		x
	Annual	91	01-01-2054	31-12-2054			x									x	x		x
	Annual	92	01-01-2055	31-12-2055			x									x	x		x
	5 Years	93	01-01-2056	30-12-2060			x									x	x		x
	5 Years	94	31-12-2060	31-12-2065			x									x	x		x
	5 Years	95	01-01-2066	31-12-2070			x									x	x		x
	5 Years	96	01-01-2071	31-12-2075			x									x	x		x
	5 Years	97	01-01-2076	30-12-2080			x									x	x		x
	5 Years	98	31-12-2080	31-12-2085			x									x	x		x
	5 Years	99	01-01-2086	31-12-2090			x									x	x		
	5 Years	100	01-01-2091	31-12-2095			x										x		

Appendix E:

Cumulative Drawdown Predictions

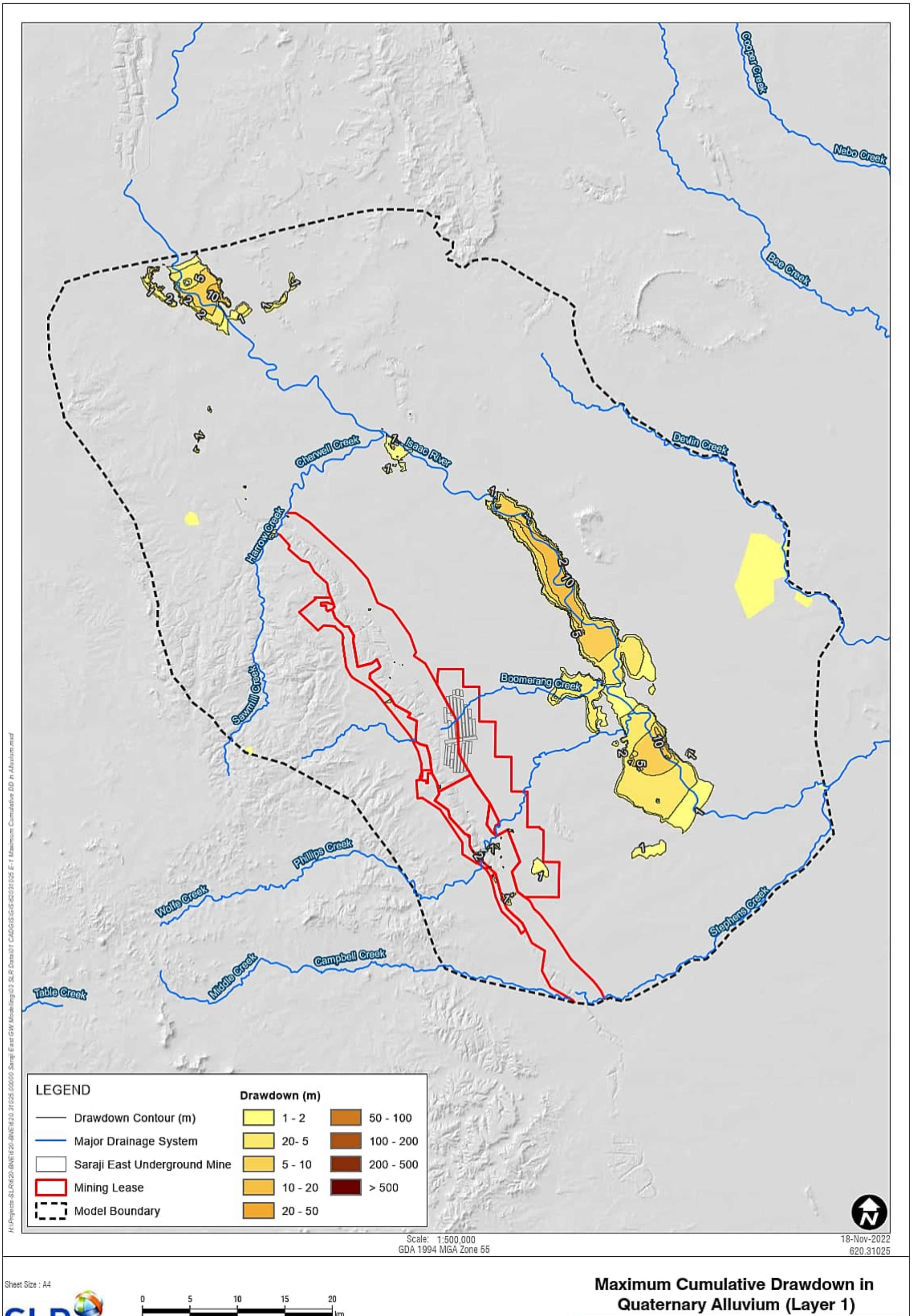

SLR
www.slrconsultingaustralia.com

Maximum Cumulative Drawdown in Quaternary Alluvium (Layer 1)

FIGURE E-1

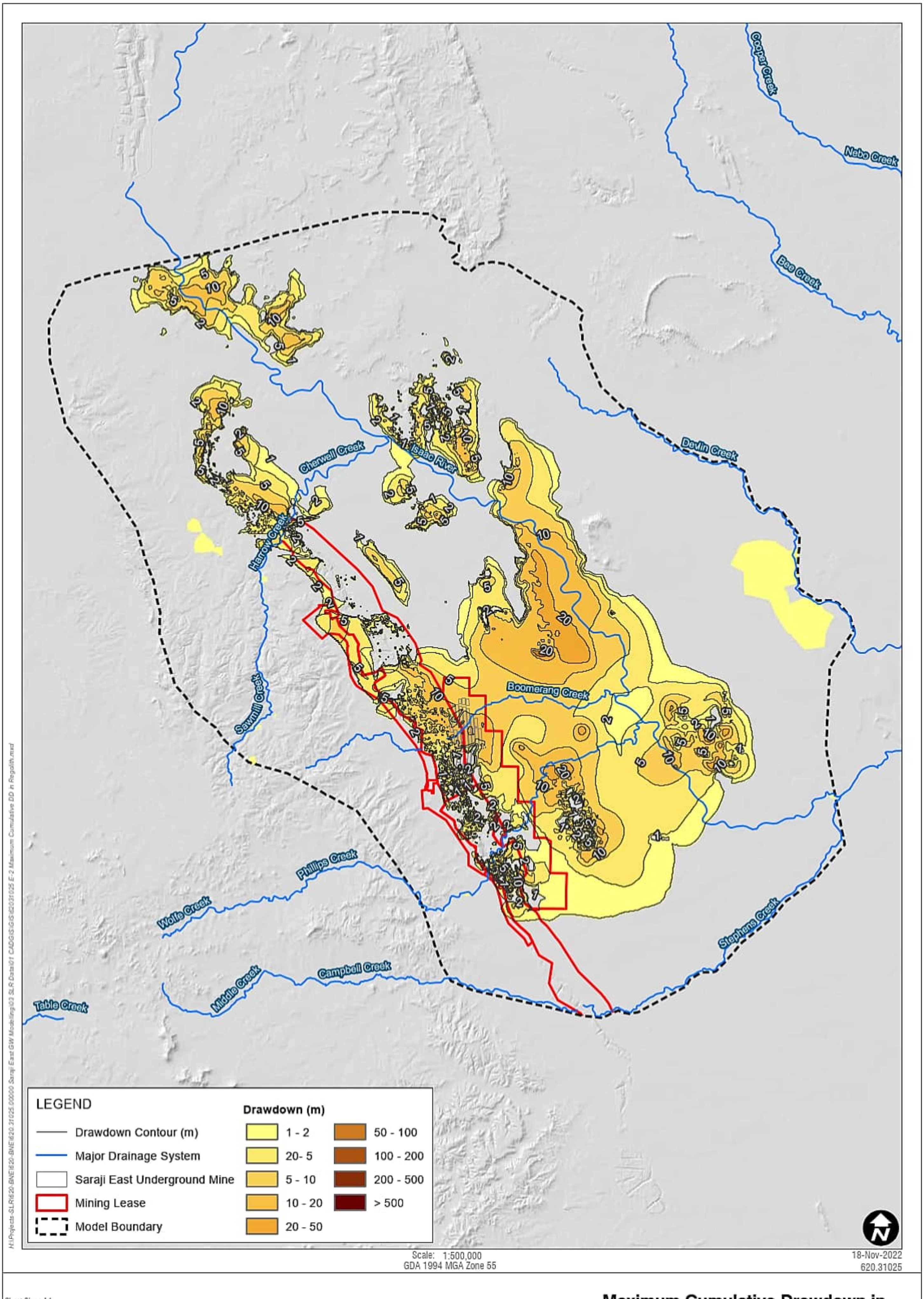

www.slrconsultingaustralia.com

Maximum Cumulative Drawdown in Regolith (Layer 2)

FIGURE E-2

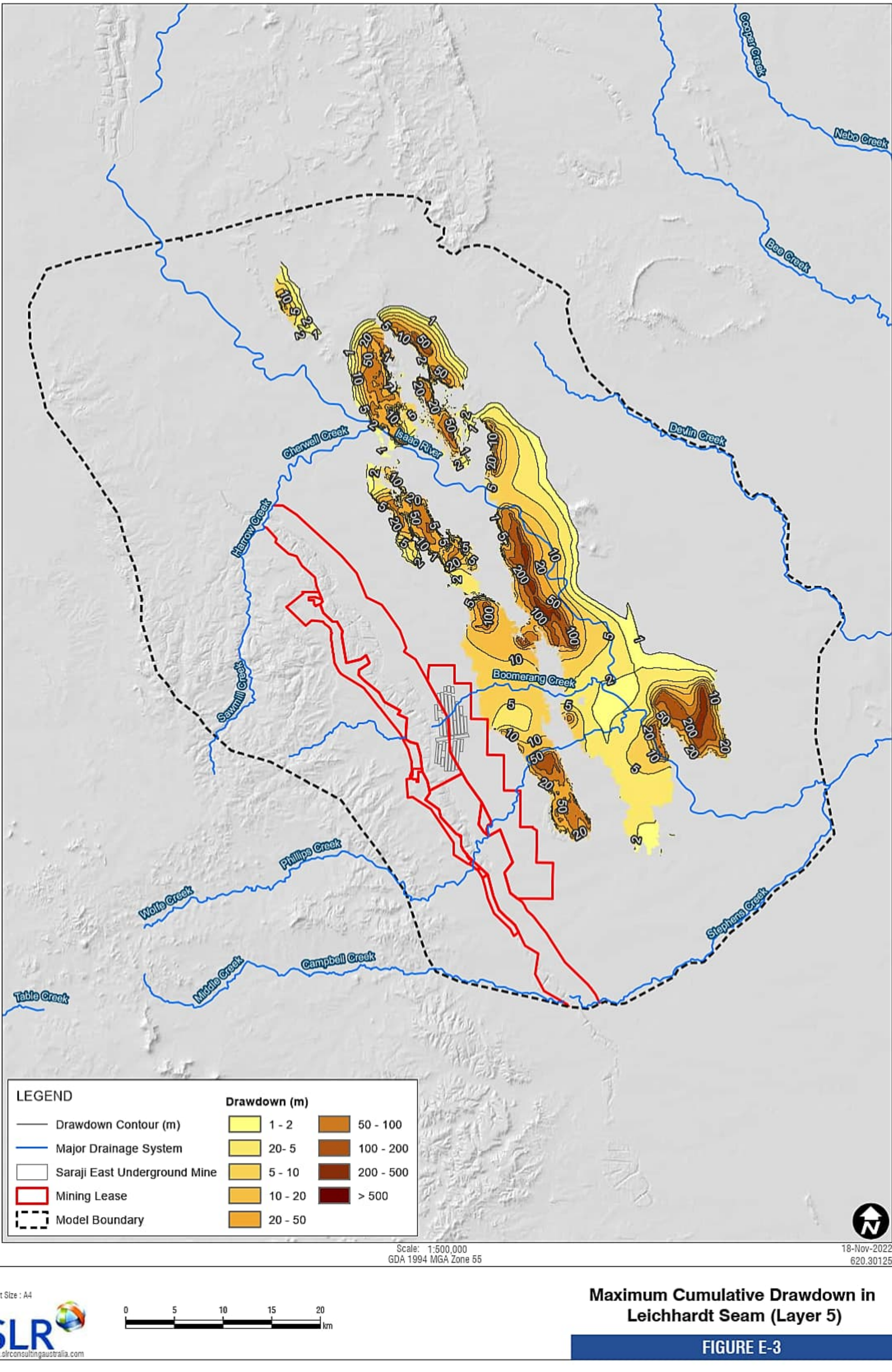

Scale: 1:500,000
GDA 1994 MGA Zone 55

18-Nov-2022
620.30125

Sheet Size : A4

SLR
www.slrconsultingaustralia.com

0 5 10 15 20 km

Maximum Cumulative Drawdown in Leichhardt Seam (Layer 5)

FIGURE E-3

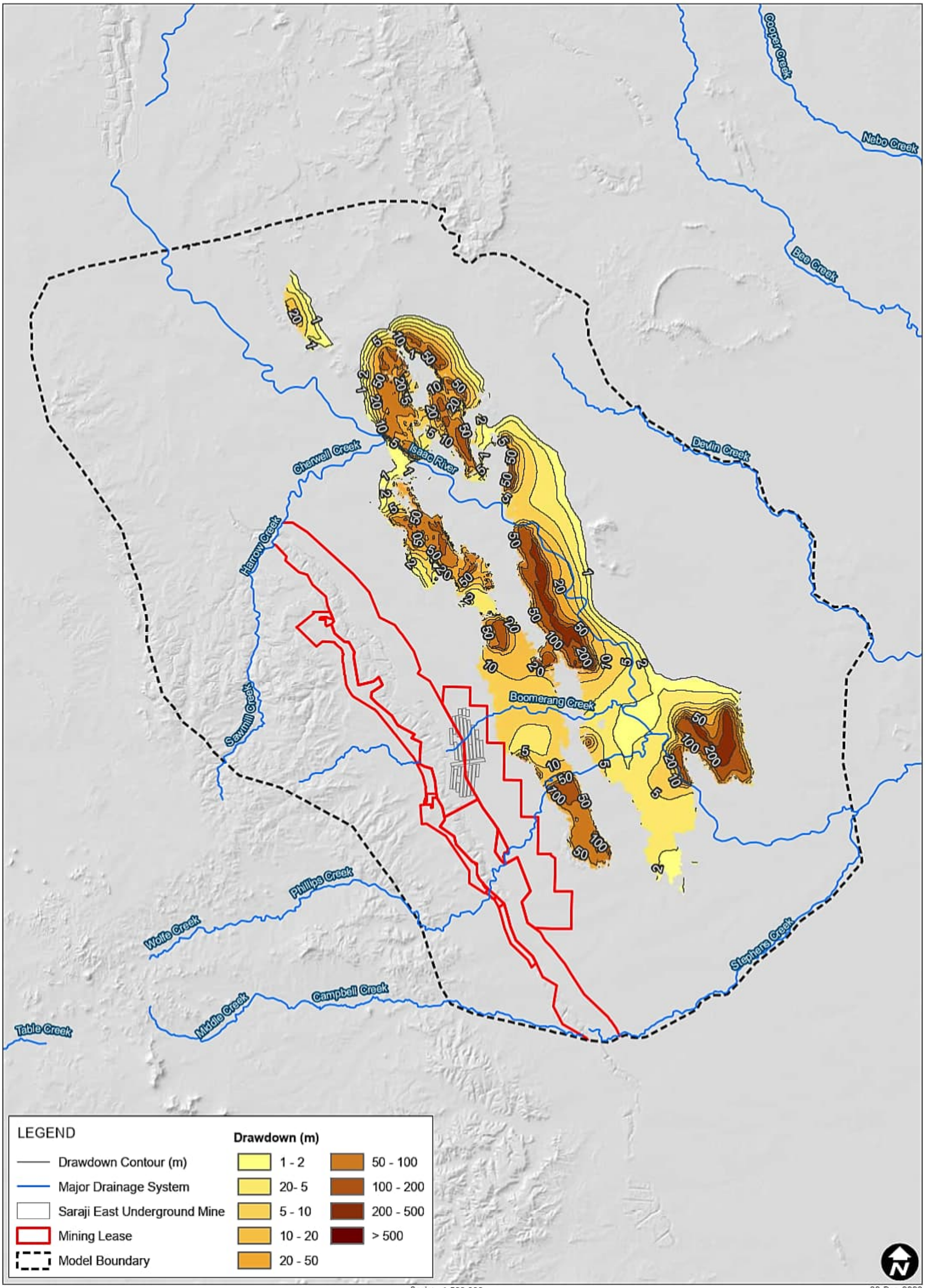

Scale: 1:500,000
GDA 1994 MGA Zone 55

22-Dec-2022
620.31025

Sheet Size : A4

SLR
www.slrconsultingaustralia.com

0 5 10 15 20 km

Maximum Cumulative Drawdown in Vermont Seam (Layer 7)

FIGURE E-4

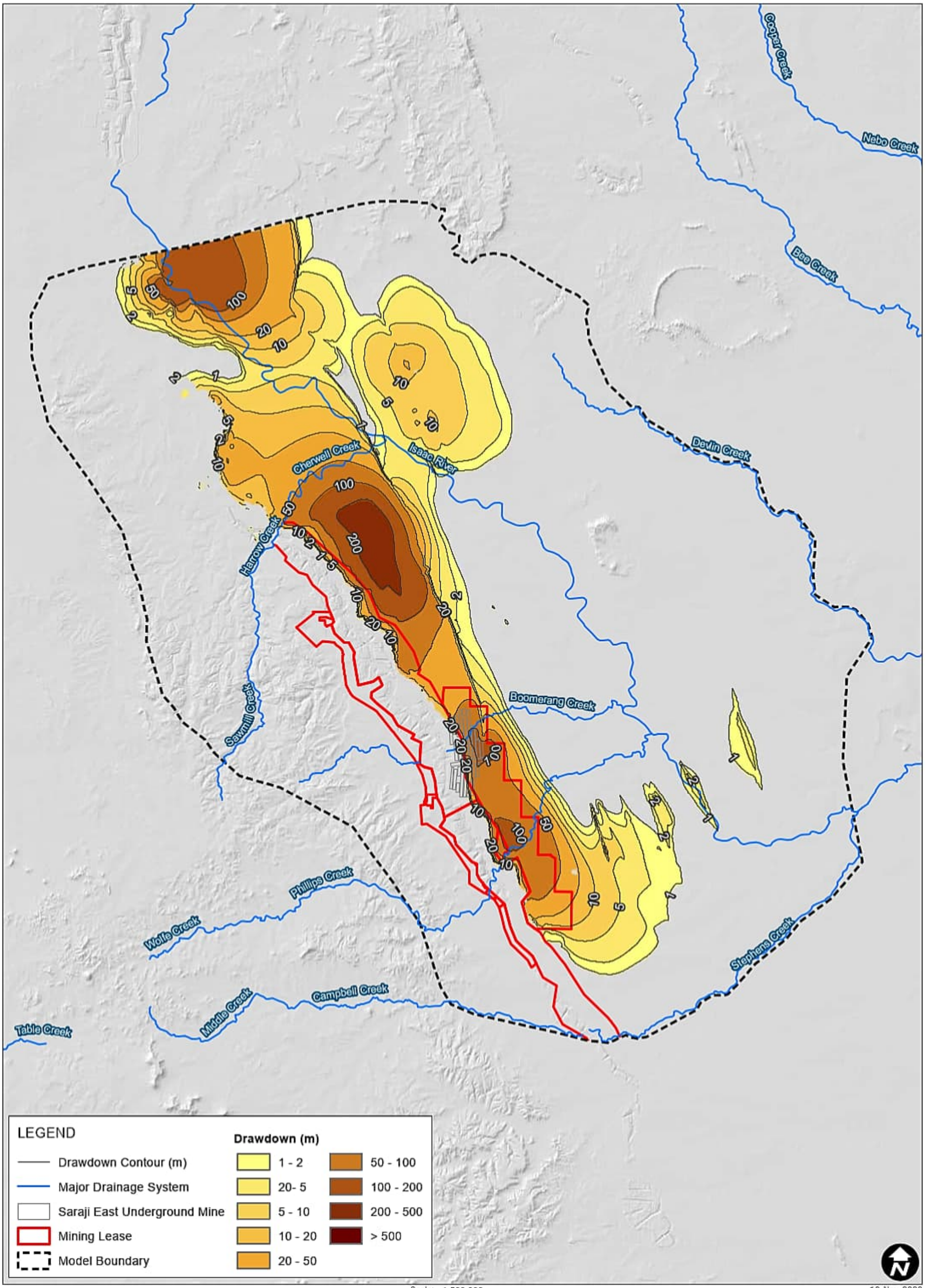

Scale: 1:500,000
GDA 1994 MGA Zone 55

18-Nov-2022
620.31025

Sheet Size : A4

SLR
www.slrconsultingaustralia.com

0 5 10 15 20 km

Maximum Cumulative Drawdown in Q Seam (Layer 12)

FIGURE E-5

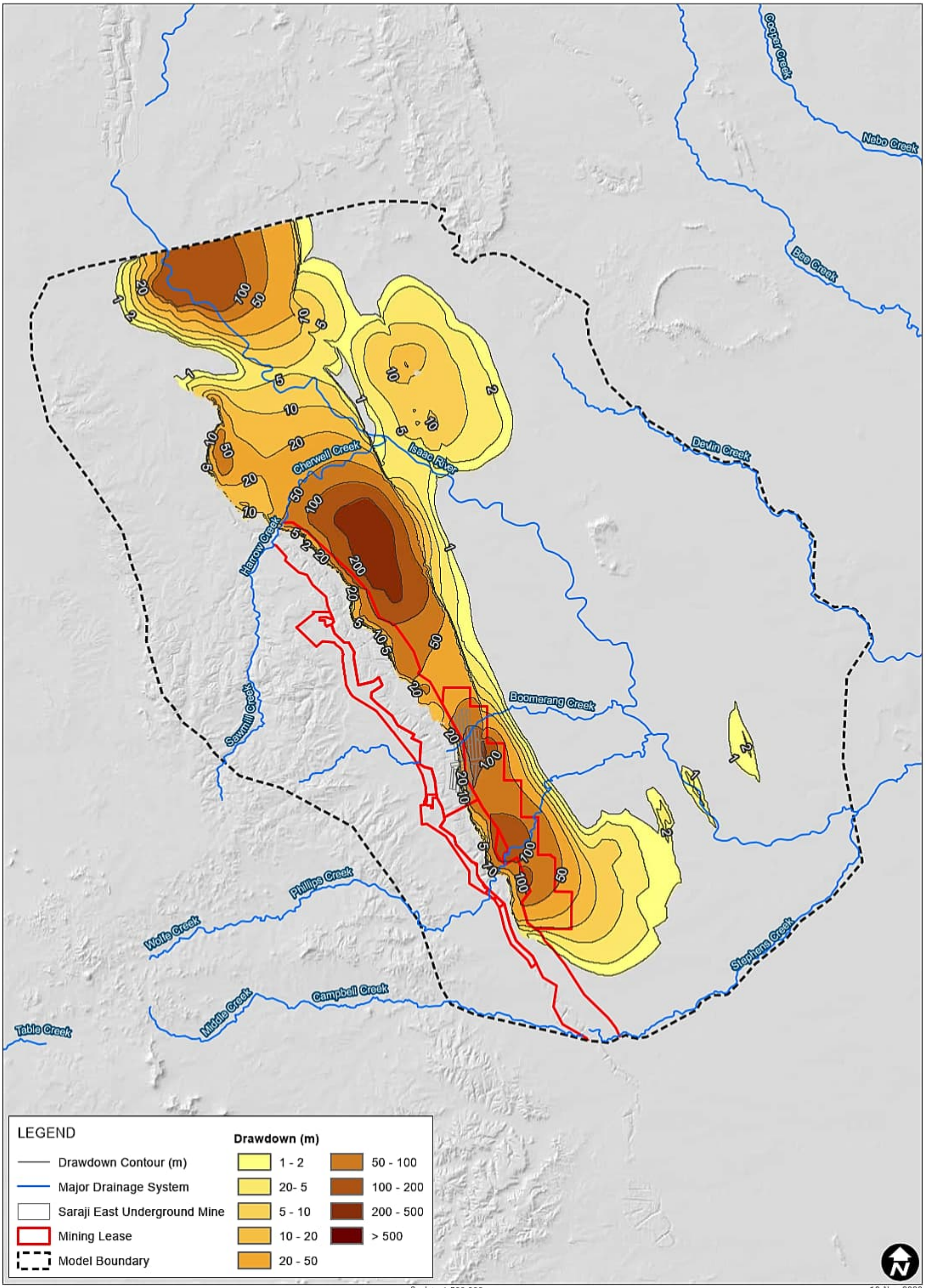

Scale: 1:500,000
GDA 1994 MGA Zone 55

18-Nov-2022
620.31025

Sheet Size : A4

SLR
www.slrconsultingaustralia.com

0 5 10 15 20 km

Maximum Cumulative Drawdown in P Seam (Layer 14)

FIGURE E-6

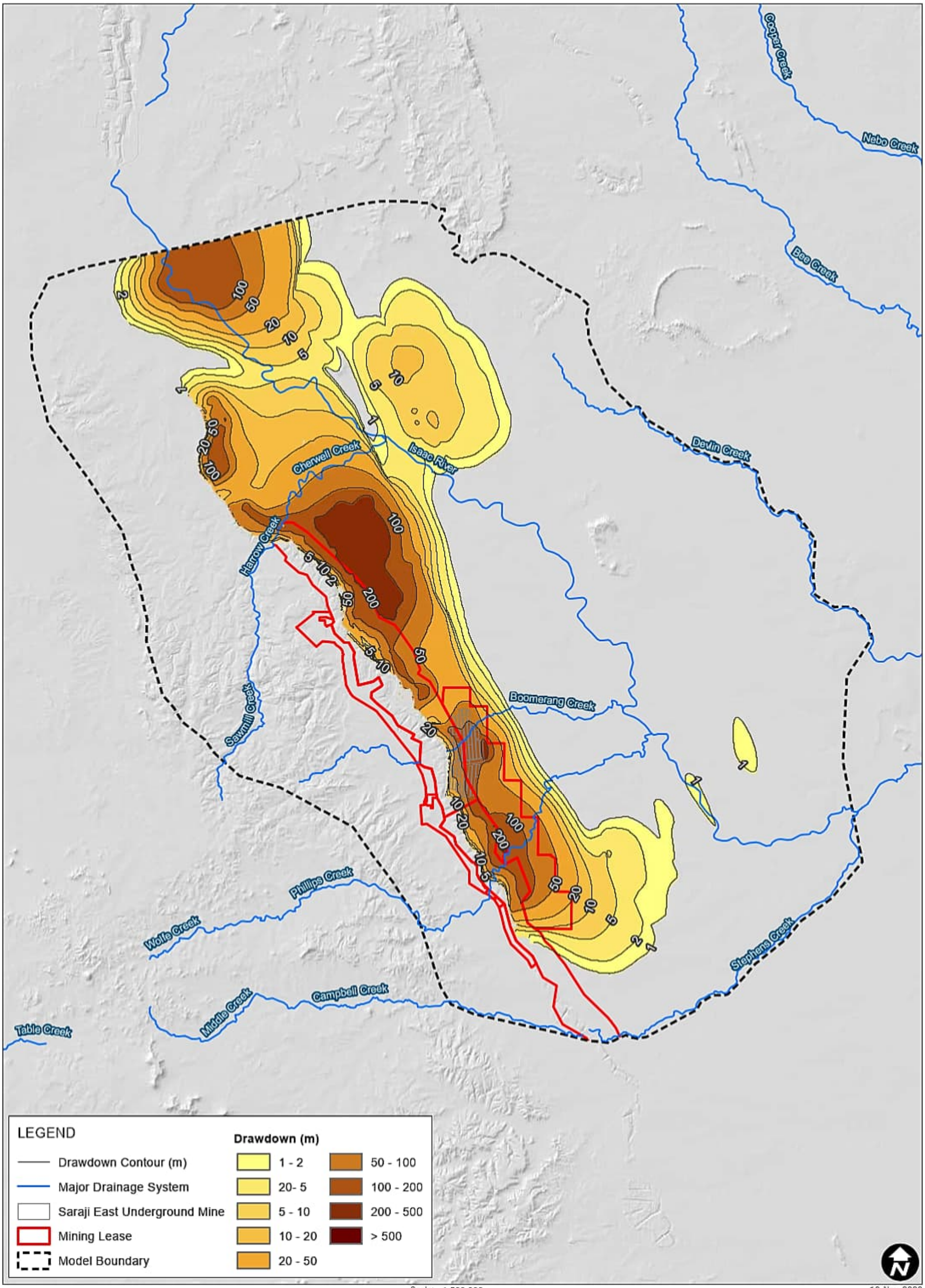

SLR
www.slrconsultingaustralia.com

Maximum Cumulative Drawdown in H Seam (Layer 16)

FIGURE E-7

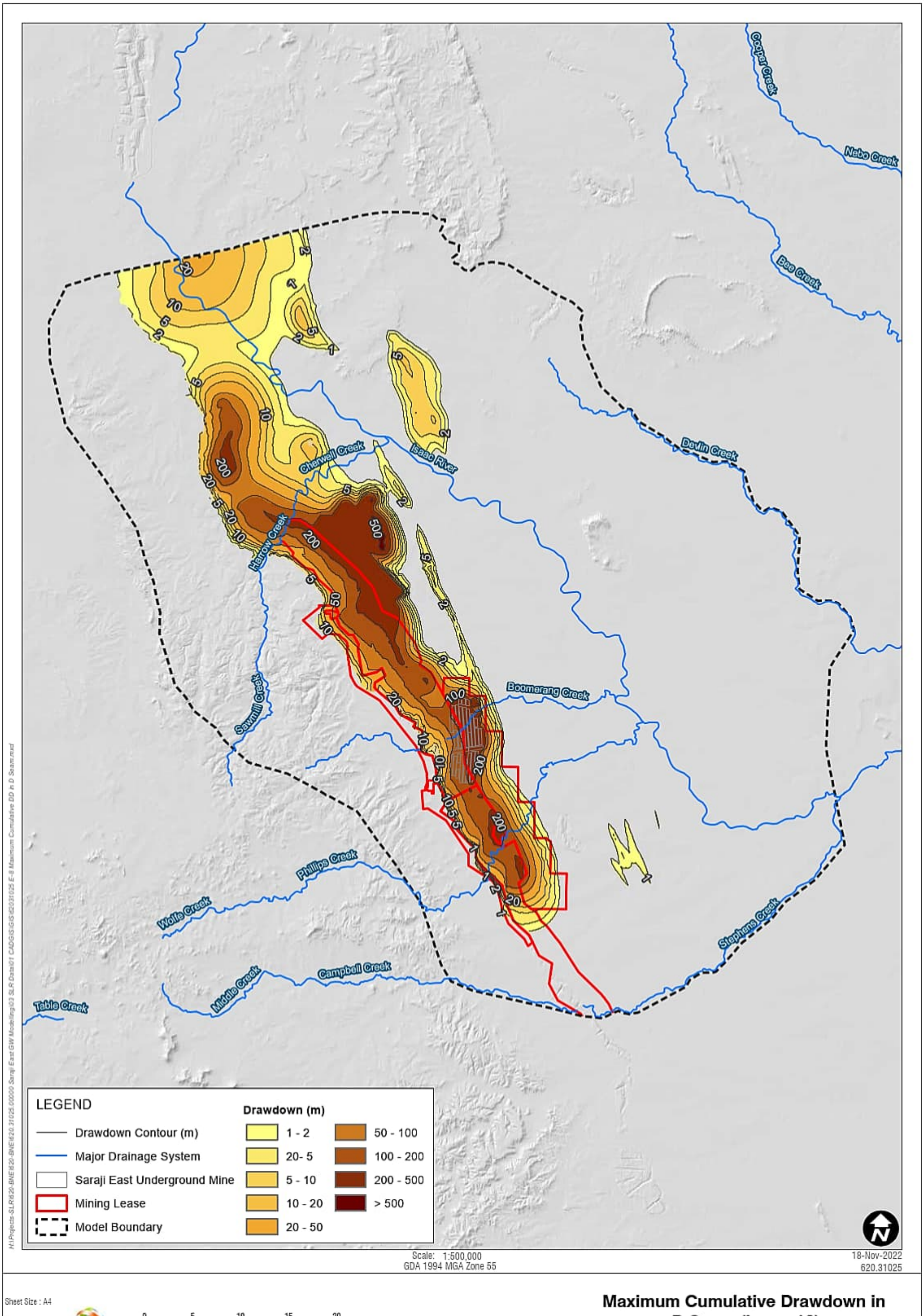

SLR
www.slrconsultingaustralia.com

Maximum Cumulative Drawdown in D Seam (Layer 18)

FIGURE E-8

Appendix F:

Uncertainty Analysis Parameter Distributions

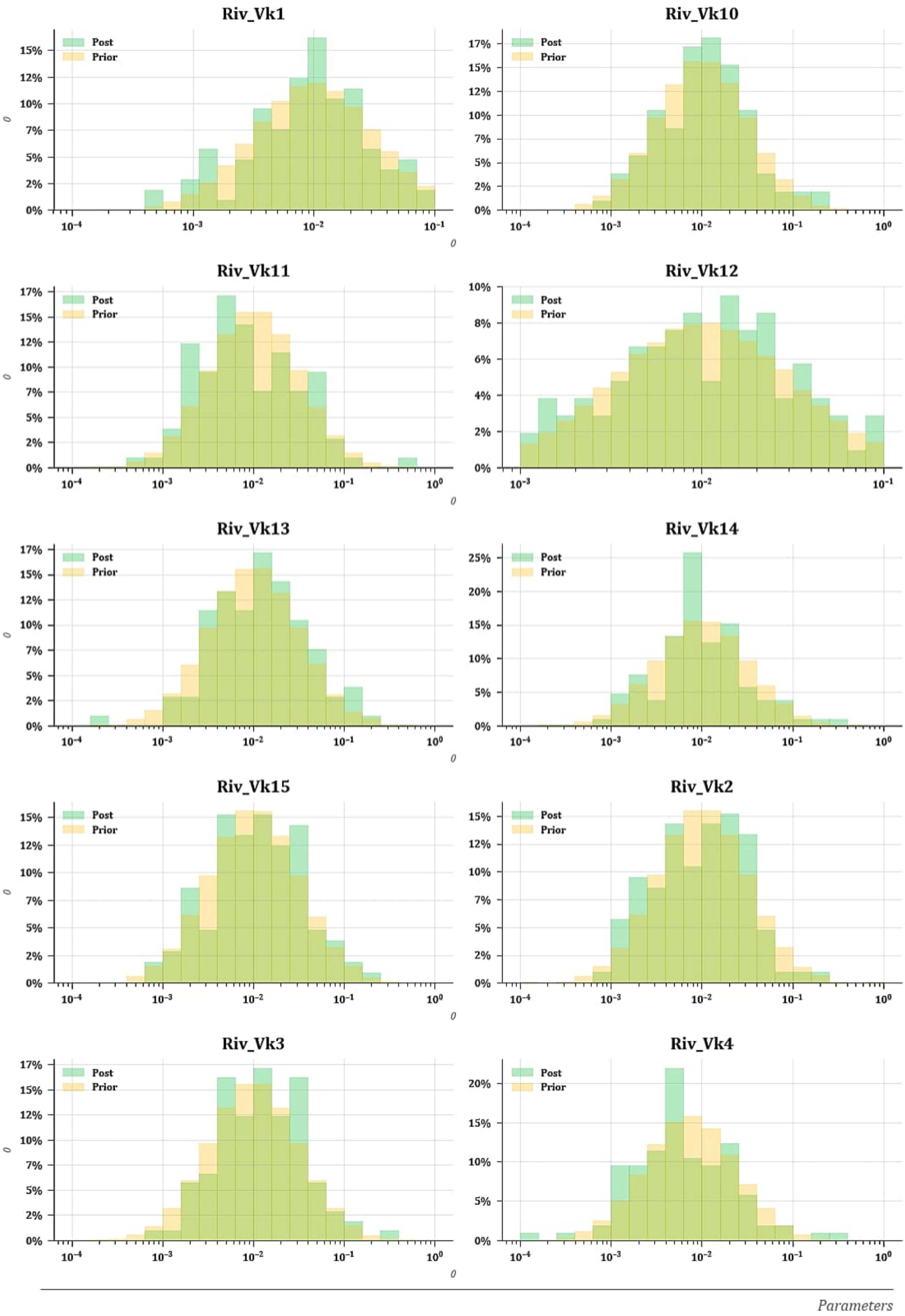
Riv_Vk1
Riv_Vk10
Riv_Vk11
Riv_Vk12
Riv_Vk13
Riv_Vk14
Riv_Vk15
Riv_Vk2
Riv_Vk3
Riv_Vk4
Post
Prior
Parameters

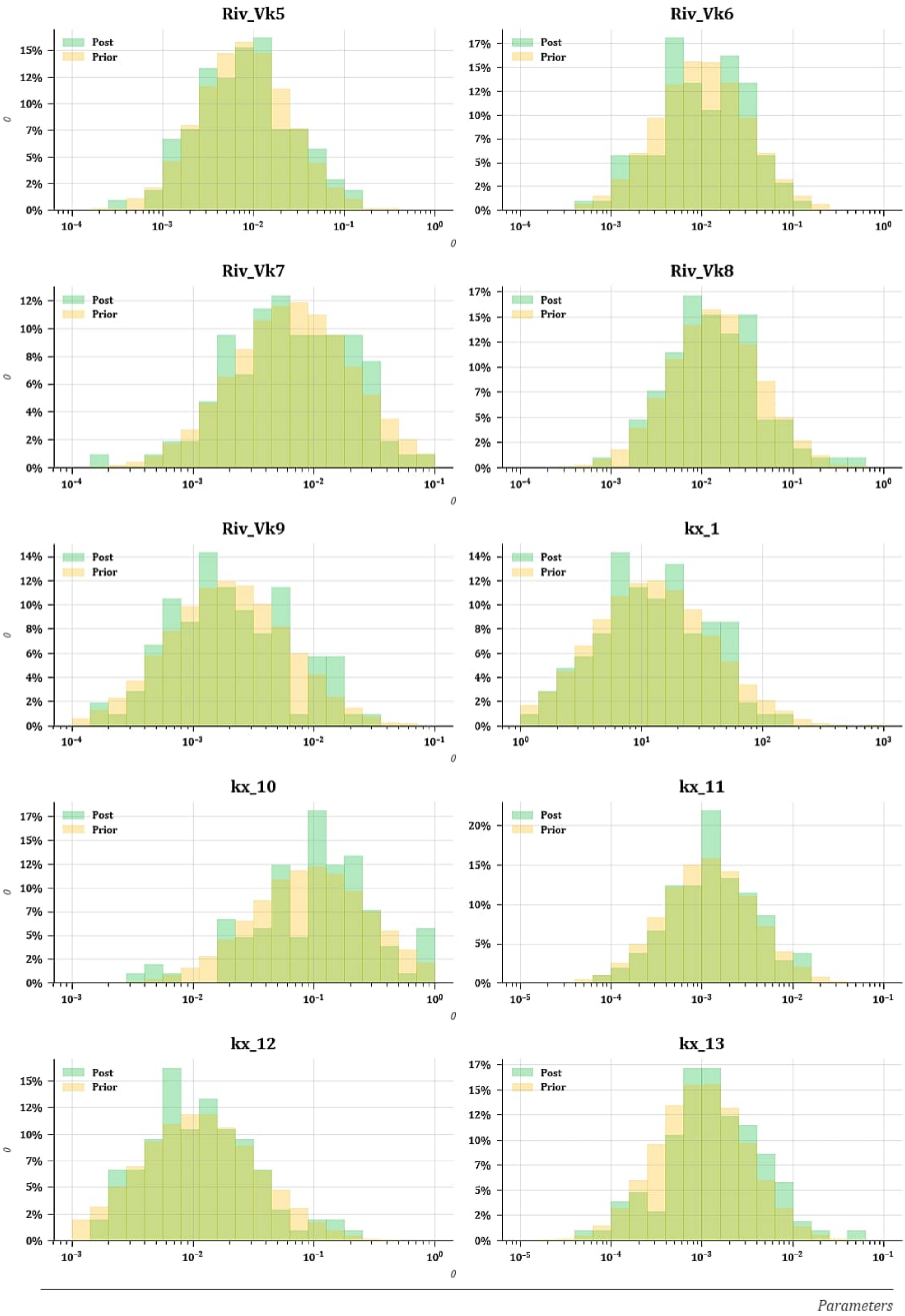

Riv_Vk5
Riv_Vk6
Riv_Vk7
Riv_Vk8
Riv_Vk9
kx_1
kx_10
kx_11
kx_12
kx_13
Post
Prior
Parameters

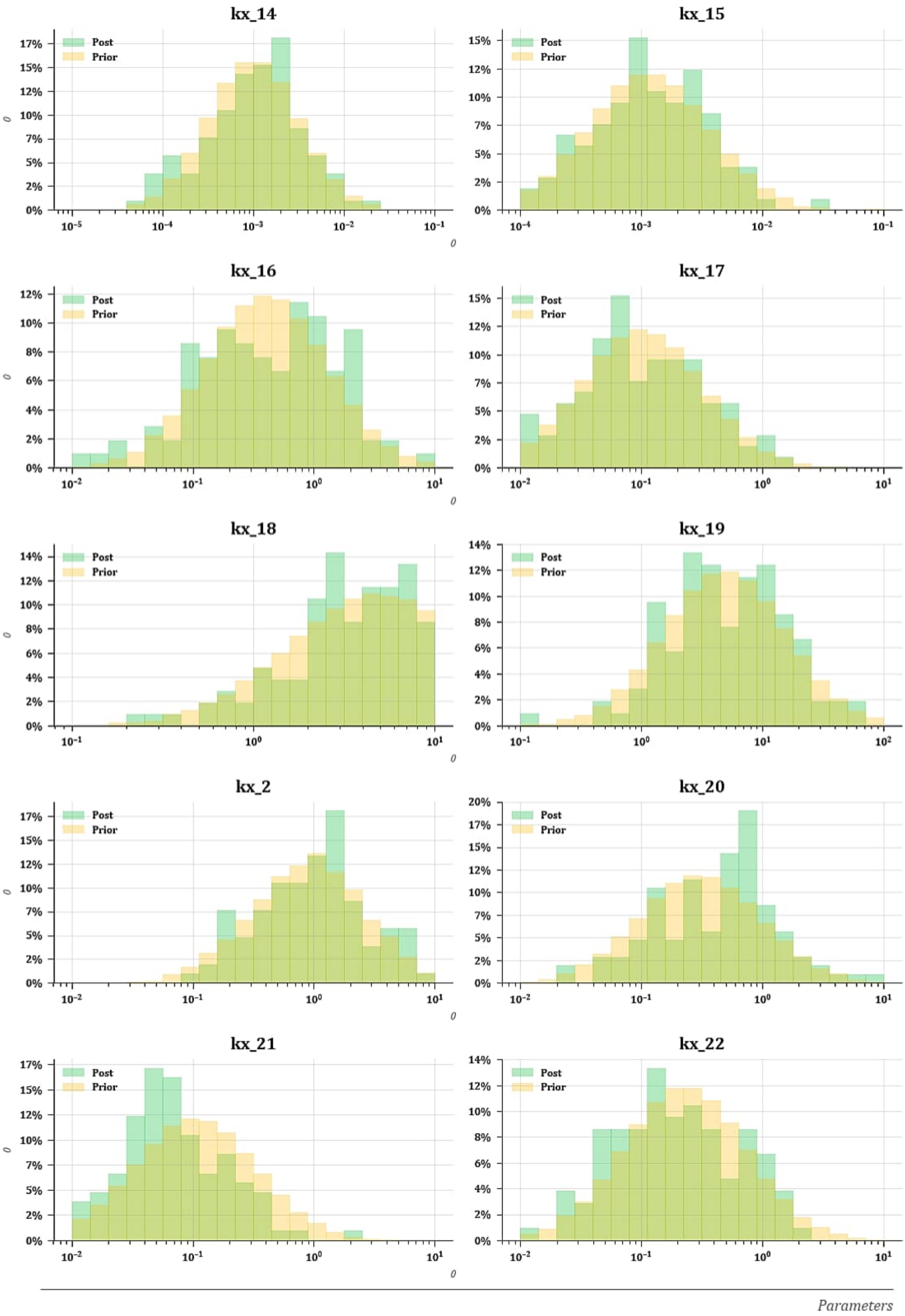
kx_14
kx_15
kx_16
kx_17
kx_18
kx_19
kx_2
kx_20
kx_21
kx_22
Post
Prior
Parameters

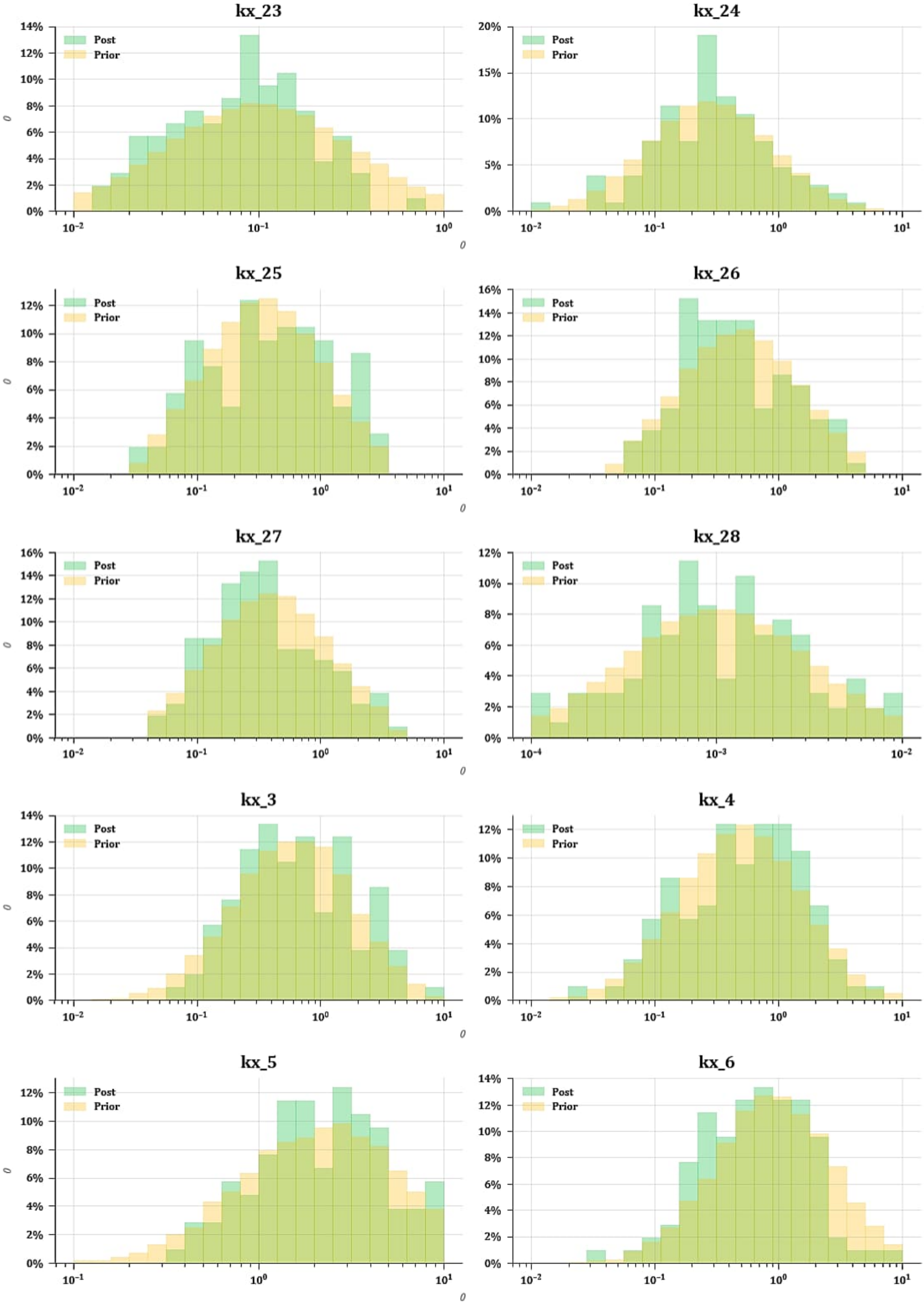

Parameters

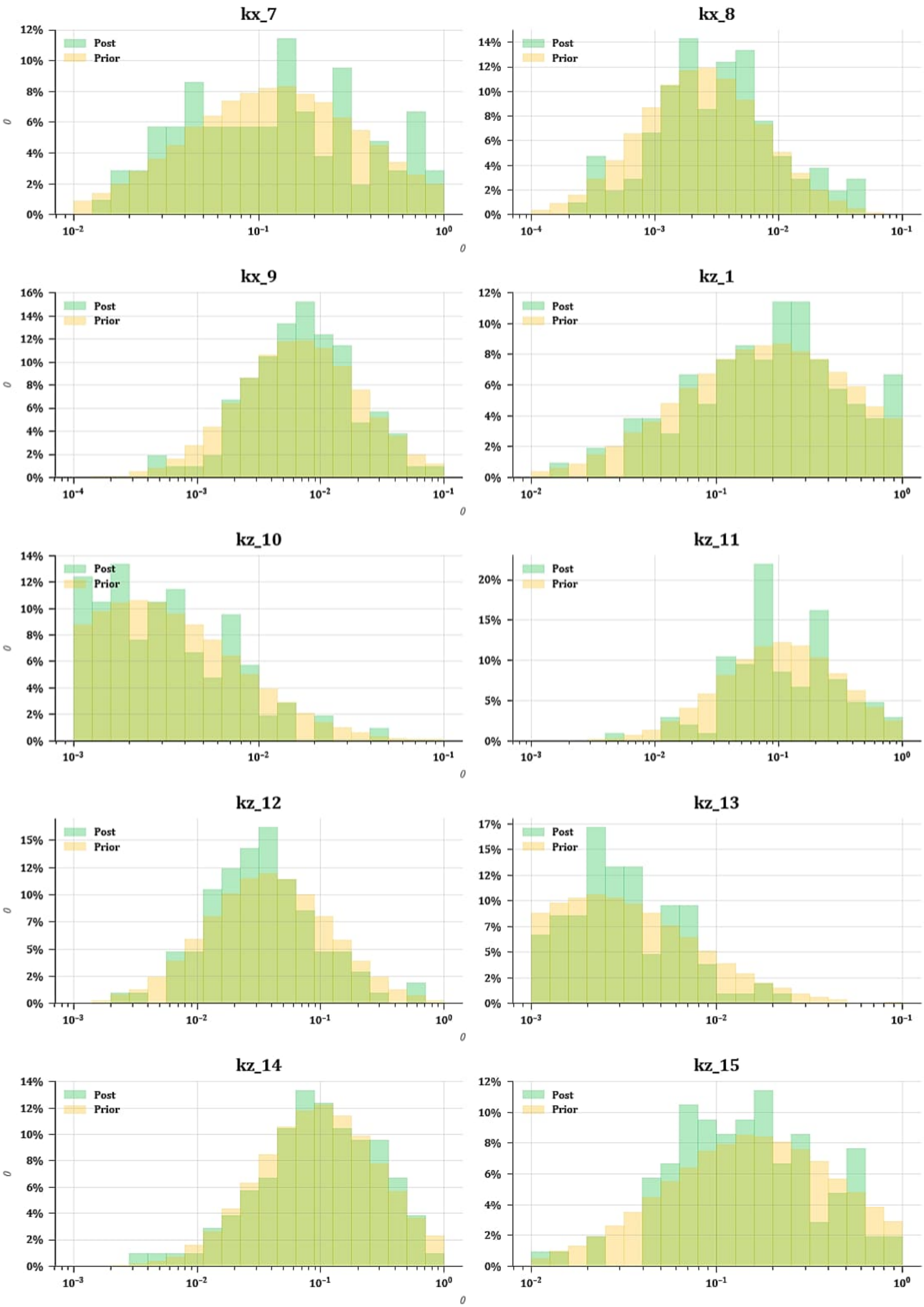

Parameters

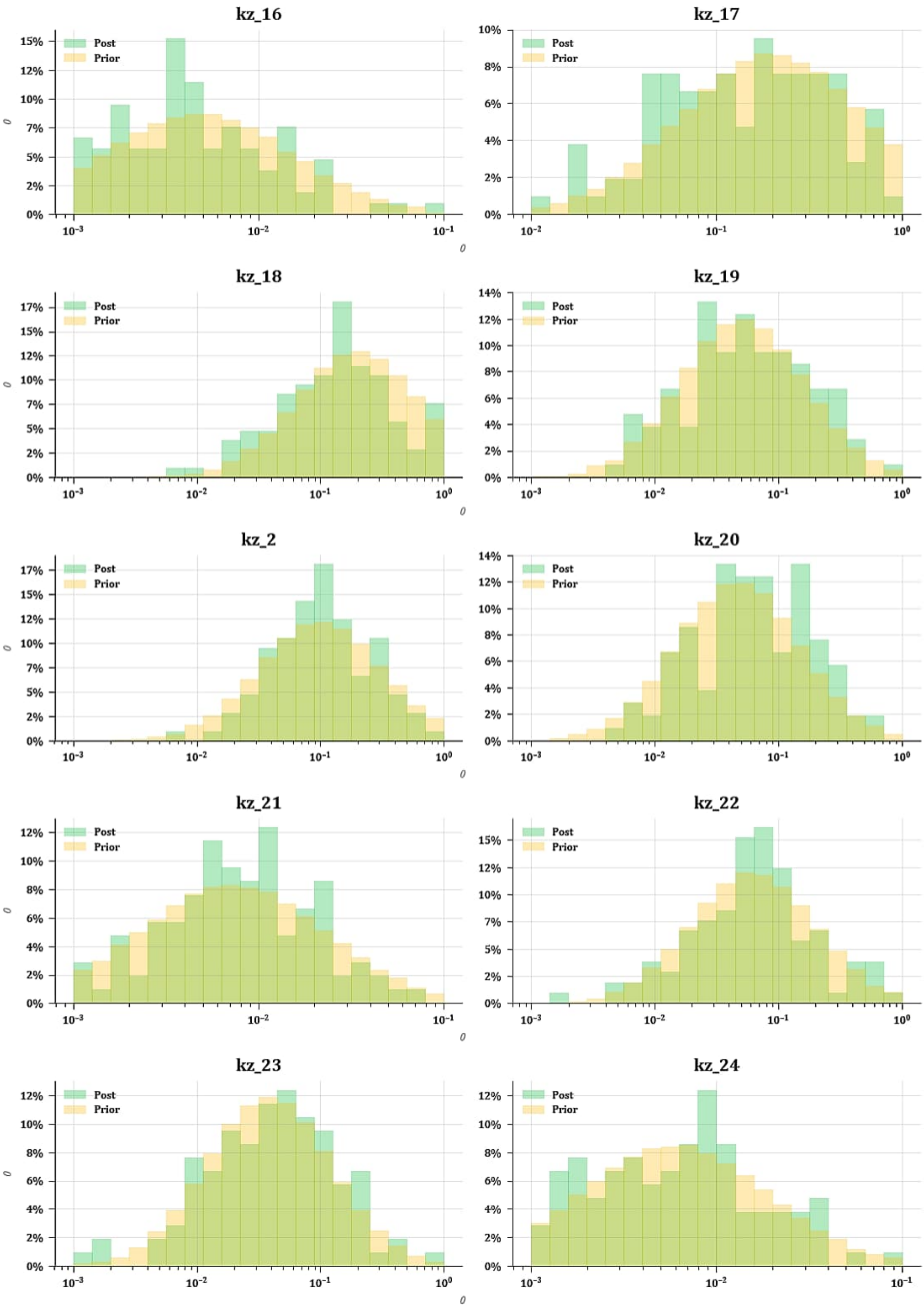
kz_16
Post
Prior
kz_17
Post
Prior
kz_18
Post
Prior
kz_19
Post
Prior
kz_2
Post
Prior
kz_20
Post
Prior
kz_21
Post
Prior
kz_22
Post
Prior
kz_23
Post
Prior
kz_24
Post
Prior

Parameters

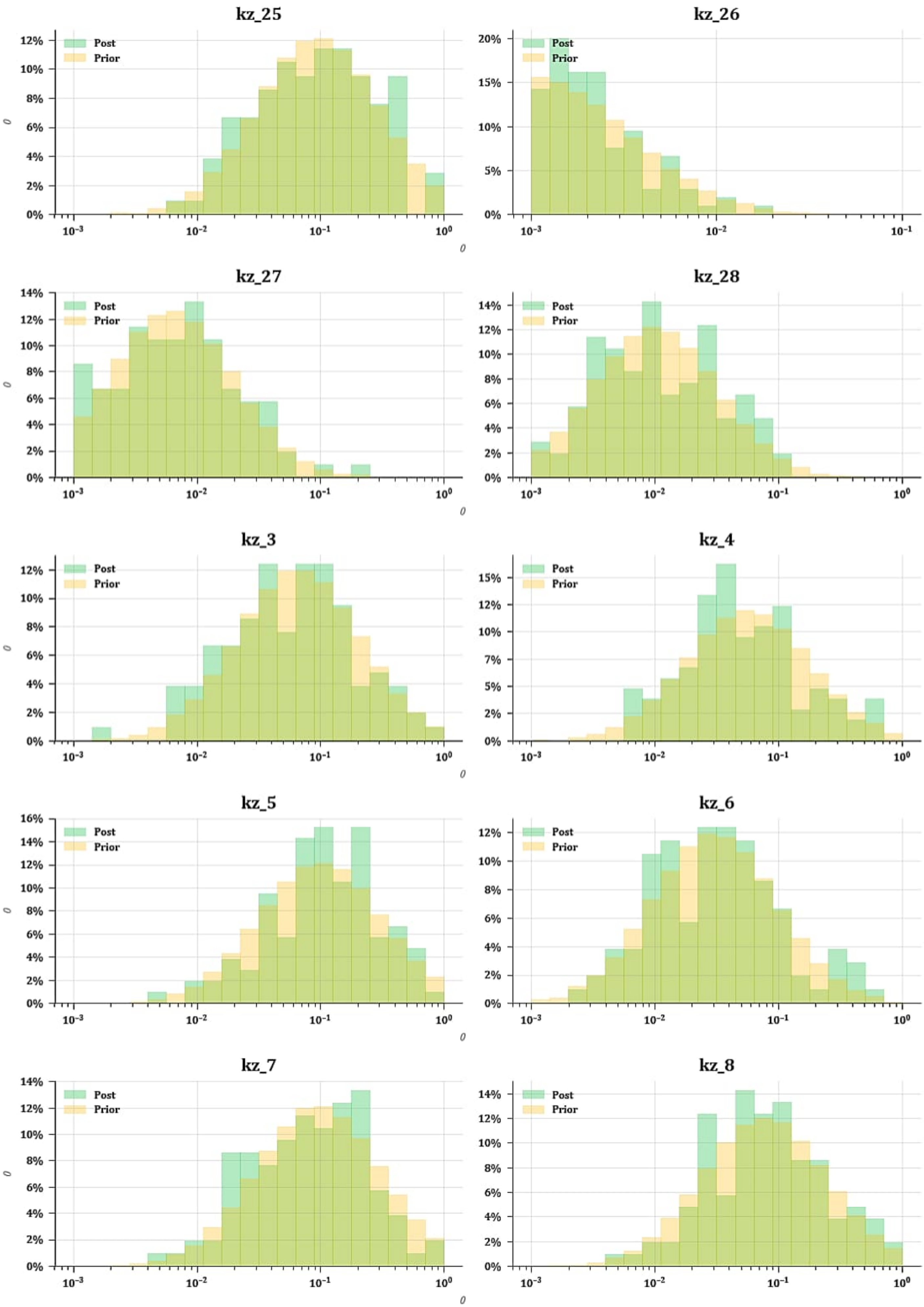
kz_25
Post
Prior
kz_26
Post
Prior
kz_27
Post
Prior
kz_28
Post
Prior
kz_3
Post
Prior
kz_4
Post
Prior
kz_5
Post
Prior
kz_6
Post
Prior
kz_7
Post
Prior
kz_8
Post
Prior

Parameters

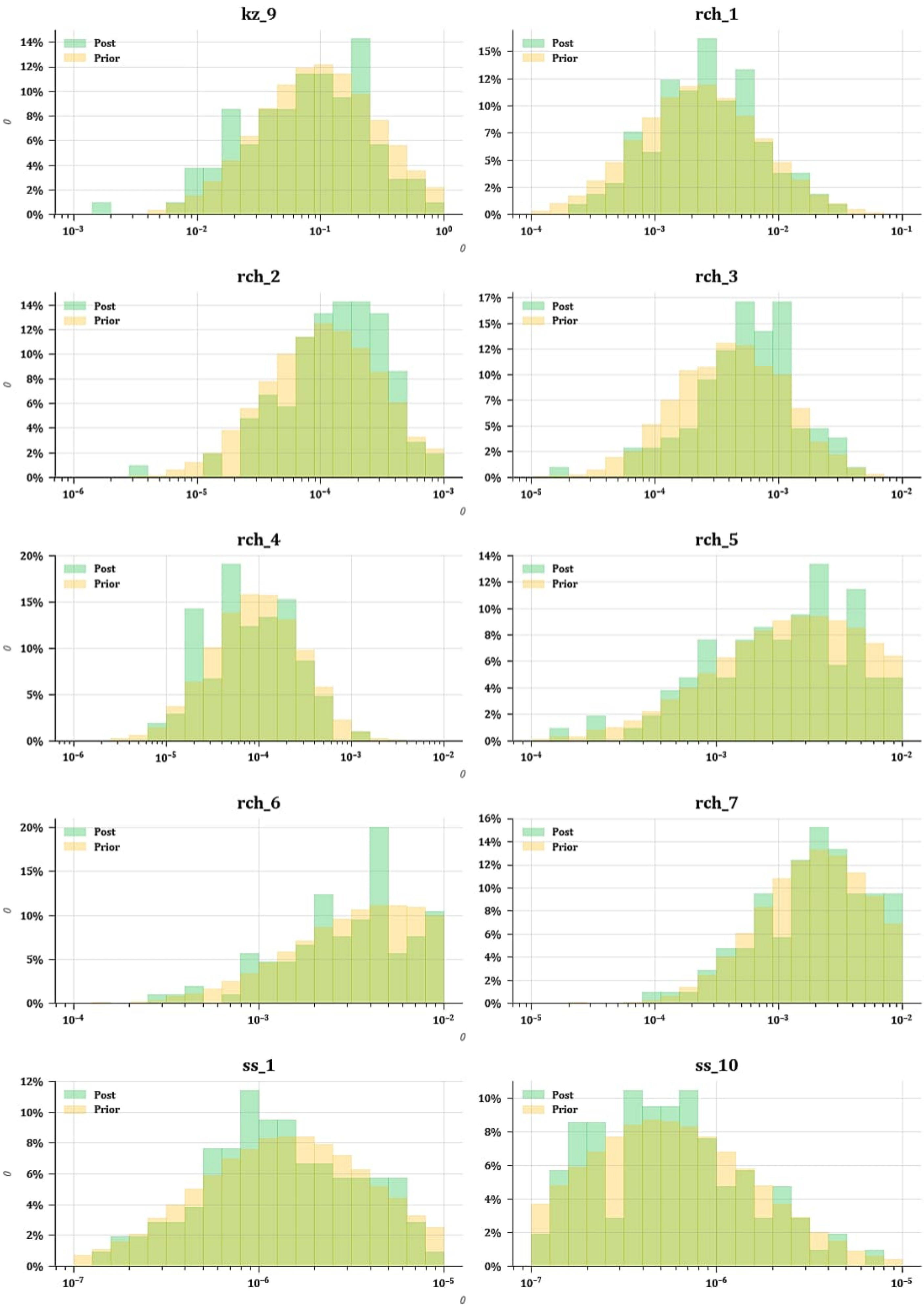

Parameters

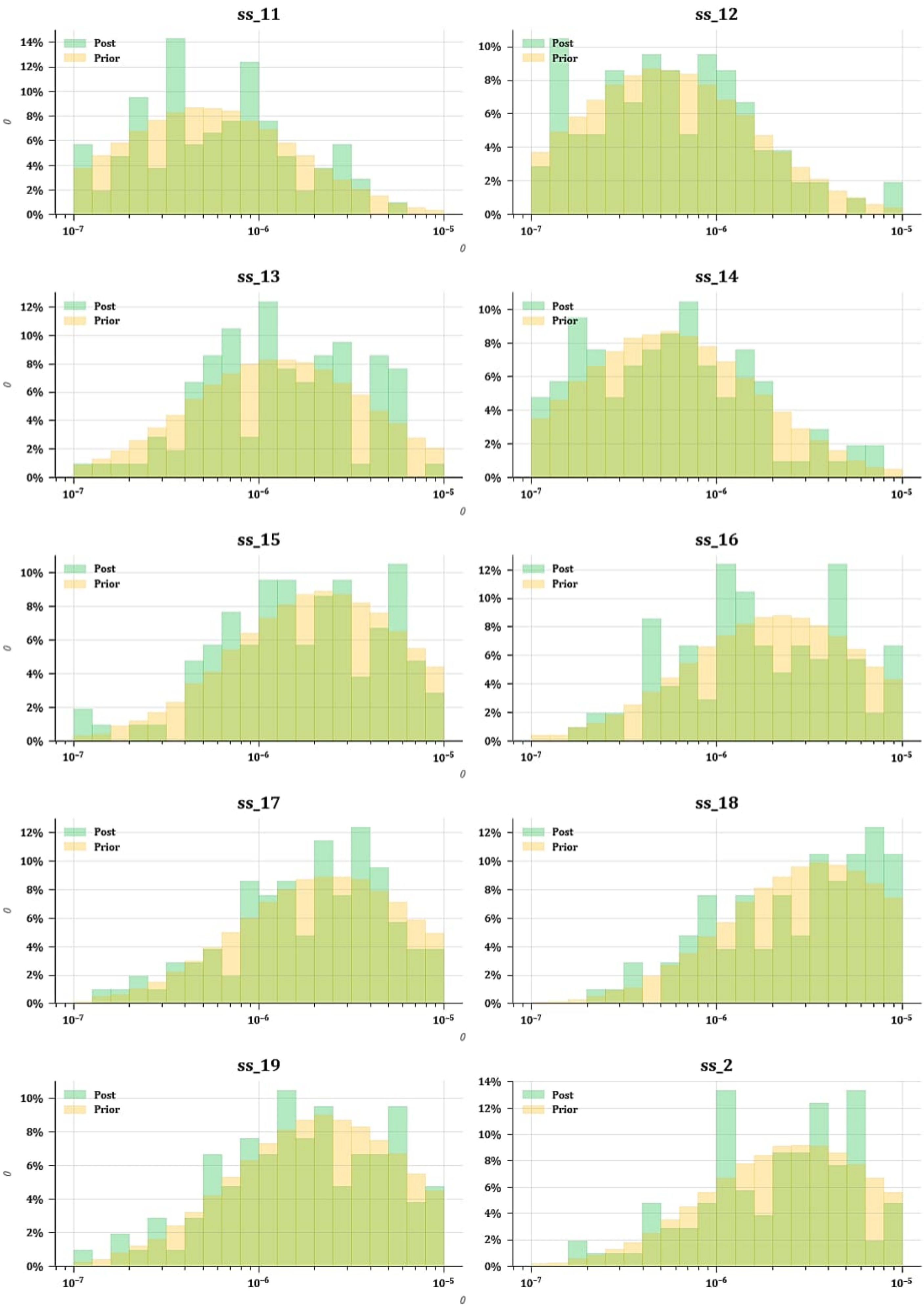
ss_11
ss_12
ss_13
ss_14
ss_15
ss_16
ss_17
ss_18
ss_19
ss_2
Post
Prior

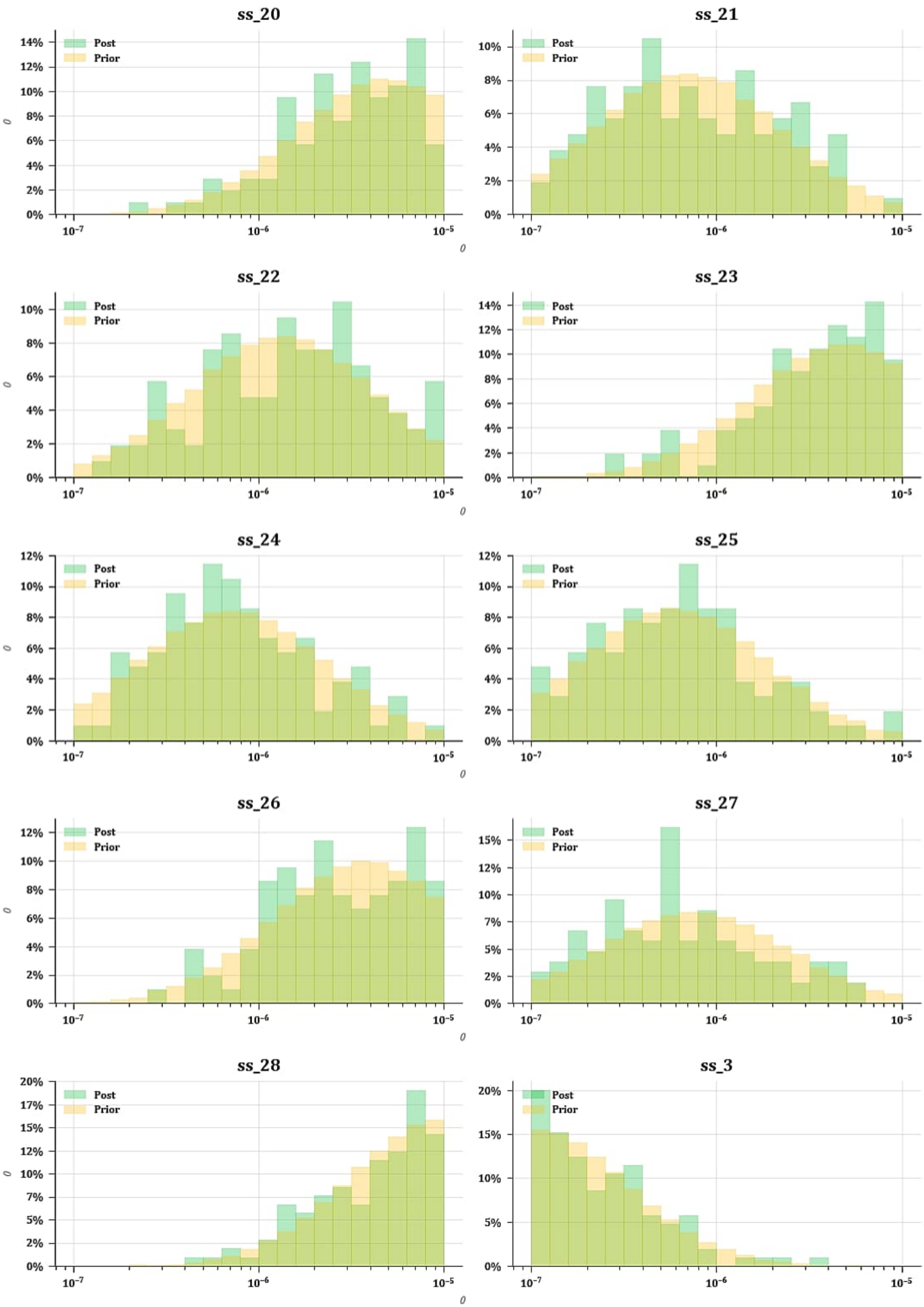
ss_20
ss_21
ss_22
ss_23
ss_24
ss_25
ss_26
ss_27
ss_28
ss_3
Post
Prior
0
10^{-7}
10^{-6}
10^{-5}

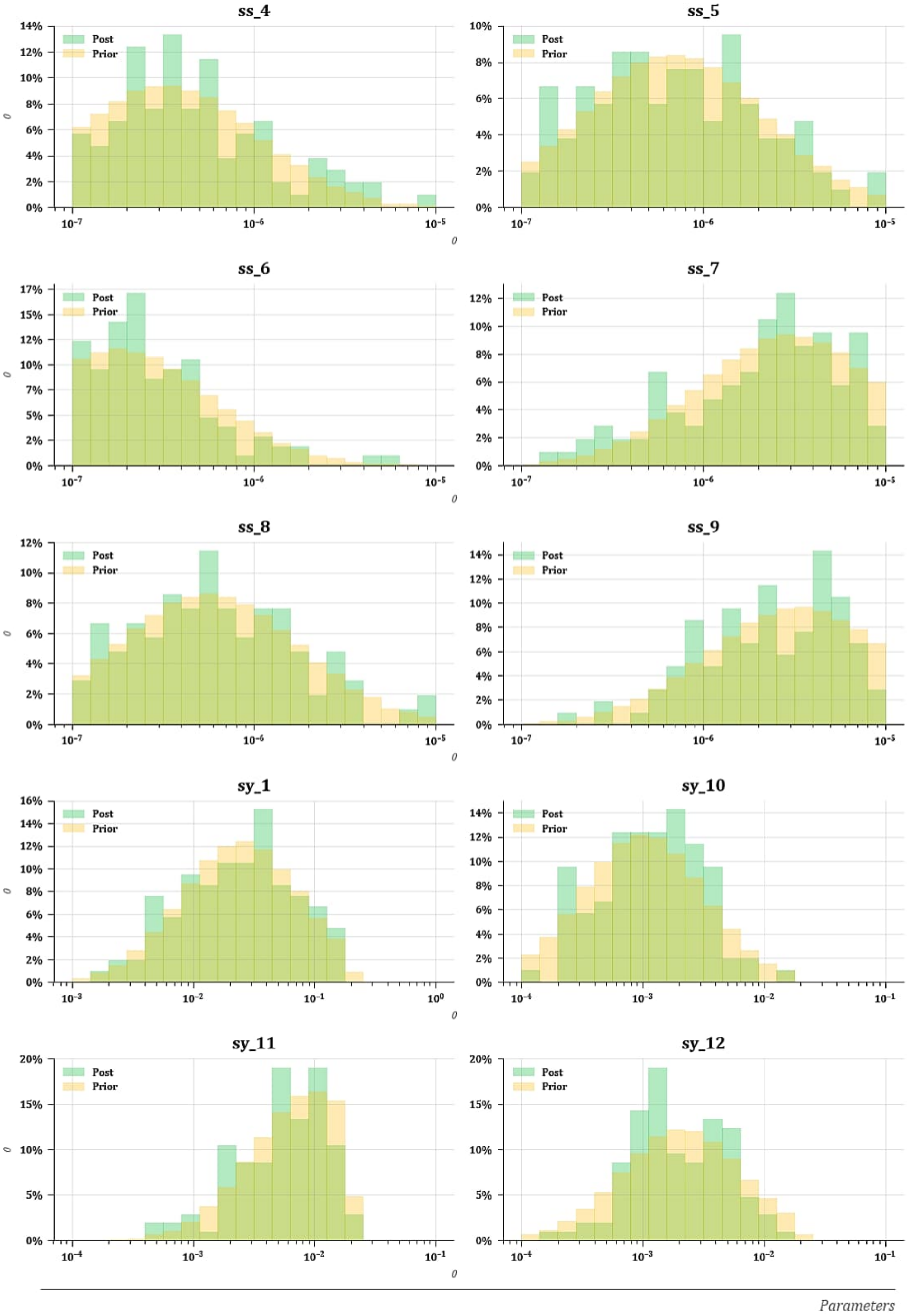
ss_4
ss_5
ss_6
ss_7
ss_8
ss_9
sy_1
sy_10
sy_11
sy_12
Post
Prior
Parameters

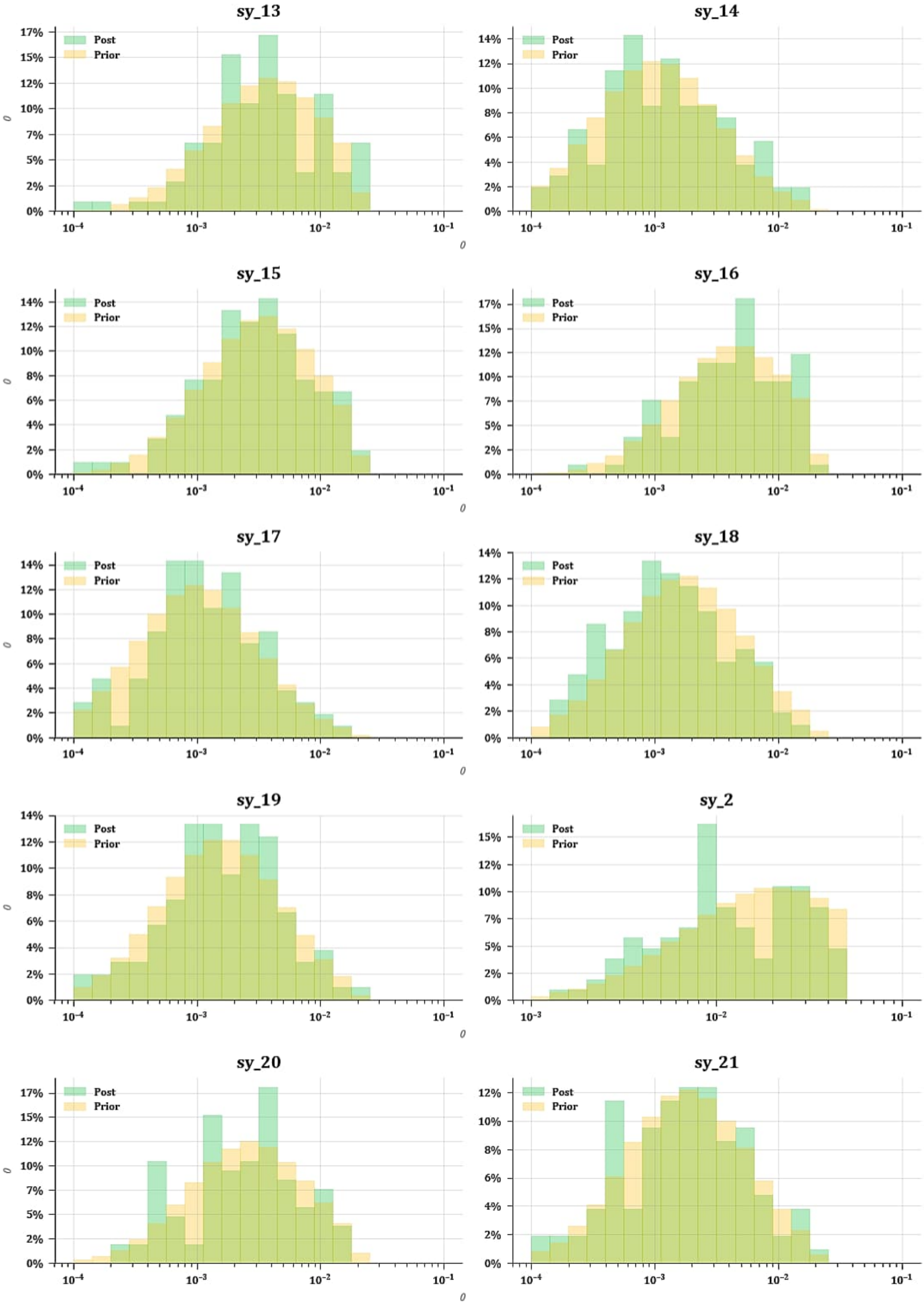
sy_13
sy_14
sy_15
sy_16
sy_17
sy_18
sy_19
sy_2
sy_20
sy_21
Post
Prior

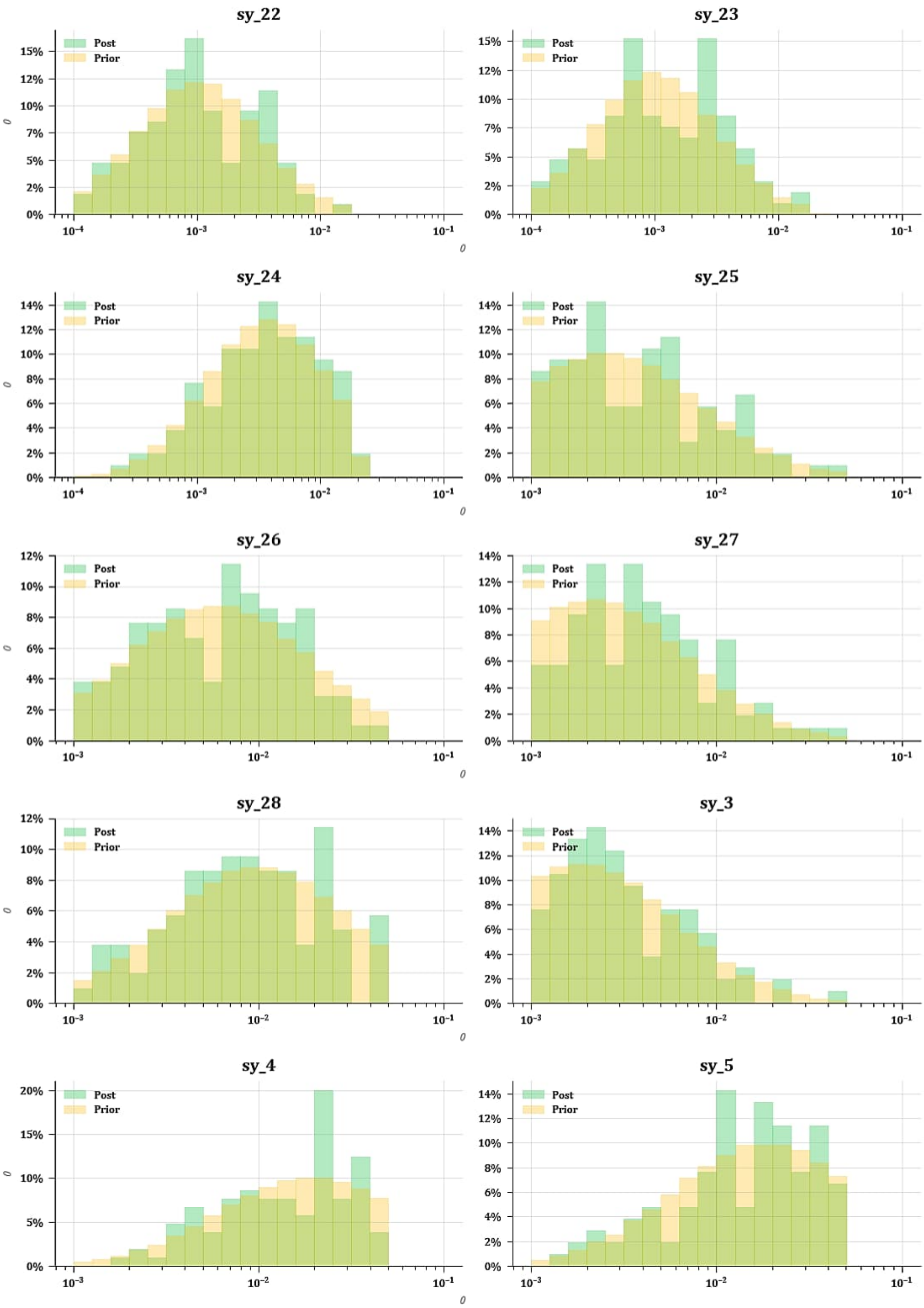
sy_22
sy_23
sy_24
sy_25
sy_26
sy_27
sy_28
sy_3
sy_4
sy_5
Post
Prior
0
15%
12%
10%
7%
5%
2%
0%
14%
8%
6%
4%
20%
10^{-4}
10^{-3}
10^{-2}
10^{-1}

Parameters

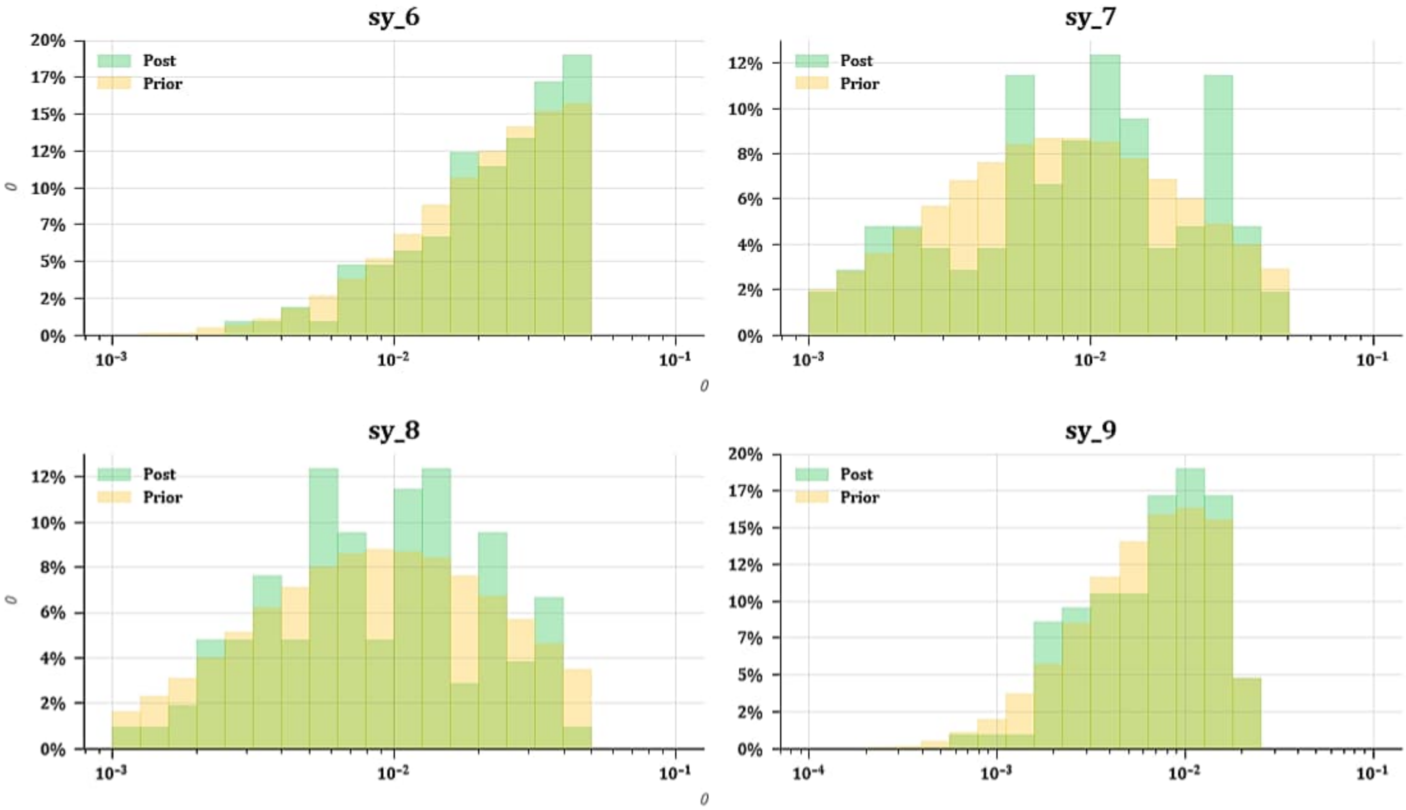
sy_6
sy_7
sy_8
sy_9
Post
Prior

ASIA PACIFIC OFFICES

BRISBANE
Level 2, 15 Astor Terrace
Spring Hill QLD 4000
Australia
T: +61 7 3858 4800
F: +61 7 3858 4801

CANBERRA
GPO 410
Canberra ACT 2600
Australia
T: +61 2 6287 0800
F: +61 2 9427 8200

DARWIN
Unit 5, 21 Parap Road
Parap NT 0820
Australia
T: +61 8 8998 0100
F: +61 8 9370 0101

GOLD COAST
Level 2, 194 Varsity Parade
Varsity Lakes QLD 4227
Australia
M: +61 438 763 516

MACKAY
21 River Street
Mackay QLD 4740
Australia
T: +61 7 3181 3300

MELBOURNE
Level 11, 176 Wellington Parade
East Melbourne VIC 3002
Australia
T: +61 3 9249 9400
F: +61 3 9249 9499

NEWCASTLE
10 Kings Road
New Lambton NSW 2305
Australia
T: +61 2 4037 3200
F: +61 2 4037 3201

NEWCASTLE CBD
Suite 2B, 125 Bull Street
Newcastle West NSW 2302
Australia
T: +61 2 4940 0442

PERTH
Ground Floor, 503 Murray Street
Perth WA 6000
Australia
T: +61 8 9422 5900
F: +61 8 9422 5901

SYDNEY
Tenancy 202 Submarine School
Sub Base Platypus
120 High Street
North Sydney NSW 2060
Australia
T: +61 2 9427 8100
F: +61 2 9427 8200

TOWNSVILLE
12 Cannan Street
South Townsville QLD 4810
Australia
T: +61 7 4722 8000
F: +61 7 4722 8001

WOLLONGONG
Level 1, The Central Building
UoW Innovation Campus
North Wollongong NSW 2500
Australia
T: +61 2 4249 1000

AUCKLAND
Level 4, 12 O'Connell Street
Auckland 1010
New Zealand
T: 0800 757 695

NELSON
6/A Cambridge Street
Richmond, Nelson 7020
New Zealand
T: +64 274 898 628